

**DISCOVERY OF TISSUE-SPECIFIC  
FUNCTIONS OF ATYPICAL E2FS IN  
CANCER**

Eva Moreno Iglesias

The research described in this thesis was performed at the Department of Biomolecular Health and Sciences, Division of Cell Biology, Metabolism & Cancer, Faculty of Veterinary Medicine, Utrecht University, Utrecht, The Netherlands.

The printing of this thesis was financially supported by Bio Services.

*Bio*  *Services*

ISBN: 978-94-6416-663-7  
Cover & layout design: Publiss | [www.publiss.nl](http://www.publiss.nl)  
Print: Ridderprint | [www.ridderprint.nl](http://www.ridderprint.nl)  
Cover: Immunohistochemistry image of liver tissue from the transgenic mice.

© Copyright 2021: Eva Moreno Iglesias

All rights reserved. No part of this publication may be reproduced, stored in a retrieval system, or transmitted in any form or by any means, electronic, mechanical, by photocopying, recording, or otherwise, without the prior written permission of the author.

# DISCOVERY OF TISSUE-SPECIFIC FUNCTIONS OF ATYPICAL E2FS IN CANCER

NIEUWE WEEFSEL SPECIFIEKE FUNCTIES  
VAN ATYPISCHE E2FS IN KANKER

(met een samenvatting in het Nederlands)

## **Proefschrift**

ter verkrijging van de graad van doctor aan de  
Universiteit Utrecht  
op gezag van de  
rector magnificus, prof.dr. H.R.B.M. Kummeling,  
ingevolge het besluit van het college voor promoties  
in het openbaar te verdedigen op

donderdag 30 september 2021 des ochtends te 10.15 uur

door

**Eva Moreno Iglesias**

geboren op 16 september 1991  
te Madrid, Spanje

**Promotor:**

Prof. dr. A. de Bruin

**Copromotor:**

Dr. B. Westendorp

The research described in this thesis was financially supported by Dutch Cancer Society grant (KWF: UU2013-5777, 11941/2018-2, to B. Westendorp and A. de Bruin), and Utrecht Life Sciences Infrastructure grant (call 2014-I) and ZonMW (91116011).



*Para papá y mamá;*



## **Table of contents**

<b>Chapter 1</b>	Introduction	9
	Outline of the thesis	20
<b>Chapter 2</b>	E2F7 is a potent inhibitor of liver tumor growth in mice	29
<b>Chapter 3</b>	Atypical E2Fs either counteract or cooperate with RB during tumorigenesis depending on tissue context.	67
<b>Chapter 4</b>	Polyploidization in non-alcoholic fatty liver disease promotes steatosis and inhibits liver tumor progression.	95
<b>Chapter 5</b>	General discussion	123
<b>Chapter 6</b>	<b>Addendum</b>	143
	Nederlandse Samenvatting	144
	Summary	146
	Resumen	148
	Acknowledgements	151
	About the author: Curriculum vitae & Publication list	157



14-18 mg/kg adipose tissue

Organ	Sex	Age	Color	Weight	Measurements
Heart					
Lung					
Spleen					
Stomach					
Small Intestine					
Large Intestine					
Bladder					
Uterus					
Ovary					
Testis					
Prostate					
Penis					
Prepuce					
Skull					
Brain					
Eye					
Ear					
Thyroid					
Trachea					
Esophagus					
Diaphragm					
Pericardium					
Peritoneum					
Pericyst					
Other					

Necropsy comments:

~~1. Liver (L1, L2, L3, L4, L5, L6, L7, L8, L9, L10, L11, L12) - spleen~~  
~~2. Kidney~~  
~~3. Intestine (transverse)~~  
~~4. Adipose tissue~~  
~~5. Fat~~  
~~6. Skin~~  
~~7. Muscle~~  
~~8. Bone~~  
~~9. Cartilage~~  
~~10. Other~~

Sample	Volume	Container	Notes	
Blood				
EDTA				
Clot				
Plasma				
Whole Blood				
Other				
Tissues				
Brain				
Heart				
Liver				
Lung				
Spleen				
Stomach				
Small Intestine				
Large Intestine				
Bladder				
Uterus				
Ovary				
Testis				
Prostate				
Penis				
Prepuce				
Skull				
Brain				
Eye				
Ear				
Thyroid				
Trachea				
Esophagus				
Diaphragm				
Pericardium				
Peritoneum				
Pericyst				
Other				

# Chapter 1

---

## General Introduction

Cancer, or malignant neoplasia, refers to cells with unscheduled cellular proliferation which have the ability to form macroscopic tumors that invade the surrounding tissue and can even disseminate to distant sites or other organs, namely metastases. To date, there are more than 200 distinct cancer types that are generally named after the organ and tissue of origin. Due to the high complexity of cancer biology and the diversity of cancers, researchers Hanahan and Weinberg tried to unify common aspects and functional capabilities that cancer cells must acquire, irrespective of the etiology, to become malignant. This initial proposal of an unifying framework to understand the fundamental biology of cancer was called “Hallmarks of Cancer” (1) which, despite being frequently updated (2), continues to serve as the key concept for understanding the molecular biology of cancer.

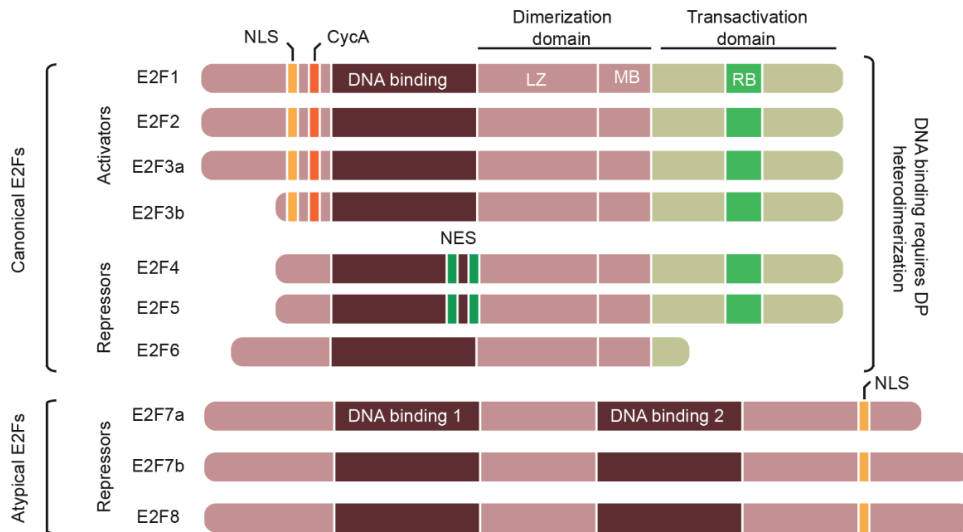
One of these Hallmarks of Cancer is the insensitivity to anti-growth signals. Interestingly, the E2F family members and its key regulators the pocket proteins including the Retinoblastoma protein (RB) play a crucial role in arbitrating these antiproliferative signals.

The introduction chapter of this thesis provides an overview about the E2F transcription factors, their function in controlling the cell cycle, and their impact on cancer progression. After the introduction, three research chapters are outlined which include several transgenic mouse model studies to explore the role of the newest members of E2F family, the atypical E2Fs (E2F7 and -8) and RB in cancer progression. The final chapter contains an extensive discussion of the data presented in this thesis and an outlook towards future perspective.

## **The E2F family**

Back in the late eighties, a cellular factor with transcriptional activity capable of activating the adenoviral E2 gene promoter was identified and named adenoviral early region 2 binding factor (E2F) (3,4). Since then, a total of eight members (E2F1-8) have been identified. The E2F family members share highly conserved DNA binding domains which are necessary to directly bind to the classic E2F consensus motif (TTT[C/G][C/G]CGC) (5). These motifs are usually located in very close proximity of the transcriptional start sites of target genes and thereby E2F transcription factors control their expression. Chromatin immune-precipitation analysis and gene analysis experiments have revealed that many E2F-target genes are involved in DNA synthesis, DNA metabolism, DNA repair and cell cycle progression (6-8).

On the basis of structural analysis, E2Fs can be classified into canonical E2Fs (E2F1-6) and atypical E2Fs (E2F7-8). Briefly, canonical E2Fs require dimerization, via the dimerization domain, with a partner protein (DP) to form hetero-dimers and bind DNA. In contrast, atypical E2Fs lack a DP binding domain and, instead, have an additional DNA binding domain. Interestingly, atypical E2Fs have the ability to form homo- and heterodimers with each other and bind to the promoter of target genes independent of DP (9-12) (Figure 1). Therefore, both the DP domain and the DNA binding domain are the minimal requirements that differentiate



**▲Figure 1: Structural diagram of mammalian E2F family members.** All E2F family members contain a conserved DNA binding domain (DBD). Based on their transcriptional activity, E2Fs can be broadly divided into activators and repressors. Canonical E2Fs require dimerization with a member of the transcription factor dimerization partner (DP1 or -2) in order to bind DNA. The dimerization domain which consists of leucine zipper (LZ) and marked box (MB) domains grants this binding. Transcription induced by canonical E2Fs is mainly regulated by Retinoblastoma protein (RB) and the other pocket proteins p107/p130, which binds to the transactivation domain. However, unlike canonical repressors, E2F7 and E2F8 contain two DNA binding domains and lack the dimerization and transactivation domains. Therefore, their repression function is presumed to occur independently of RB and related pocket proteins. All E2F proteins contain a putative nuclear localization signal (NLS). The NLS of canonical E2Fs is localized in their N-terminal region, whereas atypical E2Fs hold a bipartite NLS in their C-terminal tail. E2F3 and E2F7 encode for two isoforms, a and -b. NLS: Nuclear Localization Signal. NES: Nuclear Export Signal. CycA: CyclinA Binding site. LZ: Leucine Zipper Domain. MB: Marked Box Domain. RB: pocket protein binding domain. Illustration modified from Chet et al. 2009.

canonical from atypical E2Fs. In addition, canonical E2Fs, with the exception of E2F6, also possess a transactivation domain, which is essential to facilitate the interaction with the family of pocket proteins (p107, p130 and Rb) to regulate the E2F transcriptional activity (13,14). Atypical E2Fs do not contain this domain and therefore their repressor functions are suggested to occur independent of Rb. Nevertheless, canonical and atypical E2Fs regulate an overlapping network of cell cycle genes involved in DNA replication, DNA metabolism and DNA repair (15-18).

## E2Fs control cell cycle progression and apoptosis

The E2F family members are tightly controlled during the cell cycle by transcriptional, post-transcriptional and post-translational mechanisms. This is important to prevent deregulation of E2F-dependent transcription and consequently unscheduled proliferation and tumorigenesis (19). Notably, E2Fs are highly conserved throughout evolution and different species (20). Upon growth stimulation, cyclin proteins and cyclin dependent kinases (CDKs) hyper-phosphorylate Rb, leading to the release and activation of E2F1-3. This action leads to the induction of E2F target gene expression responsible to promote G1-S transition (21-23). In S to G2, E2F6-8 are responsible for repressing target gene expression to control cell cycle progression at this stage (9,13,15,21-25). Finally, E2F4-5 remain constitutively expressed throughout all phases of the cell cycle, but they are only present in the nucleus in non-cycling cells to transcriptionally repress cell cycle genes. Therefore, they play an important role in the maintenance of quiescence (26,27). Thus, the interplay and oscillation pattern between E2F “activators” and “repressors” is thought to ensure accurate DNA replication and cell division (Figure 2). While this is their best-known function, most of these results were obtained from cell lines where the cellular microenvironment is highly controlled and the results might be rather oversimplified. Expression and regulation of E2Fs in tissues turned out to be more complex. Beyond the cell cycle regulation, individual E2F proteins have been described to have additional properties. These include the regulation of genes involved in cell differentiation, polyploidization and cell survival. Moreover, the roles of E2F family members depends on tissue context and cellular microenvironment. For example, E2F1-3 switch from activators in intestinal progenitor cells to repressors in differentiating intestinal cells (28). Moreover, repressor E2Fs can bind to the promoters of activators and *vice versa*, resulting in a rather complex negative feedback loop (27). An example of this phenomenon is that repression of E2F1 expression by atypical E2Fs prevents excessive cell death (29). Paradoxically, E2F activity can promote both cell proliferation and cell death. These conflicting results were firstly observed in fibroblasts, which underwent extensive cell death upon E2F1 overexpression (30). Although the pro-apoptotic function of dysregulated E2F activity was mainly attributed to E2F1, later it was demonstrated by *in vitro* and *in vivo* studies that other E2Fs can also induce apoptosis (31-34). Although in most cases this effect is p53-dependent, E2Fs can induce also apoptosis in a p53-independent manner (35-37). Nevertheless, the contribution of E2F to the pro-apoptotic phenotype also appears to be context- and tissue-dependent. For instance, DNA damage can increase the selectivity of E2F1 for a specific subsets of pro-apoptotic E2F target genes (38). Intriguingly, some pro-apoptotic E2F target genes such as the tumor suppressor *ARF* gene, are only activated in the presence of cellular stresses (21,39). It remains unclear what mechanisms trigger the activation of a specific subset of genes in response to cellular stresses.

In tissues, the dual function of E2Fs in controlling cell cycle progression and apoptosis has a clear impact on embryonic development. For example, *E2f7* and *E2f8* double-knockout



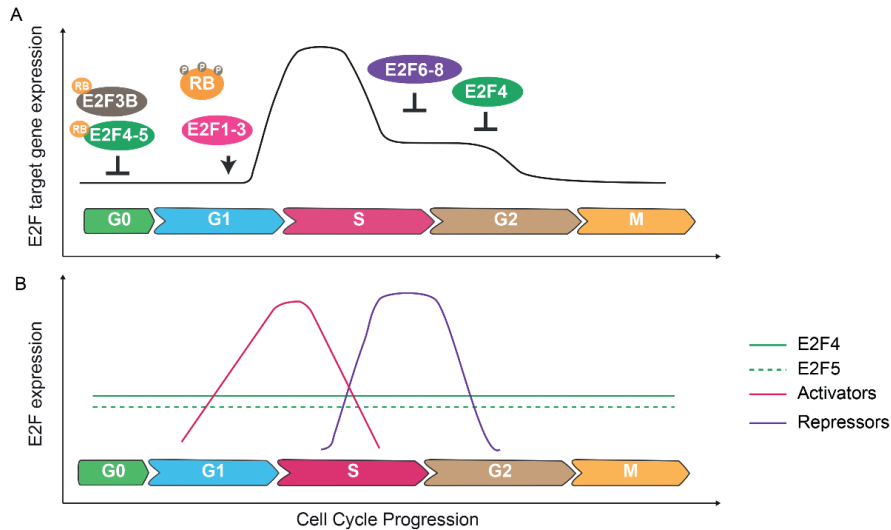
mouse embryos display increased levels of E2F1 and widespread apoptosis. Removal of E2F1 was sufficient to suppress this pro-apoptotic phenotype (29). Based on these developmental studies, it was hypothesized that similar effects could exist in cancer. However, manipulation of E2F activity in different cancer-prone mouse models provides some unexpected outcomes and revealed distinct tissue-specific functions for different E2Fs. For instance, E2F1 deficiency significantly diminished the development of different tumors in *Rb* heterozygous mice (40). Interestingly, loss of *E2f3* in *Rb* heterozygous mice suppressed pituitary tumors but promoted development and metastasis of medullary thyroid tumors (41). Whether this reflects a tissue-specific E2F activity on cell cycle progression and/or apoptosis remains unknown. Lastly, copy number gains in *E2f1* or *E2f3b* led to increased incidence of spontaneous hepatocellular carcinoma (HCC) in the absence of excessive apoptosis (42). These results indicate that pro-apoptotic function of E2Fs might be relevant only in certain tissues, for example depending on accessibility of pro-apoptotic target promoters or on post-translational modification of E2Fs (43).

Understanding the difference between the pro-proliferative and pro-apoptotic functions of E2F activity may be of critical importance to explain the apparent paradox roles of E2Fs as both tumor suppressors and oncogenes.

## **Importance of balanced E2F-dependent transcription on proliferation/ differentiation decisions.**

In general, proliferation and differentiation processes are mutually exclusive. Although in *Drosophila*, for instance, a unique transcription factor appears to simultaneously promote both cell cycle arrest and neural differentiation (44). Consistently, E2F-mediated regulation of target genes is used to link cell cycle progression at some targets while simultaneously providing repression at others (45). This evidence supports a direct link between transcriptional regulation of genes involved in cell cycle and cell differentiation (46). Indeed, together with the studies presented above, several researchers have shown that the RB/E2F pathway is essential not only for control of cell cycle progression but also for differentiation and proper embryonic development in mice, *Drosophila* and *Xenopus* (47-50).

Activation of differentiating genes and/or suppressing cell cycle progression must be a decision that depends on the balanced interplay between E2F activators and repressors on the regulation of E2F targets. One way in which this is achieved is through binding site recognition specificities. The majority of E2F target promoters are regulated by several E2Fs. However, some promoters are regulated by specific E2Fs. For instance, while E2F1 can bind and repress the *Mcl-1* promoter to contribute to apoptosis, E2F4 is unable to bind to this same promoter (51). Therefore, E2F activators and repressors might have different binding affinity for specific promoters. Moreover, their oscillating expression pattern causes that specific E2F members are available at different phases of the cell cycle (50,52-54). In addition, RB/E2F members can interact with other transcriptional regulators, such as MyoD, C/EBPs and HBP1 to regulate



**▲Figure 2: Model of E2F regulation throughout the cell cycle.** (A) Regulation of E2F dependent transcription by E2Fs and pocket proteins during the cell cycle. In G0 (quiescent or differentiation), RB form inhibitory complexes with canonical E2F repressors (E2F4-5) and E2F3b to repress E2F target gene expression. Upon growth stimulus, E2F4-5 are shuttled from the nucleus to the cytoplasm and CDKs phosphorylate and inactivate RB, which lead to binding of E2F1-3 activators to the target promoters and consequently peak of target genes at the G1-S transition. As S phase progresses, E2F targets get repressed by the action of E2F6 and atypical E2F7/8 repressors. During late G2, E2F4 can be detected in the nucleus to further repress E2F targets. (B) Regulation of E2F expression throughout the cell cycle. E2F4 and -5 constitutively express in all phases of the cell cycle but only have repressive functions when shuttle from cytoplasm to the nucleus. Activators (E2F1-3) peak activity is during G1-S transition, when they are release from RB. This activation induces cell cycle genes including *E2F7* and *E2F8*. During S phase and G2, E2F6-8 peak activity to control cell cycle progression. Protein. RB: Retinoblastoma. P: phosphorylation. Illustration adapted from Kent et al. 2019.

together the differentiation process (55–57). Therefore, the interplay between E2F activity and the cell fate decision goes beyond affinity for certain promoters but might be more related to the availability of the different E2Fs and their interaction with transcriptional co-regulators .

However this transcriptional regulation of cell cycle and differentiation genes might also be dependent on the tissue or cell type. The generation of E2F knockout mice for each family members (single knockouts) or combinations, has revealed that E2Fs have tissue-specific roles during development. For instance, both E2F1 and E2F2 had been shown to be important for T-cell proliferation and development. Interestingly, the murine knockout studies revealed a role for E2F1 in regulating proliferation of mature T-lymphocytes and tumor formation while E2F2 is important for regulating proliferation of immature T-lymphocytes and preventing autoimmune diseases (58,59). Lineage specificity was also suggested for E2F4 and E2F5. Mice

lacking E2F4 or E2F5 exhibited different developmental defects that resulted from defective differentiation of various cell lineages (60-62). These studies are consistent with the role of E2F in the regulation of cell-fate making decisions, but also suggest that this function might be restricted to specific tissues.

Lastly, an imbalance between proliferation and differentiation during tumorigenesis might determine the initiation and progression of precancerous and cancer cells. The presence or absence of E2Fs activity affect these cell-fate decisions (63). Therefore, it is possible that the balance between E2F activators and E2F repressors will determine whether cells continue to proliferate or undergo cell cycle arrest and switch on a differentiation program.

## The Yin and Yang of E2Fs in cancer.

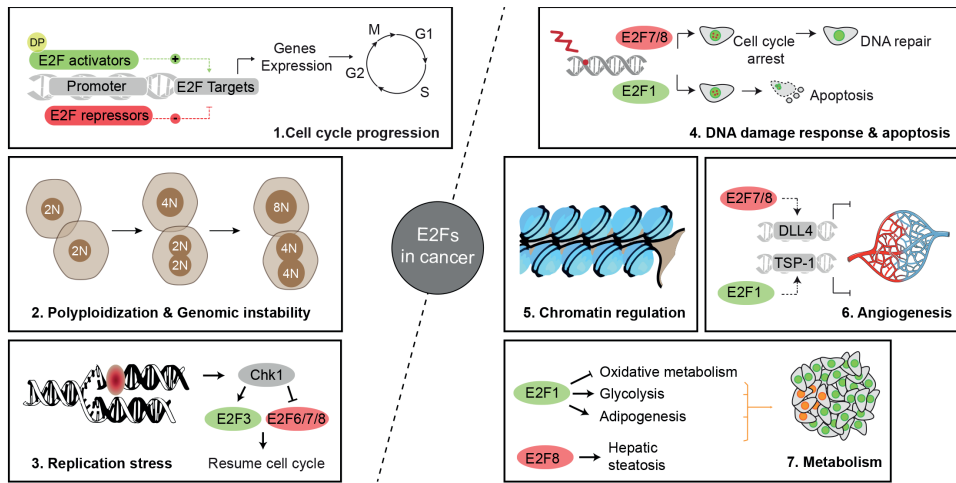
Unrestrained E2F-dependent transcription is linked to tumor progression and poor prognosis. This has led to the view that disruption of the RB/E2F pathway, responsible for regulating E2F transcriptional activity, is an universal requirement for cancer development (64,65). Depending on the activating or repressing role of the E2F members, they are expected to behave as oncogenes or tumor suppressors, respectively. Accordingly, overexpression of E2F1 and -3 has been detected in many human cancers (66-69) and whole body copy number gains in *E2f1* or *E2f3b* are sufficient to induce spontaneous liver tumorigenesis in a dosage-dependent manner, suggesting that the liver appears more sensitive to oncogenic E2F activity than other tissues (42). Moreover, conditional deletion of E2F repressors, namely E2F7 and -8, led to liver tumorigenesis, supporting their role as tumor suppressors (17,34). Nevertheless, conflicting results have suggested that E2F7 and in particular E2F8 can also have oncogenic effects (70,71). These studies are based on the notion that E2F7 and E2F8 mRNA expression are consistently high in many cancer types and this correlates with poor prognosis. However, this upregulation might simply reflect the high percentage of proliferating cells of those aggressive tumors, as *E2f7* and *E2f8* transcripts peak during S/G2-phase of the cell cycle.

Mechanistically, how E2Fs and their transcriptional targets could contribute to cancer development and progression can be broadly categorized into 7 groups (Figure 3).

1. **Cell cycle progression:** Many E2F target genes participate in facilitating the transition between phases of the cell cycle, mainly G1-S transition. Importantly, E2F activation correlates directly with the ability of a cell to overcome the G1/S restriction point (72,73). This indicates that E2Fs can be activated and cells will be forced to proliferate even in the absent of mitogen stimulation. Accordingly, amplification of E2F activators or oncogene-induce E2F activation is frequently observed in cancer cells. Moreover, there is cumulative evidence that manipulation of E2F activity is used by cancer cells to develop resistance against molecular cancer therapy by, for instance, forcing cell cycle progression or increasing DNA repair. This is in particular the case for PARP and CDK4/6 inhibitors

(74). Although most of these findings are obtained from *in vitro* settings, there are now several *in vivo* studies implicating the relevance of regulating cell cycle progression by E2Fs critical is for tumorigenesis. For instance, in the second chapter of this thesis we provide evidence that manipulation of E2F dependent transcription by overexpressing the E2F atypical repressors, E2F7 and E2F8, can block liver tumor growth in mice by the repression of E2F target genes.

2. Polypliodization and genomic instability: Besides controlling normal cell cycle progression, the E2F family members are also involved in the regulation of atypical or abortive cell cycles that lead to duplication of complete sets of chromosomes. This phenomenon is known as polypliodization and it occurs physiologically in all mammalian species during development and aging in selected tissues such as liver, pancreas, heart or placenta. The liver represents one of the few mammalian organs that display changes in ploidy depending on the circumstances. On one hand, progressive polypliodization during development or aging indicate regulation of tissue homeostasis or terminal differentiation, respectively. On the other hand, increased of hepatocyte polypliodization is frequently observed during (oxidative) stress or DNA damage. Hence, polypliodization may also represent a pathological state(75). Interestingly, polypliodization is frequently observed in different cancer types (reviewed in(76)), although whether it drives or protects from tumorigenesis is still under debate. This phenomenon could function as a buffer against gene-inactivating mutations, due to presence of extra copies of a tumor suppressor, or buffer against tumor-suppressor loss of heterozygosity (77). However, multiple studies also suggested that polypliod cells are more susceptible to chromosome segregation errors and consequently aneuploidy and genomic instability, therefore supporting oncogenic properties (78). It is therefore not surprising that mechanisms which prevent the proliferation of polypliod cells have evolved. For instance, activation of p53 pathway limits the proliferation of polypliod cells to protect genomic integrity and tumorigenesis (79). In the liver, polypliody is partly triggered by timely repression of E2F-dependent transcription. Accordingly, dysregulation of the E2F activity leads to changes in polypliodization of hepatocytes (80-82). Experimental studies with mouse models demonstrated that livers with conditional deletion of *E2f7/8* have less polypliod hepatocytes and developed spontaneous liver tumors (17). In addition, *E2f1* depleted livers resulted in enhanced polypliodization and less DEN-induced liver tumors (42,82). These data suggest that control of polypliodization, via E2Fs, helps to prevent tumor development.



**▲Figure 3: E2Fs contribute to cancer development and progression by controlling different mechanisms.** Several studies of the E2F family have uncovered critical roles of some of these members in the control of transcription, cell cycle, apoptosis and metabolism. In this figure we aim to depict some of the mechanisms that contribute to cancer development and/ or progression and are regulated by E2F family members. The details from this illustration are explained in the corresponding sections of the text.

- 3. Replication stress:** Replication stress (RS) is defined as stalling or collapsing of replication forks. One of the sources of replication stress is oncogenic events that deregulate cell cycle progression. For instance, oncogenic HRAS<sup>V12</sup> drives proliferation and induces RS by stimulating RNA synthesis and increasing global transcription rates (83). Consequently, cells with excessive replication stress resulted in collapsed of forks into DNA damage. To cope with these threats, cells mostly rely on the activation of the intra- S phase checkpoint (ATR/ Chk1) to repair this damage which otherwise can result in genomic instability, a well-known hallmark of cancer. Interestingly, extensive evidence showed that high E2F activity is maintained under DNA damage conditions and links E2Fs with the recovery and tolerance of RS (84–87). To initiate replication, a protein complex named *replisome* needs to be loaded on the DNA. This is facilitated by the action of replicative helicases minichromosome maintenance complex 2–7 (MCM2–7) at replication origins. Of note, MCM proteins, as well as other replication factors such as cell division cycle 6 (CDC6) or DNA replication factor 1 (CDT1), are regulated by E2Fs. Therefore, one could speculate that increasing or decreasing E2F-dependent transcription during S phase, increases or decreases replication capacity, respectively, and can result in replication stress and DNA damage. In agreement with this, *in vitro* cultures showed indeed that up regulation of E2F transcription during S phase, by knocking down E2F6, increased the DNA synthesis rate without directly inducing replication stress but increasing unresolved DNA damage over time (88). Additionally, extensive evidence

using *in vivo* models supports the impact of deregulated E2F-dependent transcription on the replication rates and tumorigenesis. For example, overexpression of CDC6, CDT1 or FBXO5 induced disruption of normal replication mechanisms and genomic instability which results in cellular transformation in mice (89,90). Strikingly, repression of E2F transcription also causes replication stress although can have dual effects on tumorigenesis, blocking tumor proliferation or increasing cancer risk (91,92). Taken together, upregulation of E2F activity via oncogenic stimulus is frequently encountered in cancer cells. This upregulation causes replication stress, however it is also speculated that it could contribute to how cells can tolerate replication stress.

4. DNA damage response and apoptosis: E2Fs are also involved in the DNA damage response and apoptosis. Both phenomena represent barriers against genomic instability and tumorigenesis. Under DNA damaging conditions, cells rely on a highly conserved DNA damage response (DDR) mechanism which involves activation of several pathways including checkpoint kinases (Chk1 and Chk2). These kinases directly phosphorylate multiple substrates to modulate their activity, stability and subcellular localization (93). For instance, Chk2 phosphorylates BRCA1 to control the selectivity of the repair events upon DNA damage (94). There is increased evidence that E2F activity is necessary to ensure proper DNA damage repair and continuation of the cell cycle upon completeness of the repair (33,95-97). Notably, the checkpoint kinases have been identified as direct regulators of E2F activity (85,87,98). For instance, Chk1 phosphorylates atypical E2Fs to prevent a permanent cell cycle arrest and allow DNA repair (87). In addition to participating on the DNA damage response, specific E2Fs, mainly E2F1, can induce apoptosis in response to DNA damage, although this largely depends on context (expression levels), severity of the DNA damage and specific cell types (99,100).

In conclusion, the role of E2Fs on modulating the DNA damage response and apoptosis is part of their complex regulation to maintain genomic integrity.

5. Chromatin regulation: E2Fs are transcription factors that can directly control gene transcription. In addition, several studies showed that E2Fs can also affect gene transcription in a more indirect manner by interacting with chromatin regulatory complexes (101). For instance, recruitment of Pontin/Reptin by E2F1 opens the chromatin at E2F target genes facilitating the capacity of other E2F factors (E2f1 and E2f3) to bind and enhance the E2F transcriptional response in liver tumors (102). Therefore, chromatin regulatory complexes might determine the activating or repressing effects of individual E2Fs. This additional regulatory mechanism makes it more complex to predict whether individual E2Fs will function as tumor suppressors or oncogenes in specific cancer types.

Moreover, few studies showed that some E2Fs can localize at DNA damage sites and can modify the chromatin environment to facilitate DNA damage repair (97,103,104). Therefore, transcriptional independent roles of E2Fs might also contribute to maintain the genomic stability. However, the role of E2Fs in chromatin modulation is largely unexplored.

6. **Angiogenesis:** Blood vessel formation towards and within tumors is another important hallmark of cancer and E2Fs have been implicated in the regulation of tumor angiogenesis (105,106). For instance, atypical E2Fs might inhibit intra-tumoral vessel branching via induction of DLL4 (105). Moreover, E2F1 could activate the transcription of Thrombospondin 1 (TSP-1) resulting in inhibition of tumor angiogenesis and tumor growth (106). Inhibiting tumor angiogenesis is of critical for tumor progression because it enables more accessibility to growth factors and oxygen resources for cancer cells. Cancer cells are very dependent on high energy resources and deficient endothelial cell proliferation can result in ischemia and tissue necrosis. Previous studies have shown that genes involved in angiogenesis and tumor progression, such as VEGF receptors, have potential E2F binding sites in their promoter. Accordingly, we showed that atypical E2Fs can transcriptionally activate VEGFA in cooperation with hypoxia inducible factor 1 (HIF1)(107). In addition, VEGF stimulation resulted in dissociation of Rb/E2F1 complex and robust binding of E2F1 and activation of VEGF promoter (108,109). Given that high levels of VEGF receptors are frequently detected in cancer patients and are associated with poor prognosis (110,111), targeting activator E2Fs might be a promising approach to complement standard anti-angiogenic treatments of cancer patients.
7. **Metabolism:** E2F transcription factors also regulate metabolic genes. For instance, E2F1 have been implicated in the regulation of glycolysis, adipogenesis and oxidative metabolism via a mechanism that implies transcriptional regulation(112-114). In addition, E2F8 promote steatosis in zebrafish livers by regulating the fatty acid binding protein 3 (*fabp3*) (115). The role of these E2Fs in regulating metabolic genes could have potential impact on the initiation or progression of cancer. Recently, reprogramming of energy metabolism has emerged as a hallmark of cancer and some oncogenes and tumor suppressors such as Myc or p53 play an important role in adapting metabolic pathways (116,117). The impact of E2Fs on cancer metabolism still needs to further be explored, but current studies on E2F1 suggest that E2Fs may also control tumorigenesis via reprogramming of metabolic pathways.

In summary, E2F transcription factors can affect a multitude of cancer-related processes, however most of these studies are based on *in vitro* experiments. This thesis explores the consequences of dysregulated E2F-dependent transcription on normal tissue development and cancer formation in multiple mouse models by manipulation atypical E2F repressors *in vivo*. The ensuing chapters of this thesis will present multiple investigations displaying the importance of proper balancing E2F activity during development and cancer, and will discuss the possibility of new venues for the treatment of cancer patients.

## SCOPE AND OUTLINE OF THIS THESIS

In this thesis we studied the consequences of manipulating E2F-dependent transcription in tumor formation and progression and their interaction with other tumor suppressors during liver tumorigenesis. These studies provide new insights on the important role of E2F activity in cancer progression and contribute towards the potential of manipulating E2Fs as putative novel cancer therapy. In **Chapter 2** we developed transgenic mice overexpressing atypical E2Fs which allowed to demonstrate that atypical E2Fs block liver tumor growth by inducing replication stress and DNA damage in cycling hepatocytes. In **Chapter 3** we studied how atypical E2Fs affect tumorigenesis driven by RB loss in multiple different transgenic and knockout mouse models. We propose that E2Fs and Rb cooperate to maintain genomic stability throughout the different phases of the cell cycle in a tissue-specific manner. In **Chapter 4** we explored the role of polyploidization in liver metabolism and tumorigenesis through deleting atypical E2Fs in a mouse model of fatty liver disease. Finally, in **Chapter 5**, we discuss the overall results of the studies presented in this thesis and we propose future strategies to target E2Fs as potential anti-cancer treatment.



## REFERENCES

- (1) Hanahan D, Weinberg RA. The Hallmarks of Cancer. *Cell* 2000 -01-07;100(1):57-70.
- (2) Hanahan D, Weinberg RA. Hallmarks of Cancer: The Next Generation. *Cell* 2011 -03-04;144(5):646-674.
- (3) Kovetski I, Reichel R, Nevins JR. Identification of a cellular transcription factor involved in E1A trans-activation. *Cell* 1986 Apr 25;45(2):219-228.
- (4) Yee AS, Reichel R, Kovetski I, Nevins JR. Promoter interaction of the E1A-inducible factor E2F and its potential role in the formation of a multi-component complex. *EMBO J* 1987 Jul;6(7):2061-2068.
- (5) Helin K, Harlow E. Heterodimerization of the transcription factors E2F-1 and DP-1 is required for binding to the adenovirus E4 (ORF6/7) protein. *J Virol* 1994 -8;68(8):5027-5035.
- (6) Zwicker J, Liu N, Engeland K, Lucibello FC, Müller R. Cell cycle regulation of E2F site occupation in vivo. *Science* 1996 Mar 15;271(5255):1595-1597.
- (7) Wells J, Graveel CR, Bartley SM, Madore SJ, Farnham PJ. The identification of E2F1-specific target genes. *Proc Natl Acad Sci U S A* 2002 Mar 19;99(6):3890-3895.
- (8) Ogawa H, Ishiguro K, Gaubatz S, Livingston DM, Nakatani Y. A complex with chromatin modifiers that occupies E2F- and Myc-responsive genes in G0 cells. *Science* 2002 May 10;296(5570):1132-1136.
- (9) de Bruin A, Maiti B, Jakoi L, Timmers C, Buerki R, Leone G. Identification and characterization of E2F7, a novel mammalian E2F family member capable of blocking cellular proliferation. *J Biol Chem* 2003;278(43):42041-42049.
- (10) Logan N, Graham A, Zhao X, Fisher R, Maiti B, Leone G, et al. E2F-8: an E2F family member with a similar organization of DNA-binding domains to E2F-7. *Oncogene* 2005;24(31):5000-5004.
- (11) Maiti B, Li J, de Bruin A, Gordon F, Timmers C, Opavsky R, et al. Cloning and characterization of mouse E2F8, a novel mammalian E2F family member capable of blocking cellular proliferation. *J Biol Chem* 2005;280(18):18211-18220.
- (12) Di Stefano L, Jensen MR, Helin K. E2F7, a novel E2F featuring DP-independent repression of a subset of E2F-regulated genes. *EMBO J* 2003 -12-1;22(23):6289-6298.
- (13) Attwooll C, Lazzarini Denchi E, Helin K. The E2F family: specific functions and overlapping interests. *EMBO J* 2004 Dec 08;23(24):4709-4716.
- (14) Cobrinik D. Pocket proteins and cell cycle control. *Oncogene* 2005 Apr 18;24(17):2796-2809.
- (15) Westendorp B, Mokry M, Groot Koerkamp, Marian J A, Holstege FCP, Cuppen E, de Bruin A. E2F7 represses a network of oscillating cell cycle genes to control S-phase progression. *Nucleic Acids Res* 2012;40(8):3511-3523.
- (16) Ishida S, Huang E, Zuzan H, Spang R, Leone G, West M, et al. Role for E2F in control of both DNA replication and mitotic functions as revealed from DNA microarray analysis. *Mol Cell Biol* 2001 Jul;21(14):4684-4699.
- (17) Kent L, Rakijas J, Pandit S, Westendorp B, Chen H, Huntington J, et al. E2f8 mediates tumor suppression in postnatal liver development. *J Clin Invest* 2016;126(8):2955-2969.
- (18) Ren B, Cam H, Takahashi Y, Volkert T, Terragni J, Young RA, et al. E2F integrates cell cycle progression with DNA repair, replication, and G(2)/M checkpoints. *Genes Dev* 2002 Jan 15;16(2):245-256.

- (19) Chen H, Tsai S, Leone G. Emerging roles of E2Fs in cancer: an exit from cell cycle control. *Nat Rev Cancer* 2009;9(11):785-797.
- (20) Cross FR, Buchler NE, Skotheim JM. Evolution of networks and sequences in eukaryotic cell cycle control. *Philos Trans R Soc Lond B Biol Sci* 2011 Dec 27;366(1584):3532-3544.
- (21) DeGregori J, Leone G, Miron A, Jakoi L, Nevins JR. Distinct roles for E2F proteins in cell growth control and apoptosis. *Proc Natl Acad Sci U S A* 1997 Jul 08;94(14):7245-7250.
- (22) Wenzel PL, Chong J, Sáenz-Robles MT, Ferrey A, Hagan JP, Gomez YM, et al. Cell proliferation in the absence of E2F1-3. *Dev Biol* 2011 Mar 01;351(1):35-45.
- (23) Frolov MV, Huen DS, Stevaux O, Dimova D, Balczarek-Strang K, Elsdon M, et al. Functional antagonism between E2F family members. *Genes Dev* 2001 Aug 15;15(16):2146-2160.
- (24) Christensen J, Cloos P, Toftegaard U, Klinkenberg D, Bracken AP, Trinh E, et al. Characterization of E2F8, a novel E2F-like cell-cycle regulated repressor of E2F-activated transcription. *Nucleic Acids Res* 2005;33(17):5458-5470.
- (25) Giangrande PH, Zhu W, Schlisio S, Sun X, Mori S, Gaubatz S, et al. A role for E2F6 in distinguishing G1/S- and G2/M-specific transcription. *Genes Dev* 2004 Dec 01;18(23):2941-2951.
- (26) Chong J, Wenzel P, Sáenz Robles MT, Nair V, Ferrey A, Hagan J, et al. E2f1-3 switch from activators in progenitor cells to repressors in differentiating cells. *Nature* 2009;462(7275):930-934.
- (27) Wong JV, Dong P, Nevins JR, Mathey-Prevot B, You L. Network calisthenics: control of E2F dynamics in cell cycle entry. *Cell Cycle* 2011 Sep 15;10(18):3086-3094.
- (28) Chong J, Wenzel PL, Sáenz-Robles MT, Nair V, Ferrey A, Hagan JP, et al. E2F1-3 Switch from Activators in Progenitor Cells to Repressors in Differentiating Cells. *Nature* 2009 -12-17;462(7275):930-934.
- (29) Li J, Ran C, Li E, Gordon F, Comstock G, Siddiqui H, et al. Synergistic function of E2F7 and E2F8 is essential for cell survival and embryonic development. *Dev Cell* 2008 Jan;14(1):62-75.
- (30) Kowalik TF, DeGregori J, Schwarz JK, Nevins JR. E2F1 overexpression in quiescent fibroblasts leads to induction of cellular DNA synthesis and apoptosis. *J Virol* 1995 Apr;69(4):2491-2500.
- (31) Iaquinta PJ, Lees JA. Life and death decisions by the E2F transcription factors. *Curr Opin Cell Biol* 2007 -12;19(6):649-657.
- (32) Chen D, Chen Y, Forrest D, Bremner R. E2f2 induces cone photoreceptor apoptosis independent of E2f1 and E2f3. *Cell Death Differ* 2013 -07;20(7):931-940.
- (33) Martinez LA, Goluszko E, Chen H, Leone G, Post S, Lozano G, et al. E2F3 Is a Mediator of DNA Damage-Induced Apoptosis. *Mol Cell Biol* 2010 -1;30(2):524-536.
- (34) Thurlings I, Martínez López LM, Westendorp B, Zijp M, Kuiper R, Tooten P, et al. Synergistic functions of E2F7 and E2F8 are critical to suppress stress-induced skin cancer. *Oncogene* 2017;36(6):829-839.
- (35) Stiewe T, Pützer BM. Role of the p53-homologue p73 in E2F1-induced apoptosis. *Nat Genet* 2000 Dec;26(4):464-469.
- (36) Urist M, Tanaka T, Poyurovsky MV, Prives C. p73 induction after DNA damage is regulated by checkpoint kinases Chk1 and Chk2. *Genes Dev* 2004 Dec 15;18(24):3041-3054.
- (37) Kowalik TF, DeGregori J, Leone G, Jakoi L, Nevins JR. E2F1-specific induction of apoptosis and p53 accumulation, which is blocked by Mdm2. *Cell Growth Differ* 1998 Feb;9(2):113-118.
- (38) Pediconi N, Ianari A, Costanzo A, Belloni L, Gallo R, Cimino L, et al. Differential regulation of E2F1 apoptotic target genes in response to DNA damage. *Nat Cell Biol* 2003 Jun;5(6):552-558.

- (39) Bates S, Phillips AC, Clark PA, Stott F, Peters G, Ludwig RL, et al. p14ARF links the tumour suppressors RB and p53. *Nature* 1998 Sep 10;395(6698):124-125.
- (40) Yamasaki L, Bronson R, Williams BO, Dyson NJ, Harlow E, Jacks T. Loss of E2F-1 reduces tumorigenesis and extends the lifespan of Rb1(+/-)mice. *Nat Genet* 1998;18(4):360-364.
- (41) Ziebold U, Lee E, Bronson R, Lees J. E2F3 loss has opposing effects on different pRB-deficient tumors, resulting in suppression of pituitary tumors but metastasis of medullary thyroid carcinomas. *Mol Cell Biol* 2003;23(18):6542-6552.
- (42) Kent L, Bae S, Tsai S, Tang X, Srivastava A, Koivisto C, et al. Dosage-dependent copy number gains in E2f1 and E2f3 drive hepatocellular carcinoma. *J Clin Invest* 2017;127(3):830-842.
- (43) Zheng S, Moehlenbrink J, Lu Y, Zalmas L, Sagum CA, Carr S, et al. Arginine methylation-dependent reader-writer interplay governs growth control by E2F-1. *Mol Cell* 2013 -10-10;52(1):37-51.
- (44) Li L, Vaessin H. Pan-neural Prospero terminates cell proliferation during Drosophila neurogenesis. *Genes Dev* 2000 01/15;14(2):147-151.
- (45) Dimova DK, Stevaux O, Frolov MV, Dyson NJ. Cell cycle-dependent and cell cycle-independent control of transcription by the Drosophila E2F/RB pathway. *Genes Dev* 2003 09/15;17(18):2308-2320.
- (46) Cell cycle: To differentiate or not to differentiate? *Current Biology* 2000 /04/15;10(8):R302-R304.
- (47) Suzuki A, Hemmati-Brivanlou A. Xenopus Embryonic E2F Is Required for the Formation of Ventral and Posterior Cell Fates during Early Embryogenesis. *Molecular Cell* 2000 -02-01;5(2):217-229.
- (48) Myster DL, Bonnette PC, Duronio RJ. A role for the DP subunit of the E2F transcription factor in axis determination during Drosophila oogenesis. *Development* 2000 Aug;127(15):3249-3261.
- (49) Lipinski MM, Jacks T. The retinoblastoma gene family in differentiation and development. *Oncogene* 1999 /12;18(55):7873-7882.
- (50) Müller H, Bracken AP, Vernell R, Moroni MC, Christians F, Grassilli E, et al. E2Fs regulate the expression of genes involved in differentiation, development, proliferation, and apoptosis. *Genes Dev* 2001 -2-1;15(3):267-285.
- (51) Croxton R, Ma Y, Song L, Haura EB, Cress WD. Direct repression of the Mcl-1 promoter by E2F1. *Oncogene* 2002 /02;21(9):1359-1369.
- (52) DeGregori J, Johnson DG. Distinct and Overlapping Roles for E2F Family Members in Transcription, Proliferation and Apoptosis. *Curr Mol Med* 2006 Nov;6(7):739-748.
- (53) Hurford RK, Cobrinik D, Lee MH, Dyson N. pRB and p107/p130 are required for the regulated expression of different sets of E2F responsive genes. *Genes Dev* 1997 Jun 01;11(11):1447-1463.
- (54) DeGregori J. The genetics of the E2F family of transcription factors: shared functions and unique roles. *Biochim Biophys Acta* 2002 Jun 21;1602(2):131-150.
- (55) Gu W, Schneider JW, Condorelli G, Kaushal S, Mahdavi V, Nadal-Ginard B. Interaction of myogenic factors and the retinoblastoma protein mediates muscle cell commitment and differentiation. *Cell* 1993 -02-12;72(3):309-324.
- (56) Chen PL, Riley DJ, Chen Y, Lee WH. Retinoblastoma protein positively regulates terminal adipocyte differentiation through direct interaction with C/EBPs. *Genes Dev* 1996 -11-01;10(21):2794-2804.
- (57) Novitsch BG, Mulligan GJ, Jacks T, Lassar AB. Skeletal muscle cells lacking the retinoblastoma protein display defects in muscle gene expression and accumulate in S and G2 phases of the cell cycle. *J Cell Biol* 1996 -10;135(2):441-456.

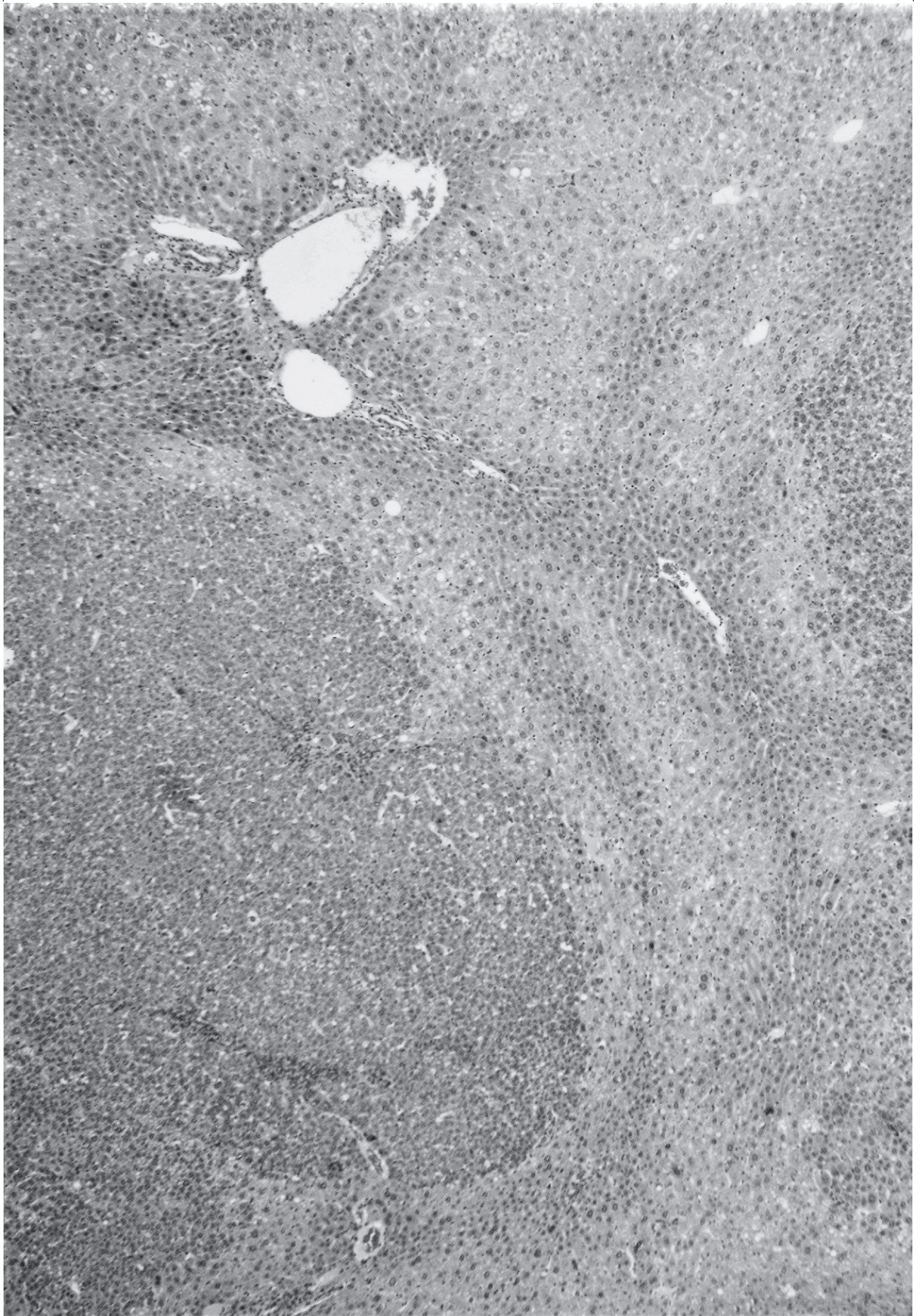
- (58) Murga M, Fernández-Capetillo O, Field SJ, Moreno B, Borlado LR, Fujiwara Y, et al. Mutation of E2F2 in mice causes enhanced T lymphocyte proliferation, leading to the development of autoimmunity. *Immunity* 2001 Dec;15(6):959-970.
- (59) Field SJ, Tsai FY, Kuo F, Zubiaga AM, Kaelin WG, Livingston DM, et al. E2F-1 functions in mice to promote apoptosis and suppress proliferation. *Cell* 1996 May 17;85(4):549-561. (60) Lindeman GJ, Dagnino L, Gaubatz S, Xu Y, Bronson RT, Warren HB, et al. A specific, nonproliferative role for E2F-5 in choroid plexus function revealed by gene targeting. *Genes Dev* 1998 Apr 15;12(8):1092-1098.
- (61) Rempel RE, Saenz-Robles MT, Storms R, Morham S, Ishida S, Engel A, et al. Loss of E2F4 activity leads to abnormal development of multiple cellular lineages. *Mol Cell* 2000 Aug;6(2):293-306.
- (62) Humbert PO, Rogers C, Ganiatsas S, Landsberg RL, Trimarchi JM, Dandapani S, et al. E2F4 is essential for normal erythrocyte maturation and neonatal viability. *Mol Cell* 2000 Aug;6(2):281-291.
- (63) Rempel R, Mori S, Gasparetto M, Glozak M, Andrechek E, Adler S, et al. A role for E2F activities in determining the fate of Myc-induced lymphomagenesis. *PLoS Genet* 2009;5(9):e1000640.
- (64) Viatour P, Sage J. Newly identified aspects of tumor suppression by RB. *Dis Model Mech* 2011 Sep;4(5):581-585.
- (65) Kent LN, Leone G. The broken cycle: E2F dysfunction in cancer. *Nat Rev Cancer* 2019 /06;19(6):326-338.
- (66) Cooper CS, Nicholson AG, Foster C, Dodson A, Edwards S, Fletcher A, et al. Nuclear overexpression of the E2F3 transcription factor in human lung cancer. *Lung Cancer* 2006 Nov;54(2):155-162.
- (67) Foster CS, Falconer A, Dodson AR, Norman AR, Dennis N, Fletcher A, et al. Transcription factor E2F3 overexpressed in prostate cancer independently predicts clinical outcome. *Oncogene* 2004 Aug 05;23(35):5871-5879.
- (68) Hovey RM, Chu L, Balazs M, DeVries S, Moore D, Sauter G, et al. Genetic alterations in primary bladder cancers and their metastases. *Cancer Res* 1998 Aug 15;58(16):3555-3560.
- (69) Olson MV, Johnson DG, Jiang H, Xu J, Alonso MM, Aldape KD, et al. Transgenic E2F1 Expression in the Mouse Brain Induces a Human-Like Bimodal Pattern of Tumors. *Cancer Res* 2007 -05-01 00:00:00;67(9):4005-4009.
- (70) Park S, Platt J, Lee J, López Giráldez F, Herbst R, Koo J. E2F8 as a Novel Therapeutic Target for Lung Cancer. *J Natl Cancer Inst* 2015;107(9).
- (71) Deng Q, Wang Q, Zong W, Zheng D, Wen Y, Wang K, et al. E2F8 contributes to human hepatocellular carcinoma via regulating cell proliferation. *Cancer Res* 2010;70(2):782-791.
- (72) Yao G, Lee TJ, Mori S, You L, Nevins JR. A bistable Rb-E2F switch underlies the restriction point. *Nature Cell Biology* 2008 Apr;10(4):476-482.
- (73) Kwon JS, Everetts NJ, Wang X, Wang W, Della Croce K, Xing J, et al. Controlling Depth of Cellular Quiescence by an Rb-E2F Network Switch. *Cell Rep* 2017 Sep 26;20(13):3223-3235.
- (74) Clements KE, Thakar T, Nicolae CM, Liang X, Wang H, Moldovan G. Loss of E2F7 confers resistance to poly-ADP-ribose polymerase (PARP) inhibitors in BRCA2-deficient cells. *Nucleic Acids Res* 2018 /09/28;46(17):8898-8907.
- (75) Gentric G, Mailliet V, Paradis V, Couton D, L'Hermitte A, Panasyuk G, et al. Oxidative stress promotes pathologic polyploidization in nonalcoholic fatty liver disease. *The Journal of clinical investigation* 2015;125(3):981-992.

- (76) Donne R, Saroul-Aïnama M, Cordier P, Celton-Morizur S, Desdouets C. Polyploidy in liver development, homeostasis and disease. *Nature Reviews Gastroenterology & Hepatology* 2020 -07;17(7):391-405.
- (77) Zhang S, Zhou K, Luo X, Li L, Tu H, Sehgal A, et al. The polyploid state plays a tumor suppressive role in the liver. *Dev Cell* 2018 -2-26;44(4):447-459.e5.
- (78) Storchova Z, Pellman D. From polyploidy to aneuploidy, genome instability and cancer. *Nat Rev Mol Cell Biol* 2004 /01;5(1):45-54.
- (79) Fujiwara T, Bandi M, Nitta M, Ivanova EV, Bronson RT, Pellman D. Cytokinesis failure generating tetraploids promotes tumorigenesis in p53 -null cells. *Nature* 2005 /10;437(7061):1043-1047.
- (80) Mayhew CN, Bosco EE, Fox SR, Okaya T, Tarapore P, Schwemmer SJ, et al. Liver-Specific pRB Loss Results in Ectopic Cell Cycle Entry and Aberrant Ploidy. *Cancer Res* 2005 -06-01 z00:00:00;65(11):4568-4577.
- (81) Chen H, Ouseph MM, Li J, Pécot T, Chokshi V, Kent L, et al. Canonical and atypical E2Fs regulate the mammalian endocycle. *Nat Cell Biol* 2012 Nov;14(11):1192-1202.
- (82) Pandit S, Westendorp B, Nantasanti S, van Liere E, Tooten PCJ, Cornelissen PWA, et al. E2F8 is essential for polyploidization in mammalian cells. *Nat Cell Biol* 2012;14(11):1181-1191.
- (83) Kotsantis P, Silva LM, Irmscher S, Jones RM, Folkes L, Gromak N, et al. Increased global transcription activity as a mechanism of replication stress in cancer. *Nat Commun* 2016 -10-11;7(1):1-13.
- (84) Carvajal L, Hamard P, Tonnessen C, Manfredi J. E2F7, a novel target, is up-regulated by p53 and mediates DNA damage-dependent transcriptional repression. *Genes Dev* 2012;26(14):1533-1545.
- (85) Bertoli C, Klier S, McGowan C, Wittenberg C, de Bruin, Robertus A M. Chk1 inhibits E2F6 repressor function in response to replication stress to maintain cell-cycle transcription. *Curr Biol* 2013;23(17):1629-1637.
- (86) Bertoli C, Herlihy A, Pennycook B, Kriston Vizi J, de Bruin, Robertus A M. Sustained E2F-Dependent Transcription Is a Key Mechanism to Prevent Replication-Stress-Induced DNA Damage. *Cell Rep* 2016;15(7):1412-1422.
- (87) Yuan R, Vos HR, van Es RM, Chen J, Burgering BM, Westendorp B, et al. Chk1 and 14-3-3 proteins inhibit atypical E2Fs to prevent a permanent cell cycle arrest. *EMBO J* 2018 03 01.;37(5).
- (88) Pennycook BR, Vesela E, Peripolli S, Singh T, Barr AR, Bertoli C, et al. E2F-dependent transcription determines replication capacity and S phase length. *Nature Communications* 2020 -07-14;11(1):1-10.
- (89) Vaidyanathan S, Cato K, Tang L, Pavey S, Haass NK, Gabrielli BG, et al. In vivo overexpression of Emi1 promotes chromosome instability and tumorigenesis. *Oncogene* 2016 10 13.;35(41):5446-5455.
- (90) Lontos M, Koutsami M, Sideridou M, Evangelou K, Kletsas D, Levy B, et al. Deregulated Overexpression of hCdt1 and hCdc6 Promotes Malignant Behavior. *Cancer Res* 2007 -11-15 00:00:00;67(22):10899-10909.
- (91) Moreno E, Toussaint MJM, van Essen S, Bongiovanni L, van Liere E, Koster M, et al. E2F7 is a potent inhibitor of liver tumor growth in adult mice. *Hepatology* 2020.
- (92) Shima N, Alcaraz A, Liachko I, Buske TR, Andrews CA, Munroe RJ, et al. A viable allele of Mcm4 causes chromosome instability and mammary adenocarcinomas in mice. *Nat Genet* 2007 Jan;39(1):93-98.
- (93) Bartek J, Lukas J. Chk1 and Chk2 kinases in checkpoint control and cancer. *Cancer Cell* 2003 -05;3(5):421-429.

- (94) Zhang J, Willers H, Feng Z, Ghosh JC, Kim S, Weaver DT, et al. Chk2 phosphorylation of BRCA1 regulates DNA double-strand break repair. *Mol Cell Biol* 2004 -01;24(2):708-718.
- (95) Panagiotis Zalmas L, Zhao X, Graham AL, Fisher R, Reilly C, Coutts AS, et al. DNA-damage response control of E2F7 and E2F8. *EMBO Rep* 2008 -03;9(3):252-259.
- (96) Carvajal LA, Hamard P, Tonnessen C, Manfredi JJ. E2F7, a novel target, is up-regulated by p53 and mediates DNA damage-dependent transcriptional repression. *Genes Dev* 2012 Jul 15;26(14):1533-1545.
- (97) Guo R, Chen J, Zhu F, Biswas AK, Berton TR, Mitchell DL, et al. E2F1 localizes to sites of UV-induced DNA damage to enhance nucleotide excision repair. *J Biol Chem* 2010 Jun 18;285(25):19308-19315.
- (98) Stevens C, Smith L, La Thangue NB. Chk2 activates E2F-1 in response to DNA damage. *Nat Cell Biol* 2003 May;5(5):401-409.
- (99) Lin W, Lin F, Nevins JR. Selective induction of E2F1 in response to DNA damage, mediated by ATM-dependent phosphorylation. *Genes Dev* 2001 07/15;15(14):1833-1844.
- (100) Shats I, Deng M, Davidovich A, Zhang C, Kwon JS, Manandhar D, et al. Expression level is a key determinant of E2F1-mediated cell fate. *Cell Death Differ* 2017 /04;24(4):626-637.
- (101) Blais A, Dynlacht BD. E2F-associated chromatin modifiers and cell cycle control. *Curr Opin Cell Biol* 2007 -12;19(6):658-662.
- (102) Tarangelo A, Lo N, Teng R, Kim E, Le L, Watson D, et al. Recruitment of Pontin/Reptin by E2f1 amplifies E2f transcriptional response during cancer progression. *Nature Communications* 2015 -12-07;6(1):1-14.
- (103) Chen J, Zhu F, Weeks RL, Biswas AK, Guo R, Li Y, et al. E2F1 promotes the recruitment of DNA repair factors to sites of DNA double-strand breaks. *Cell Cycle* 2011 Apr 15;10(8):1287-1294.
- (104) Zalmas L, Coutts AS, Helleday T, La Thangue NB. E2F-7 couples DNA damage-dependent transcription with the DNA repair process. *Cell Cycle* 2013 Sep 15;12(18):3037-3051.
- (105) Weijts, B. G. M. W., Westendorp B, Hien BT, Martínez-López LM, Zijp M, Thurlings I, et al. Atypical E2Fs inhibit tumor angiogenesis. *Oncogene* 2018 /01;37(2):271-276.
- (106) Ji W, Zhang W, Xiao W. E2F-1 Directly Regulates Thrombospondin 1 Expression. *PLoS One* 2010 -10-15;5(10).
- (107) Weijts, Bart G. M. W., Bakker WJ, Cornelissen PWA, Liang K, Schaftenaar FH, Westendorp B, et al. E2F7 and E2F8 promote angiogenesis through transcriptional activation of VEGFA in cooperation with HIF1. *EMBO J* 2012 Oct 03;31(19):3871-3884.
- (108) Qin G, Kishore R, Dolan CM, Silver M, Wecker A, Luedemann CN, et al. Cell cycle regulator E2F1 modulates angiogenesis via p53-dependent transcriptional control of VEGF. *Proc Natl Acad Sci U S A* 2006 -7-18;103(29):11015-11020.
- (109) Pillai S, Kovacs M, Chellappan S. Regulation of VEGF receptors by Rb and E2F1: Role of acetylation. *Cancer Res* 2010 -6-15;70(12):4931-4940.
- (110) Su J-, Yen C-, Chen P-, Chuang S-, Hong C-, Kuo I-, et al. The role of the VEGF-C/VEGFR-3 axis in cancer progression. *Br J Cancer* 2007 -02-26;96(4):541-545.
- (111) Su J, Yang P, Shih J, Yang C, Wei L, Hsieh C, et al. The VEGF-C/Flt-4 axis promotes invasion and metastasis of cancer cells. *Cancer Cell* 2006 -03;9(3):209-223.
- (112) Wu M, Seto E, Zhang J. E2F1 enhances glycolysis through suppressing Sirt6 transcription in cancer cells. *Oncotarget* 2015 -3-14;6(13):11252-11263.

- (113) Blanchet E, Annicotte J, Lagarrigue S, Aguilar V, Clapé C, Chavey C, et al. E2F transcription factor-1 regulates oxidative metabolism. *Nat Cell Biol* 2011 /09;13(9):1146-1152.
- (114) Fajas L, Landsberg RL, Huss-Garcia Y, Sardet C, Lees JA, Auwerx J. E2Fs Regulate Adipocyte Differentiation. *Developmental Cell* 2002 -07-01;3(1):39-49.
- (115) Shimada Y, Kuninaga S, Ariyoshi M, Zhang B, Shiina Y, Takahashi Y, et al. E2F8 promotes hepatic steatosis through FABP3 expression in diet-induced obesity in zebrafish. *Nutr Metab (Lond)* 2015 -5-20;12.
- (116) Stine ZE, Walton ZE, Altman BJ, Hsieh AL, Dang CV. MYC, Metabolism, and Cancer. *Cancer Discov* 2015 -10-01 00:00:00;5(10):1024-1039.
- (117) Flöter J, Kaymak I, Schulze A. Regulation of Metabolic Activity by p53. *Metabolites* 2017 May 20;7(2).







# Chapter 2

---

## **E2F7 is a potent inhibitor of liver tumor growth in adult mice**

Eva Moreno<sup>1</sup>, Mathilda J.M. Toussaint<sup>1</sup>, Saskia C. van Essen<sup>1</sup>, Laura Bongiovanni<sup>1</sup>, Elsbeth A. van Liere<sup>1</sup>, Mirjam H. Koster<sup>4</sup>, Ruixue Yuan<sup>1,5</sup>, Jan van Deursen<sup>2,3</sup>, Bart Westendorp<sup>1</sup>, Alain de Bruin<sup>†1,4</sup>.

Affiliations:

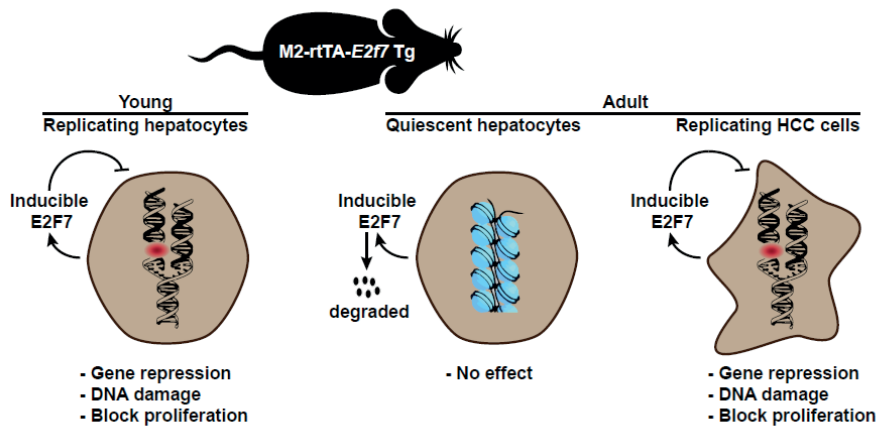
Departments of <sup>1</sup>Biomolecular Health Sciences, Division of Cell Biology, Metabolism and Cancer, Faculty of Veterinary Medicine, Utrecht University, The Netherlands; <sup>2</sup>Biochemistry and Molecular Biology, Mayo Clinic, Rochester, Minnesota; <sup>3</sup>Pediatric and Adolescent Medicine, Mayo Clinic, Rochester, Minnesota; <sup>4</sup>Pediatrics, Division Molecular Genetics, University Medical Center Groningen, University of Groningen, The Netherlands; <sup>5</sup>Pathology, Academic Medical Center, Amsterdam, The Netherlands.

† Corresponding author

*Hepatology*. 2021 Jan;73(1):303-317.

## ABSTRACT

Upregulation of the E2F-dependent transcriptional network has been identified in nearly every human malignancy and is an important driver of tumorigenesis. Two members of the E2F family, E2F7 and E2F8, are potent repressors of E2F-dependent transcription. They are atypical in that they do not bind to dimerization partner (DP) proteins and are not controlled by pRb. The physiological relevance of E2F7 and E2F8 remains incompletely understood, largely because tools to manipulate their activity in vivo have been lacking. Here, we generated transgenic mice with doxycycline-controlled transcriptional activation of *E2f7* and *E2f8* and induce their expression during postnatal development, in adulthood, and in the context of cancer. Systemic induction of *E2f7* and to lesser extent *E2f8* transgenes in juvenile mice impaired cell proliferation, caused replication stress, DNA damage and apoptosis, and inhibited animal growth. In adult mice, however, E2F7 and E2F8 induction was well tolerated, yet profoundly interfered with DNA replication, DNA integrity and cell proliferation in DEN-induced liver tumors. **Conclusion:** Collectively, our findings demonstrate that atypical E2Fs can override cell-cycle entry and progression governed by other E2F-family members, and suggest that this property can be exploited to inhibit proliferation of neoplastic hepatocytes when growth and development have subsided during adulthood.



## INTRODUCTION

The cell cycle consists of a sequence of tightly controlled and ordered events, which together ensure proper genetic inheritance. Central among these events is the oscillatory activity of the E2F transcription program. Individual E2F family members bind to hundreds of target genes, many of which are essential for DNA replication and repair. Hence entry into S-phase depends on activation of this program (1,2). Once S-phase has started, E2F-transcription becomes silenced again. E2F7 and -8 are the repressing family members that redundantly mediate this downswing during late S- and G2-phase (3-7). They are referred to as atypical E2Fs, because they possess unique structural features compared to the other E2Fs. They cannot bind to dimerization partner (DP) proteins, and instead act as homo- or heterodimers (6,8). Furthermore, their activity is not controlled by pRb. This is important, because *RB* is inactivated, mutated, or lost in a wide array of human cancers (9,10). Manipulation of E2F7/8 can uncouple E2F target gene transcription from pRb activity (11). The resulting unrestrained E2F transcription is thought to contribute to cancer progression in a variety of cancer types, including hepatocellular carcinoma (HCC). Accordingly, we observed that conditional deletion of *E2f7* and *E2f8* in mice caused upregulation of many E2F target genes, resulting in spontaneous liver cancer and accelerated skin cancer progression (12,13). These results indicate that atypical E2Fs are capable of controlling proliferation under stress conditions. For example, DNA damage can trigger a p53-dependent upregulation of E2F7 to block cell cycle progression (11,14). These data led us to hypothesize that tipping over the balance between activator and repressor E2Fs in favor of repressors might be a potent strategy to inhibit tumor proliferation. Notwithstanding these tumor-suppressing effects, *in vitro* studies aimed at overexpressing atypical E2Fs have yielded conflicting results. A number of studies indicated that E2F8 overexpression can promote proliferation of lung, breast and liver cancer cell lines (15-17). Other work demonstrated that overexpression of E2F7 and -8 is a potent inhibitor of proliferation in HeLa, MEF and U2OS cells (1,3,5,8,18).

To resolve these issues, we employed an *in vivo* genetic approach to study the consequences of inducible E2F target gene repression on proliferation of normal and cancer cells. We created doxycycline-inducible *E2f7/8*-transgenic mice and demonstrate that transgene induction markedly inhibited tissue proliferation in juvenile mice by perturbing S-phase progression. Adult mice tolerated the transgene induction better than juvenile mice. Moreover, induction of E2F7 and -8 to a lesser extent revealed a consistent reduction of liver tumor growth via repression of gene transcription.

## MATERIAL AND METHODS

### Animal experiments

Animal experiments were approved by the Utrecht University Animal Ethics Committee (approval number: AVD108002016626) and performed according to institutional and national

guidelines. Doxycycline (2g/kg) was administrated ad libitum in pellets to all experimental mice (Bio Services). All lines were generated by prof. dr. Jan van Deursen (Mayo Clinic, USA) according to previously described methodology (19) and maintained on a mixed genetic background 129/Sv x C57Bl/6 x FVB. Additional information and genotyping primers in Supplemental Material and Supporting Table S1.

### **Generation of inducible cell lines and cell culture.**

Inducible cell lines were created by introducing consecutively the pLenti-CMV-TetR and our newly synthesized E2F7/8 containing plasmids into RPE-hTert cells using third generation lentiviral packaging system. In addition to E2F7/8 we used E2F7/8 cDNAs with both DNA binding domains mutated as described previously (20). pLenti CMV TetR Blast (716-1) and pLenti CMV/TO Puro DEST (670-1) were a gift from Eric Campeau & Paul Kaufman (Addgene plasmids #17492; <http://n2t.net/addgene:17492>; RRID:Addgene\_17492; and #17293; <http://n2t.net/addgene:17293>; RRID:Addgene\_17293). The HeLa/TO E2F8<sup>DBDmut.</sup> cells were available in our lab from previous studies (1). Additional information in Supplemental Material.

HeLa and Retinal Pigment Epithelium (RPE) cells were maintained in Dulbecco's Modified Eagle Medium (DMEM) supplemented with 10% Tet System Approved Fetal Bovine Serum (Clontech, CL631106) and 1% Penicillin-Streptomycin (Pen-Strep) at 37°C, 5% CO<sub>2</sub>. Overexpression was induced by adding 0.2µg/mL doxycycline (Sigma Aldrich) to the cell culture medium. For the proliferation assay, HeLa/TO E2F7 cells were seeded at a density of 1x10<sup>5</sup> cells in 60cm petri dish. Doxycycline was refreshed every two days. Cells were harvested in duplo daily and counted using a BioRad TC20™ Automated Cell Counter.

### **Flow cytometry and FACS sorting**

For determination of DNA content, cells were trypsinized, washed with PBS 2x, fixed with 70% ethanol and stored at 4°C. Nuclei suspensions from frozen liver tissue were obtained as previously described (21). Details can be found in Supplemental Material.

FACS sorting based on EGFP fluorescence was performed on a BD-Influx. Cells were collected in cell culture medium and immediately plated at a density of 5x10<sup>3</sup> cells per well for the colony formation assay.

### **RNA isolation, cDNA and qPCR**

RNA isolation, cDNA synthesis and quantitative PCR were performed based on manufacturer's instructions for QIAGEN (RNeasy Kits), Thermo Fisher Scientific (cDNA synthesis Kits) and Bio-Rad (SYBR Green Master Mix), respectively. Reactions were performed in duplicate and relative amount of cDNA was normalized to GAPDH using the  $\Delta\Delta C_t$  method. Quantitative real-time PCR primer sequences are provided in Supporting Table S2.

## Immunoblotting

Protein lysates were obtained with RIPA buffer (50mM Tris-HCl Ph 7.5, 1mM EDTA, 150mM NaCl, 0.25% deoxycholic acid, 1% Nonidet- P40), 1mM NaF and  $\text{NaV}_3\text{O}_4$  and protease inhibitor cocktail (11873580001, Sigma Aldrich). After centrifugation at full speed (12g) for 10 min, supernatants were collected and proceed to a standard SDS-PAGE Immunoblot. Immunoblot antibodies are shown in Supporting Table S3.

## Immunohistochemistry and histopathology analysis

Tissues were embedded in paraffin and sectioned at 4 $\mu\text{m}$ . Details on antibodies, procedures and explanation of quantifications are outlined in Supplemental Material and Supporting Table S3. Liver tumors were classified as previously described (22,23).

## Fiber analysis

Cells were pulse-labelled with 25 $\mu\text{M}$  CldU followed by 250 $\mu\text{M}$  IdU for 20 min each. Rest of the protocol was performed as previously described (24). Pictures were taken with a Leica SPE-II-DMI4000 confocal microscope using a 63x objective and the LAS-AF, HCS basic module software. Track lengths and quantification of number of origins fired were manually analyzed with ImageJ software. Replication track lengths were calculated using the conversion factor 1 $\mu\text{m}$ = 2.59 kb (25).

## Colony formation assays

HeLa cells were seeded after FACS sorting in duplo at low density ( $5 \times 10^3$  per well in 6-well plates ) from three different cell clones. Cells were incubated with or without doxycycline for 10 days. For fixation, medium was removed, cells were washed twice with PBS and fixed with acetic acid/methanol 1:7 (vol/vol) for 5 min. Then, colonies were stained with 0,5% Crystal violet for 2 hours. Pictures represent entire wells (34,8mm diameter), taken with a Nikon camera. For quantification in Figure 2F and Supporting Figure S2H, pictures were loaded in Photoshop CS6. For each condition 10 fields (300x300 pixels) were randomly selected. Positive colony staining was measured with Magic Wand Tool, with tolerance value set to 16. Relative intensity was defined as the ratio of positive purple-staining area (pixels) over total area of the field.

## Statistics

The number of independent experiments, the number of mice and the type of statistical analysis for each figure are indicated in the legends. All statistical analyses were performed using SigmaPlot 13.0 software. Every cell culture experiment was repeated at least 2 times

and with conditions in duplo. Specific statistical tests for each dataset are mentioned in the figure legends. Asterisks indicate where significant differences were seen. Where relevant for understanding the figure and individual comparisons, we indicate with “n.s.” that significance was not reached.

## RESULTS

### E2F7/8 overexpression inhibits proliferation in vivo

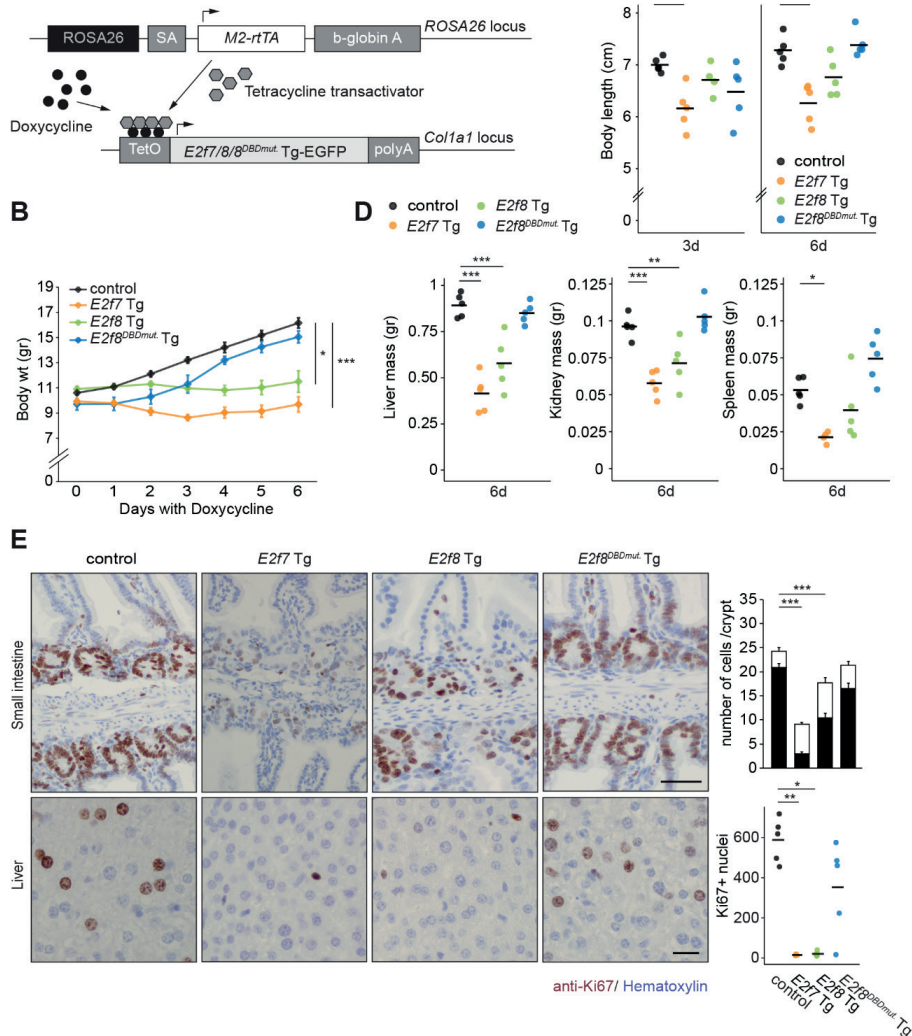
To study the physiological consequences of atypical E2F repressor activation, we generated transgenic mice with doxycycline (Dox)-inducible overexpression (OE) of E2F7 or E2F8. Gene constructs encoding EGFP-tagged E2F7 or E2F8 (hereafter *E2f7*Tg and *E2f8*Tg) under the control of a tetracycline-responsive element were inserted in the *Col1a1* locus. The M2 reverse tetracycline transactivator (M2-rtTA) is expressed from the *Rosa26* locus, allowing doxycycline-inducible expression of the transgene (Figure 1A). A third transgenic mouse carrying a mutated version of *E2f8* containing mutations in both DNA-binding domains (*E2f8*<sup>DBDmut</sup>.Tg) was created to validate that the effects of E2F8 overexpression were caused by transcriptional repression. Mice on dox chow but only expressing M2-rtTA served as negative controls.

Because expression of E2F target genes strongly correlates with proliferation rates, we anticipated the strongest impact of E2F7/8 overexpression in rapidly proliferating tissues. Therefore, we first induced the transgenes in juvenile mice immediately after weaning, when the proliferation rates are high in multiple tissues. To this end, we fed 21-days old juvenile mice with doxycycline for 3 or 6 days.

Doxycycline caused a strong induction of *E2f7*Tg and *E2f8*Tg transcripts and proteins in the respective transgenic mice (Supporting Figure S1A-C), and repressed key E2F target transcripts such as *Cdc6*, *Cdt1* and *Rad51* (Supporting Figure S1D). Immunohistochemistry on liver tissues revealed that transgenic E2F7 and E2F8 were nuclear proteins (Supporting Figure S1E). After 6 days of transgene induction, *E2f7*Tg and *E2f8*Tg mice showed a clear growth reduction, measured by body weight and length, compared to control littermates and *E2f8*<sup>DBDmut</sup>.Tg mice (Figures 1B-C). Furthermore, weights of multiple organs – including liver, kidney, spleen and thymus – were markedly reduced in the *E2f7* and, to a lesser extent, in *E2f8*Tg mice (Figure 1D, Supporting Figure S1F-G).

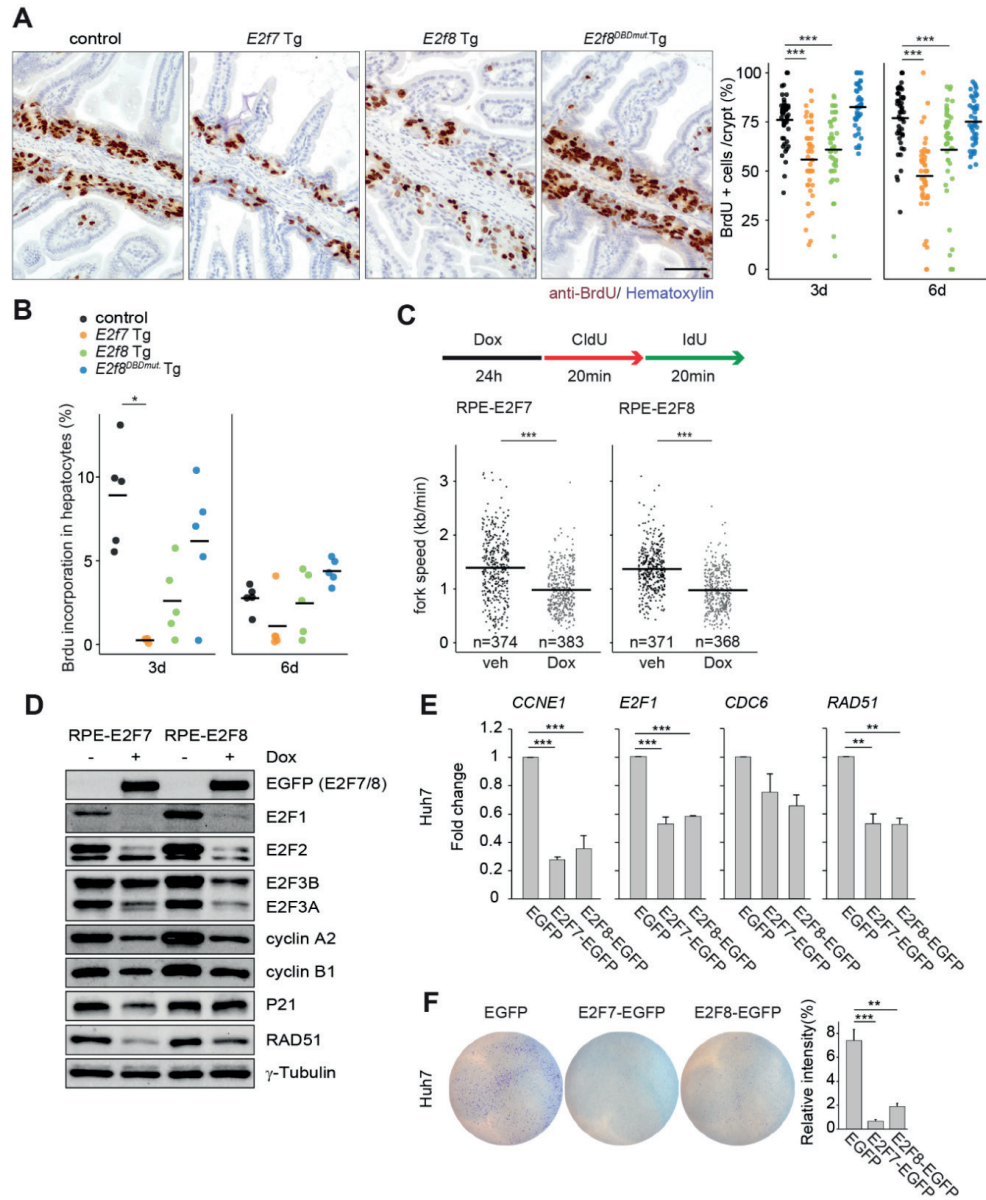
Immunohistochemistry analysis of Ki67 confirmed a marked reduction of cycling cells in small intestinal crypts of *E2f7* and *E2f8*Tg mice, thus reducing the number of cells per crypt in each transgenic model (Figure 1E and Supporting Figure S1H). These phenotypes were more profound in *E2f7*Tg mice than their *E2f8*Tg counterparts. The development of *E2f8*<sup>DBDmut</sup>.Tg mice did not deviate from normal development of controls.

Collectively, the data demonstrate that E2F7 or E2F8 overexpression is sufficient to repress cell proliferation during postnatal development through a mechanism that involves DNA binding.



**▲Figure 1. Inducible transgenic E2F7 and E2F8 expression blocks proliferation in juvenile mice.** (A) Schematic representation of the transgenic model. SA-polyA, splice acceptor-polyA; PGKp, phosphoglycerate kinase promoter; ATG, start codon; Hyg, hygromycin resistance cassette. (B) Growth curves of the transgenic mice. Error bars represents SEM ( $n=10$ , day 0-3;  $n=5$ , day 4-6 of doxycycline treatment). (C) Body lengths of juvenile mice after 3 and 6 days of transgene induction with doxycycline. Bars represent average ( $n=5$  mice) (D) Liver, kidney and spleen mass of transgenic mice after 6 days with doxycycline. Organs were weighed post-fixation with 4% paraformaldehyde. Crossbars represent averages per genotype ( $n=5$  mice). *E2f7* Tg spleen  $n=4$ . (E) Representative pictures of Ki67 showing proliferating cells in small intestines (top) and livers (bottom) of transgenic mice after 3 days of doxycycline treatment. Scale bars: 50µm (top) and 20µm (bottom). Small intestine quantification: total count and Ki67-positive nuclei per crypt of small intestines. Error bars represent SEM ( $n=45$  crypts/genotype;  $n=3$  mice/ genotype). Liver: Total Ki67-positive nuclei in ten fields (40x objective). Crossbars represent averages per genotype ( $n=5$  mice). Data information: In (B, C, D and E), \* $p<0.05$ , \*\* $p<0.01$ , \*\*\* $p<0.001$  (Kruskal Wallis One Way Analysis of Variance on Ranks and Dunnett's Method for Multiple Comparisons vs. control).







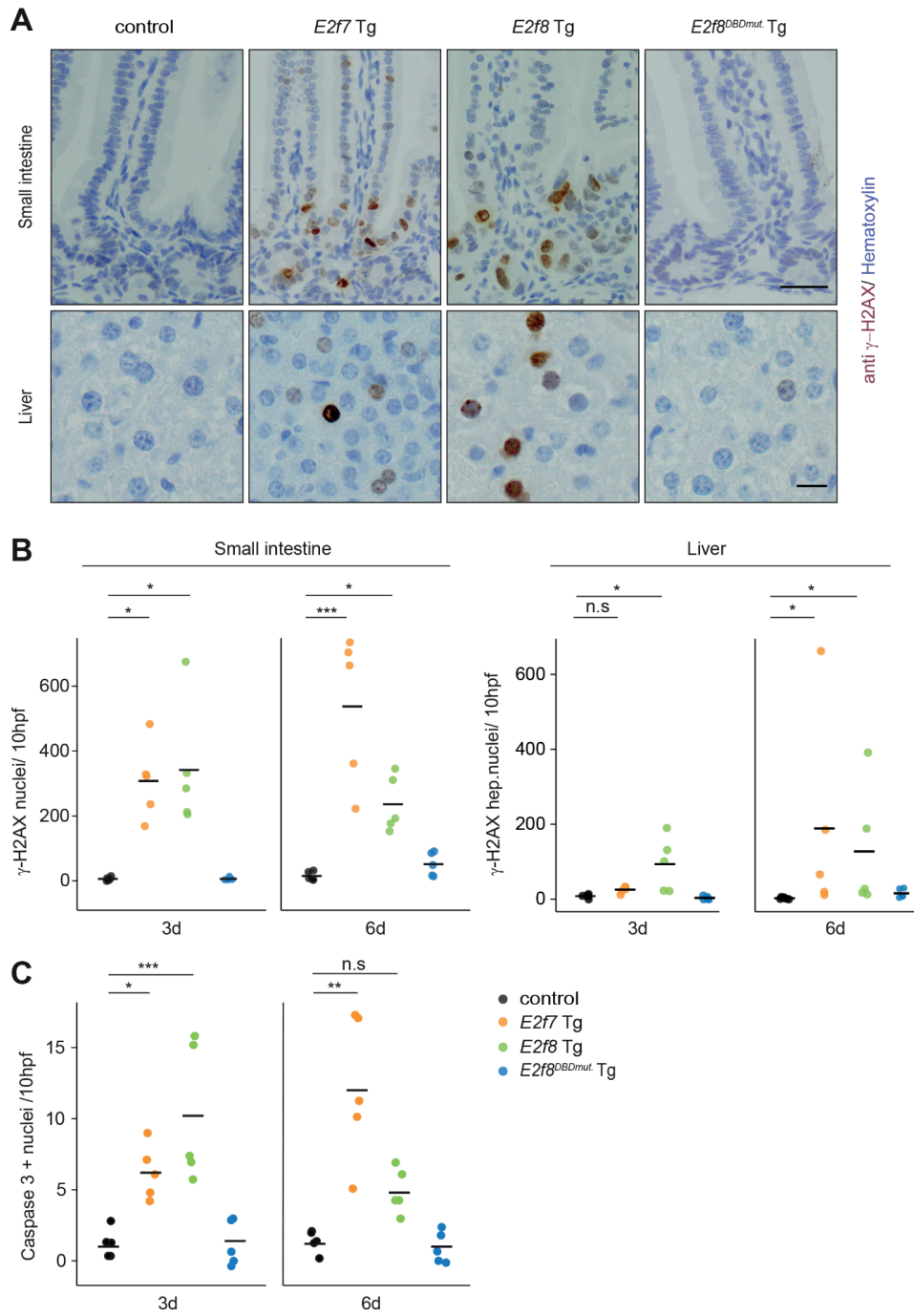
## E2F7/8 overabundance inhibits DNA replication in vivo

Next, we examined whether the observed growth inhibitions were due to perturbations in DNA replication. To this end, mice treated with dox for 3 days were injected with the thymidine analogue 5-bromo-2'-deoxyuridine (BrdU), 2 hours prior to euthanasia. Indeed, the incorporation of BrdU was reduced in both small intestinal crypts and hepatocytes of juvenile *E2f7* and *E2f8* Tg mice (Figure 2A-B and Supporting Figure S2A). Reductions were most profound in *E2f7* Tg mice, and not observed in *E2f8<sup>DBDmut</sup>* Tg. In complementary experiments, we evaluated S-phase progression upon E2F7 and -8 overexpression on human retinal pigment epithelium (RPE) cells with doxycycline-inducible expression of EGFP-tagged E2F7 and E2F8 (Supporting Figure S2B-C). DNA replication fork progression was visualized and quantified performing the DNA fiber analysis (26). We found that the speed of replication fork progression and the percentage of new origins that fired were significantly reduced by transgene induction (Figure 2C and Supporting Figure S2D-E), confirming that overexpression of our E2F7 and E2F8 fusion proteins leads to replication stress. As expected, RPE cell lines expressing the DNA-binding mutant versions of our E2F7 and -8 transgenes showed no signs of replication stress (Supporting Figure S4A-C).

In addition, expression of activator E2Fs, cyclin A2, and cyclin B1 were decreased in RPE cells upon induction of E2F7 and -8 (Figure 2D). The DNA repair protein RAD51 and CDK inhibitor P21, which are both known E2F7/8 target genes, were also strongly repressed in E2F7/8 expressing cells (Figure 2D). Surprisingly, p21 levels were profoundly induced in HeLa cells after E2F7 induction, which could potentially explained by defect checkpoint functions. Importantly, the inhibitory effect of E2F7 on proliferation was consistently observed

◀**Figure 2. E2F7 and E2F8 expression inhibits ongoing DNA replication.** (A) Immunohistochemistry using anti-BrdU to label S-phase cells in small intestines of transgenic mice treated for 6d with doxycycline. Scale bar: 50µm. Dot plot shows quantification of BrdU-positive area in 5 fields using the 20x objective. Crossbars represent averages per genotype ( $n=45$  crypts/ genotype;  $n=3$  mice/ genotype). (B) Dot plot shows the percentage of BrdU- positive hepatocyte nuclei per condition. Crossbars represent average values per condition ( $n=5$  mice). *E2f7*Tg after 3d Dox ( $n=4$ ). (C) Experimental work flow and quantification of replication fork speed in the cell lines and conditions indicated. Data from two separate experiments are pooled. Only ongoing replication forks (red+green) were included in the quantification. Crossbars represent average values per condition. (D) Protein expression of cell cycle regulators in the indicated RPE inducible cell lines after 24 hours of doxycycline treatment. (E) Transcript levels of *CDC6*, *E2F1* and *RAD51* in Huh7 cells. EGFP positive cells were sorted 24h after transfections and directly collected for RNA analysis. Fold changes were adjusted to average of EGFP controls and *GAPDH* and *RSP18* were used to normalize the expression. Data represent average  $\pm$  SEM of at least 2 different experiments. (F) Clonogenic survival assay of EGFP FACS-sorted Huh7 cells. Cells were transfected with indicated plasmids for 24h before FACS-sorting and re-plated for 72 hours. Histogram shows the quantification of relative intensity (%) from each condition. Data represents average  $\pm$  SEM (2 independent experiments were performed in at least duplo).

Data information: In (A, B, E and F), \* $p<0.05$ , \*\* $p<0.01$ , \*\*\* $p<0.001$  (Kruskal Wallis One Way Analysis of Variance on Ranks and Dunnett's Method for Multiple Comparisons vs. control). In (C) \*\*\* $p<0.001$  (Mann-Whitney Rank Sum Test).



independent from the genetic background (HeLa versus RPE) and p53/Rb status (Figure 2D, Supporting Figure S2F and S3A–D). In addition, we observed repression of DNA replication and DNA repair transcripts as well as inhibitory proliferative effect on EGFP-sorted HCC-derived cell lines with null and mutated p53, Hep3B and Huh7 respectively, upon transfection with E2F7- and E2F8-EGFP plasmids (Figure 2E–F and Supporting Figure S2G–H).

Together, these data show that overabundance of E2F7 and -8 causes DNA replication stress via transcriptional repression of multiple essential cell cycle genes.

### E2F7/8 overexpression causes DNA damage and apoptosis

Since E2F7 and -8 repress multiple DNA repair genes, their overexpression would not only predispose cells to replication stress-induced double strand breaks, but also inhibit the repair of such lesions (1,27,28). Indeed, *E2f7* and *E2f8* Tg mice showed a marked increase of  $\gamma$ -H2AX positive nuclei in intestines and livers after 3 and 6 days with doxycycline, indicating severe DNA damage in these tissues (Figure 3A–B). On the other hand, *E2f8<sup>DBDmut.</sup>* Tg mice were unaffected. In addition, we observed increased rates of apoptosis in small intestinal crypts of *E2f7* and *E2f8* Tg mice, suggesting that the DNA damage was severe enough to be fatal (Figure 3C and Supporting Figure S5A). As a second tissue, we analyzed liver, but overall apoptosis rates were extremely low, precluding reliable assessment of differences between genotypes (Supporting Figure S5B). Induction of E2F7 or E2F8 expression also caused severe DNA damage in RPE cells (Figure 2E and Supporting Figure S5C–D). Collectively, these data indicate that E2F7 and E2F8 overexpression creates replication stress-induced DNA damage.

### E2F7/8 transgene induction in liver tumors causes replication stress and inhibits neoplastic growth

To study the *in vivo* consequences of elevated E2F7/8 levels in cancer cells, we utilized our transgenic mice to induce E2F7 and E2F8 expression in a liver cancer model. To this end, control, *E2f7* Tg, *E2f8* Tg and *E2f8<sup>DBDmut.</sup>* Tg male mice were injected once with the liver-specific carcinogen DEN at postnatal day 14 (Figure 4A). After 9 months, we confirmed that 20 randomly chosen mice all had macroscopic tumors, although there was substantial variation in tumor burden between mice (Supporting Figure S6A–B). Interestingly, 1 month of transgene

**◀Figure 3. Replication stress induced by transgenic E2F7/8 expression leads to DNA damage and apoptosis.** (A) Representative pictures of  $\gamma$ -H2AX immunohistochemistry of small intestines (top) and livers (bottom) of transgenic mice after 6 days of doxycycline treatment. Scale bars: 50 $\mu$ m (top) and 20 $\mu$ m (bottom). (B) Quantification of total  $\gamma$ -H2AX positive nuclei in ten fields using 40x objective (hpf) of small intestine and liver sections after 3 and 6 days of doxycycline treatment. Crossbars represent average ( $n=5$  mice). (C) Quantification of total cleaved Caspase 3-positive nuclei in ten fields using 40x objective (hpf) of small intestine sections after 3 and 6 days of doxycycline treatment. Crossbars represent average ( $n=5$  mice). Data information: In (B and C), \* $p<0.05$ , \*\* $p<0.01$ , \*\*\* $p<0.001$  (Kruskal Wallis One Way Analysis of Variance on Ranks and Dunnett's Method for Multiple Comparisons vs. control).

induction neither affected body weights, nor did it cause obvious structural or functional abnormalities in proliferative tissues such as small intestine (Supporting Figure S6C-D). These findings suggest that mice tolerate E2F7 and E2F8 overexpression much better in adulthood than during postnatal development.

Analysis of gross liver weights and number of macroscopically visible tumors suggested that E2F7 overexpression reduced DEN-induced tumor burden, although differences did not reach statistical significance due to the large variation among animals (Figure 4B and Supporting Figure S6E). *E2f8* Tg mice showed a similar, but weaker trend, whereas the mean tumor burden in *E2f8*<sup>DBDmut.</sup> Tg mice was nearly identical to the control mice. For more in-depth analysis, we performed detailed histological analysis on seven independent liver sections of each mouse in the study. This analysis revealed a highly significant decrease in the numbers of histologically detectable tumors in *E2f7* and *E2f8* Tg livers, as well as a reduction in the ratio between tumor and normal liver tissue (Figures 4C-D, Supporting Figure S6F). Importantly, tumor nodules of *E2f7* and *E2f8* Tg mice showed reduced BrdU incorporation compared to controls, indicative of reduced DNA replication (Figure 4C and E), which was accompanied by an increase in DNA damage, as measured with  $\gamma$ -H2AX staining (Figure 4C and F).

Histological analysis revealed that the majority of the nodules in all genotypes are premalignant lesions, characterized as focal cellular alteration (FCA). HCCs were diagnosed in very low percentage in all genotypes (Supporting Figure S7A). Notably, BrdU incorporation was reduced in tumor nodules of *E2f7* and *E2f8* Tg mice independent of their grade of malignancy (Supporting Figure S7B). This data are consistent with a model in which *E2f7* and *E2f8* overexpression inhibit tumorigenesis by blocking cell proliferation in DEN-induced liver cancers. Additionally, in the absence of DEN treatment, adult *E2f7* and *E2f8* Tg mice that were long-term treated with doxycycline developed spontaneous liver tumor with decreased incidence compared to control animals (Supporting Figure S7C).

Taken together, these data suggest that E2F7 and E2F8 can inhibit tumor growth, by interfering with DNA replication, irrespective of the grade of malignancy. Importantly, adult mice were able to tolerate the induction of the transgenes with little effect on their quality of life.

## **Heterogeneity in transgene expression underlies variation in liver tumor inhibition by E2F7.**

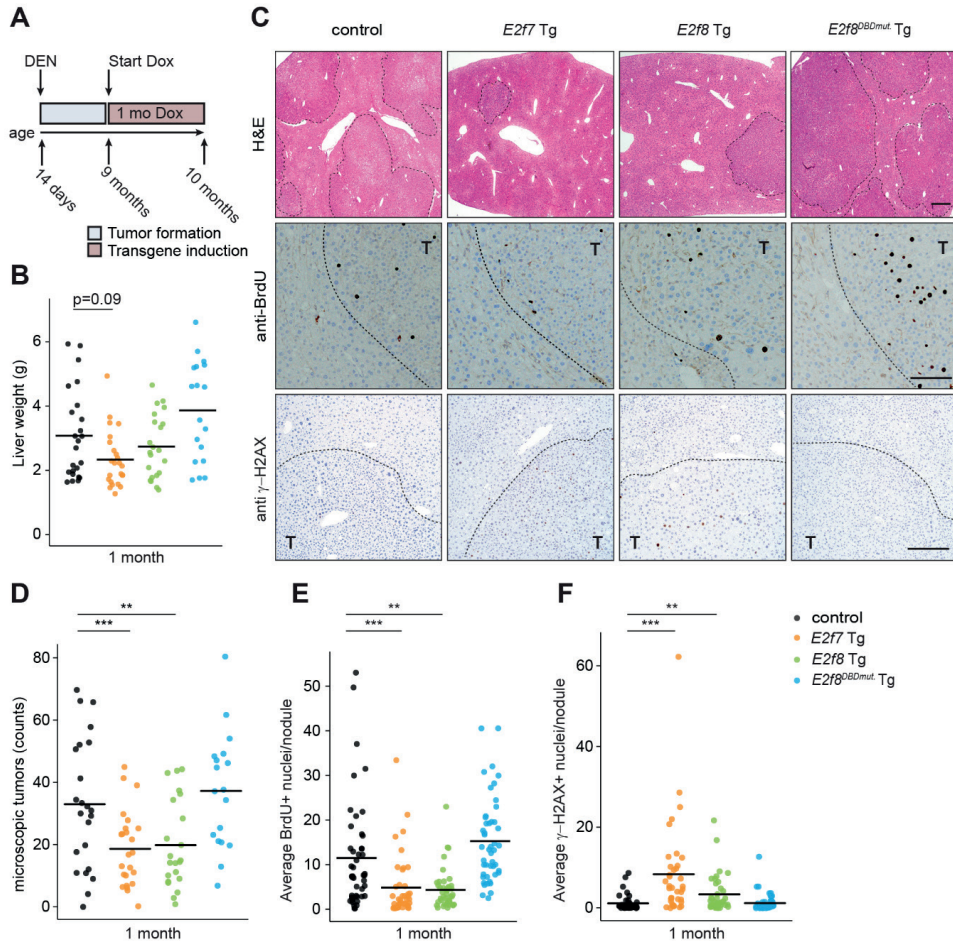
To determine whether the heterogeneity in tumor burden among E2F7 and E2F8 transgenic mice might be due to differences in transgene expression, we immunolabeled tumor level sections of DEN-treated mice for the EGFP tags of the transgenic proteins. Surprisingly, we observed completely negative tumor nodules side-by-side with strongly positive nodules in *E2f7* and, to a lesser extent, *E2f8* Tg liver tumors (Figure 5A, Supporting Figure S8A). Analysis of EGFP-positive versus negative tumor nodules did not show differences in vascularization.

Thus, variation in accessibility to doxycycline are unlikely to explain the variation in transgene expression (Supporting Figure S8B). The vast majority of the tumors from *E2f8<sup>DBDmut</sup>* Tg mice presented high numbers of EGFP-positive cells (Supporting Figure S8A), indicating that E2F7 and E2F8 transgene expression was selected against in a subset of tumors. Thus, E2F7/8 transgene induction may be such a potent mechanism of inhibiting tumorigenesis, that transgene silencing seems to be an important requirement for tumor growth (Figure 5B).

To further investigate this phenomenon, we kept an additional cohort of DEN-treated mice on prolonged transgene induction of 3 months with doxycycline (Supporting Figure S9A). Interestingly, average liver weights of control, *E2f7* and *E2f8* Tg mice were similar and all higher after 3 months than at after 1 month of transgene induction (Supporting Figure S9B). Moreover, quantification of EGFP-stained tissue sections revealed a marked increase in the percentages of completely EGFP-negative nodules over time in *E2f7* and *E2f8* Tg mice (Figure 5C). In contrast, *E2f8<sup>DBDmut</sup>* Tg mice presented very low percentages of EGFP-negative nodules. We also saw that the average number of EGFP-positive cells per nodule clearly decreased in the period from 1 month to 3 months with doxycycline in the *E2f7* and *E2f8* Tg mice (Figure 5D). Importantly, genotyping of 3 months treated tumor samples showed presence of the transgene locus, indicating that loss of transgene locus is an unlikely scenario (Supporting Figure S9C). However, despite comparable mRNA expression of the Tet activator (rTA) in juvenile livers and liver tumors after 3 months of doxycycline, we observed a strong reduction of EGFP mRNA in the tumor samples (Supporting Figure S9D). This indicates that transgene expression in tumor cells might be epigenetically silenced, which is a known phenomenon for tetracycline-inducible CMV promoters (29–33).

To further support this concept of E2F7/8-mediated selection pressure, we then set out to mimic it *in vitro*. To test this, we cultured HeLa cell lines with stable doxycycline-inducible expression of EGFP tagged-E2F7. We previously demonstrated strong inhibition of proliferation, and induction of apoptosis for up to 4 days (1,18), but now we induced E2F7 overexpression for up to 20 days. Quantitative PCR and flow cytometry analysis revealed a near-complete loss of E2F7-EGFP expressing cells within 12 days (Figure 6A and Supporting Figure S10A). Genotyping PCRs on these HeLa/Tet On cell lines demonstrated that the E2F7-EGFP locus was still clearly detectable after 20 days of doxycycline. This data again suggest epigenetic silencing of the inducible E2F7-EGFP (Supporting Figure S10B). Accordingly, E2F7-EGFP cell lines cultured for 20 days in doxycycline proliferated at a similar rate as non-induced cells, whereas acute induction caused a near-complete inhibition of proliferation (Figure 6B). Importantly, a control cell line carrying doxycycline-inducible EGFP had very stable expression levels over the course of 20 days, suggesting again that the loss of expression in E2F7-EGFP cell lines is due to the selection pressure caused by the antiproliferative effect of E2F7 (Figure 6A and Supporting Figure S10A). We then FACS-sorted inducible HeLa E2F7-EGFP based on expression levels shortly after doxycycline induction (16 hours), and we analyzed the colony-forming capacity of these cells. This assay revealed that HeLa cells with high expression of E2F7





**▲Figure 4. Proliferation of DEN-induced liver tumors is inhibited by induction of transgenic E2F7 expression.** (A) Schematic overview of the tumor experiment. (B) Gross liver weights after 1 month of doxycycline treatment. Black crossbars indicate the average per genotype. (control  $n=24$ ;  $E2f7$  Tg  $n=24$ ;  $E2f8$  Tg  $n=22$ ;  $E2f8^{DBDmut.}$  Tg  $n= 18$  mice). (C) Representative pictures of H&E- (top) BrdU- (middle) and  $\gamma$ -H2AX- stained (bottom) liver sections after 1 month of doxycycline treatment. Liver tumors (T) are outlined with dashed lines. Scale bars: 500 $\mu$ m (top), 100 $\mu$ m (middle) and 50 $\mu$ m (bottom). (D) Dot plot showing the numbers of microscopic liver tumors detected in H&E-stained sections per mouse after 1 month of doxycycline. Crossbars represent average per genotype (control  $n=23$ ;  $E2f7$  Tg  $n=24$ ;  $E2f8$  Tg  $n=22$ ;  $E2f8^{DBDmut.}$  Tg  $n= 18$  mice). (E) Quantification of BrdU IHC- stained liver sections from C. Each dot represents the average of BrdU positive hepatocytes, counted in five fields (40x objective), per nodule. At least 3 random tumor nodules were analyzed per mouse,  $n= 10$  mice/genotype). (control  $n=46$ ;  $E2f7$  Tg  $n=40$ ;  $E2f8$  Tg  $n=42$ ;  $E2f8^{DBDmut.}$  Tg  $n= 47$  nodules). (F) Average number of  $\gamma$ -H2AX positive hepatocyte nuclei per field (five fields, 40x objective) per tumor nodule. At least 3 random tumor nodules were analyzed per animal,  $n= 10$  mice/ genotype. Crossbars represent average values per genotype. (control  $n=41$ ;  $E2f7$  Tg  $n=38$ ;  $E2f8$  Tg  $n=38$ ;  $E2f8^{DBDmut.}$  Tg  $n= 50$  nodules).

Data information: In (B, D, E and F), \* $p<0.05$ , \*\* $p<0.01$ , \*\*\* $p<0.001$  (Kruskal Wallis One Way Analysis of Variance on Ranks and Dunnett's Method for Multiple Comparisons vs. control).

cannot survive long-term, compared to negative or very low expressers and vehicle condition (Figure 6C-D). Even when we removed the doxycycline after sorting and replating, high E2F7 expressing cells did not proliferate indicating that they are irreversibly damaged after only 16 hours of E2F7 induction (Supporting Figure S10C). The colony-forming capacity of cells expressing E2F7<sup>DBDmut.</sup> was not affected, confirming that transcriptional repression is the mechanism of DNA damage induction (Supporting Figure S10D).

Collectively, our data reveal that transgenic expression of E2F7 has a strong dose-dependent antiproliferative effect on cancer cells *in vivo*. This creates a strong growth advantage for cancer cells losing transgene expression.

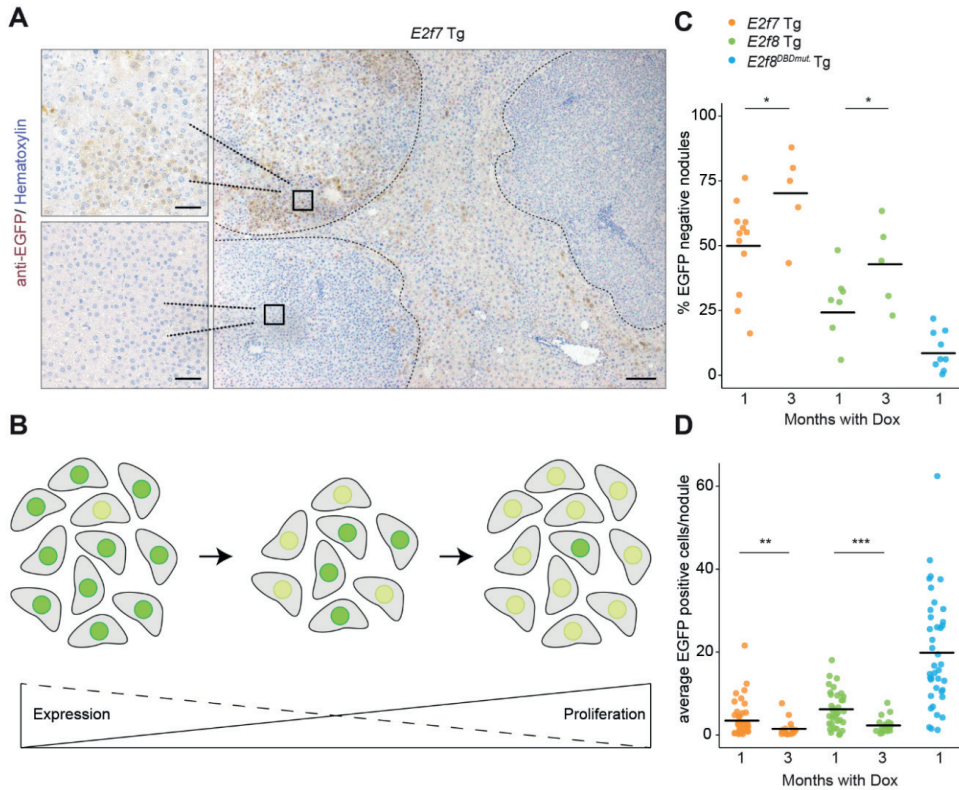
### **Deregulation of E2F-dependent transcription is associated with disease progression and poor survival.**

To determine the relevance of our findings to human HCC, we compared HCC patients (TCGA-LIHC) with high versus low expression of E2F7 and -8 target genes (Supporting Figure S11A). We observed that deregulated expression of these target genes was strongly associated with poor survival. Interestingly, when we divided patients according to tumor stage (AJCC stage I-III) we observed only a strong correlation in the advanced stages of HCC (II and III, Supporting Figure S11B). Collectively, these results further support the notion that E2F-dependent transcription contributes cell proliferation and disease progression resulting in poor clinical outcome in HCC cancer patients.

## **DISCUSSION**

Upregulation of E2F-dependent transcription due to alterations in the CDK/RB/E2F pathways is an important characteristic of hepatocellular carcinomas. Our *in vitro* and *in vivo* studies demonstrates that boosting atypical E2F repressor activity can efficiently block deregulated E2F-dependent transcription leading to reduced proliferation of neoplastic hepatocytes. Mechanistically, we show that overexpressing of E2F7 or E2F8 represses transcription of E2F target genes involved in DNA replication and DNA repair resulting in DNA replication stress and DNA damage. Importantly we show that ubiquitous induction of atypical E2F activity inhibits liver tumor growth without a major impact on the health status of adult mice. These findings could open a novel therapeutic avenue for HCC patients through increasing the transcriptional repressor activity of atypical E2Fs.

The transgenic mouse model presented here provides a powerful tool to inactivate E2F-dependent transcription at any desired time and allowed us to evaluate this effect during mouse development and liver cancer progression. The notion that E2F7 overexpression virtually blocks postnatal development is consistent with previous work showing that combined loss of the activators *E2f1* and *E2f3a* results in growth retardation, dysplasia of multiple tissues, and



**▲Figure 5. Antiproliferative effects of E2F7/8 overexpression cause the appearance of liver tumor nodules lacking transgene expression.** (A) Representative anti-EGFP immunohistochemistry pictures showing E2F7-EGFP Tg expression in livers treated for one month with doxycycline. Scale bars: 200 $\mu$ m (main), 50 $\mu$ m (side pictures). Dashed lines delineate tumor nodules. (B) Proposed model of the observed and described variation in expression and proliferative capacity of cells overexpressing E2F7 both in cell culture system and in mice. Dark green and yellow nuclei represent high and low E2F7-EGFP expression levels, respectively. (C) Percentage of IHC-stained EGFP-negative nodules relative to the total number of microscopic tumors in the indicated genotype. Bars represents average per genotype. \* $p < 0.05$  (t-test). (D) Dot plot represents the count of EGFP-positive hepatocyte nuclei in five fields (40x objective) per nodule. At least 3 random tumor nodules were analyzed per animal,  $n =$  at least 10 mice/genotype). \*\* $p < 0.01$ , \*\*\* $p < 0.001$  (Mann-Whitney Rank Sum Test)

multi-organ failure (34). However, loss of activator E2Fs can either cause impaired S-phase entry or S-phase progression. Thus, in that model it is difficult to distinguish the relative importance of these two functions. In addition, E2F1-3 can switch from activators to repressors, depending on tissue context and Rb status (35). The advantage of inducible E2F7/8 induction is that its effect is largely confined to S/G2-phase progression: we previously demonstrated that both endogenous and exogenous E2F7 and -8 are highly efficiently degraded via APC/C<sup>Cdh1</sup> during G1 (18). This means that the transgenic E2F7/8 only accumulates once S-phase



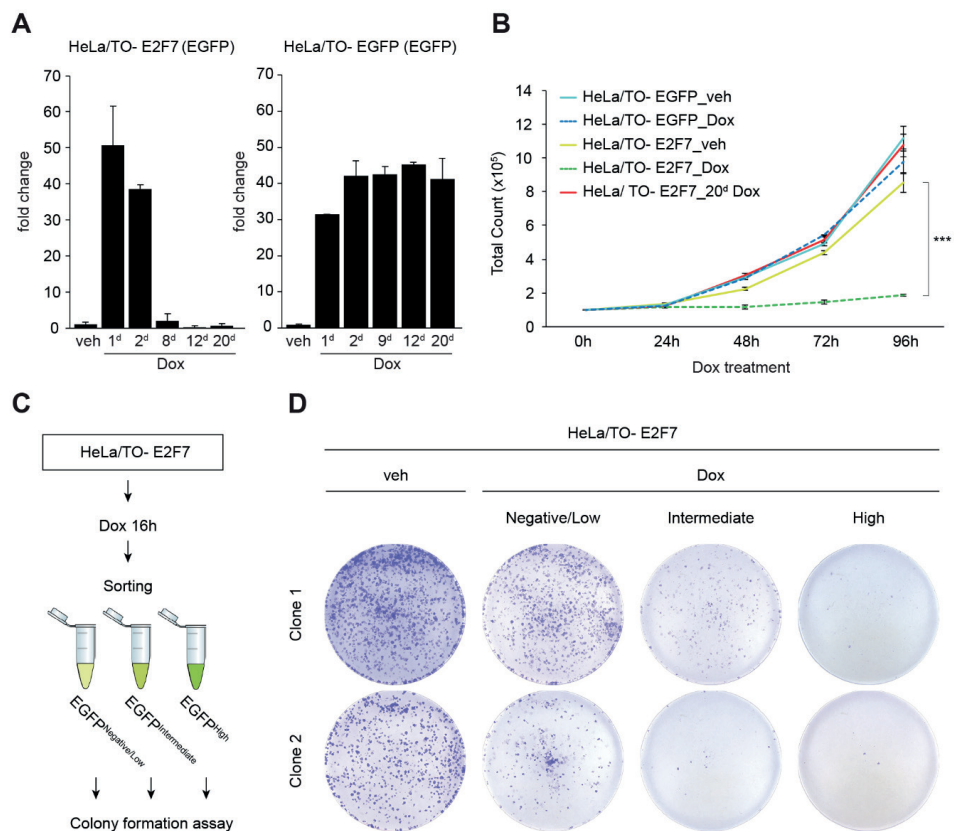
has already begun. Therefore, the cell cycle defects in multiple organs in the juvenile E2F7/8 transgenic mice described here now unequivocally show that unscheduled inactivation of E2F-transcription during S-phase strongly impairs cell cycle progression.

Inhibition of cell cycle progression by the E2F7 and -8 transgenes in normal cells as well as cancer cells clearly supports their role as tumor suppressors. Nevertheless, E2F7 and in particular E2F8 have also been suggested to have oncogenic effects. This idea is based on the notion that E2F7 and E2F8 are highly expressed in cancer, and that their transcript levels positively correlate with poor prognosis (15-17). However, E2F7 and -8 are E2F target genes themselves, whose expression levels peak during S-phase. Therefore, high *E2F7/8* mRNA levels simply correlate with a high percentage of cycling cells, and hence poor prognosis. To understand the biological actions of atypical E2Fs on tumor growth, it should be taken into account that they are tightly regulated by multiple post-translational mechanisms, including APC/*C<sup>dh1</sup>* and CHK1, indicating that mRNA levels do not necessarily reflect high activity of atypical E2Fs (18,28). A second notion is that some *in vitro* studies using cancer cell lines suggested that overexpression of E2F8 promoted tumor cell proliferation (15-17,36,37). However, we now demonstrate that E2F7/8 overexpression invokes a strong selection pressure on cells. Thus generation of stable E2F7/8-overexpressing cell lines could be problematic, because it would favor the selection of severely adapted cell lines. Nevertheless, we cannot exclude that cell-type context or concomitant mutations in cancer-related genes uncover oncogenic functions of E2F7 or -8.

Our study shows that severe repression of E2F-dependent transcription during S-phase causes clear signs of DNA replication stress. Because replication stress is often seen in cancer cells, it is likely that tipping over the balance between atypical repressors and activator E2Fs towards the former will have a particular strong impact on the cell cycle progression of cancer cells under DNA damaging conditions. In this respect, it is interesting to note that CHK1 inhibits repressor E2F activity under conditions of replication stress to maintain a high level of E2F-dependent transcription for boosting DNA repair and restarting DNA replication (27,38).

As a consequence, the cell cycle arrest seen in CHK1-depleted cells is rescued by additional loss of atypical E2Fs (28). Together with these insights, our data suggest that low levels of E2F-dependent transcription sensitize cancer cells to replication stress. In further support of this notion, recent work showed that high levels of E2F-dependent transcription, via loss of E2F7, promotes resistance of cancer cells towards Poly (ADP-ribose) polymerase (PARP) inhibitors and interstrand-crosslinking drugs such as cisplatin or mitomycin C (39,40).

In conclusion, the inducible transgenic mouse model presented here strongly suggests that a basal level of E2F-dependent transcription is essential for the proliferation of mammalian cells. In addition, we provide a strong rationale to combine the inhibition of E2F-dependent transcription during S-phase with DNA-damaging reagents to achieve synergistic cancer-killing effects. Future studies should explore whether the transcriptional repressor activity of atypical E2Fs can be boosted in HCC patients for example by applying small molecules that specifically inhibit the degradation of E2F7/8.



**▲Figure 6. Selection pressure by inducible overexpression of E2F7 *in vitro* favors proliferation of cells with low levels of E2F7-EGFP.** (A) Quantitative PCR results showing EGFP transcript expression in inducible E2F7-EGFP HeLa cells and -EGFP after 1, 2, 8, 12 and 20 days of doxycycline administration. Two independent experiments. (B) Proliferation curves of HeLa cells with inducible E2F7-EGFP and -EGFP after doxycycline treatment. Color lines represent average  $\pm$  s.d. of two technical replicates for each time point. Representative curves of two independent experiments. (C) Experimental scheme of FACS-sorting experiment to determine E2F7-EGFP overexpression levels on clonogenic capacity of HeLa cells. (D) Representative images of colony formation assay with cells sorted in C from two independent clones. Two independent experiments were performed in duplo for three different cell clones of inducible E2F7-EGFP HeLa cell lines.

**Financial support:** This work was financially supported by the Dutch Cancer Society funding (KWF: UU2013-5777 & 11941/2018-2) to Bart Westendorp and Alain de Bruin, an Utrecht Life Sciences Infrastructure Grant (call 2014-I), and ZonMW grant 91116011.

**Acknowledgements:** We thank Wout Puijk and the rest of animal care takers for excellent care of our mice during experiments. Ger Arkesteijn (Faculty of Veterinary Medicine, Utrecht University, NL) and Reinier van der Linden (Hubrecht Institute, Utrecht, NL) for providing professional assistance with the FACS sorting. We also thank Rosan Heijboer for the generation of the RPE inducible cell lines and Rachel Thomas for her contribution to the manuscript revision.

**Author contributions:** EM, BW, EAvL and RY performed experiments. HTMT and SCvE provided technical assistance during mice necropsies and tissue processing. SCvE and MHK performed IHC stainings. LB performed the histopathological analysis of tumors. BW, EAvL and RY designed and tested construct to develop the mouse models. JvD generated the mice. All authors contributed to the revision of the manuscript. EM, BW, AdB conceived the study design and experimental approaches and data analysis. EM, JvD, BW, AdB wrote the manuscript.

## SUPPLEMENTARY MATERIAL

**Supporting Table S1:** PCR primers for transgene detection

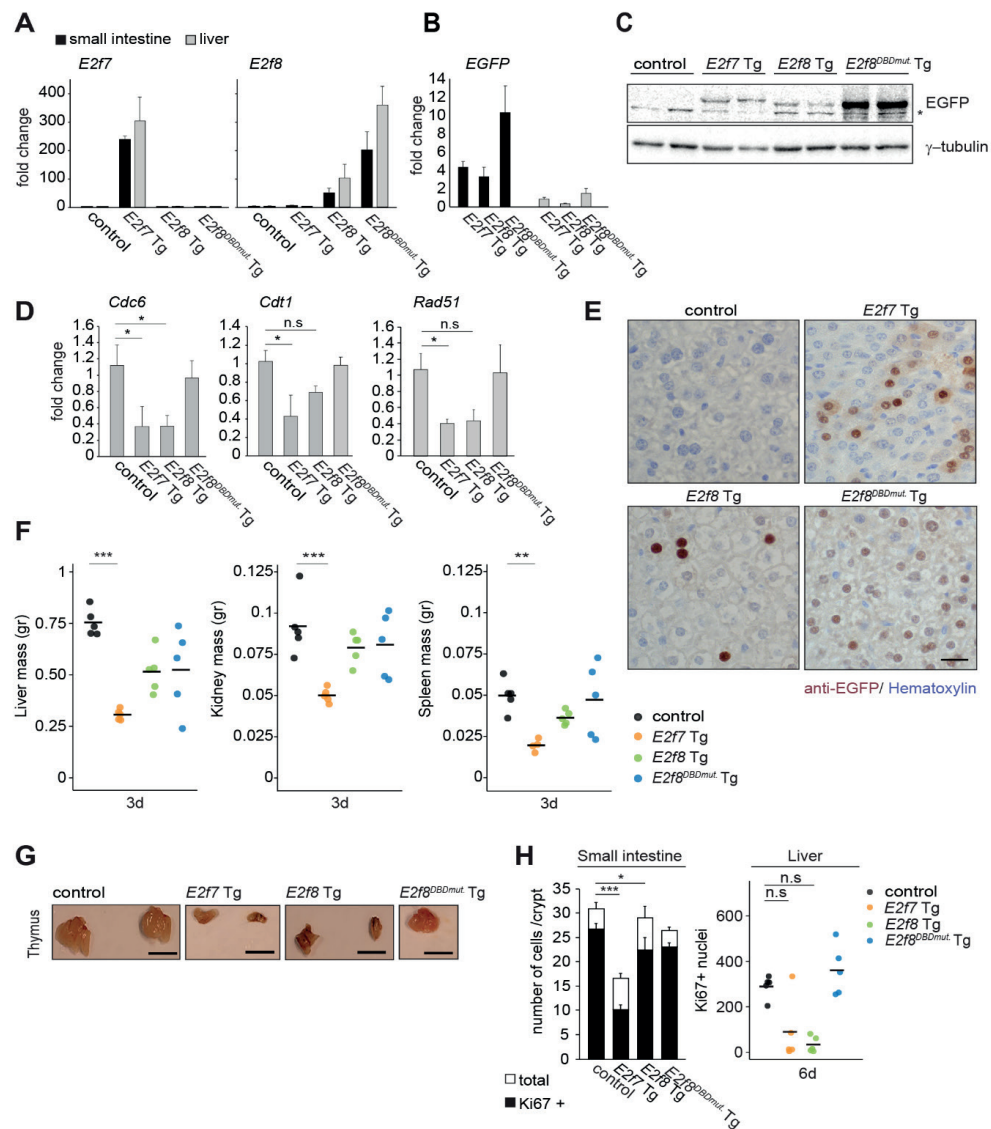
Primer	Sequence (5'-3')
TA Tg_ for 1	GCG AAG AGT TTG TCC TCA ACC
TA Tg_ rev1	AAA GTC GCT CTG AGT TGT TAT
TA Tg_ rev2	AAA GTC GCT CTG AGT TGT TAT
E2f7, E2f8 Tg and E2f8 <sup>DBDmut</sup> Tg_ for1	CCC TCC ATG TGT GAC CAA GG
E2f7, E2f8 Tg and E2f8 <sup>DBDmut</sup> Tg_ rev1	GCA CAG CAT TGC GGA CAT GC
E2f7, E2f8 Tg and E2f8 <sup>DBDmut</sup> Tg_ rev2	GCA GAA GCG CGG CCG TCT GG

**Supporting Table S2:** qPCR primers

	Forward primer (5'-3')	Reverse primer (3'-5')
E2F7; mouse	GATGCGTTTCGTGAACTCCCTG	AGAAACTTCTGGCACAGCAGCC
E2F7; human	CTCCTGTGCCAGAAGTTTC	CATAGATGCGTCTCCTTTCC
E2F8; mouse	GAGAAATCCCAGCCGAGTC	CATAAATCCGCCGACGTT
E2F8; human	AATATCGTGTGGCAGAGATCC	AGGTTGGCTGTCGGTGTC
GAPDH; mouse	GAAGGTCGGTGTGAACGG	TGAAGGGGTCGTTGATGG
GAPDH; human	CTCTGCTCCTCCTGTTCG	GCCCAATACGACCAAATCC
EGFP	CACTACCAGCAGAACACCCC	GTCACGAACTCCAGCAGGAC
CDC6; mouse	AGTTCTGTGCCCCGAAAGTG	AGCAGCAAAGAGCAAACCAGG
CDC6; human	AAACCCGATCCCAGGCACAG	AGGCAGGGCTTTTACACGAGGAG
CDT1; mouse	ACAGCCGGGCAAGATCCCCT	GGCTCCCAACTTCCGTGCC
M2-rtTA; mouse	CTGGGAGTTGAGCAGCCTAC	AGAGCACAGCGGAATGACTT
TP53; human	GTTCCGAGAGCTGAATGAGG	TCTGAGTCAGGCCCTTCTGT
RB1; human	GAGACACAAGCAACCTCAGC	GCTCAGACAGAAGGCGTTC
RAD51; mouse	CTCATGCGTCAACCACCAG	GCTTCAGGAAGACAGGGAGAG
RAD51; human	TGCTTATTGTAGACAGTGCCACC	CACCAAACCTCATCAGCGAGTC
E2F1; human	GACCACCTGATGAATATCTG	TGCTACGAAGGTCCTGAC
CCNE1; human	GACACCATGAAGGAGGACGG	ATTGTCCCAAGGCTGGCTC
RSP18; human	AGTTCCAGCATATTTTGCAG	CTCTTGGTGAGGTCAATGTC

**Supporting Table S3:** Antibodies for immunoblots and immunohistochemistry

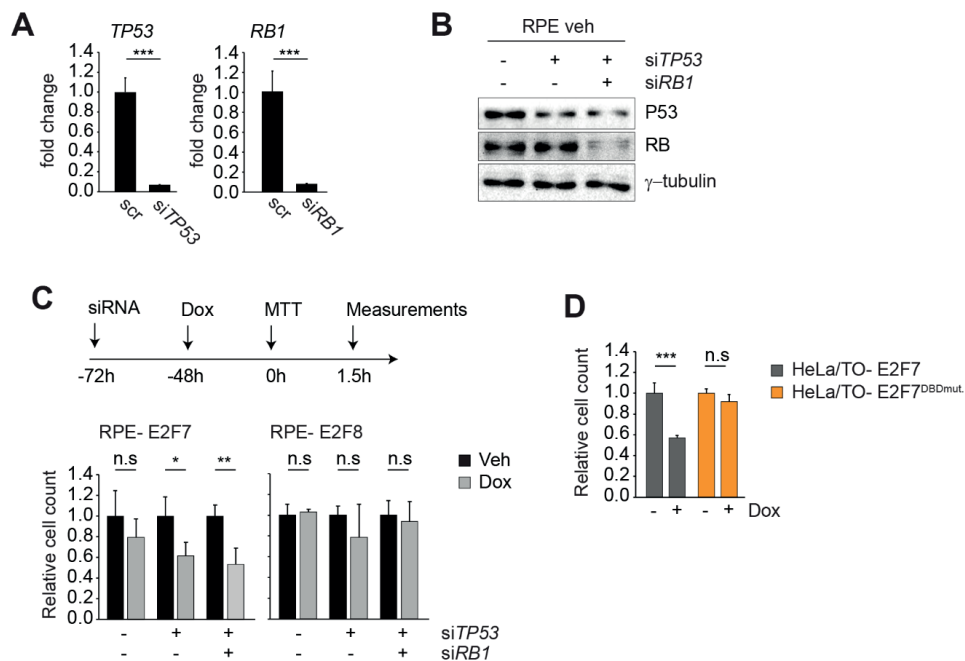
Application	Name	Company	Cat #	Dilution	
Immunoblot	GFP	Abcam	AB6673	1:1000	
	E2F1	Santa Cruz	Sc-193	1:1000	
	E2F2	Santa Cruz	(C-20) sc-633	1:1000	
	E2F3	Santa Cruz	(C-18) sc-878	1:5000	
	cyclin A2	Santa Cruz	Sc-751	1:1000	
	cyclin B1	Santa Cruz	Sc-245	1:1000	
	P21	Santa Cruz	(M-19) sc-471	1:1000	
	RAD51	Santa Cruz	(H-92) sc-8349	1:1000	
	P53	Calbiochem	OP03	1:500	
	RB	Santa Cruz	(C-15) sc-50	1:1000	
	$\gamma$ -tubulin (clone GTU-88)	Sigma	T6557	1:1000	
	Immunohistochemistry	GFP	Abcam	AB6673	1:800
		Ki67	Thermo Scientific	RM-9106	1:75
BrdU		DAKO	M0744	1:50	
$\gamma$ -H2AX		Cell Signaling	S139	1:500	
Caspase-3		R&D systems	AF835	1:400	
Isolectin B4		Vector Labs	B-1205	1:100	



◀**Supporting Figure 1.** (A) Transcript levels of *E2f7* and *E2f8* in livers and small intestines after doxycycline treatment for 6 days in the indicated genotypes measured by quantitative PCR. Fold changes were adjusted to average of controls and *Gapdh* and *Actb* were used to normalize the expression. Data represent average  $\pm$  SEM of 5 different mice. (B) Transcript levels of *EGFP* in small intestines (black bars) livers (grey bars) small intestines after doxycycline treatment for 6 days in the indicated genotypes measured by quantitative PCR. Fold changes were adjusted to average of controls and *Gapdh* and *Actb* were used to normalize the expression. Data represent average  $\pm$  SEM of 5 different mice. (C) Protein expression of exogenous E2F7, E2F8 and E2F8<sup>DBDmut.</sup> in liver lysates of mice harvested after 6 days with doxycycline treatment.  $\gamma$ -tubulin was used as loading control. Each lane represents a different mouse. Asterisk indicates unspecific bands. (D) Transcript levels of E2F target genes *Cdc6*, *Cdt1* and *Rad51* in liver tissue in the indicated genotype. Data represents average  $\pm$  SEM of 5 different mice. (E) Representative anti-EGFP immunohistochemistry pictures to detect transgene expression in livers treated 6d with doxycycline. Scale bars: 20 $\mu$ m. (F) Liver, kidney and spleen weights after 3 days of transgene induction in juvenile mice. Organs were weighed after fixation with 4% paraformaldehyde. Bars represent averages per genotype ( $n=5$  mice; *E2f7*Tg spleen  $n=4$ ). (G) Representative macroscopic pictures of the thymuses from mice with the indicated genotypes after 6 days with doxycycline. Scale bars: 5mm. (H) Quantification of Ki67- staining from Figure 1E after 6 days of doxycycline treatment. Small intestine quantification: total count and Ki67-positive nuclei per crypt of small intestines. Error bars represent SEM ( $n=45$  crypts/genotype;  $n=3$  mice/ genotype). Liver: Total Ki67-positive nuclei in ten fields (40x objective). Crossbars represent averages per genotype ( $n=5$  mice).

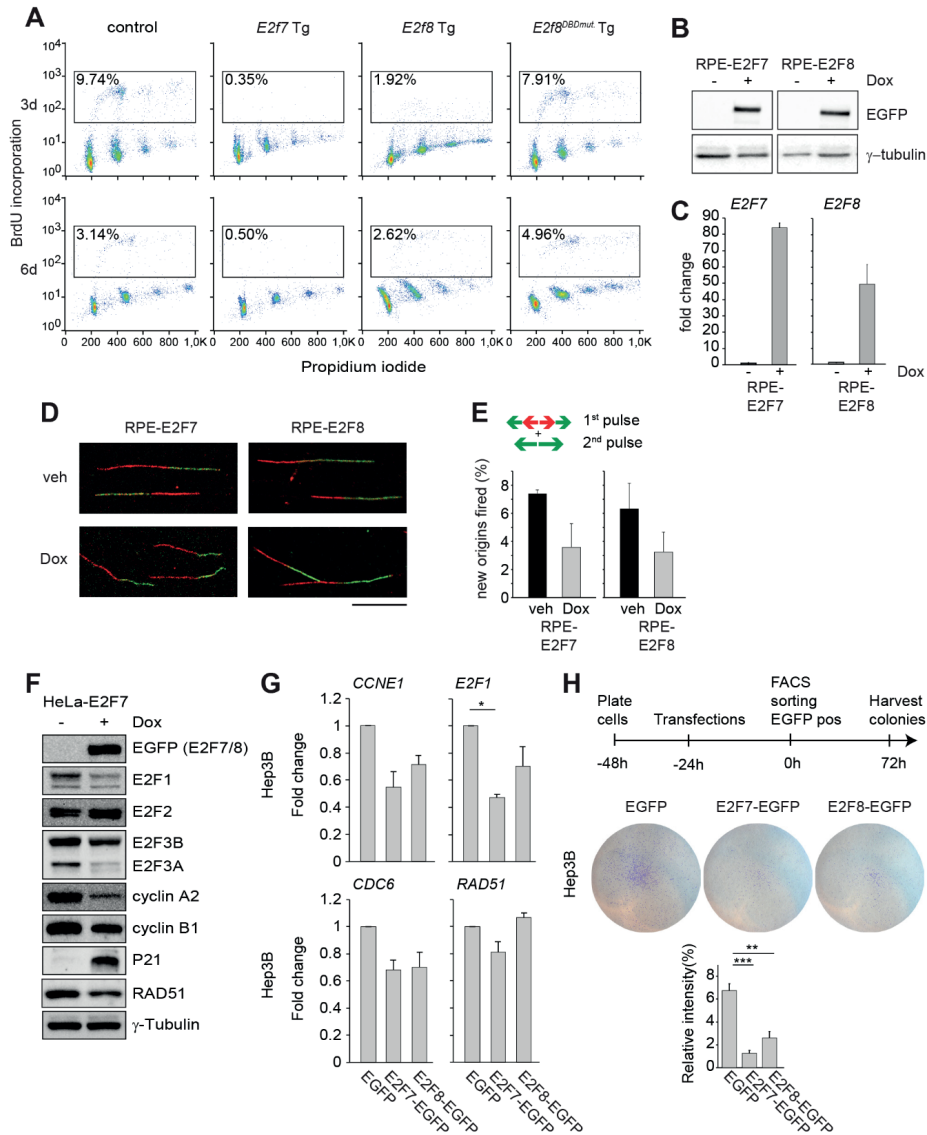
Data information: In (F and H), \* $p<0.05$ , \*\* $p<0.01$ , \*\*\* $p<0.001$  (Kruskal Wallis One Way Analysis of Variance on Ranks and Dunnett's Method for Multiple Comparisons vs. control).





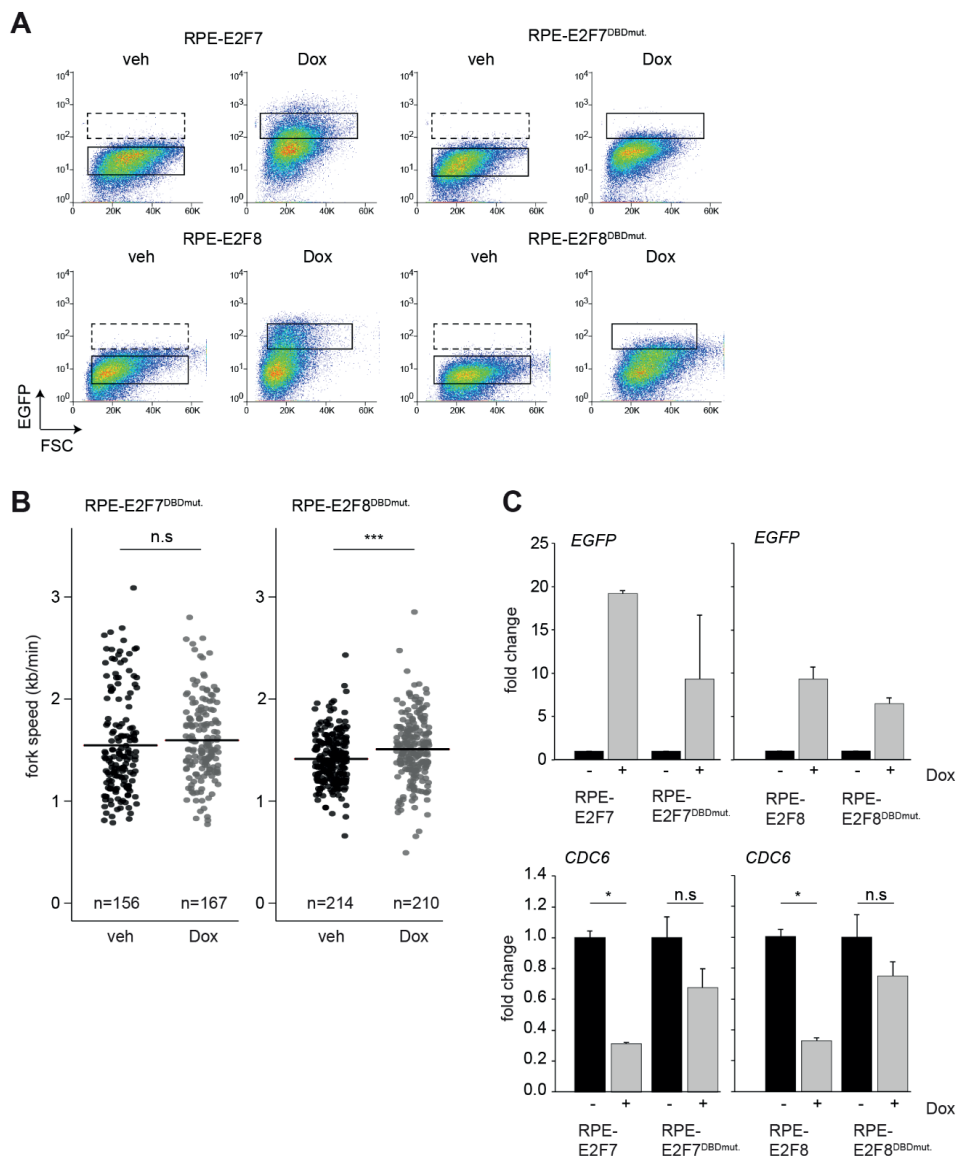
**▲ Supporting Figure 2.** (A) Representative flow cytometry plots showing BrdU incorporation (y-axes) versus DNA content (propidium iodide, x-axis) of isolated nuclei from the indicated genotypes livers after 3 and 6d with doxycycline treatment. (B) Immunoblots showing induced expression of exogenous E2F7 and E2F8 in RPE-TetOn cell lysates after 24h of doxycycline administration.  $\gamma$ -tubulin was used as loading control. (C) Transcript levels of *E2F7* and *E2F8* genes in RPE cells with inducible E2F7 or E2F8 overexpression, respectively, after 24h treatment with doxycycline, measured by quantitative PCR. Fold changes were adjusted to vehicles and *GAPDH* was used to normalize the expression. (D) Representative images of ongoing DNA replication in vehicle-(veh) and doxycycline-treated-(dox) RPE cells with Tet/On inducible E2F7/8-EGFP expression. Scale bar; 10 $\mu$ m. (E) New origins fired are shown as percentage of origins fired during 1<sup>st</sup> pulse (green-red-green) and 2<sup>nd</sup> pulse (green) relative to the total number of fibers in the indicated condition ( $n=2$  experiments/ condition; at least 350 tracks/ condition in each experiment). Error bars represent SD. (F) Protein expression of cell cycle regulators in the indicated HeLa inducible cell lines after 24 hours of doxycycline treatment. (G) Transcript levels of *CDC6*, *E2F1* and *RAD51* in Hep3B cells. EGFP positive cells were sorted 24h after transfections and directly collected for RNA analysis. Fold changes were adjusted to average of EGFP controls and *GAPDH* and *RSP18* were used to normalize the expression. Data represent average  $\pm$  SEM of at least 2 different experiments. (H) Schematic overview of the experimental settings and representative images of colonies of EGFP FACS-sorted Hep3B cells. Cells were transfected with indicated plasmids for 24h before FACS-sorting and re-plated for 72 hours. Histogram shows the quantification of relative intensity (%) from each condition. Data represents average  $\pm$  SEM (2 independent experiments were performed in at least duplo).

Data information: In (G and H), \* $p < 0.05$ , \*\* $p < 0.01$ , \*\*\* $p < 0.001$  (Kruskal Wallis One Way Analysis of Variance on Ranks and Dunnett's Method for Multiple Comparisons vs. EGFP control).



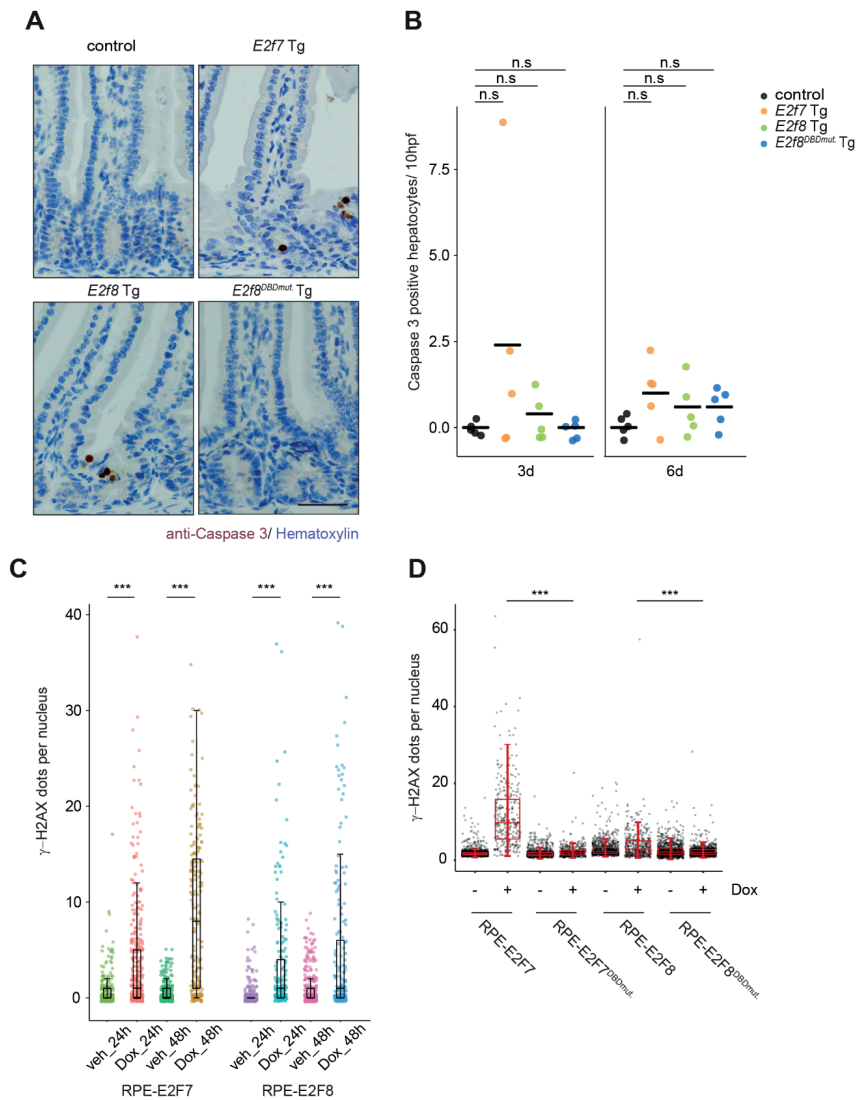
**▲Supporting Figure 3.** (A) Transcript levels of *TP53* and *RB1* in RPE cells 24h post-transfections with the indicated siRNA. (B) Immunoblot analysis for the validation of the efficient siRNA-mediated knockdown of P53 and Rb in RPE E2F7 and -8 cells 24h post-transfections. Hydroxyurea (2mM, Sigma-Aldrich) was added 16h before harvesting to all samples to induce clear P53 expression.  $\gamma$ -tubulin was used as loading control. (C) Schematic overview of the experimental setting and proliferation of RPE-E2F7 and RPE-E2F8, measured by MTT assays. Cells were transfected with the indicated siRNA and incubated for 48h with doxycycline before starting the MTT assay. (D) Proliferation of HeLa/TO-E2F7 cells after 48h incubation with doxycycline, measured with MTT assay.

Data information: In (A, C and D), \* $p < 0.05$ , \*\* $p < 0.01$ , \*\*\* $p < 0.001$ , n.s no significant (t-test). Bars represent means of  $n=3$  biological replicates.



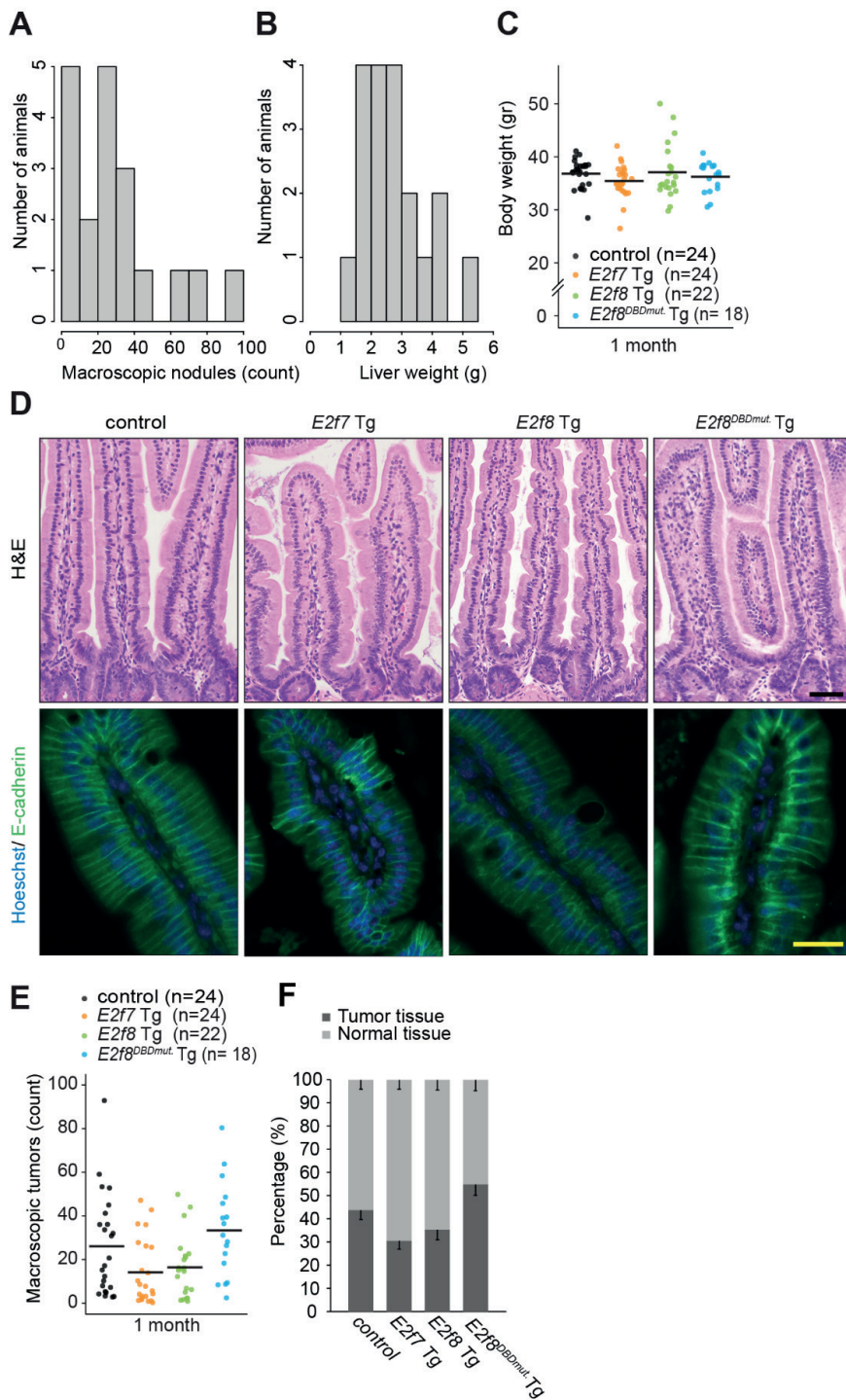
**▲Supporting Figure 4. (A)** FACS profiles showing EGFP expression in the indicated RPE cells. Solid encircled areas indicate the gates used to sort EGFP expressing cells. **(B)** Quantification of replication fork speed in the cell lines and conditions indicated. Only ongoing replication forks (red+green) were included in the quantification. Crossbars represent average values per condition. **(C)** Transcript levels of *EGFP* and *CDC6* genes in RPE cells with inducible *E2F7*, *E2F8* or *E2F7<sup>DBDmut.</sup>* overexpression after 24h treatment with doxycycline, measured by quantitative PCR. Fold changes were adjusted to the condition without doxycycline and *GAPDH* was used to normalize the expression.

Data information: In **(B)** \*\*\* $P < 0.001$  (Mann-Whitney Rank Sum Test). In **(C)** \* $P < 0.05$  (t-test).



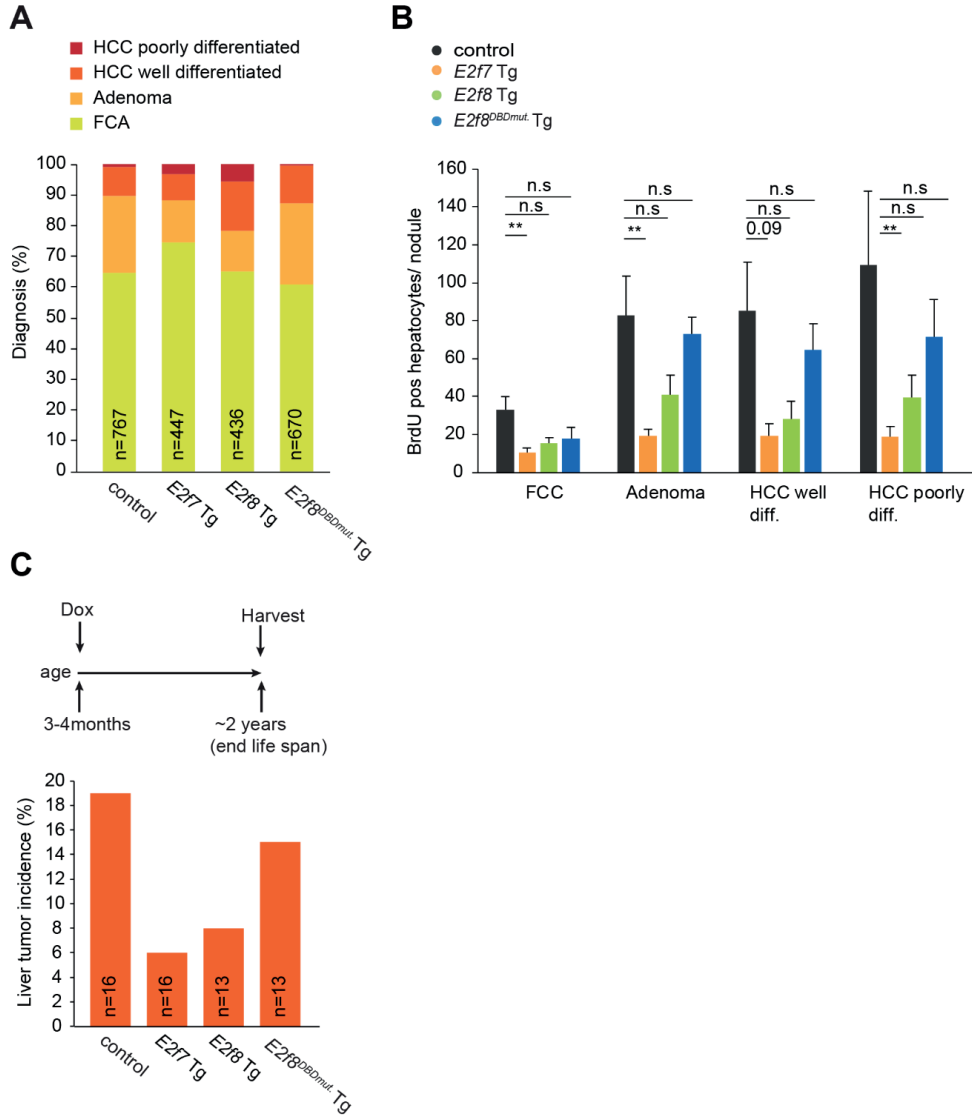
**▲Supporting Figure 5.** (A) Cleaved Caspase 3 IHC staining in intestinal tissue of the indicated genotypes after 3d of doxycycline treatment. Scale bars: 50 $\mu$ m. (B) Quantification of cleaved Caspase 3 IHC staining in liver tissue of the indicated genotypes after 3 and 6d of doxycycline treatment. (C) Immunofluorescence staining showing the total count of  $\gamma$ -H2AX dots per nuclei in RPE inducible cells lines. Cells were incubated for 24 and 48h with doxycycline (Dox) before harvesting. Nuclear DNA was stained with DAPI. For quantification at least 200 cells were included. (D) Immunofluorescence staining showing total count of  $\gamma$ -H2AX dots per nuclei in RPE inducible cells lines. Cells were incubated 48h with doxycycline (Dox) before harvesting. Nuclear DNA was stained with DAPI. For quantification at least 200 cells were included.

Data information: In (B) n.s.; no significant difference (Kruskal Wallis One Way Analysis of Variance on Ranks and Dunnett's Method for Multiple Comparisons vs. control). In (C and D), \*\*\* $p < 0.001$  (Mann-Whitney Rank Sum Test).



◀**Supporting Figure 6.** (A) Histogram showing the frequency distribution of total number of macroscopic tumors per mouse at time point 0h ( $n=20$  mice). (B) Histogram showing the frequency distribution liver weights from the animals harvested at time point 0h ( $n=20$  mice). (C) Dot plot showing the body weights after 1 month of doxycycline treatment in transgenic mice with DEN-induced liver tumors. (D) Representative pictures of H&E- (top) and E-cadherin immunofluorescent staining (bottom) of intestinal sections after 1 month of doxycycline treatment. Scale bars:  $50\mu\text{m}$  (top) and  $30\mu\text{m}$  (bottom). (E) Dot plot showing the number of macroscopic tumors after 1 month of doxycycline treatment in transgenic mice with DEN-induced liver tumors. (F) Bar chart showing the ratio between liver tumor and normal liver tissue in histology sections after 1 month of doxycycline; measured by a board-certified pathologist. We analyzed 18-24 animals/ genotype and two slides with 7 different sections of the liver per animal.

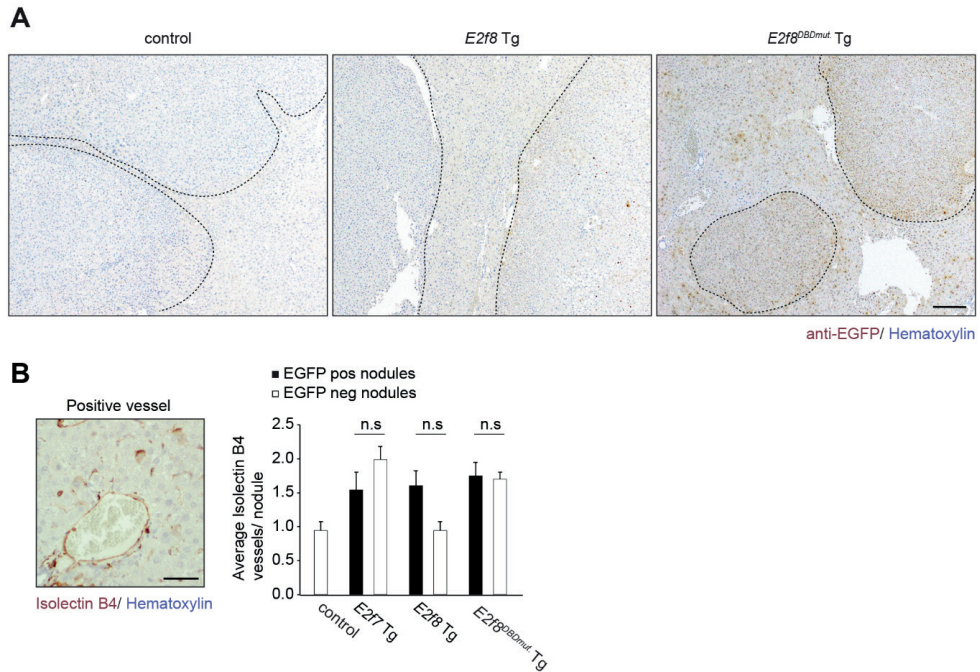
Data information: In (C, E and F) no significance detected (Kruskal Wallis One Way Analysis of Variance on Ranks and Dunnett's Method for Multiple Comparisons vs. control).



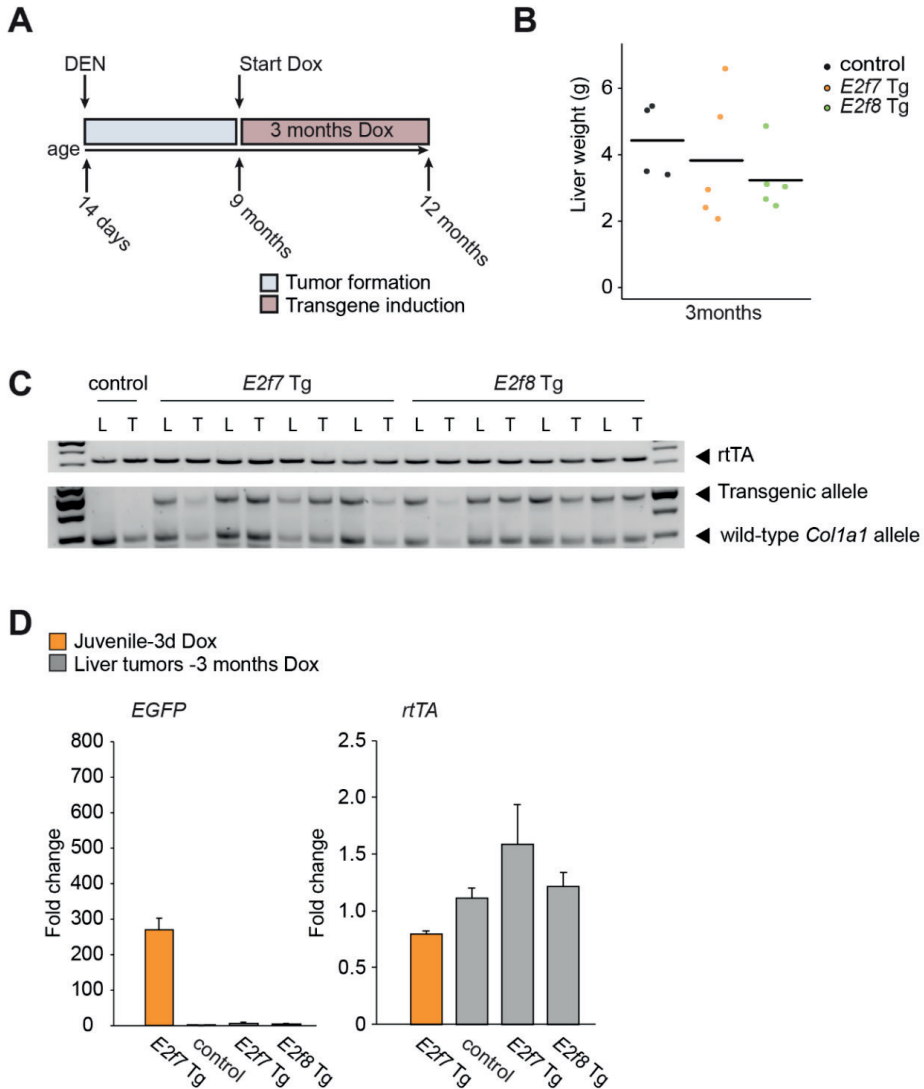
**▲Supporting Figure 7. (A)** Histopathological analysis of DEN-induced liver tumors after one month of transgene induction with doxycycline. Total number of tumors analyzed per genotype were grouped together. We analyzed 18-24 animals/ genotype. **(B)** Quantification of BrdU-positive cells in 5 fields using the 40x objective in nodules of the different histopathological categories for each genotype. Histogram represent averages of the total number of BrdU positive cells per nodule per genotype (*n*=10 nodules per genotype; poorly differentiated HCC: *E2f8<sup>DBDmut</sup>* (*n*=3), control (*n*= 5). **(C)** Schematic overview of the experimental setting and histogram showing the percentage of spontaneous liver tumor incidence in aged mice.

Data information: In **(B)** \**p*<0.05, \*\**p*<0.01, \*\*\**p*<0.001, n.s no significant (Kruskal Wallis One Way Analysis of Variance on Ranks and Dunnett's Method for Multiple Comparisons vs. control). In **(A and C)** n.s no significant (Chi-square).

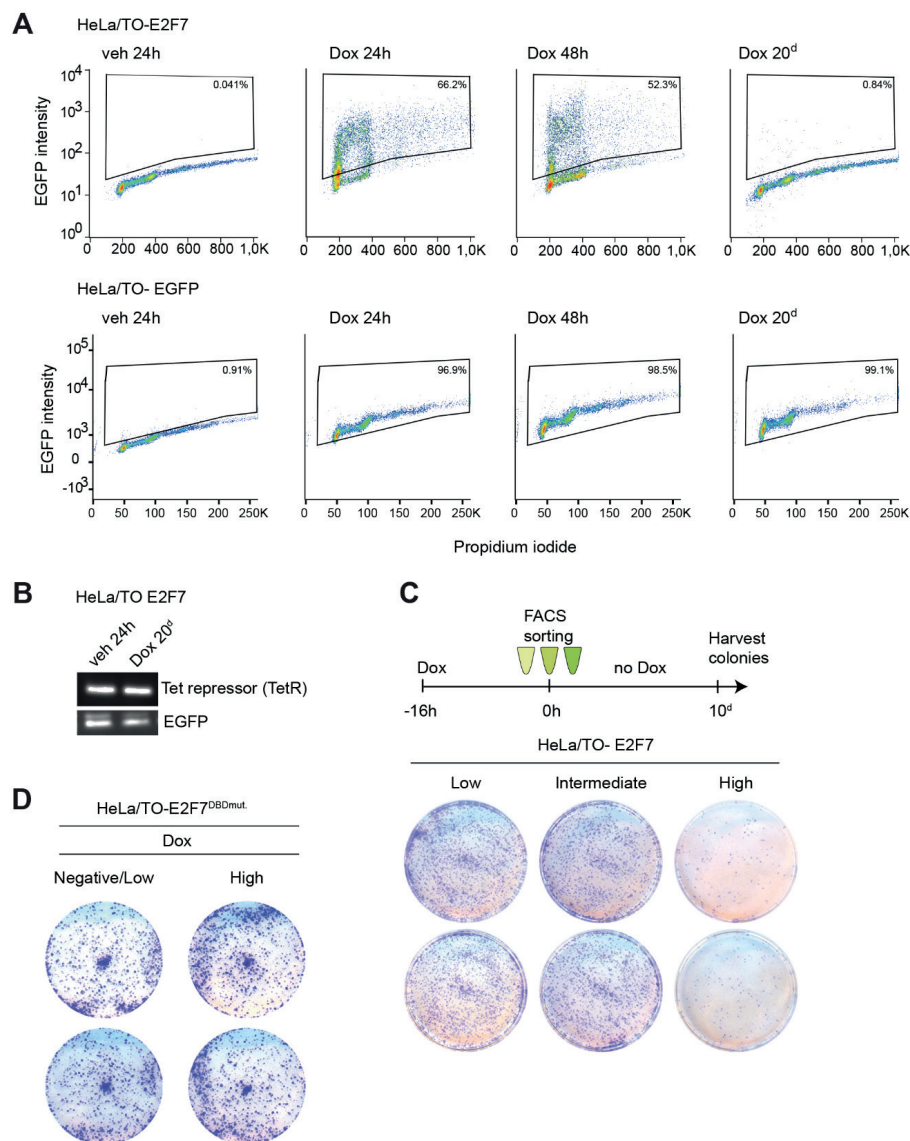




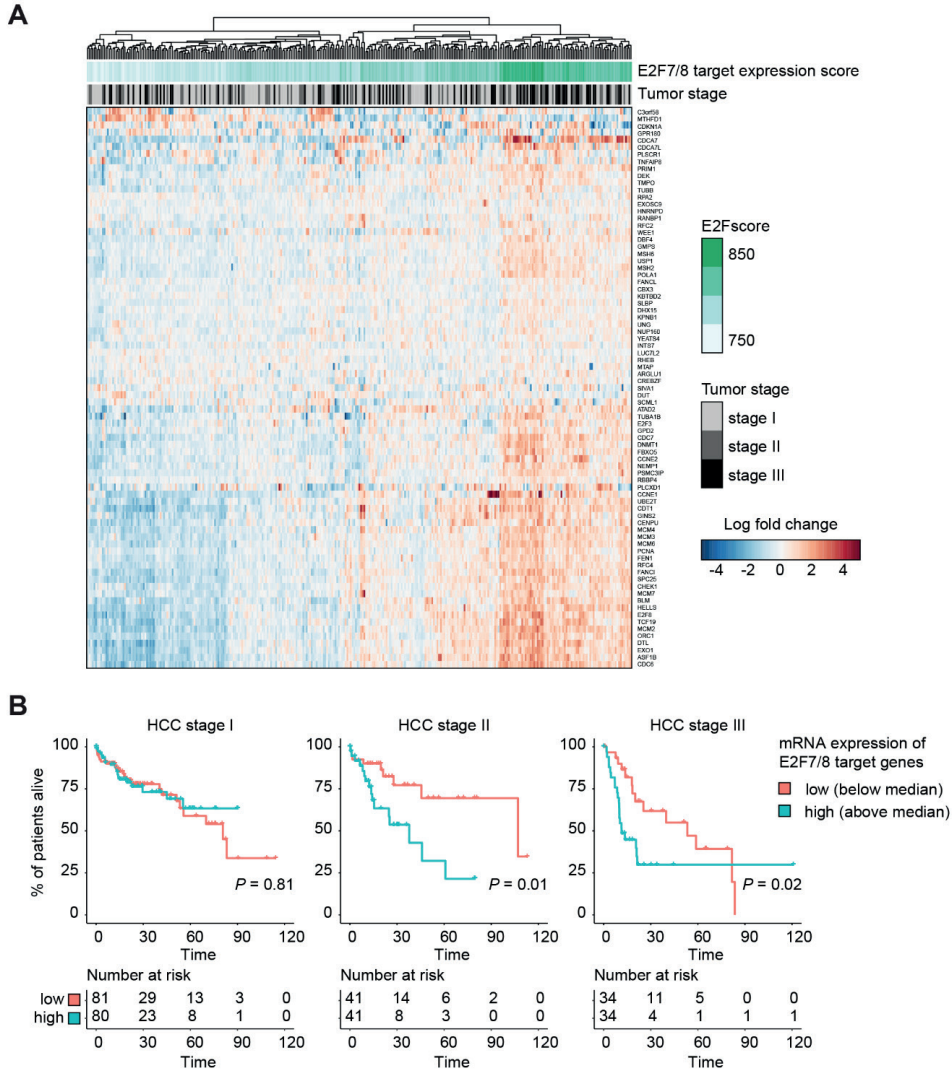
**▲Supporting Figure 8. (A)** Representative EGFP immunohistochemistry pictures of DEN-induced liver tumors after 1 month of transgene induction with doxycycline. Scale bars: 200  $\mu$ m. Black dashed lines delimitate tumor nodules. **(B)** Representative Isolectin B4 (endothelial cell marker) positive vessel picture and histograms showing the quantification of Isolectin B4 positive blood vessels staining in EGFP-positive and -negative tumor nodules ( $n > 6$  EGFP positive/negative nodules per genotype; *E2F8<sup>DBDmut</sup>* negative  $n=2$ ). Scale bar: 50  $\mu$ m. n.s no significant (t-test).



**▲Supporting Figure 9.** (A) Schematic overview of long-term induced-liver cancer experiment. A cohort of mice were kept for 3 months on doxycycline after the appearance of macroscopic DEN-induced liver tumors at the age of 9 months. (B) Dot plot showing liver weights from mice from with DEN-induced liver tumors treated for 3 months with doxycycline. Crossbars indicate average ( $n=4-5$  animals / genotype). (C) Genotyping PCRs on genomic DNA isolated from normal and tumor tissue after 3 months of doxycycline treatment of the indicated genotypes. The upper panel shows the presence of M2-rtTA transgene. The lower panel shows the transgenic alleles (*E2f7/8* Tg integrated into *Col1a1* locus, upper band) as well as the wild type allele of the *Col1a1* locus (no transgene inserted, lower band). (D) Transcript levels of M2-rtTA (tet activator) and EGFP in tumors treated 3 months with doxycycline. Juvenile livers of *E2f7* Tg mice (3d Dox) were used as positive controls. *GAPDH* was used to normalize expression. Bars represent  $n=5$  tumors.



**▲Supporting Figure 10. (A)** FACS plots showing DNA content on the x-axis (propidium iodide) and EGFP intensity on the y-axes of inducible HeLa/TetOn cells with inducible expression of E2F7-EGFP (upper row) or EGFP (lower row), after 24 hours, 48 hours and 20 days of doxycycline treatment. The same gate was applied for vehicle- and doxycycline- treated cells to determine the percentage of positive cells. **(B)** PCR gel showing the presence of the TetR gene and *EGFP* in HeLa/TO-E2F7 cells before (veh 24h) and after 20 days of doxycycline treatment. **(C)** Schematic overview of the experimental settings and representative images of colony formation assays of sorted HeLa/TO-E2F7 cells based on EGFP expression. Recovery was determined after withdrawal of doxycycline for 10 days. **(D)** Representative images of colony formation assays of sorted HeLa/TO-E2F7<sup>DBDmut.</sup> expressing cells. ( $n=2$  independent experiments in duplo)



**▲Supporting Figure 11. (A)** Heatmap showing expression of a previously identified set of E2F7/8 target genes in HCC patients. Expression values represent log fold changes in normalized counts, obtained from the RNA-sequencing data of the TCGA-LIHC cohort. The columns are labeled by disease stage, and by cumulative expression of all indicated target genes (E2F score). **(B)** Overall survival of HCC patients in TCGA study. Patients were stratified according to low (below median) or high (above median) cumulative expression of a ser of E2F7/8 target genes. Patients with early (stage I) and advanced disease (stage II and III, American Joint Committee on Cancer staging system) were separately analyzed to rule out potential bias caused by disease stage. P values were determined using log-rank analysis.

## REFERENCES

- (1) Westendorp B, Mokry M, Groot Koerkamp, Marian J A, Holstege FCP, Cuppen E, de Bruin A. E2F7 represses a network of oscillating cell cycle genes to control S-phase progression. *Nucleic Acids Res* 2012;40(8):3511-3523.
- (2) Bertoli C, Skotheim JM, de Bruin, Robertus A. M. Control of cell cycle transcription during G1 and S phases. *Nat Rev Mol Cell Biol* 2013 -8;14(8):518-528.
- (3) Di Stefano L, Jensen M, Helin K. E2F7, a novel E2F featuring DP-independent repression of a subset of E2F-regulated genes. *EMBO J* 2003;22(23):6289-6298.
- (4) de Bruin A, Maiti B, Jakoi L, Timmers C, Buerki R, Leone G. Identification and characterization of E2F7, a novel mammalian E2F family member capable of blocking cellular proliferation. *J Biol Chem* 2003;278(43):42041-42049.
- (5) Maiti B, Li J, de Bruin A, Gordon F, Timmers C, Opavsky R, et al. Cloning and characterization of mouse E2F8, a novel mammalian E2F family member capable of blocking cellular proliferation. *J Biol Chem* 2005;280(18):18211-18220.
- (6) Logan N, Graham A, Zhao X, Fisher R, Maiti B, Leone G, et al. E2F-8: an E2F family member with a similar organization of DNA-binding domains to E2F-7. *Oncogene* 2005;24(31):5000-5004.
- (7) Chen H, Tsai S, Leone G. Emerging roles of E2Fs in cancer: an exit from cell cycle control. *Nat Rev Cancer* 2009;9(11):785-797.
- (8) Logan N, Delavaine L, Graham A, Reilly C, Wilson J, Brummelkamp T, et al. E2F-7: a distinctive E2F family member with an unusual organization of DNA-binding domains. *Oncogene* 2004;23(30):5138-5150.
- (9) Weinberg RA. The retinoblastoma protein and cell cycle control. *Cell* 1995 May 05; ;81(3):323-330.
- (10) Nevins JR. The Rb/E2F pathway and cancer. *Hum Mol Genet* 2001;10(7):699-703.
- (11) Aksoy O, Chicas A, Zeng T, Zhao Z, McCurrach M, Wang X, et al. The atypical E2F family member E2F7 couples the p53 and RB pathways during cellular senescence. *Genes Dev* 2012;26(14):1546-1557.
- (12) Kent L, Rakijas J, Pandit S, Westendorp B, Chen H, Huntington J, et al. E2f8 mediates tumor suppression in postnatal liver development. *J Clin Invest* 2016;126(8):2955-2969.
- (13) Thurlings I, Martínez López LM, Westendorp B, Zijp M, Kuiper R, Tooten P, et al. Synergistic functions of E2F7 and E2F8 are critical to suppress stress-induced skin cancer. *Oncogene* 2017;36(6):829-839.
- (14) Carvajal L, Hamard P, Tonnessen C, Manfredi J. E2F7, a novel target, is up-regulated by p53 and mediates DNA damage-dependent transcriptional repression. *Genes Dev* 2012;26(14):1533-1545.
- (15) Ye L, Guo L, He Z, Wang X, Lin C, Zhang X, et al. Upregulation of E2F8 promotes cell proliferation and tumorigenicity in breast cancer by modulating G1/S phase transition. *Oncotarget* 2016;7(17):23757-23771.
- (16) Lv Y, Xiao J, Liu J, Xing F. E2F8 is a Potential Therapeutic Target for Hepatocellular Carcinoma. *J Cancer* 2017;8(7):1205-1213.
- (17) Park S, Platt J, Lee J, López Giráldez F, Herbst R, Koo J. E2F8 as a Novel Therapeutic Target for Lung Cancer. *J Natl Cancer Inst* 2015;107(9).
- (18) Boekhout M, Yuan R, Wondergem A, Segeren H, van Liere E, Awol N, et al. Feedback regulation between atypical E2Fs and APC/CCdh1 coordinates cell cycle progression. *EMBO Rep* 2016;17(3):414-427.

- (19) Nam H, van Deursen J. Cyclin B2 and p53 control proper timing of centrosome separation. *Nat Cell Biol* 2014;16(6):538-549.
- (20) Li J, Ran C, Li E, Gordon F, Comstock G, Siddiqui H, et al. Synergistic function of E2F7 and E2F8 is essential for cell survival and embryonic development. *Dev Cell* 2008 Jan;14(1):62-75.
- (21) Pandit S, Westendorp B, Nantasanti S, van Liere E, Tooten PCJ, Cornelissen PWA, et al. E2F8 is essential for polyploidization in mammalian cells. *Nat Cell Biol* 2012;14(11):1181-1191.
- (22) Da Costa, Rui M Gil, Paula Santos N, Rocha A, Colaço A, Lopes C, Oliveira P. The N-nitrosodiethylamine mouse model: sketching a timeline of evolution of chemically-induced hepatic lesions. *Anticancer Res* 2014;34(12):7029-7037.
- (23) Thoolen B, Maronpot R, Harada T, Nyska A, Rousseaux C, Nolte T, et al. Proliferative and nonproliferative lesions of the rat and mouse hepatobiliary system. *Toxicol Pathol* 2010;38(7 Suppl):5S-81S.
- (24) Benedict B, van Harn T, Dekker M, Hermesen S, Kucukosmanoglu A, Pieters W, et al. Loss of p53 suppresses replication-stress-induced DNA breakage in G1/S checkpoint deficient cells. *Elife* 2018;7.
- (25) Jackson DA, Pombo A. Replicon clusters are stable units of chromosome structure: evidence that nuclear organization contributes to the efficient activation and propagation of S phase in human cells. *J Cell Biol* 1998;140(6):1285-1295.
- (26) Tuduri S, Tourrière H, Pasero P. Defining replication origin efficiency using DNA fiber assays. *Chromosome Res* 2010;18(1):91-102.
- (27) Bertoli C, Herlihy A, Pennycook B, Kriston Vizi J, de Bruin, Robertus A M. Sustained E2F-Dependent Transcription Is a Key Mechanism to Prevent Replication-Stress-Induced DNA Damage. *Cell Rep* 2016;15(7):1412-1422.
- (28) Yuan R, Vos HR, van Es RM, Chen J, Burgering BM, Westendorp B, et al. Chk1 and 14-3-3 proteins inhibit atypical E2Fs to prevent a permanent cell cycle arrest. *EMBO J* 2018 03 01;37(5).
- (29) Nuo MT, Yuan JL, Yang WL, Gao XY, He N, Liang H, et al. Promoter methylation and histone modifications affect the expression of the exogenous DsRed gene in transgenic goats. *Genet Mol Res* 2016;15(3).
- (30) Ngai S, Rosli R, Al Abbar A, Abdullah S. DNA methylation and histone modifications are the molecular lock in lentivirally transduced hematopoietic progenitor cells. *Biomed Res Int* 2015;2015:346134.
- (31) Yu Y, Lowy M, Elble R. Tet-On lentiviral transductants lose inducibility when silenced for extended intervals in mammary epithelial cells. *Metab Eng Commun* 2016;3:64-67.
- (32) Zhu P, Aller MI, Baron U, Cambridge S, Bausen M, Herb J, et al. Silencing and un-silencing of tetracycline-controlled genes in neurons. *PLoS ONE* 2007;2(6):e533.
- (33) Gödecke N, Zha L, Spencer S, Behme S, Riemer P, Rehli M, et al. Controlled re-activation of epigenetically silenced Tet promoter-driven transgene expression by targeted demethylation. *Nucleic Acids Res* 2017;45(16):e147.
- (34) Tsai S, Opavsky R, Sharma N, Wu L, Naidu S, Nolan E, et al. Mouse development with a single E2F activator. *Nature* 2008;454(7208):1137-1141.
- (35) Chong J, Wenzel P, Sáenz Robles MT, Nair V, Ferrey A, Hagan J, et al. E2f1-3 switch from activators in progenitor cells to repressors in differentiating cells. *Nature* 2009;462(7275):930-934.
- (36) Chang H, Song J, Wu J, Zhang Y. E2F transcription factor 8 promotes cell proliferation via CCND1/p21 in esophageal squamous cell carcinoma. *Onco Targets Ther* 2018;11:8165-8173.

- (37) Deng Q, Wang Q, Zong W, Zheng D, Wen Y, Wang K, et al. E2F8 contributes to human hepatocellular carcinoma via regulating cell proliferation. *Cancer Res* 2010;70(2):782-791.
- (38) Bertoli C, Klier S, McGowan C, Wittenberg C, de Bruin, Robertus A M. Chk1 inhibits E2F6 repressor function in response to replication stress to maintain cell-cycle transcription. *Curr Biol* 2013;23(17):1629-1637.
- (39) Clements KE, Thakar T, Nicolae CM, Liang X, Wang H, Moldovan G. Loss of E2F7 confers resistance to poly-ADP-ribose polymerase (PARP) inhibitors in BRCA2-deficient cells. *Nucleic Acids Res* 2018 /09/28;46(17):8898-8907.
- (40) Mitxelena J, Apraiz A, Vallejo Rodríguez J, García Santisteban I, Fullaondo A, Alvarez Fernández M, et al. An E2F7-dependent transcriptional program modulates DNA damage repair and genomic stability. *Nucleic Acids Res* 2018;46(9):4546-4559.





# Chapter 3

---

## **Atypical E2Fs either counteract or cooperate with RB during tumorigenesis depending on tissue context**

Eva Moreno<sup>1\*</sup>, Shusil K. Pandit<sup>1,2\*</sup>, Mathilda J.M. Toussaint<sup>1</sup>, Laura Bongiovanni<sup>1,3</sup>, Liesbeth Harkema<sup>1</sup>, Saskia C. van Essen<sup>1</sup>, Elsbeth A. van Liere<sup>1</sup>, Bart Westendorp<sup>1</sup>, Alain de Bruin<sup>1,3 †</sup>.

Affiliations:

Departments of <sup>1</sup>Biomolecular Health Sciences, Division of Cell Biology, Metabolism and Cancer, Faculty of Veterinary Medicine, Utrecht University, Utrecht, The Netherlands; <sup>2</sup>Department of Pathology, Kerk School of Medicine, University of Southern California, Los Angeles, USA. <sup>3</sup>Department of Pediatrics, Division Molecular Genetics, University Medical Center Groningen, University of Groningen, Groningen, The Netherlands;

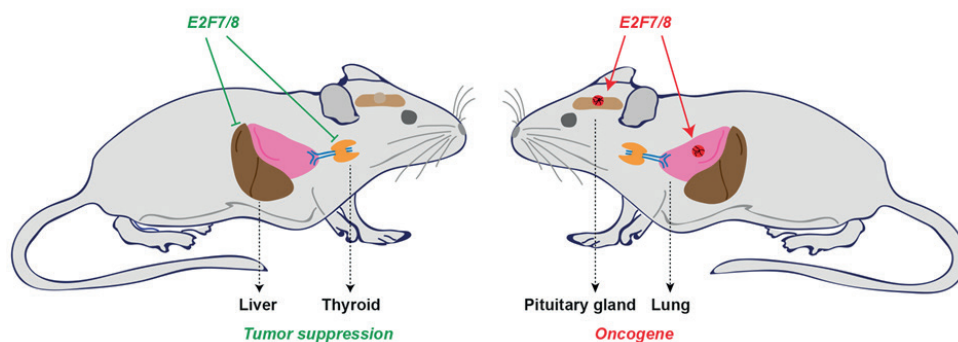
\* These authors contributed equally to this work

† Corresponding author

*Cancers*. 2021. 13(9), 203

## ABSTRACT

E2F-transcription factors activate many genes involved in cell cycle progression, DNA repair, and apoptosis. Hence, E2F-dependent transcription must be tightly regulated to prevent tumorigenesis, and therefore metazoan cells possess multiple E2F regulation mechanisms. The best-known is the Retinoblastoma protein (RB), which is mutated in many cancers. Atypical E2Fs (E2F7 and -8) can repress E2F-target gene expression independently of RB and are rarely mutated in cancer. Therefore, they may act as emergency brakes in RB-mutated cells to suppress tumor growth. Currently, it is unknown if and how RB and atypical E2Fs functionally interact *in vivo*. Here, we demonstrate that mice with liver-specific combinatorial deletion of *Rb* and *E2f7/8* have reduced life-spans compared to *E2f7/8* or *Rb* deletion alone. This was associated with increased proliferation and enhanced malignant progression of liver tumors. Hence, atypical repressor E2Fs and RB cooperatively act as tumor suppressors in hepatocytes. In contrast, loss of either *E2f7* or *E2f8* largely prevented the formation of pituitary tumors in *Rb*<sup>+/-</sup> mice. To test whether atypical E2Fs can also function as oncogenes independent of RB loss, we induced long-term overexpression of *E2f7* or *E2f8* in mice. E2F7 and -8 overexpression increased the incidence of tumors in the lungs, but not in other tissues. Collectively, these data show that atypical E2Fs can promote but also inhibit tumorigenesis depending on tissue type and RB status. We propose that the complex interactions between atypical E2Fs and RB on maintenance of genetic stability underlie this context-dependency.



## INTRODUCTION

The CDK/RB/E2F axis is the core of G1-S regulation, and thus is essential to ensure proper DNA replication (1). Upon growth factor signaling, RB gets hyperphosphorylated by Cyclin-CDK complexes and releases the activator E2Fs to induce cell cycle entry. In contrast, the hypophosphorylated form of RB maintains cells in G1 (2). This notion classifies RB as a cell-proliferation inhibitor. Consequently, mutations affecting RB are frequently encountered in a wide array of human cancers (3,4). RB binds and inhibits activator E2Fs via a motif known as the pocket domain. Two other proteins, p107 and p130, possess such pocket domains, and like Rb, also appear to regulate cell cycle progression. However, these other two pocket proteins are rarely mutated in tumors (5-8). The growth-suppressive properties of RB are thought to be largely dependent on its ability to interact with E2Fs, but also non-canonical functions have been described (9). RB loss leads to untimely release of activator E2Fs and consequently to upregulation of E2F dependent transcription. This contributes to unscheduled S-phase entry, genomic instability, and eventually cancer progression (10,11).

However, apart from RB (and the related pocket proteins P107 and P130), E2F-dependent transcription is also negatively regulated by repressor E2F family members. In cycling cells, this function is mainly carried out by E2F7 and -8, also known as atypical E2F repressors (12). Unlike canonical E2Fs, E2F7 and E2F8 lack a pocket protein binding domain and possess an additional DNA binding domain, which suggests that their repressor functions occur independent of RB (13-17). Moreover, these atypical E2F members redundantly regulate expression of the E2F target genes during late S- and G2 phase, unlike RB/canonical E2Fs which mainly control the G1/S transition (18-20). To date, it is unknown if and how these two seemingly independent E2F-inhibitory mechanisms interact *in vivo*. In fact, inactivation of RB leads to upregulation of E2F7 and -8 in liver tumorigenesis and cellular senescence (21). This notion suggest that atypical E2Fs could potentially compensate for the loss of RB. In addition, both RB and atypical E2Fs are thought to play important roles in mediating DNA repair and cell cycle arrest in response to genotoxic reagents (22-29). Hence, to fully understand how control of E2F-dependent transcription affects tumorigenesis, their genetic interaction must be studied *in vivo*.

Here, we employed multiple different transgenic and knockout mouse models to study how atypical E2Fs affect tumorigenesis driven by RB loss. We found that loss of atypical E2Fs accelerated the onset of liver tumors but delayed pituitary tumorigenesis in Rb-deficient cells. Moreover, we found enhanced lung tumor formation in transgenic mice with chronic overexpression E2F7 or -8. Thus, atypical E2Fs appear to play a dual role as tumor promoters or protectors and can either compensate or aggravate the tumorigenic effect of RB loss, depending on tissue context.

## MATERIAL AND METHODS

### Animal experiments

Animal experiments were approved by the Utrecht University Animal Ethics Committee and performed according to institutional and national guidelines. E2f7 and E2f8 knockout mice and doxycycline-inducible transgenic lines were already present in the lab (30,31). Albumin-Cre mice were derived from Jackson laboratory. *Rb* conditional knockout mice were provided by Dr. A. Berns (Netherlands Cancer Institute, Amsterdam, The Netherlands). Mice from Figures 1–3 were bred into FVB (Figure 1–2: 5th FVB generation; Figure 3: 15th FVB generation) while transgenic mice were maintained on a mixed genetic background 129/Sv (25%) × C57Bl/6 (25%) × FVB (50%) background. Doxycycline (2 g/kg) was administered ad libitum in pellets to all experimental transgenic mice (Bio Services). BrdU (858811, Sigma-Aldrich) was injected intraperitoneally 2h prior to euthanasia in doses of 30 µg/g for 4weeks-old mice.

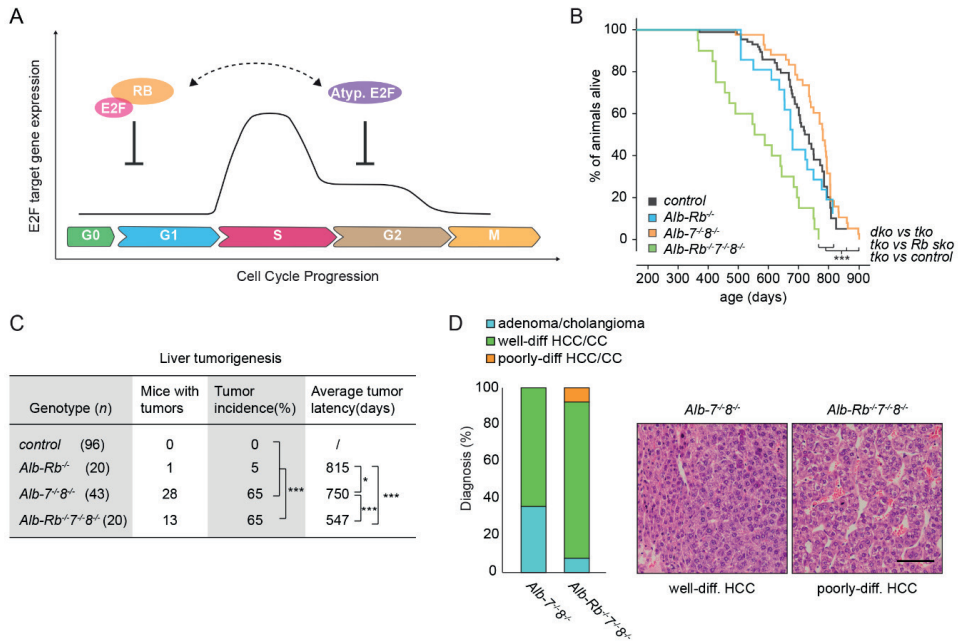
### Flow cytometry

Liver or tumor cell suspensions were prepared from fresh or frozen tissues followed by fixation in 70% ethanol overnight at 4°C. Cells were washed in PBS and then treated with pepsin (0.5mg/ml and 0.1N in HCl) to isolate hepatocyte nuclei. Nuclei were stained with anti-BrdU-FITC (Becton Dickinson, 347583, 1:250) and/or propidium iodide (5µg/ml PI and 250µg/ml RNase in PBS) and analyzed with a FACS Calibur flow cytometer (Becton Dickinson) and BD CellQuest Pro software.

### Immunohistochemistry and histological analysis

Immunohistochemical staining was performed on formalin-fixed and paraffin embedded tissues with a thickness of 4 µm. Endogenous peroxidase activity was blocked with 1% H<sub>2</sub>O<sub>2</sub>. We used 10 mM Citrate buffer (pH 6) for heat-induced antigen retrieval. Sections were stained with standard hematoxylin and eosin (HE). For immunohistochemistry analysis, this involved: anti-Ki67 (Biogenex, MU297-UC; 1:75 in PBS), anti-EGFP (Abcam, Ab6673; 1:800 in PBS), anti γH2AX (Cell signaling, S139, 1:500 in PBS), and anti-Caspase 3 (R&D systems, AF835; 1:400 in PBS). Secondary antibodies were biotinylated. Vectastain Elite ABC reagents (Vector Labs) were used according to the manufacturer's instructions. Slides were counterstained with hematoxylin. Images were taken using a DP25 camera, Labsens soft imaging version 1.1, and Olympus BX45 microscope.

All the HE slides were analyzed by board certified veterinary pathologists (LB, LH and AdB) according to corresponding nomenclature and diagnostic criteria. Quantification of Ki67 in liver slides represents the average of Ki67 positive cells in 5 fields using 40× objective for each condition (non tumor vs. tumor/genotype). Total number of Ki67 positive cells in 5 fields using 40× objective was quantified per lung tumor nodule.



**▲Figure 1: Atypical E2Fs and RB cooperate to prevent liver cancer.** (A) Schematic representation of the regulation of E2F dependent transcription by RB and atypical E2Fs in the cell cycle. (B) Kaplan-Meier overall survival curves of control ( $n=96$ ), *Alb-Rb*<sup>-/-</sup> (Rb sko;  $n=20$ ), *Alb-7<sup>-/-</sup>8<sup>-/-</sup>* (dko;  $n=43$ ) and *Alb-Rb*<sup>-/-</sup>*7<sup>-/-</sup>8<sup>-/-</sup>* (tko;  $n=20$ ) mice. (C) Table indicating tumor incidence (%) and tumor latency (days) of the indicated genotypes at the end of life span. (D) Histological classification of tumors from *Alb-7<sup>-/-</sup>8<sup>-/-</sup>* ( $n=28$ ) and *Alb-Rb*<sup>-/-</sup>*7<sup>-/-</sup>8<sup>-/-</sup>* ( $n=13$ ) mice. In the right representative pictures of well and poorly differentiated HCC tumors. Scale bar: 50 $\mu$ m.

Data information: In (B and C); \*  $p<0.05$ , \*\*\* $p<0.001$  (Log Rank Mantel-Cox test and Chi-square (tumor incidence)).

## RNA isolation, cDNA and qPCR

RNA isolation, cDNA synthesis and quantitative PCR were performed based on manufacturer's instructions for QIAGEN (RNeasy Kits), Thermo Fisher Scientific (cDNA synthesis Kits) and Bio-Rad (SYBR Green Master Mix), respectively. Reactions were performed in duplicate and relative amount of cDNA was normalized to house-keeping genes indicated on figure legends using the  $\Delta\Delta C_t$  method. Sequences of primers used for qPCR listed on Supplemental Table 2.

## RNA sequencing

Total RNA was isolated from livers using the RNeasy Kit (Qiagen). We used 4 livers per condition. To deplete for ribosomal RNA, 5 $\mu$ g of total RNA was used to isolate Poly(A) RNA using poly (A)purist MAG kit (Life Technologies, AM1922) followed by purification using



mRNA only eukaryotic mRNA isolation kit (Illumina, MOE41024). Purified mRNA was used to construct transcriptome libraries using SOLiD total RNA-seq kit (Applied Biosystems Life Technologies, 4445374) using manufacturers' instructions for low input. Size selected cDNA was amplified, barcoded, and subsequently sequenced using a 5500 W Series Genetic Analyzer (Fisher Scientific) to produce 40-bp-long reads. Sequencing reads were mapped against the reference genome (mm9, NCBI37) using BWA (-c -l 25 -k 2 -n 10) software. Gene count tables were then made using FeatureCounts (32). The R package DESeq2 was used to call differentially expressed genes between controls and knock-out tumor samples with a Benjamini-Hochberg-adjusted *p* value of less than 0.05 (33). Heatmaps were generated using the R package pheatmap. GEO accession number: GSE172508.

## Statistics

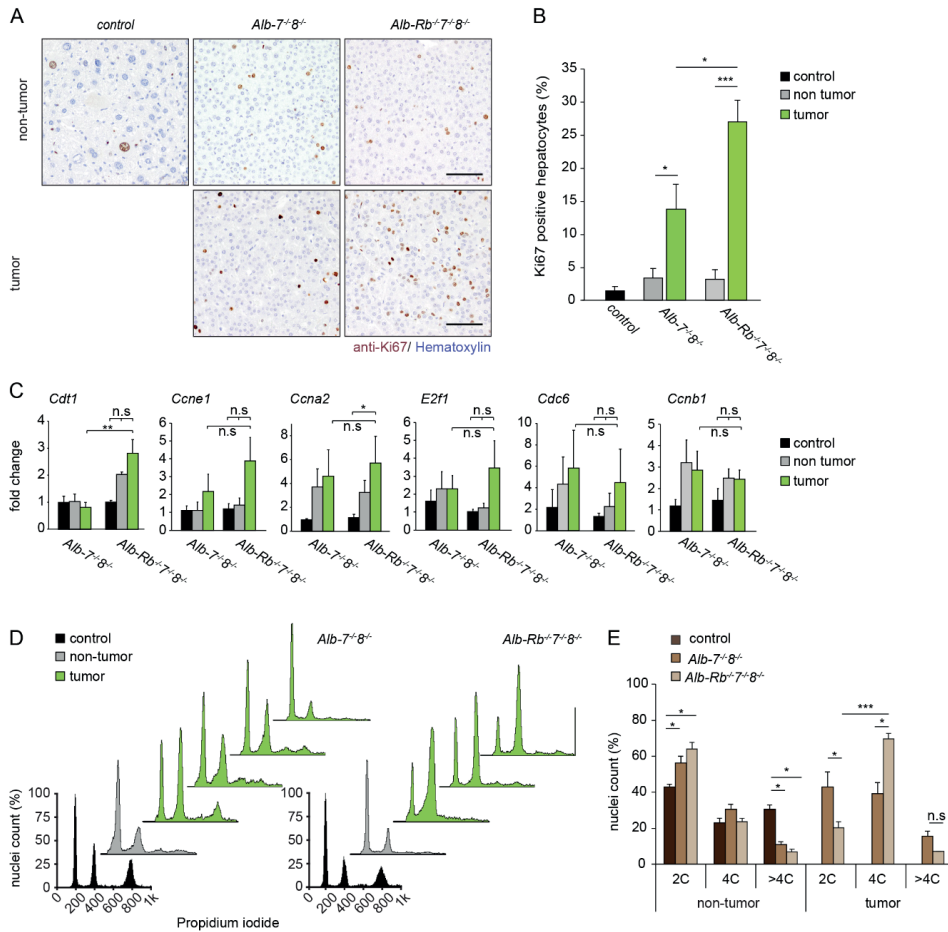
The number of mice and the specific statistical tests for each figure are indicated in the legends. All statistical analyses were performed using SPSS statistical package or SigmaPlot 13.0 software. Asterisks indicate where significant differences were seen. Where relevant for understanding the figure and individual comparisons, we indicate with "n.s." that significance was not reached.

## RESULTS

### RB and atypical E2F cooperate to prevent liver cancer.

Previous studies showed that loss of RB enhanced tumor formation in livers exposed to the hepatocarcinogen diethylnitrosamine (DEN)(34). Those tumors expressed high levels of RB/E2F target genes, indicating that tumorigenesis in RB deficient livers may result from the deregulation of E2F dependent transcription. Atypical E2Fs are downstream targets of RB and their expression is frequently increased in tumors. Paradoxically, atypical E2Fs act as tumor suppressors in the liver (10,31). Therefore, we asked whether atypical E2Fs could at least in part compensate for the loss of RB, via repression of E2F-responsive genes (Figure 1A). Thus, deletion of E2f7 and -8 would exacerbate the formation of Rb-deficient liver tumors. To test this hypothesis, we conditionally deleted E2f7, E2f8, and Rb (*Alb-Rb<sup>-/-</sup>E2f7<sup>-/-</sup>E2f8<sup>-/-</sup>*) in murine livers using the Cre/LoxP transgenic approach under the control of the hepatocyte-specific albumin promoter (*Alb-Cre*). We then compared lifespans and spontaneous liver tumor incidence of these triple knockout mice with E2f7 and E2f8 double knockout (*Alb-E2f7<sup>-/-</sup>E2f8<sup>-/-</sup>*), Rb single knockout (*Alb-Rb<sup>-/-</sup>*), and control littermates (Supplemental Figure S1A). Mice were either found dead, or were euthanized when they were moribund. Deletion of atypical E2fs or Rb alone did not significantly alter the lifespan, but *Alb-Rb<sup>-/-</sup>E2f7<sup>-/-</sup>E2f8<sup>-/-</sup>* mice, namely males, lived significantly shorter lives than control mice, *Alb-Rb<sup>-/-</sup>* mice, and *Alb-E2f7<sup>-/-</sup>E2f8<sup>-/-</sup>* mice (Figures 1B and Supplemental S1B). Post-mortem analysis of the livers showed that 65% of *Alb-Rb<sup>-/-</sup>E2f7<sup>-/-</sup>E2f8<sup>-/-</sup>* mice had liver tumors, whereas only one *Rb<sup>-/-</sup>* single knockout mouse





**▲Figure 2: Combined loss of E2F7/8 and RB results in rapidly proliferating liver tumors. (A)** Representative pictures of Ki67 showing proliferating cells in non-tumor and tumor areas of livers from the indicated genotypes. Tumors were collected at the end of life span. Scale bars: 50µm. **(B)** Quantification of Ki67 immunohistochemistry in 5 fields (40x objective) in tumor and adjacent non tumor areas of the livers from the indicated genotypes. Controls represent Alb-Cre negative littermates analyzed at the same time point as Alb-Cre positive ones. The data are presented as average ±SEM (1 tumor analyzed /mouse; n= 6-7 mice). **(C)** Transcript levels of E2F target genes in the indicated areas from *Alb-7<sup>-</sup>8<sup>-</sup>* and *Alb-Rb<sup>-</sup>7<sup>-</sup>8<sup>-</sup>* mice. Fold changes were adjusted to average of controls and *Actb* and *Gapdh* were used to normalize the expression. Data represent average ± SEM (n= 5-6 mice). **(D)** Representative cell cycle profiles analyzed by flow cytometry of the indicated areas and genotypes. **(E)** Quantification of nuclei from the cell cycle profiles in D. Data represent average ± SEM (n= 3-5). Data information: In **(B)** \*p<0.05, (Mann-Whitney Rank Sum test); **(C and E)** \*p<0.05, \*\*p<0.01, \*\*\*p<0.001 (One Way ANOVA).

carried a liver tumor (Figure 1C). There was a strong gender bias in liver tumor incidence, because nearly all tumors were seen in males (Supplemental Figure S1C). This suggests that male *Alb-Rb<sup>-/-</sup>7<sup>-/-</sup>8<sup>-/-</sup>* mice develop tumors earlier than *Alb-7<sup>-/-</sup>8<sup>-/-</sup>* mice. Indeed, *Alb-7<sup>-/-</sup>8<sup>-/-</sup>* mice also developed liver tumors at the same incidence rate, however the tumor latency was longer compared to *Alb-Rb<sup>-/-</sup>7<sup>-/-</sup>8<sup>-/-</sup>* (Figure 1C and Supplemental Figure S1D). These findings indicate that addition deletion of RB in E2F7/8 deficient liver has no major impact on tumor initiation, but results in enhanced tumor progression. Histopathology analysis revealed that *Alb-Rb<sup>-/-</sup>7<sup>-/-</sup>8<sup>-/-</sup>* mice had an increased incidence of malignant liver tumors (hepatocellular carcinomas) compared to *Alb-7<sup>-/-</sup>8<sup>-/-</sup>* mice, although this difference did not reach statistical significance (Figure 1D). Most HCCs were well differentiated, but 10% of those HCCs in *Alb-Rb<sup>-/-</sup>7<sup>-/-</sup>8<sup>-/-</sup>* mice were poorly-differentiated, suggesting a faster progression. Body and liver weights did not significantly differ between *Alb-7<sup>-/-</sup>8<sup>-/-</sup>* and *Alb-Rb<sup>-/-</sup>7<sup>-/-</sup>8<sup>-/-</sup>* mice (Supplemental Figure S1E,F). No other pathologies were observed in the livers of the male *Alb-Rb<sup>-/-</sup>7<sup>-/-</sup>8<sup>-/-</sup>* mice, suggesting that their decreased lifespan was directly related to the liver tumors seen in these mice.

Together, these data show that atypical E2Fs cooperate with RB to suppress liver cancer and that their combined loss causes liver cancer-associated mortality.

### **Loss of RB results in enhanced proliferation and deregulation of cell cycle control in atypical E2F-deficient liver tumors.**

We performed immunohistochemical analysis of Ki67 expression in the tumors and the adjacent normal liver tissues. This analysis revealed a significant increase in percentage of Ki67 positive hepatocytes in *Alb-Rb<sup>-/-</sup>7<sup>-/-</sup>8<sup>-/-</sup>* and *Alb-7<sup>-/-</sup>8<sup>-/-</sup>* tumors compared to adjacent non-tumor tissue (Figure 2A,B). Furthermore, *Alb-Rb<sup>-/-</sup>7<sup>-/-</sup>8<sup>-/-</sup>* liver tumors showed significantly higher levels of Ki67-positive cells than those from *Alb-7<sup>-/-</sup>8<sup>-/-</sup>* mice, indicating that additional deletion of Rb enhanced proliferation of tumor cells.

The growth-suppressive properties of RB are thought to be largely dependent on its ability to interact with E2F1/2/3 to regulate E2F-dependent transcription, although non-canonical functions have been described (9). Importantly, we showed previously that the main tumor suppressive mechanism of atypical E2Fs is their repressive function on E2F-dependent transcription (10,31). We therefore investigated whether the enhanced proliferation and tumorigenesis in the triple-knockout mice could be explained by further deregulation of E2F dependent transcription in those livers. Firstly, we analyzed proliferation and E2F target gene expression in juvenile livers, when tumors are not yet present and the proliferation rate of hepatocytes is high. The DNA replication rates, shown by BrdU incorporation, were increased in *Alb-Rb<sup>-/-</sup>7<sup>-/-</sup>8<sup>-/-</sup>* compared to *Alb-7<sup>-/-</sup>8<sup>-/-</sup>* livers (Supplemental Figure S2A). However, a similar increase was seen when comparing the Cre-negative littermates of *Alb-Rb<sup>-/-</sup>7<sup>-/-</sup>8<sup>-/-</sup>*

livers to *Alb-7<sup>-/-</sup>8<sup>-/-</sup>* livers, indicating that additional deletion of Rb was not responsible for an increase in DNA replication at 4 weeks of age (Supplemental Figure S2A). Consistently, E2F target gene expression was not increased in juvenile *Alb-Rb<sup>-/-</sup>7<sup>-/-</sup>8<sup>-/-</sup>* livers compared to *Alb-7<sup>-/-</sup>8<sup>-/-</sup>* livers (Supplemental Figure S2B). We then analyzed the expression of multiple E2F-dependent genes in tumor and adjacent tumor areas. Consistent with our observations in the juvenile mice, there was not a significant up-regulation in *Alb-Rb<sup>-/-</sup>7<sup>-/-</sup>8<sup>-/-</sup>* tumors compared to *Alb-7<sup>-/-</sup>8<sup>-/-</sup>* tumors, with the exception of the licensing factor Cdt1 (Figure 2C). To explore gene expression changes in an unbiased manner, we performed RNA sequencing analysis on non-tumor tissue from controls and *Alb-7<sup>-/-</sup>8<sup>-/-</sup>* and *Alb-Rb<sup>-/-</sup>7<sup>-/-</sup>8<sup>-/-</sup>* tumors. Pathway analysis of differentially expressed genes in the tumor samples revealed up-regulation of genes associated with cell cycle and cancer-related signaling pathways in tumors of both genotypes compared to wild-type control livers (Supplemental Figure S2C). Downregulated pathways were mostly involved in energy metabolism (Supplemental Figure S2C). Strikingly, we only identified 44 genes which were significantly differentially expressed between *Alb-Rb<sup>-/-</sup>7<sup>-/-</sup>8<sup>-/-</sup>* and *Alb-7<sup>-/-</sup>8<sup>-/-</sup>* tumors compared to controls, indicating that these tumors are remarkably similar (Supplemental Figure S2D and Supplemental Table 1). We then plotted expression of a panel of well-described E2F target genes. This analysis did not reveal differences between the tumor samples from *Alb-Rb<sup>-/-</sup>7<sup>-/-</sup>8<sup>-/-</sup>* and *Alb-7<sup>-/-</sup>8<sup>-/-</sup>* livers, consistent with the qPCR data shown in (Supplemental Figure S2E). Together, these data indicate that the cooperation between RB and atypical E2Fs in tumor suppression extends beyond compensatory E2F target gene repression.

Next, we determined whether the combined deletion of Rb/E2f7/8 changed the polyploidization status and cell cycle profile of hepatocytes, since these cell cycle genes have been shown to control liver cell polyploidization and cell cycle progression. Previous studies demonstrated that loss of RB enhances liver cell polyploidization, whereas ablation of E2F7/8 prevents polyploidization (34,35). Consistent with previous studies, our *Alb-7<sup>-/-</sup>8<sup>-/-</sup>* juvenile livers showed a marked reduction of 4C and 8C nuclei compared to control littermates (Supplemental Figure S2F). Remarkably, we found a similar ploidy reduction in juvenile *Alb-Rb<sup>-/-</sup>7<sup>-/-</sup>8<sup>-/-</sup>* triple knockout hepatocyte nuclei (Supplemental Figure S2F), indicating that atypical E2Fs counteract RB in regulating liver cell polyploidization. We then analyzed the ploidy status in liver tumors and their adjacent normal tissue. In line with the observations in the juvenile mice, *Alb-7<sup>-/-</sup>8<sup>-/-</sup>* and *Alb-Rb<sup>-/-</sup>7<sup>-/-</sup>8<sup>-/-</sup>* hepatocytes remained mostly diploid in non-tumor areas. Interestingly, in liver tumors, we observed an altered cell cycle profile marked by an increase of 4C cell populations in *Alb-Rb<sup>-/-</sup>7<sup>-/-</sup>8<sup>-/-</sup>* tumors compared to *Alb-7<sup>-/-</sup>8<sup>-/-</sup>* tumors (Figure 2D,E). Tetraploidization or presence of G2-like cells could represent an early event in the tumorigenesis of *Alb-Rb<sup>-/-</sup>7<sup>-/-</sup>8<sup>-/-</sup>* livers, indicating enhanced genomic instability. To explore whether genomic instability was enhanced in *Alb-Rb<sup>-/-</sup>7<sup>-/-</sup>8<sup>-/-</sup>* tumors, we plotted a gene signature related to chromosomal instability (36). This signature contains

many genes involved in G2/M progression. Although expression of this signature was increased in most tumors compared to wild type livers, we did not observe a difference between *Alb-Rb<sup>-/-</sup>7<sup>-/-</sup>8<sup>-/-</sup>* and *Alb-7<sup>-/-</sup>8<sup>-/-</sup>* tumors (Supplemental Figure S2G), consistent with our notion that the emergence of 4C cells had been an early event. In line with this, DNA damage, measured by quantification of  $\gamma$ H2AX-positive hepatocytes, was not different between *Alb-Rb<sup>-/-</sup>7<sup>-/-</sup>8<sup>-/-</sup>* and *Alb-7<sup>-/-</sup>8<sup>-/-</sup>* tumors (Supplemental Figure S2H).

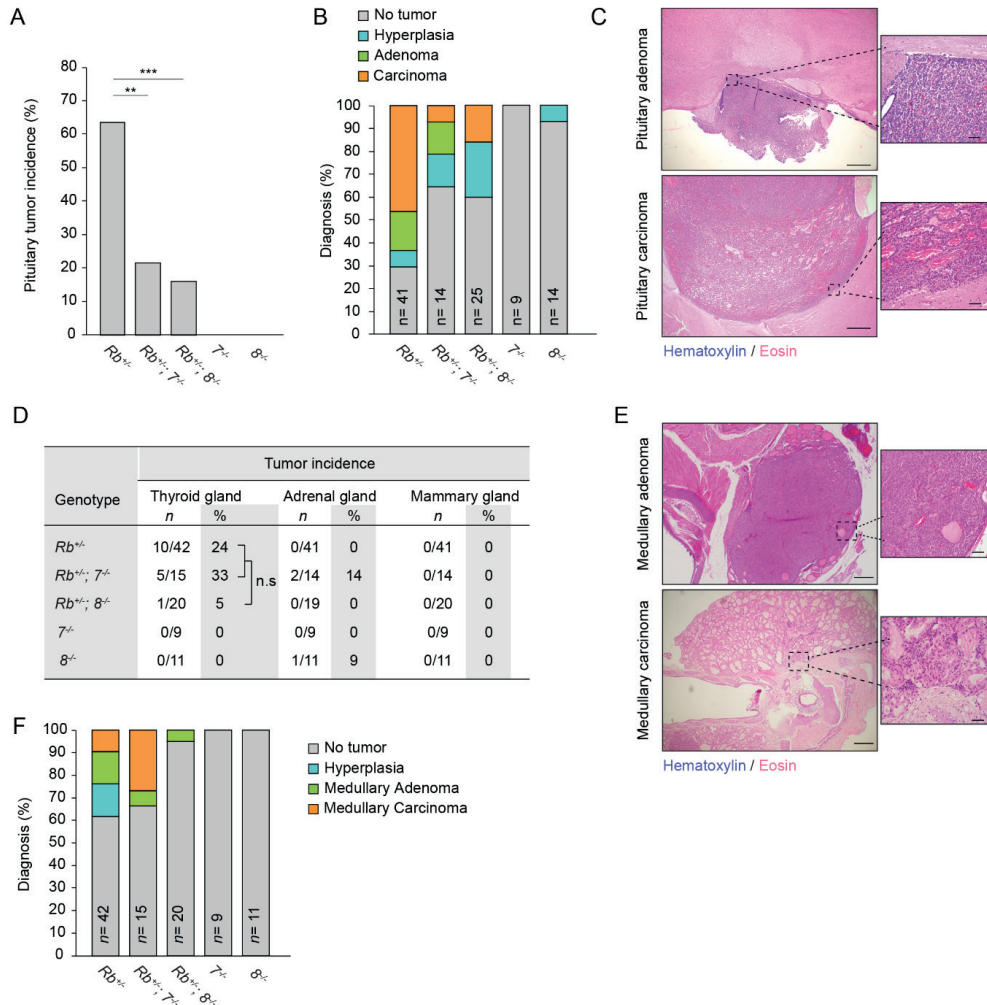
Previous studies have shown that deletion of Rb in livers can cause defects in mitotic entry and activation of the DNA damage checkpoint (37). Furthermore, the E2F7/8 loss can cause defects in the DNA damage checkpoint (38). Thus, combined loss of RB and atypical E2Fs could cause altered cell cycle fates of damaged cells to eventually promote tumorigenesis.

Together, our data demonstrate that atypical E2Fs act as tumor suppressors and negative regulators of proliferation in RB-null livers. Although they are active during different phases of the cell cycle, Rb during G1/S transition and atypical E2Fs during S/G2 (Figure 1A), their combined action could be required to maintain genomic integrity and prevent oncogenesis in the liver.

### **E2F7 and -8 promote tumorigenesis in pituitary gland of Rb<sup>+/-</sup> mice.**

We next sought to investigate if the genetic interaction between RB and atypical E2Fs would be different in other tissues. To this end, we investigated the consequences of E2F7 and E2F8 loss in *Rb<sup>+/-</sup>* mice, a well-established loss-of-heterozygosity model characterized by the emergence of tumors in the pituitary and thyroid glands. Because global combined deletion of *E2f7* and *E2f8* results in embryonic lethality due to a placental phenotype (30,39), we crossed conventional knock-out mice with single homozygous deletion of *E2f7* or *E2f8* with *Rb<sup>+/-</sup>* mice to generate the following experimental cohorts: *Rb<sup>+/-</sup>*; *Rb<sup>+/-</sup>7<sup>-/-</sup>*; *Rb<sup>+/-</sup>8<sup>-/-</sup>*; *7<sup>-/-</sup>* and *8<sup>-/-</sup>* mice. We performed a cross-sectional pathology study at the age of 14 months. Consistent with previous reports, a high percentage of adult *Rb<sup>+/-</sup>* mice developed spontaneous pituitary tumors. Surprisingly, additional deletion of *E2f7* or *E2f8* resulted in significantly lower pituitary tumor incidence compared to *Rb<sup>+/-</sup>* mice (Figure 3A). Mice with single deletion of *E2f7* or -8 did not develop any spontaneous pituitary tumors.

We further examined those pituitary tumors by performing pathological analysis. Histology showed that the pituitary glands of single E2f7 (*7<sup>-/-</sup>*) or E2f8 (*8<sup>-/-</sup>*) mutant littermates appeared completely normal (Supplemental Figure S3A). The histological features of *Rb<sup>+/-</sup>* pituitary tumors were entirely consistent with previous studies where carcinomas originated from the intermediate lobe were highly prevalent (40) (Supplemental Figure S3B). The percentage of malignant tumors was reduced in *Rb<sup>+/-</sup>7<sup>-/-</sup>* and *Rb<sup>+/-</sup>8<sup>-/-</sup>* compared to *Rb<sup>+/-</sup>* mice (Figure 3B,C). These results strongly suggest that E2F7 and -8 might act as oncogenes in Rb-deficient pituitaries.



**▲Figure 3: E2F7 and -8 promote tumorigenesis in pituitary glands with RB loss. (A)** Pituitary tumor incidence (%) in 14 months old mice from the indicated genotypes. Data collected from  $Rb^{+/+}$  n= 41;  $Rb^{+/-}$ ,  $7^{-/-}$  n= 14;  $Rb^{+/-}$ ,  $8^{-/-}$  n=25;  $7^{-/-}$  n= 9;  $8^{-/-}$  n= 14. **(B)** Histological diagnoses of pituitary glands from A. **(C)** Representative images of histological features of pituitary tumors. Scale bars: left picture 500 $\mu$ m; right 50  $\mu$ m. **(D)** Microscopic tumor incidence of additional neuroendocrine glands from mice in A. **(E)** Representative images of histological features of thyroid tumors. Scale bars: left picture 500 $\mu$ m; right 50  $\mu$ m. **(F)** Histological diagnoses of thyroid tumors from E. Data information: In **(A and D)**; n.s not significant, \* $p < 0.05$ , \*\* $p < 0.01$ , \*\*\* $p < 0.001$  (chi-square)

Beside pituitary tumors,  $Rb^{+/-}$  mice are also predisposed to develop c-cell hyperplasia, which subsequently can progress into medullary thyroid carcinomas (41,42). We therefore also histologically examined the incidence of hyperplasia and tumorigenesis in the thyroid gland

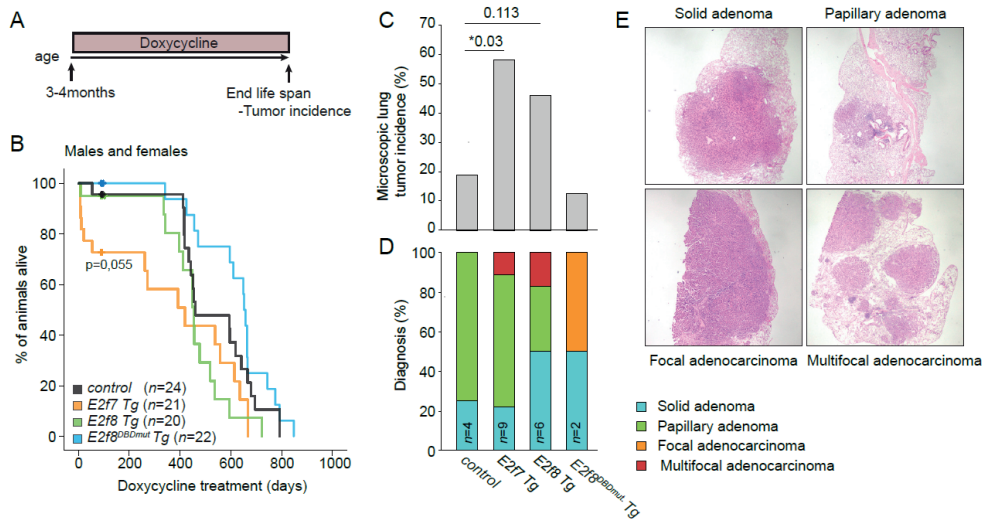
and other glands, namely adrenal and mammary glands. We observed a slight trend, although not a significant one, of increased thyroid tumor incidence in  $Rb^{+/-}7^{-/-}$  compared to  $Rb^{+/-}$  mice (Figure 3D). The opposite trend occurred in  $Rb^{+/-}8^{-/-}$  mice, where loss of E2F8 reduced the incidence of Rb-deficient thyroid tumors. Pathological analysis revealed that four out of the five  $Rb^{+/-}7^{-/-}$  tumor lesions were medullary thyroid carcinomas, suggesting that loss of E2F7 aggravates the malignant progression of Rb-deficient thyroid tumors (Figure 3E,F). We also analyzed the adrenals and mammary glands of these mice, but we only incidentally observed tumors, with no statistically increased incidence in any of the analyzed genotypes (Figure 3D). Early lesions (hyperplasia) were frequently encountered but there were no significant differences between genotypes (Supplemental Figure S3C). Overall, these data demonstrate that E2F7 and E2F8 clearly contribute to the tumor formation in the pituitary glands of  $Rb^{+/-}$  mice, while in the thyroid glands, loss of atypical E2Fs does not have a significant impact on RB loss dependent tumorigenesis. This demonstrates that the interaction between atypical E2Fs and RB is highly tissue-specific.

### **E2F7 and -8 overexpression promotes spontaneous lung tumorigenesis.**

Having discovered that atypical E2Fs can have oncogenic functions in a Rb-mutant background, we asked if overexpression of E2F7 or -8 by itself could be sufficient to drive tumorigenesis. Previously we developed E2f7 and E2f8 transgenic (Tg) mice capable of blocking the proliferation of chemically-induced hepatocellular carcinomas, consistent with their role as tumor suppressors in the liver (31). These mice carry ubiquitously expressed doxycycline-inducible E2f7/8 alleles. We now induced long-term overexpression of atypical E2Fs and analyzed tumor incidence in aged mice. We maintained a cohort of male and female control, E2f7, E2f8, and E2f8<sup>DBDmut</sup> Tg mice on lifelong doxycycline chow, starting from young adulthood- 3-4 months old (Figure 4A). E2f8<sup>DBDmut</sup> mice carrying mutations in both DNA-binding domains were included as an additional control group because they are transcriptionally inactive (31). Chronic E2F7 or E2F8 overexpression did not significantly affect lifespan, although we noticed that a subset of male and female E2f7 Tg mice died within the first weeks of doxycycline induction (Figure 4B and Supplemental Figure S4A).

Immunohistochemistry staining showed that transgenic E2F7-EGFP and E2F8-EGFP were mainly found in proliferative adult tissues (Supplemental Figure S4B). This is consistent with previous findings describing that E2F7/8 proteins are efficiently degraded in non-cycling cells (10,20). We also observed a decline in EGFP expression over time (Supplemental Figure S4C). This decrease in transgene expression can be explained by a decrease in overall proliferation rates during aging, but also by the negative selection pressure on transgenic cells caused by the antiproliferative effect of atypical E2Fs. Furthermore, we found increased





**▲Figure 4: E2F7 or -8 overexpression promotes spontaneous lung tumorigenesis. (A)** Experimental scheme of the long-term induction of E2F7 and -8 in the transgenic mice. **(B)** Kaplan-Meier overall survival of males and females *control* (n=24); *E2f7* Tg (n=21); *E2f8* Tg (n=20); *E2f8<sup>DBDmut</sup>*. Tg (n= 22) mice. **(C)** Microscopic lung tumor incidence in the indicated genotypes of mice euthanized at the end of life-span. *Control* (n=16); *E2f7* Tg (n=12); *E2f8* Tg (n=13); *E2f8<sup>DBDmut</sup>*. Tg (n= 16) mice. **(D)** Pathological analysis of the lung tumors. **(E)** Representative images of the different pathological diagnoses in E.

Data information: In **(B)** Log-rank Mantel-Cox test. In **(C and D)** n.s not significant, \*p<0.05 (chi-square).

apoptosis in small intestinal crypts of *E2f7* Tg mice treated for 3 months with doxycycline (Supplemental Figure S4D), which could also contribute to the lower number EGFP positive cells observed in aged Tg mice. Thus, inhibition of cell proliferation in intestinal epithelium and other rapidly dividing tissues, could at least partially explain why some *E2f7* Tg mice presented early lethality (Figure 4B and Supplemental Figure S4A).

To initially screen for tumors, we performed necropsy on *control*, *E2f7*, *E2f8*, and *E2f8<sup>DBDmut</sup>* Tg mice. Interestingly, we observed an increased presence of tumors in the lungs of transgenic mice, but not in any other organ (Supplemental Figure S5A). To confirm and quantify this observation, we performed microscopic analysis of at least 5 different lung sections per mouse. Both *E2f7* and *E2f8* Tg mice indeed presented a higher microscopic lung tumor incidence than controls and *E2f8<sup>DBDmut</sup>* Tg (Figure 4C and Supplemental Figure S5B). Lung tumors are often observed in ageing mice, especially in the FVB strain (43), and these findings suggest that overexpression of atypical E2Fs may drive oncogenesis in some tumor-prone tissue contexts. Histopathology revealed that the vast majority of the tumors in all genotypes were focal adenomas with rather low proliferation rates (Supplemental Figure S5C). Nonetheless, we



found a few cases of more aggressive multifocal adenocarcinomas in *E2f7* and *E2f8* Tg mice, and not in the other genotypes shown in (Figure 4E,F). Importantly, *E2f8<sup>DBDmut</sup>* Tg mice, which carry mutations in the DNA binding domain of E2f8, did not show increased lung tumor incidence, which strongly suggests that the oncogenic action of atypical E2Fs in the lungs is due to mis-regulation of target gene transcription rather than due to another mechanism.

This raises the question of whether the E2F target gene expression was repressed or activated in the lung epithelium. To answer this, we analyzed target gene expression after 3 days of E2F7/8 induction in 21 year-old juvenile Tg mice for 3 days as previously described (31). Doxycycline caused an induction of *E2f7* Tg and *E2f8* Tg proteins, which was analyzed by EGFP-IHC staining, and mild repression of E2F target transcripts (Supplemental Figure S5D,E). These results show that long term in vivo overexpression of atypical E2Fs can promote tumor growth in the lungs, most likely via a mechanism involving transcriptional repression.

## DISCUSSION

The results presented here highlight the complexity of the E2F/RB pathway in tumorigenesis. Unrestrained E2F-dependent transcription is linked to tumor progression and poor prognosis in several cancer types. However, the consequences of deleting RB and atypical E2Fs—two independent mechanisms that both repress E2F-dependent transcription—were strikingly context and tissue-specific. While atypical E2Fs and RB cooperate to prevent liver tumorigenesis, they counteract each other in pituitary glands. In line with this, we revealed that long-term expression of atypical E2F enhances spontaneous lung tumorigenesis. This suggests that E2F7/8 can act as oncogenes besides their tumor suppressor functions.

Although surprising, our findings are consistent with previous studies that also revealed dual roles for other E2F family members. For example, various mouse models unequivocally showed that E2f1 and E2f3 can both act as tumor suppressors or oncogenes, depending on tissue context (10,41). But what determines the tissue specific functions of atypical E2Fs? In chemical-induced skin carcinogenesis, we previously showed that atypical E2Fs block tumorigenesis by mediating a cell cycle arrest in cells with unresolved DNA damage (11).

In the genetic models presented here, levels of genotoxic stress are much lower and possibly other downstream effects of atypical E2Fs come into play. In the liver, the maintenance of cell cycle checkpoints appears to be critical herein. We demonstrated previously that E2F7 and -8 suppress tumor growth in the liver via transcriptional repression of E2F targets and possibly through promoting polyploidization (10,31). Although RB loss in the liver results in elevated expression of the same target genes (22), the timing during the cell cycle is completely different (1,19,44). RB prevents cells from making the G1-S transition, whereas atypical E2Fs repress target genes during late S and G2. Hence atypical E2Fs are involved in the DNA damage checkpoint (18,45), whereas RB activates the G1/S checkpoint (1,46). Manipulating

both checkpoints by combined deletion of E2F7/8 and RB would thus further enhance the risk of genomic instability and cancer than either one of these interventions alone.

This checkpoint-based hypothesis does not explain our observations that E2f7 or E2f8 deletion prevented pituitary tumor formation in the *Rb*<sup>+/-</sup> model. It should be kept in mind this is a different tumor model, in which loss of heterozygosity (LOH) of the Rb gene is a key early event in the formation of pituitary tumors, whereas Rb is homozygously deleted in our Alb-Cre model. Therefore, it is possible that atypical E2Fs promote LOH in the pituitary tissue. Although it is difficult to experimentally address this possibility, previous studies showed that inhibition of DNA repair genes could cause LOH (47). This fits with our previous observations that E2F7 and -8 repress multiple DNA repair factors during G2 (18). However, it is not clear why the pituitary tissue would be so exquisitely sensitive to E2F7/8-induced LOH of the Rb locus. No other tissues in the *Rb*<sup>+/-</sup> mice showed evidence that E2F7/8 loss promoted LOH.

Our long-term E2F7/8 overexpression studies suggest that lung is another tissue in which atypical E2Fs can act as oncogenes in vivo. This is consistent with previous in vitro work claiming an oncogenic function of E2F8 in lung cancer cell lines (48). The question then arises if LOH plays a role in the emergence of the lung adenomas and adenocarcinomas in the *E2f7/8* Tg mice. Our Tg mice were bred one generation into the FVB background. FVB mice are more prone to develop these spontaneous lung tumors than other strains, suggesting a genetic predisposition (43). Possibly, FVB mice first acquire a heterozygous mutation in a key lung tumor suppressor gene, and LOH is an important second hit event for these tumors to appear. Therefore, LOH in this model is difficult to prove but again conceivable. Nevertheless, cell non-autonomous effects could also play a role in lung tumorigenesis. We reported before that *E2f7/8* Tg mice inhibits proliferation of rapidly dividing tissues. This could include white blood cells, and immunosurveillance of (pre-)malignant cells in the lungs could thus be impaired in *E2f7/8* Tg mice.

Taken together, the in vivo studies presented here indicate that atypical E2Fs and RB both control multiple mechanisms that are required to maintain genomic integrity. The importance of balancing E2F-dependent transcription extends far beyond controlling the G1/S transition and apoptosis. Its role in maintenance of genomic stability is highly complex and tissue-dependent. Moreover, we showed previously evidence that E2F-dependent transcription can be highly heterogeneous between single cancer cells (38). Therefore, it will be important to study how variation in E2F-dependent transcription in both RB-mutant and RB-intact tumors will affect for example prognosis and anti-cancer drug responses.

**Financial support:** This work was financially supported by the Dutch Cancer Society funding (KWF: UU2013-5777 & 11941/2018-2) to Bart Westendorp and Alain de Bruin, and Utrecht Life Sciences Infrastructure Grant (call 2014-I), and ZonMW grant 91116011.

**Acknowledgements:** We thank Prof. Jan van Deursen for the generation of the transgenic mice (Figure 4) and Wout Puijk and the rest of the animal caretakers for excellent care of our mice.

**Author contributions:** Conceptualization, E.M., S.K.P.; M.J.M.T, B.W, A.d.B.; Data curation, E.M.; Formal analysis, E.M., S.K.P.; M.J.M.T; Funding acquisition, B.W, A.d.B; Investigation, E.M., S.K.P.; M.J.M.T, L.B, L.H, E.v.L., B.W.; Methodology, E.M., S.K.P.; Project administration, A.d.B; Resources, E.M., S.K.P.; M.J.M.T and S.C.v.E.; Supervision, B.W, A.d.B; Validation, E.M., S.K.P.; Visualization, E.M.; Writing – original draft, E.M.; Writing – review & editing, S.K.P.; M.J.M.T, L.B, L.H, B.W, A.d.B.

## SUPPLEMENTARY MATERIAL

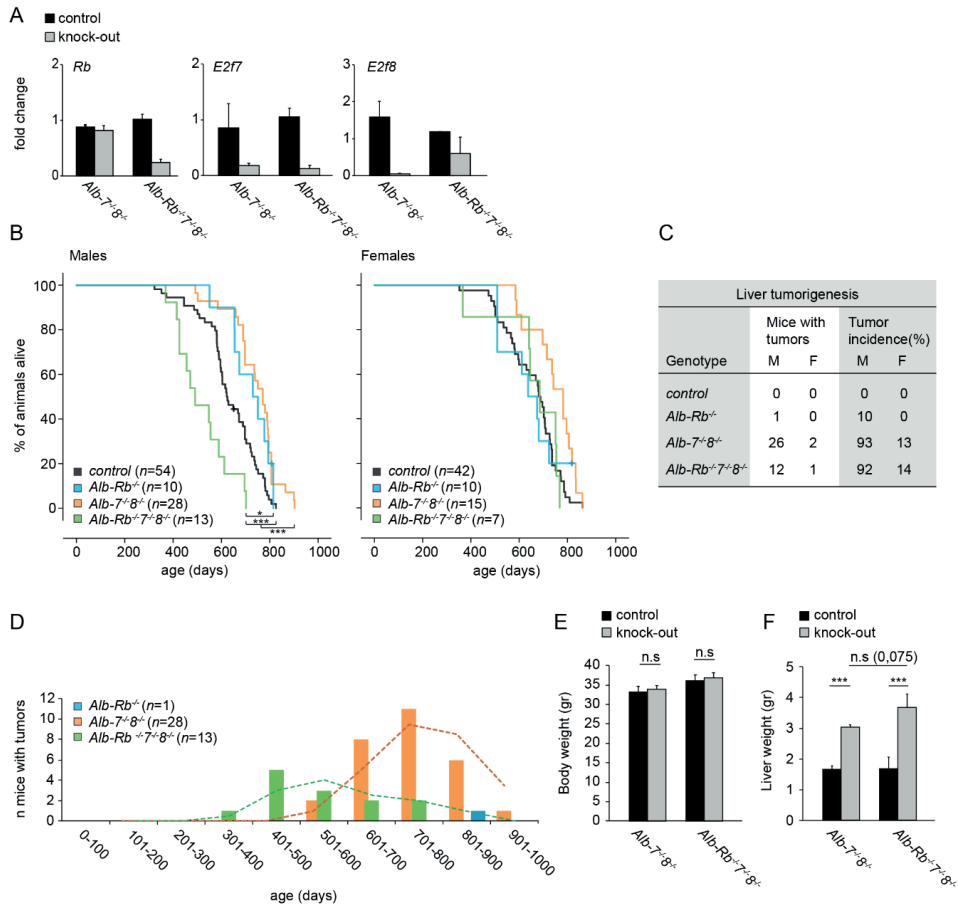
**Supplemental Table 1:** The table list the 44 differentially expressed genes that were significantly up- or down- regulated in *Alb-Rb<sup>-/-</sup>7<sup>-/-</sup>8<sup>-/-</sup>* versus *Alb- 7<sup>-/-</sup>8<sup>-/-</sup>* tumors.

Gene symbol	Gene name	Log2 fold change
<b>Upregulated</b>		
<i>Mbnl3</i>	Muscle blind-Like Splicing Regulator 3	2,37
<i>Tenn3</i>	Teneurin Transmembrane Protein 3	1,83
<i>Ttc30b</i>	Tetratricopeptide Repeat Domain 30B	1,60
<i>Ndufb7</i>	NADH: Ubiquinone Oxidoreductase Subunit B7	1,10
<i>Gpr19</i>	G protein-coupled receptor 19	1,08
<i>Tfap4</i>	Transcription factor AP-4	1,03
<i>Oaz1-ps</i>	Ornithine decarboxylase antizyme 1, pseudogene	0,93
<i>Fuom</i>	Fucose mutarotase	0,90
<i>Haus4</i>	HAUS augmin-like complex, subunit 4	0,75
<i>Tsen34</i>	tRNA splicing endonuclease subunit 34	0,74
<i>Cdk4</i>	Cyclin-dependent kinase 4	0,72
<i>Wdr6</i>	WD repeat domain 6	0,71
<i>Ptges2</i>	Prostaglandin E synthase 2	0,65
<i>Dip2a</i>	Disco interacting protein 2 homolog A	0,64
<i>Cpt1a</i>	Carnitine palmitoyltransferase 1A	0,63
<i>Zfp687</i>	Zinc finger protein 687	0,60
<i>Tshz1</i>	Teashirt zinc finger family member 1	0,55
<i>Dcaf8</i>	DDB1 and CUL4 associated factor 8	0,45
<b>Downregulated</b>		
<i>Son</i>	Son DNA binding protein	-0,38
<i>Nrd1</i>	Nardilysin, N-arginine dibasic convertase, NRD convertase 1	-0,48
<i>Nckap1</i>	NCK-associated protein 1	-0,75
<i>Abca5</i>	ATP-binding cassette, subfamily A (ABC1) member 5	-0,76
<i>Klhl7</i>	Kelch-like 7	-0,85
<i>Atg4c</i>	Autophagy related 4C, cysteine peptidase	-0,86
<i>Rb1</i>	RB transcriptional corepressor 1	-1,02
<i>Akr1d1</i>	Aldo-keto reductase family 1 member D1	-1,04
<i>Sult1d1</i>	Sulfotransferase family 1D member 1	-1,09
<i>Fmnl2</i>	Formin-like 2	-1,14
<i>Gdpd1</i>	Glycerophosphodiester phosphodiesterase domain containing 1	-1,31
<i>Fgl2</i>	Fibrinogen-like protein 2	-1,40
<i>Acmsd</i>	Amino carboxymuconate semialdehyde decarboxylase	-1,64
<i>Serpine1</i>	Serine (or cysteine) peptidase inhibitor, clade E, member 1	-1,80
<i>Tspan8</i>	Tetraspanin 8	-2,39
<i>Olfir1033</i>	Olfactory receptor 1033	-2,53

Gene symbol	Gene name	Log2 fold change
<i>Ostamp</i>	Osteoclast stimulatory transmembrane protein	-2,66
<i>Itih5</i>	Inter-alpha (globulin) inhibitor H5	-2,70
<i>Prom1</i>	Prominin 1	-2,77
<i>Phlda2</i>	Pleckstrin homology like domain, family A, member 2	-2,86
<i>Them7</i>	Thioesterase superfamily member 7	-2,94
<i>Adcy1</i>	adenylate cyclase 1	-3,20
<i>Hist1h1d</i>	H1.3 linker histone, cluster member	-3,24
<i>Tmprss4</i>	Transmembrane protease, serine 4	-3,29
<i>Afp</i>	Alpha fetoprotein	-3,43
<i>Col6a6</i>	Collagen, type VI, alpha 6	-3,72

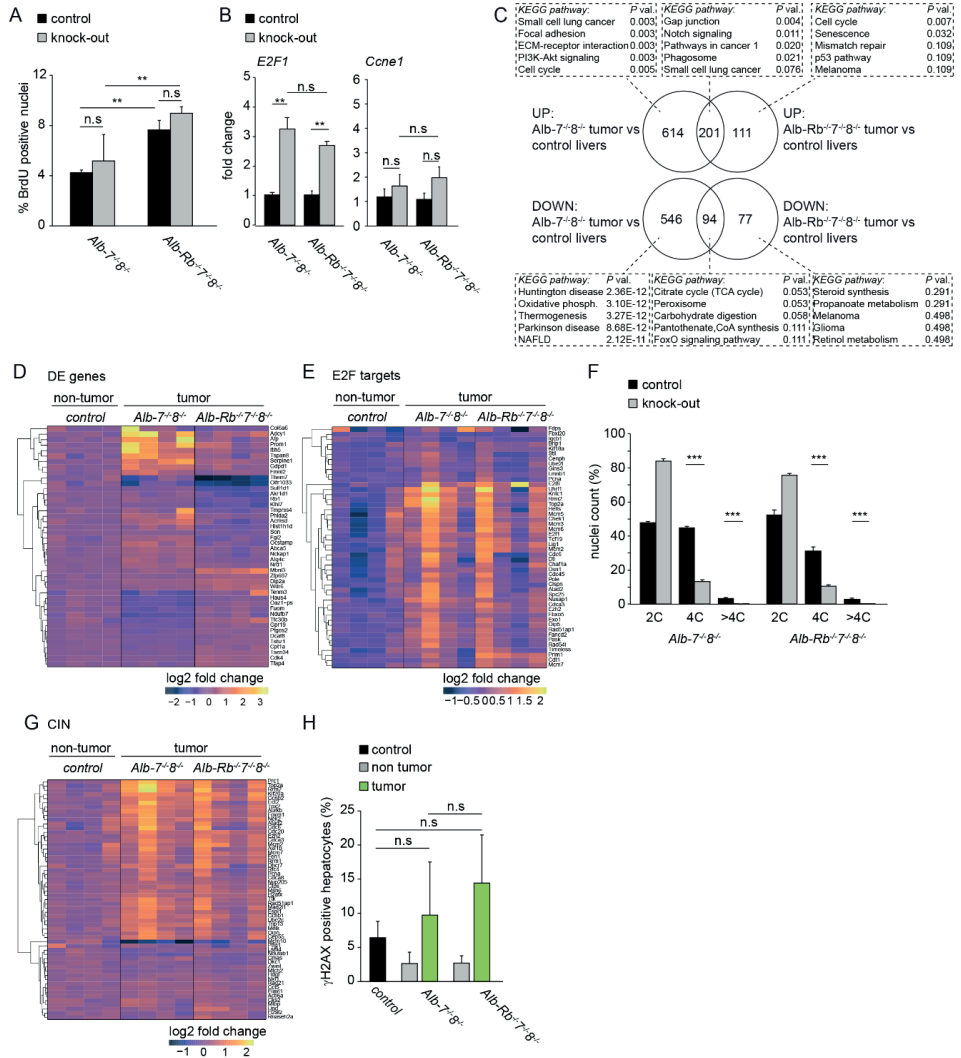
**Supplemental Table 2:** mouse qPCR primers

	<i>Forward primer (5'-3')</i>	<i>Reverse primer (3'-5')</i>
<i>Actb</i>	AGTCCTTCGTTGCCGGTCCA	TTTGCACATGCCGGAGCCGTTG
<i>Cdc6</i>	AGTTCTGTGCCCGCAAAGTG	AGCAGCAAAGAGCAAACCAGG
<i>Cdt1</i>	ACAGCCGGGCAAGATCCCCT	GGCTCCCAACTTCCGTGCC
<i>Ccnb1</i>	AAAGGGAAGCAAAAACGCTAGG	TGTTCAAGTTCAGGTTCAGGCTC
<i>Ccne1</i>	AGCGAGGATAGCAGTCAGCC	GGTGGTCTGATTTTCCGAGG
<i>Ccna2</i>	CTTCTTCCTTTTCCCTTGGC	TTTCAGAGTCCCAGTGACCC
<i>E2f1</i>	ACATCACCAATGTCCTGGAGGG	AGCCGCTTACCAATCCCCAC
<i>E2f7</i>	GATGCGTTCGTGAACTCCCTG	AGAAACTTCTGGCACAGCAGCC
<i>E2f8</i>	GAGAAATCCCAGCCGAGTC	CATAAATCCGCCGACGTT
<i>Gapdh</i>	GAAGTTCGGTGTGAACGG	TGAAGGGGTCGTTGATGG
<i>Mcm2</i>	TCTCTCTCAGCATCTAGCCCTG	AGACTCATCTTCAAATGGGGG
<i>Rad51</i>	CTCATGCGTCAACCACCAG	GCTTCAGGAAGACAGGGAGAG
<i>Rb1</i>	TCTCCAGGGTAACCATACTGC	CAAGGGAGGTAGATTTCAATGG



**▲ Supplemental Figure 1: Atypical E2Fs and RB cooperate to prevent liver cancer.** (A) Transcript levels of Rb, E2f7 and E2f8 from *Alb-7-/-8-/-* and *Alb-Rb-/-7-/-8-/-* mice in non-tumor areas. Fold changes were adjusted to average of controls and Actb, Gapdh and Rsp18 were used to normalize the expression. Data represent average  $\pm$  SEM ( $n=4-5$  mice). (B) Kaplan-Meier overall survival curves of males and females from control, *Alb-Rb-/-*, *Alb-7-/-8-/-* and *Alb-Rb-/-7-/-8-/-* mice. (C) Table indicating tumor incidence (%) of males and females of the indicated genotypes. Tumors collected at the end of life span. (D) Tumor latency distribution. Bar charts represent number of animals with tumors at the indicated age period. Dash lines indicate distribution of the data. (E) Body weights of control and *Alb-7-/-8-/-* and *Alb-Rb-/-7-/-8-/-* knock-out mice. Data represents average  $\pm$  SEM ( $n=15-20$  controls;  $n=20$  *Alb-Rb-/-7-/-8-/-* ko;  $n=10$  *Alb-7-/-8-/-* ko). (F) Liver weights of control and *Alb-7-/-8-/-* and *Alb-Rb-/-7-/-8-/-* ko mice. Data represents average  $\pm$  SEM ( $n=15-20$  controls;  $n=20$  *Alb-Rb-/-7-/-8-/-* ko;  $n=10$  *Alb-7-/-8-/-* ko).

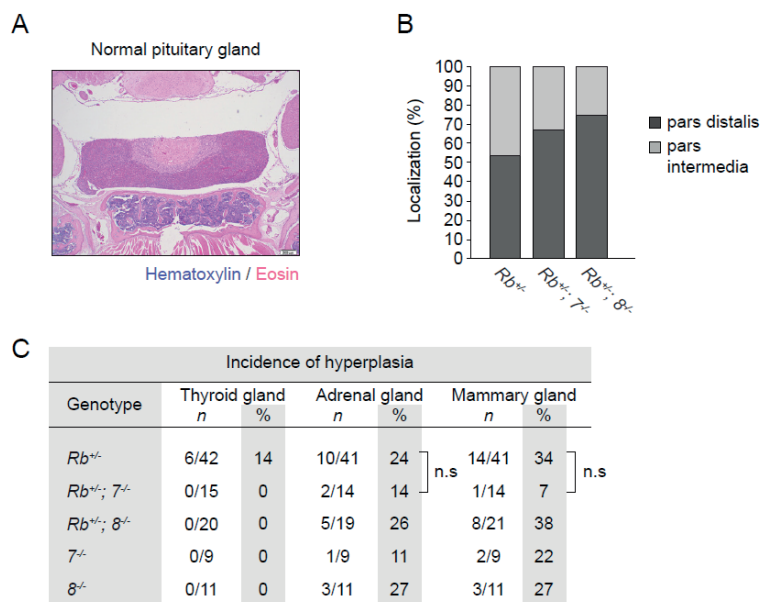
Data information: in (B: survival and C: latency) Log Rang (Mantel-Cox) test and in (E and F) Mann-Whitney Rank Sum test; n.s not significant, \* $p<0.05$ , \*\* $p<0.01$ , \*\*\* $p<0.001$



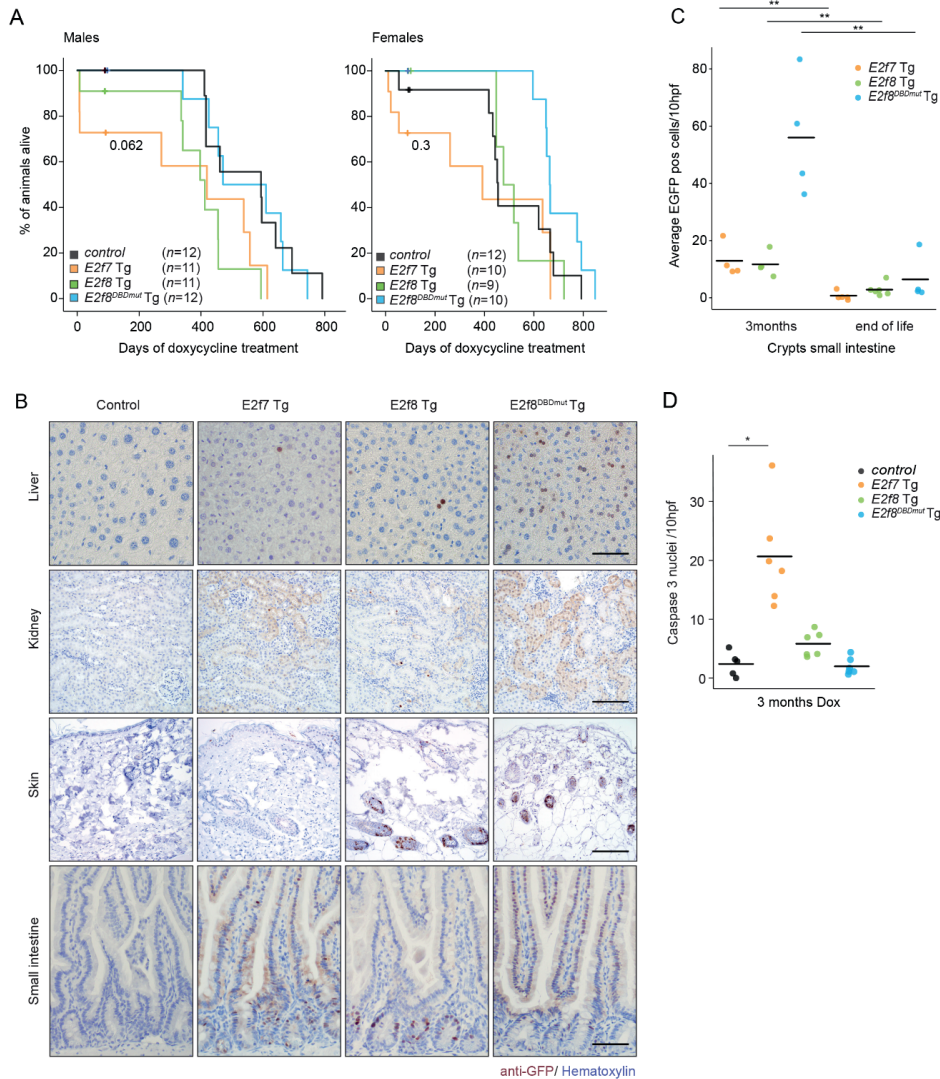


◀**Supplemental Figure 2: Loss of RB results in deregulation of cell cycle control in atypical E2F-deficient liver tumors.** (A) Quantification of the percentage of BrdU-positive nuclei in control (Cre-negative) and knockout (Cre-positive) livers from *Alb-7-/-8-/-* and *Alb-Rb-/-7-/-8-/-* mice, 4 weeks after birth, measured by FACS. Data represent average  $\pm$  SEM ( $n= 7-14$  mice). (B) Transcript levels of E2F targets from *Alb- 7-/-8-/-* and *Alb-Rb-/-7-/-8-/-* 4 weeks old mice. Fold changes were adjusted to average of controls and *Actb* and *Gapdh* were used to normalize the expression. Data represent average  $\pm$  SEM ( $n= 4-5$  mice). (C) Venn diagram showing KEGG pathway enrichment analysis from the genes significantly up- or down-regulated in liver tumor samples from *Alb- 7-/-8-/-* and *Alb-Rb-/-7-/-8-/-* mice compared to non-tumor control livers in RNA sequencing ( $n=4$  mice/ condition). *P val.*= Benjamini-Hochberg-corrected P value. (D) RNA-sequencing analysis of transcripts that were significantly differentially expressed in *Alb-Rb-/-7-/-8-/-* versus *Alb- 7-/-8-/-* tumor samples. Color scale represents  $\log_2$ -fold changes relative to the normal control livers in RNA sequencing ( $n=4$ ). (E) RNA-sequencing data showing expression of E2F targets in samples from the indicated genotypes ( $n=4$  livers/ genotype). Color scale represents  $\log_2$ -fold changes relative to age-matched wild-type livers ( $n=4$ ). (F) Quantification of 2C, 4C and >4C nuclei in 4 weeks old livers from control and knock-out *Alb-7-/-8-/-* and *Alb-Rb-/-7-/-8-/-* mice. Data represent average  $\pm$  SEM ( $n= 7-14$  mice). (G) RNA sequencing data showing expression of CIN (chromosomal instability)-associated genes (signature CIN70) from the indicated genotypes ( $n=4$  livers/ genotype). Color scale represents  $\log_2$ -fold changes relative to age-matched wild-type livers ( $n=4$ ). (H) Quantification of  $\gamma$ -H2AX immunohistochemistry in 5 fields (40x objective) in tumor and adjacent non tumor areas of the livers from the indicated genotypes. Controls represent Alb-Cre negative littermates analyzed at the same time point as Alb-Cre positive ones. The data are presented as average  $\pm$ SEM (1 tumor per mice was analyzed/mouse;  $n= 6$  mice).

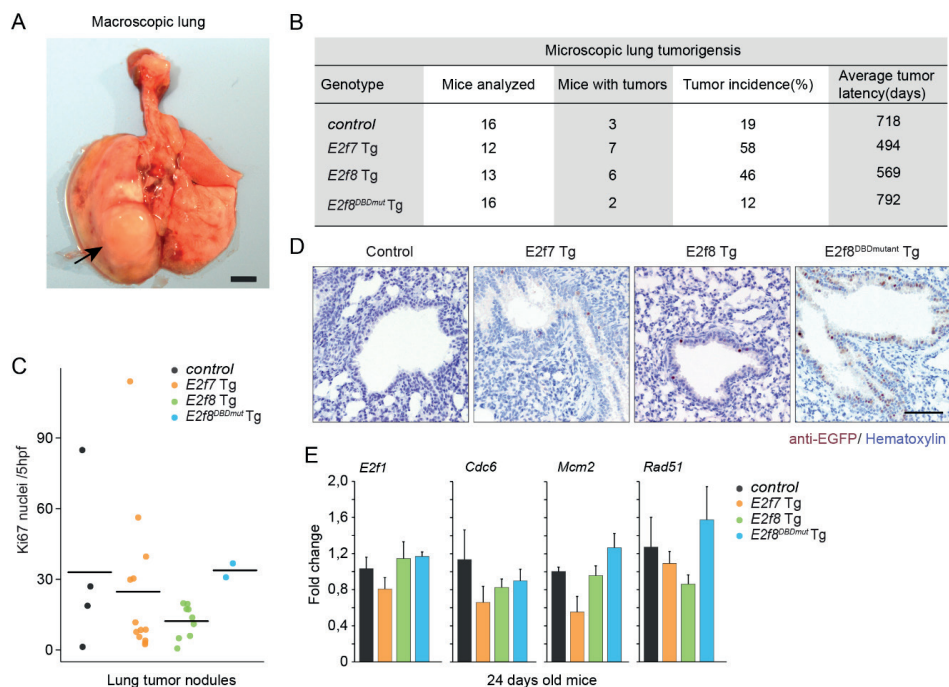
Data information: in (A, B, F and H) n.s not significant, \* $p<0.05$ , \*\* $p<0.01$ , \*\*\* $p<0.001$  (Mann-Whitney Rank Sum test).



**▲Supplemental Figure 3: Effect of E2F7 and -8 deletion in pituitary glands of RB heterozygous mice.** (A) Representative HE-stained image of a normal mouse pituitary gland. (B) Percentage of the location of the pituitary tumors in the indicated genotypes. (C) Incidence of hyperplasia in the additional neuroendocrine glands analyzed by a board-certified veterinary pathologist. n.s non significant (Chi-square).



**▲ Supplemental Figure 4: Overexpression of atypical E2Fs affects rapidly proliferating tissues in mice.** (A) Kaplan-Meier overall survival of transgenic mice, split by gender. (B) Representative anti-EGFP immunohistochemistry pictures in the indicated tissues showing transgene expression in the indicated genotypes after 3 months of doxycycline treatment. Scale bars: 100 μm. (C) Dot plot representing the counts of EGFP-positive cells in ten fields (40x objective) of the small intestinal crypts of 3 months-old and mice harvested at the end of life. Cross black line represents average. \*\* $p < 0.01$  (Mann-Whitney Rank Sum Test). (D) Dot plot representing the counts of Caspase 3-positive nuclei in ten fields (40x objective) of the small intestinal crypts of mice treated for 3 months with doxycycline. Cross black line represents average. \* $p < 0.05$  (Kruskal Wallis One Way Analysis of Variance on Ranks and Dunnett's Method for Multiple Comparisons vs. control).



**Supplemental Figure 5: E2F7 or -8 overexpression promotes spontaneous lung tumorigenesis.** (A) Representative image of a macroscopic lung lesion. Arrow indicates a lung lesion. Scale bar: 50mm. (B) Microscopic lung tumor incidence (%) and latency (days) of the indicated genotypes. Tumor incidence was determined on mice at the end of their life span. (C) Dot plot representing the counts of Ki67-positive nuclei in five fields (40x objective) of lung tumor nodules from the different genotypes. Cross black line represents average/ tumor nodule (*control* ( $n=4$ ); *E2f7 Tg* ( $n=13$ ); *E2f8 Tg* ( $n=9$ ); *E2f8<sup>DBDmut</sup> Tg* ( $n= 2$ ) mice. (D) Representative anti-EGFP immunohistochemistry pictures to detect transgene expression in lungs of 24 days old mice treated 3d with doxycycline. Scale bar: 50µm. (E) Transcript levels of E2F targets in lungs of juvenile mice from the indicated genotypes treated for 3 days with doxycycline. Fold changes were adjusted to average of *controls* and *Gapdh* was used to normalize the expression. Data represent average  $\pm$  SEM ( $n= 5$  mice).

## REFERENCES

- (1) Bertoli C, Skotheim JM, de Bruin, Robertus A. M. Control of cell cycle transcription during G1 and S phases. *Nat Rev Mol Cell Biol* 2013 -8;14(8):518-528.
- (2) Chen PL, Scully P, Shew JY, Wang JY, Lee WH. Phosphorylation of the retinoblastoma gene product is modulated during the cell cycle and cellular differentiation. *Cell* 1989 Sep 22;58(6):1193-1198.
- (3) Nevins JR. The Rb/E2F pathway and cancer. *Hum Mol Genet* 2001;10(7):699-703.
- (4) Weinberg RA. The retinoblastoma protein and cell cycle control. *Cell* 1995 May 05;81(3):323-330.
- (5) Ewen ME, Faha B, Harlow E, Livingston DM. Interaction of p107 with cyclin A independent of complex formation with viral oncoproteins. *Science* 1992 -01-03;255(5040):85-87.
- (6) Cobrinik D, Whyte P, Peeper DS, Jacks T, Weinberg RA. Cell cycle-specific association of E2F with the p130 E1A-binding protein. *Genes Dev* 1993 12/01;7(12a):2392-2404.
- (7) Hurford RK, Cobrinik D, Lee MH, Dyson N. pRB and p107/p130 are required for the regulated expression of different sets of E2F responsive genes. *Genes Dev* 1997 Jun 01;11(11):1447-1463.
- (8) Cobrinik D. Pocket proteins and cell cycle control. *Oncogene* 2005 Apr 18;24(17):2796-2809.
- (9) Dick F, Goodrich D, Sage J, Dyson N. Non-canonical functions of the RB protein in cancer. *Nat Rev Cancer* 2018;18(7):442-451.
- (10) Kent L, Rakijas J, Pandit S, Westendorp B, Chen H, Huntington J, et al. E2f8 mediates tumor suppression in postnatal liver development. *J Clin Invest* 2016;126(8):2955-2969.
- (11) Thurlings I, Martínez López LM, Westendorp B, Zipp M, Kuiper R, Tooten P, et al. Synergistic functions of E2F7 and E2F8 are critical to suppress stress-induced skin cancer. *Oncogene* 2017;36(6):829-839.
- (12) Kent LN, Leone G. The broken cycle: E2F dysfunction in cancer. *Nat Rev Cancer* 2019 /06;19(6):326-338.
- (13) Di Stefano L, Jensen M, Helin K. E2F7, a novel E2F featuring DP-independent repression of a subset of E2F-regulated genes. *EMBO J* 2003;22(23):6289-6298.
- (14) Maiti B, Li J, de Bruin A, Gordon F, Timmers C, Opavsky R, et al. Cloning and characterization of mouse E2F8, a novel mammalian E2F family member capable of blocking cellular proliferation. *J Biol Chem* 2005;280(18):18211-18220.
- (15) Logan N, Graham A, Zhao X, Fisher R, Maiti B, Leone G, et al. E2F-8: an E2F family member with a similar organization of DNA-binding domains to E2F-7. *Oncogene* 2005;24(31):5000-5004.
- (16) Logan N, Delavaine L, Graham A, Reilly C, Wilson J, Brummelkamp T, et al. E2F-7: a distinctive E2F family member with an unusual organization of DNA-binding domains. *Oncogene* 2004;23(30):5138-5150.
- (17) de Bruin A, Maiti B, Jakoi L, Timmers C, Buerki R, Leone G. Identification and characterization of E2F7, a novel mammalian E2F family member capable of blocking cellular proliferation. *J Biol Chem* 2003;278(43):42041-42049.
- (18) Yuan R, Liu Q, Segeren H, Yuniati L, Guardavaccaro D, Lebbink R, et al. Cyclin F-dependent degradation of E2F7 is critical for DNA repair and G2-phase progression. *EMBO J* 2019;38(20):e101430.
- (19) Westendorp B, Mokry M, Groot Koerkamp, Marian JA, Holstege FCP, Cuppen E, de Bruin A. E2F7 represses a network of oscillating cell cycle genes to control S-phase progression. *Nucleic Acids Res* 2012;40(8):3511-3523.
- (20) Boekhout M, Yuan R, Wondergem A, Segeren H, van Liere E, Awol N, et al. Feedback regulation between atypical E2Fs and APC/CCdh1 coordinates cell cycle progression. *EMBO Rep* 2016;17(3):414-427.

- (21) Aksoy O, Chicas A, Zeng T, Zhao Z, McCurrach M, Wang X, et al. The atypical E2F family member E2F7 couples the p53 and RB pathways during cellular senescence. *Genes Dev* 2012;26(14):1546-1557.
- (22) Srinivasan S, Mayhew C, Schwemberger S, Zagorski W, Knudsen E. RB loss promotes aberrant ploidy by deregulating levels and activity of DNA replication factors. *J Biol Chem* 2007;282(33):23867-23877.
- (23) Zheng L, Flesken-Nikitin A, Chen P, Lee W. Deficiency of Retinoblastoma Gene in Mouse Embryonic Stem Cells Leads to Genetic Instability. *Cancer Res* 2002 -05-01 00:00:00;62(9):2498-2502.
- (24) Zheng L, Lee W. Retinoblastoma tumor suppressor and genome stability. *Adv Cancer Res* 2002;85:13-50.
- (25) Brugarolas J, Moberg K, Boyd SD, Taya Y, Jacks T, Lees JA. Inhibition of cyclin-dependent kinase 2 by p21 is necessary for retinoblastoma protein-mediated G1 arrest after  $\gamma$ -irradiation. *PNAS* 1999 -02-02 00:00:00;96(3):1002-1007.
- (26) Harrington EA, Bruce JL, Harlow E, Dyson N. pRB plays an essential role in cell cycle arrest induced by DNA damage. *PNAS* 1998 -09-29 00:00:00;95(20):11945-11950.
- (27) Carvajal L, Hamard P, Tonnessen C, Manfredi J. E2F7, a novel target, is up-regulated by p53 and mediates DNA damage-dependent transcriptional repression. *Genes Dev* 2012;26(14):1533-1545.
- (28) Huang PH, Cook R, Zoumpoulidou G, Luczynski MT, Mittnacht S. Retinoblastoma family proteins: New players in DNA repair by non-homologous end-joining. *Mol Cell Oncol* 2015 -6-10;3(2).
- (29) Vélez-Cruz R, Manickavinayaham S, Biswas AK, Clary RW, Premkumar T, Cole F, et al. RB localizes to DNA double-strand breaks and promotes DNA end resection and homologous recombination through the recruitment of BRG1. *Genes Dev* 2016 -11-15;30(22):2500-2512.
- (30) Li J, Ran C, Li E, Gordon F, Comstock G, Siddiqui H, et al. Synergistic function of E2F7 and E2F8 is essential for cell survival and embryonic development. *Dev Cell* 2008 Jan;14(1):62-75.
- (31) Moreno E, Toussaint MJM, van Essen S, Bongiovanni L, van Liere E, Koster M, et al. E2F7 is a potent inhibitor of liver tumor growth in adult mice. *Hepatology* 2020.
- (32) Liao Y, Smyth GK, Shi W. featureCounts: an efficient general purpose program for assigning sequence reads to genomic features. *Bioinformatics* 2014 -04-01;30(7):923-930.
- (33) Love MI, Huber W, Anders S. Moderated estimation of fold change and dispersion for RNA-seq data with DESeq2. *Genome Biol* 2014;15(12):550.
- (34) Mayhew C, Carter S, Fox S, Sexton C, Reed C, Srinivasan S, et al. RB loss abrogates cell cycle control and genome integrity to promote liver tumorigenesis. *Gastroenterology* 2007;133(3):976-984.
- (35) Pandit S, Westendorp B, Nantasanti S, van Liere E, Tooten PCJ, Cornelissen PWA, et al. E2F8 is essential for polyploidization in mammalian cells. *Nat Cell Biol* 2012;14(11):1181-1191.
- (36) Carter SL, Eklund AC, Kohane IS, Harris LN, Szallasi Z. A signature of chromosomal instability inferred from gene expression profiles predicts clinical outcome in multiple human cancers. *Nat Genet* 2006 -09;38(9):1043-1048.
- (37) Bourgo RJ, Ehmer U, Sage J, Knudsen ES. RB deletion disrupts coordination between DNA replication licensing and mitotic entry in vivo. *Molecular biology of the cell* 2011 Apr;22(7):931-939.
- (38) Segeren HA, van Rijnberk LM, Moreno E, Riemers FM, van Liere EA, Yuan R, et al. Excessive E2F Transcription in Single Cancer Cells Precludes Transient Cell-Cycle Exit after DNA Damage. *Cell Rep* 2020 Dec 01;33(9):108449.

- (39) Ouseph M, Li J, Chen H, Pécot T, Wenzel P, Thompson J, et al. Atypical E2F repressors and activators coordinate placental development. *Dev Cell* 2012;22(4):849-862.
- (40) Hu N, Gutschmann A, Herbert DC, Bradley A, Lee WH, Lee EY. Heterozygous Rb-1 delta 20/+ mice are predisposed to tumors of the pituitary gland with a nearly complete penetrance. *Oncogene* 1994 Apr;9(4):1021-1027.
- (41) Yamasaki L, Bronson R, Williams BO, Dyson NJ, Harlow E, Jacks T. Loss of E2F-1 reduces tumorigenesis and extends the lifespan of Rb1(+/-) mice. *Nat Genet* 1998;18(4):360-364.
- (42) Williams BO, Remington L, Albert DM, Mukai S, Bronson RT, Jacks T. Cooperative tumorigenic effects of germline mutations in Rb and p53. *Nat Genet* 1994 Aug;7(4):480-484.
- (43) Mahler JF, Stokes W, Mann PC, Takaoka M, Maronpot RR. Spontaneous lesions in aging FVB/N mice. *Toxicol Pathol* 1996 Nov-Dec;24(6):710-716.
- (44) Cuitiño MC, Pécot T, Sun D, Kladney R, Okano-Uchida T, Shinde N, et al. Two Distinct E2F Transcriptional Modules Drive Cell Cycles and Differentiation. *Cell Rep* 2019 -06-18;27(12):3547-3560.e5.
- (45) Yuan R, Vos HR, van Es RM, Chen J, Burgering BM, Westendorp B, et al. Chk1 and 14-3-3 proteins inhibit atypical E2Fs to prevent a permanent cell cycle arrest. *EMBO J* 2018 03 01;37(5).
- (46) Shan B, Durfee T, Lee WH. Disruption of RB/E2F-1 interaction by single point mutations in E2F-1 enhances S-phase entry and apoptosis. *Proc Natl Acad Sci U S A* 1996 Jan 23;93(2):679-684.
- (47) Andersen MP, Nelson ZW, Hetrick ED, Gottschling DE. A genetic screen for increased loss of heterozygosity in *Saccharomyces cerevisiae*. *Genetics* 2008 Jul;179(3):1179-1195.
- (48) Park S, Platt J, Lee JW, López-Giráldez F, Herbst RS, Koo JS. E2F8 as a Novel Therapeutic Target for Lung Cancer. *J Natl Cancer Inst* 2015 -6-18;107(9).





# Chapter 4

---

## **Polyploidization in non-alcoholic fatty liver disease promotes steatosis and inhibits liver tumor progression**

Ramadhan B. Matondo<sup>1\*</sup>, Eva Moreno<sup>1\*</sup>, Laura Bongiovanni<sup>1</sup>, Martijn R. Molenaar<sup>1</sup>, Mathilda J.M. Toussaint<sup>1</sup>, Saskia C. van Essen<sup>1</sup>, Martin Houweling<sup>1</sup>, J. Bernd Helms<sup>1</sup>, Bart Westendorp<sup>1</sup>, Alain de Bruin<sup>1,2†</sup>.

Affiliations:

Departments of <sup>1</sup>Biomolecular Health Sciences, Division of Cell Biology, Metabolism and Cancer, Faculty of Veterinary Medicine, Utrecht University, Utrecht, The Netherlands;

<sup>2</sup>Department of Pediatrics, Division Molecular Genetics, University Medical Center Groningen, University of Groningen, Groningen, The Netherlands;

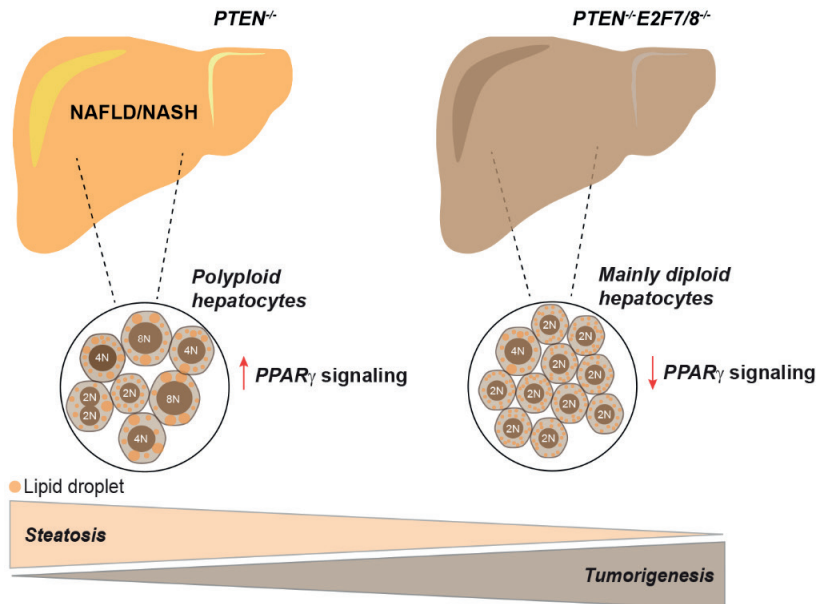
\* These authors contributed equally to this work

† Corresponding author

*Manuscript in preparation*

## ABSTRACT

Non-alcoholic fatty liver disease (NAFLD) is the most common liver disorder and a high risk factor for primary liver cancer. The global burden of NAFLD is on the rise due to increased incidence of obesity. Recent analysis in NAFLD patients demonstrated a significant increase in the percentage of polyploid hepatocytes, carrying 4 or more complete sets of chromosomes. Despite the clear correlation between NAFLD and pathological polyploidy, it is unknown whether polyploidization has an impact on the development of NAFLD and its progression towards liver cancer. Here, we used a liver-specific conditional knockout approach to delete *Pten*, a known suppressor of NAFLD and liver cancer, in combination with deletion of *E2f7/8*, known key inducers of polyploidization. As expected, *Pten* deletion caused severe steatosis and liver tumors accompanied by enhanced polyploidization. Additional deletion of *E2f7/8* inhibited polyploidization, alleviated steatosis and accelerated liver tumor progression. Global transcriptomic analysis showed that inhibition of polyploidization in *Pten*-deficient livers resulted in reduced expression of genes involved in energy metabolism, including PPAR- $\gamma$  signaling. However, we find no evidence that deregulated genes in *Pten*-deficient livers are direct transcriptional targets of E2F7/8, supporting that reduction in steatosis and progression towards liver cancer are consequences of inhibiting polyploidization. Moreover, single cell analysis on isolated wildtype primary mouse hepatocytes provided further support that polyploid cells can accumulate more lipid droplets than diploid hepatocytes. Collectively, pathological polyploidization enhances the severity of steatosis and function as an important barrier against liver tumor progression in NAFLD.





## INTRODUCTION

Non-alcoholic fatty liver disease (NAFLD) is characterized by excessive accumulation of fat in the liver, and it is emerging as a global public health issue with a prevalence of near 30%(1). Obesity and type 2 diabetes are strong risk factors of NAFLD (2,3). Importantly, NAFLD is often accompanied by inflammation, i.e. non-alcoholic steatohepatitis (NASH). Individuals with NASH can eventually develop cirrhosis and liver cancer (4). Nevertheless, the mechanisms underlying the association between lipid accumulation, inflammation and liver cancer are still incompletely understood. In addition, NAFLD is characterized by increased hepatocyte polyploidization, but the pathophysiological consequences of this polyploidization in disease progression are unknown (5).

During normal postnatal development hepatocytes can undergo successive rounds of genome duplication in the absence of cytokinesis to become polyploid (6,7). The percentage of polyploid hepatocytes in mammalian livers ranges from up to 90% in rodents to 30% in humans (8,9). Programmed polyploidization occurs in the liver during postnatal development, starting at 3 weeks of age in mice (10). This developmental hepatocyte polyploidization program is at least in part driven by insulin signaling and involves transcriptional inhibition of cytokinesis genes as well as the PIDosome components *Casp2* and *Pidd1* via the E2F7 and -8 repressors (10-13). However, a substantial increase in hepatocyte polyploidization is frequently observed as a result of liver injury or cell stress, which is referred to as pathological polyploidization (14-16). It has been proposed that pathological polyploidization may act as a mechanism to increase genetic diversity and stress-resistant hepatocyte clones (17). Other studies suggest that the increase in cell size that comes with polyploidization could rewire the energy metabolism of hepatocytes. For example, polyploidization shifted ATP synthesis from mitochondrial oxidative phosphorylation towards glycolysis(18). Furthermore, liver cell polyploidization is associated with increased lipid accumulation (5). And impairment of insulin signaling, which is commonly seen in metabolic disorders, reduces the formation of polyploid hepatocytes (11).

We and others have previously shown that physiological polyploidization in the mouse liver can be inhibited by deletion of atypical E2Fs (10,12). Surprisingly, blocking hepatocyte polyploidization had no major impact on liver cell differentiation, apoptosis or regeneration (10). Mice with livers composed of predominantly diploid hepatocytes had the same life expectancy compared to mice with normal polyploid livers. Interestingly, end of life analysis revealed that mice with reduced polyploidy had an increased incidence of liver tumors compared to mice with normal polyploid livers (19). The fact that enhanced polyploidization is associated with NAFLD suggests that pathological polyploidization is induced by metabolic stress. However, it remains obscure whether polyploidization in hepatocytes with enhanced metabolic activity has impact on NAFLD development and its progression towards liver cancer.

In the present study, we combined liver-specific deletion of *E2f7/8* to inhibit liver cell polyploidization with deletion of *Pten*. Liver-specific *Pten* deletion is an established mouse

model for NAFLD and liver cancer (20,21). Here we evaluated long-term consequences of abolishing polyploidization in this model on lipid accumulation and liver tumorigenesis. We show that polyploidy promotes steatosis and inhibits liver tumor formation under metabolic stress conditions induced by overactivation of the PI3K/Akt pathway. Our data strongly suggest that polyploidization functions as a potent barrier against liver tumor formation in NAFLD, despite facilitating lipid accumulation.

## MATERIAL AND METHODS

### Animal experiments

Animal experiments were approved by the Utrecht University Animal Ethics Committee (approval number: 2011.III.02.019) and performed according to institutional and national guidelines (experimental protocol: 103976-2). Mice were housed under standard conditions of temperature and housing. Breeding and generation of *Albumin-cre*, *Pten<sup>f/f</sup>*, and *E2f7/8<sup>f/f</sup>* mice for experiments have been previously described (10,22). Genotyping was performed using allele-specific primers (Supplementary Table 1). Mouse lines were maintained on at least 6<sup>th</sup> generation of FVB background. Figure 1-3 were

generated with liver specific knock out male and female mice harvested at the age of 16 weeks old. For the long-term cross sectional study, male and female mice with liver specific loss of *E2f7/8* (*78<sup>Δ/Δ</sup>*, n=18), *Pten* (*Pten<sup>Δ/Δ</sup>*, n=18), and or combination of the three genes (*78Pten<sup>Δ/Δ</sup>*, n=21), together with controls (*78Pten<sup>f/f</sup>*, n=20) littermates were sacrificed at the age of 10 months, and analyzed for macroscopic and microscopic tumors.

### Flow cytometry

Determination of hepatocyte ploidy by propidium iodide staining was done as previously described (10). Briefly, Pepsin (0.5mg/ml 0.1N in HCl) was used to generate the nuclei suspensions from frozen livers. Afterwards, the nuclei were washed twice with TBS and then stained with a propidium iodide (20µg/ml propidium iodide, 250µg/ml RNase A and 0.1% bovine serum albumin). All samples were measured on a BD FACS Canto II (BD Biosciences) and further analyzed using FlowJo software.

### Hepatocyte isolation, culture and IF staining of neutral lipids

Hepatocytes isolation and staining was done as previously described (9), and cultured overnight in high glucose Dulbecco's Modified Eagle's Medium (DMEM) containing 2% Fetal Bovine serum, 1mM penicillin/streptomycin and 10mM HEPES. Staining for imaging was done by plating the hepatocytes on coverslips overnight and incubated them for 24 hours with exogenous lipids C18:1 (200µM). After that period, hepatocytes were fixed with 1%

paraformaldehyde, washed with PBS 2x, blocked with 2%BSA and 0.2% Saponin in PBS for an hour and stained. Antibodies: 0.5 $\mu$ g/mL of LD540 and  $\beta$ -catenin (1:1000 diluted on PBS containing 1% BSA and 0.2% saponin; AB6302). 15 $\mu$ g/mL Hoechst 33342 (B2261, Sigma). Quantification of lipid droplets per cell was done using cell profiler software.

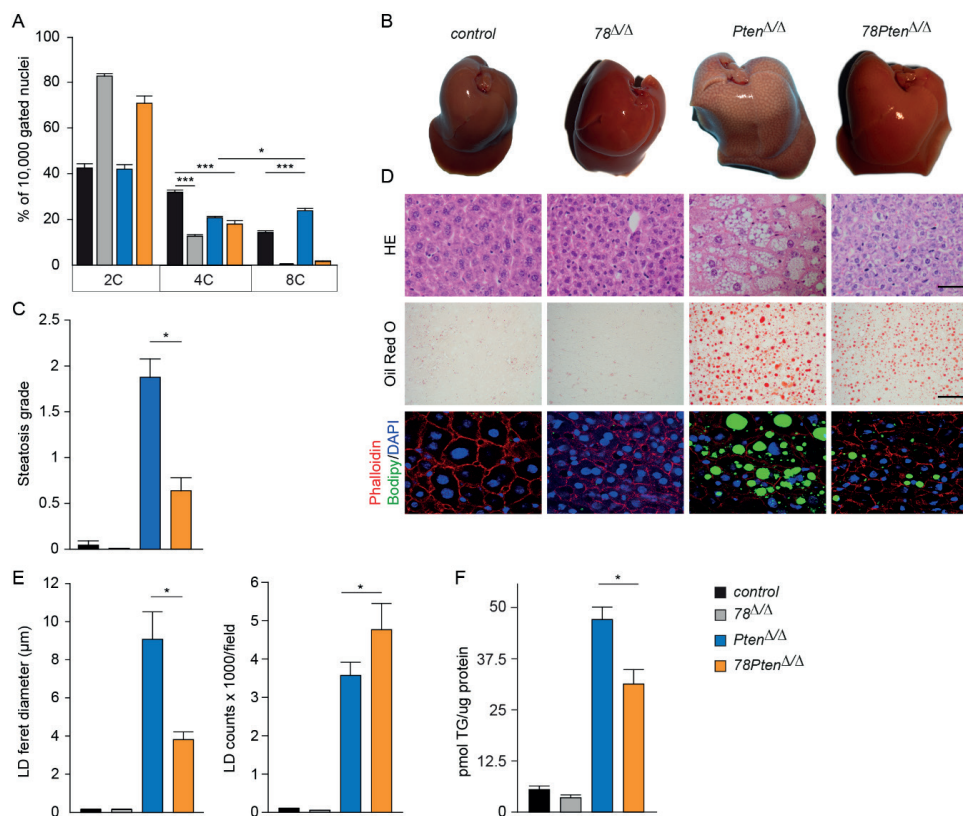
### **Neutral lipid staining in frozen liver tissue**

Frozen liver samples from mice aged 4 month were cut at 8  $\mu$ m thickness, air dried (1min), fixed in 3% paraformaldehyde (10min) and stained with filtered oil red O dye. Images were taken within 3 hours after staining. All histological images were acquired using Labsens soft imaging software version 1.1 and DP25 camera mounted on Olympus BX45 microscope. For immunofluorescent staining, sections were incubated with blocking solution containing 10% goat serum, 0.2% BSA, 1mM CaCl<sub>2</sub> and MgCl<sub>2</sub>, and 0.1% Tween-20 for 1 hour at room temperature. After blocking, sections were incubated with staining solution containing Bodipy (1:50), Alexa-fluor 568 phalloidin (1:400; A12380, Invitrogen) and DAPI (5mg/ml; 1:4000; D1306 Invitrogen) for 30 minutes at room temperature.

4

### **Immunoblotting**

Protein lysates were obtained with RIPA buffer (50mM Tris-HCl Ph 7.5, 1mM EDTA, 150mM NaCl, 0.25% deoxycholic acid, 1% Nonidet- P40), 1mM NaF and NaV<sub>3</sub>O<sub>4</sub> and protease inhibitor cocktail (11873580001, Sigma Aldrich). After centrifugation at full speed (12000xg) for 10 min, supernatants were collected and proceed to a standard SDS-PAGE Immunoblot. Antibodies used for western blots included pAKT-Thr308 (9272, Cell Signalling), pAKT-Ser473 (BD560378, BD biosciences), anti-AKT (9272S, Cell Signalling) at 1:1000 dilution.



**▲Figure 1: Loss of E2f7/8 prevents polyploidization and steatosis in Pten deficient livers. (A)** Ploidy status of 16 weeks-old livers from the indicated genotypes (*control*  $n=10$ ;  $78^{\Delta/\Delta}$   $n=5$ ;  $Pten^{\Delta/\Delta}$   $n=8$ ;  $78Pten^{\Delta/\Delta}$   $n=5$  mice/genotype). Bar graphs represent average and SEM. **(B)** Representative macroscopic images of 16 weeks-old livers from the indicated genotypes. **(C)** Steatosis grade of liver sections determined by a board-certified veterinary pathologist. ( $n$ =at least 5 mice/ genotype). **(D)** Representative microscopic pictures of HE (Scale bar  $20\mu\text{m}$ ), Oil Red O (lipid droplets, scale bar  $20\mu\text{m}$ ) and Bodipy (lipid droplets)/ Phalloidin (hepatocyte membrane)/ DAPI(nuclei) ( $6300\times$  magnification) stained liver sections from 16 weeks-old livers from the indicated genotypes. **(E)** Quantification of lipid droplet (LD) size and counts from 8-10 Oil Red O-stained images per liver section from the indicated genotypes.  $n=4$  mice/genotype. **(F)** Quantification of triglyceride content in liver homogenates. Bar graphs represent average and SEM ( $n=5$ ).

Data information: In **(A)**,  $*p<0.05$ ,  $***p < 0.001$  (t'test). In **(C, E and F)**,  $*p<0.05$  (Kruskal Wallis One Way Analysis of Variance on Ranks and Dunn's post hoc correction).



## **Immunohistochemistry**

Tissues were embedded in paraffin and sectioned at 4 $\mu$ m. Endogenous peroxidase activity was blocked with 1% H<sub>2</sub>O<sub>2</sub>. 10mM Citrate buffer (pH 6) was used for heat-induced antigen retrieval. Rabbit anti-Ki67 at 1:75 dilution in PBS (RM-9106-S0, Labvision/Neomarkers) was used for immunohistochemistry. Slides were counterstained with hematoxylin.

## **RNA isolation, cDNA and quantitative PCR.**

RNA isolation, cDNA synthesis and quantitative PCR were performed based on manufacturer's instructions for QIAGEN (RNeasy Kits), Thermo Fisher Scientific (cDNA synthesis Kits) and Bio-Rad (SYBR Green Master Mix), respectively. Reactions were performed in duplicate and relative amount of cDNA was normalized to GAPDH and Actin using the  $\Delta\Delta$ Ct method. qPCR primer sequences are provided in Supplementary Table 2.

## **RNA-sequencing.**

Liver samples taken from 4 months old mice were used. Library preparation and RNA sequencing were done at the Utrecht Sequencing Facility according to standard procedures. Barcoded cDNA libraries were prepared with a cDNA TruSeq® Stranded mRNA poly A kit (Illumina). All 16 barcoded samples were mixed and sequenced simultaneously with a 1x75 bp run on a NextSeq500 sequencer (Illumina). All samples passed a quality control using FastQC v0.10.1. The sequencing reads were then mapped to the mouse genome (assembly GRCm38/mm10) using ENCODE's STAR software (version 2.4.2a). The mapped reads were further analyzed using the R packages EdgeR (23), Deseq2 (24) and Pheatmap. Differential expression analysis was done on raw counts using Deseq2, and an FDR-corrected value of  $P < 0.05$  was considered statistically significant. Gene set enrichment analysis was done using Enrichr (25). A minimum of 5 genes and Benjamini-Hochberg-corrected  $P < 0.05$  were taken as cut-off for significant enrichment.

## **Pathological analysis: steatosis and tumors**

Pathological analysis was performed by a board-certified veterinary pathologist. Pathological changes were classified according to the nomenclature and diagnostic criteria for hepatobiliary lesions in rats and mice (26).

## **Statistics**

The number of independent experiments, the number of mice and the type of statistical analysis for each figure are indicated in the legends. Differences between groups were compared with one-way analysis of variance with Tukey's correction. Where data were not normally distributed,

groups were tested by Kruskal–Wallis tests with Dunn’s post hoc correction. Asterisks indicate where significant differences were seen ( $p < 0.05$ ). Where relevant for understanding the figure and individual comparisons, we indicate with “n.s.” that significance was not reached.

## RESULTS

### **Inhibition of polyploidization via deletion of E2f7/8 prevents accumulation of large lipid droplets in Pten-deficient livers.**

Lipid accumulation and polyploidy are positively correlated during NAFLD in both humans and mice (5). We first investigated whether inhibiting of polyploidization via ablation of E2F7 and -8 affects lipid accumulation in a mouse model of NAFLD. To this end we conditionally deleted *E2f7*, *E2f8* and *Pten* (hereafter *78Pten<sup>Δ/Δ</sup>*) in mouse livers using Cre/LoxP technology under the control of the hepatocyte-specific albumin promoter (Alb-Cre). We performed a cross-sectional pathology study at 16 weeks of age with controls (Alb-Cre negative), double *E2f7* and -8 (*78<sup>Δ/Δ</sup>*) mutant mice, single *Pten* knock-out (*Pten<sup>Δ/Δ</sup>*) and triple knockout mice (*78Pten<sup>Δ/Δ</sup>*). In line with previous work, single deletion of *Pten* caused polyploidy, as seen by an increase in the percentage of 8C nuclei compared to control livers (Figure 1A). We noted that *E2f7* and *E2f8* mRNA levels are elevated after *Pten* single deletion, indicating that pathological polyploidy could be mediated by these transcription factors (Supplementary Figure S1A). Consistent with this, the liver polyploidy was strongly reduced in the absence of atypical E2Fs, leading to mainly diploid hepatocytes in *78<sup>Δ/Δ</sup>* as well as *78Pten<sup>Δ/Δ</sup>* livers (Figure 1A). In addition, *Pten<sup>Δ/Δ</sup>* livers showed a marked increase in liver weight and size characterized by pale, bright and grossly visible boundaries of the liver lobules, indicative of steatosis (Figure 1B and Supplementary Figure S1B). Histological examination by a board-certified veterinary pathologist confirmed severe hepatic steatosis in *Pten<sup>Δ/Δ</sup>* livers, which was substantially ameliorated in *78Pten<sup>Δ/Δ</sup>* livers (Figure 1C, D). Liver weights of *78Pten<sup>Δ/Δ</sup>* mice were not significantly reduced compared to *Pten<sup>Δ/Δ</sup>* livers, suggesting that increased cell density in *78Pten<sup>Δ/Δ</sup>* might compensate for the presence of enlarged hepatocytes in *Pten<sup>Δ/Δ</sup>* livers (Supplementary Figure S1B).

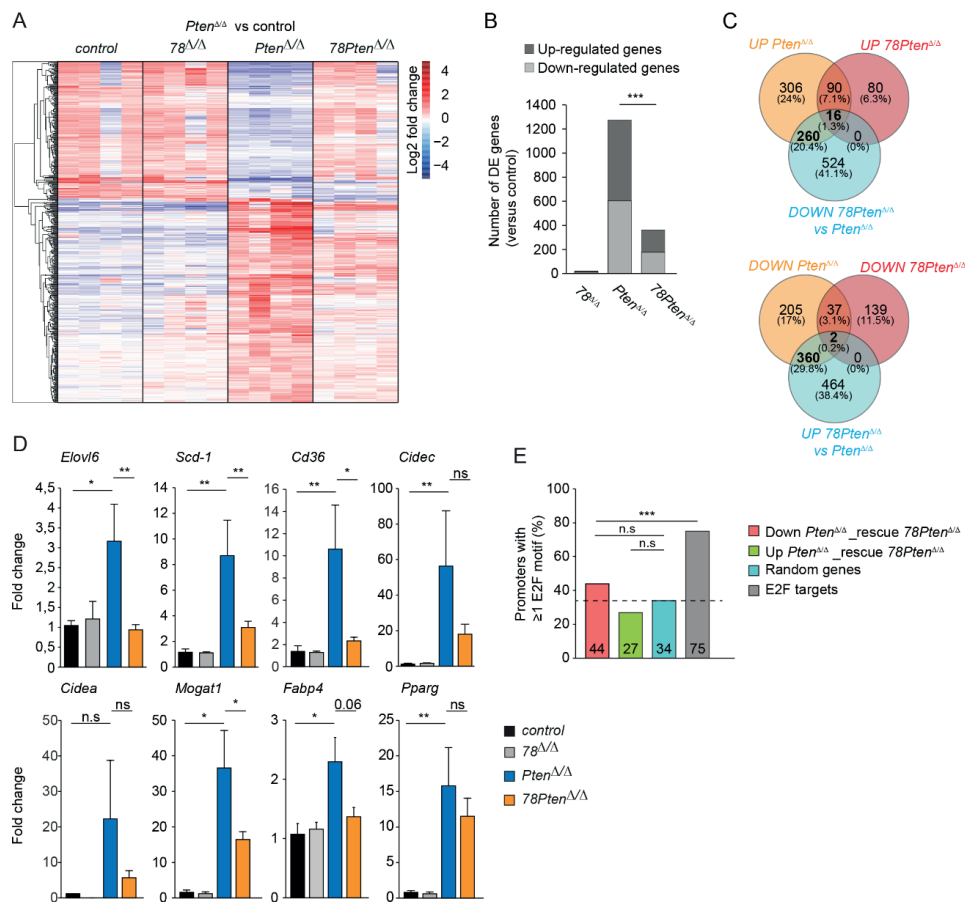
Microscopic analysis confirmed that *Pten<sup>Δ/Δ</sup>* livers accumulated large lipid droplets in hepatocytes, as shown with hematoxylin & eosin, lipid specific oil red O and bodipy staining (Figure 1D). Morphometric analysis revealed that livers with additional deletion of *E2f7* and *E2f8* (*78Pten<sup>Δ/Δ</sup>*) carried substantially smaller lipid droplets compared to *Pten<sup>Δ/Δ</sup>* livers, although the total number of lipid droplets was increased (Figure 1E). This resulted in a significantly reduced triglyceride content in the *78Pten<sup>Δ/Δ</sup>* compared to *Pten<sup>Δ/Δ</sup>* livers (Figure 1F). Together, these findings shows that PI3K/AKT-induced liver polyploidization and steatosis can be inhibited by additional deletion of atypical E2Fs.

## Polyploid hepatocytes promote lipid biosynthesis by enhancing PPAR gamma signaling

To gain comprehensive insights into how polyploidization promotes lipid accumulation in *Pten*<sup>Δ/Δ</sup> livers, we first analyzed whether PI3K-AKT signaling was affected by inhibiting polyploidization through deletion of *E2f7/8*. We found that PTEN loss caused a strong increase in AKT phosphorylation, which was not significantly decreased by additional deletion of atypical E2Fs (Supplemental Figure S2A).

We then performed differential expression (DE) analysis on the liver samples of 16 week old mice via RNA-sequencing. Strikingly, we observed that the far majority of expression changes caused by *Pten* deletion was partly or completely rescued by additional deletion of *E2f7/8* (Figure 2A). In addition, far less genes were differentially expressed in *78Pten*<sup>Δ/Δ</sup> versus control livers than in *Pten*<sup>Δ/Δ</sup> versus control livers (Figure 2B). Specifically, 276 transcripts that were upregulated through *Pten* deletion were rescued downwards upon additional deletion of *E2f7/8*. In addition, 362 transcripts that were downregulated in *Pten*<sup>Δ/Δ</sup> livers were rescued upwards when *Pten* was deleted together with atypical *E2fs* (Figure 2C). *E2f7/8* deletion by itself did not cause any notable alterations in gene expression (Figure 2A-B). Together these data strongly indicate that aberrant gene expression after deletion of *Pten* is, to a large extent, rescued by additional deletion of atypical E2Fs.

Although the lists DE genes in *Pten*<sup>Δ/Δ</sup> versus control livers comprised hundreds of genes, these lists were not strongly enriched for specific pathways or molecular processes, indicating that these genes are involved in a wide variety of different processes (Supplementary Figure S2B). The strongest functional enrichments among genes upregulated in *Pten*<sup>Δ/Δ</sup> livers were PPAR signaling and triglyceride metabolism (Supplemental Figure S2B-C; Supplementary Table 3). Previous studies demonstrated that PPARγ and its direct target are key inducers of steatosis in *Pten*-deficient livers (20,27). Given this importance of PPARγ and its direct targets in steatosis, we asked to which extent this pathway was normalized in *78Pten*<sup>Δ/Δ</sup> livers. Indeed, additional deletion of atypical E2Fs in *Pten*-deficient livers resulted in reduced expression of *Pparg* and a set of its target genes, which we validated by quantitative PCR analysis (Figure 2D, Supplementary Figure S3A). Apart from this partial rescue in PPAR signaling, we did not find significant enrichment for any pathway or GO molecular process in the list of 276 genes upregulated in *Pten*<sup>Δ/Δ</sup> compared to control livers and rescued downwards in *78Pten*<sup>Δ/Δ</sup> livers (Supplementary Figure S2B-C). Of note, hippo signaling and multiple processes linked to transcription regulation were the strongest enriched pathways among the downregulated genes in *Pten*<sup>Δ/Δ</sup> livers (Supplementary Figure S2B-C). This is consistent with the role of Hippo in negative regulation of growth in mammalian livers (28). However, when analyzing genes that were downregulated in *Pten*<sup>Δ/Δ</sup> livers and significantly rescued upwards in *78Pten*<sup>Δ/Δ</sup> livers we did not find evidence that Hippo signaling or transcription factor programs were rescued. Instead, we found a rescue of gene products known to be involved in ribosome functions



**▲Figure 2: Polypliod hepatocytes promote lipid biosynthesis by enhancing PPAR gamma signaling.** (A) Differential gene expression analysis of gene transcripts identified in RNA seq samples from the indicated genotypes (*n*=4). Heatmap showing 2log<sub>2</sub>-fold change in expression of transcripts that were differentially expressed in *Pten*<sup>Δ/Δ</sup> compared to control livers. (B) Stack histogram showing the numbers of differentially expressed genes (up or down regulated) in the indicated genotypes compared to control livers. (C) Venn diagram showing overlapping genes identified in RNAseq samples between the comparisons indicated. UP or DOWN comparisons are versus controls. (D) Transcript levels of PPARγ target gene expression in liver tissue of 16 weeks-old mice. Fold changes were adjusted to average of controls and GAPDH and β-Actin were used to normalize the expression. Data represent average ± SEM (*n*=6 controls; *n*=4 78Pten<sup>Δ/Δ</sup>; *n*=9 *Pten*<sup>Δ/Δ</sup>; *n*=8 78Pten<sup>Δ/Δ</sup>). (E) Histogram showing overall percentage of promoters with at least 1 E2F consensus motif.

Data information: In (B and E), \*\*\* *p*<0,001, n.s non-significant (Chi square). In (D), \* *p*<0,05, \*\* *p*<0,01, \*\*\**p*<0,001; n.s non-significant (Mann-Whitney Rank Sum Test).

(*Rplp1*, *Rps2* and *Rps18*; Supplementary Figure S2B) as well as protein synthesis (*Mrps24*, *Rps5*, *Pabpc4*; Supplementary Figure S2C). Notably, processes related to protein processing in ER and cellular response to ER stress were significantly downregulated in *78Pten<sup>Δ/Δ</sup>* livers compared to controls suggesting that polyploidization is used for cellular adaptation (Supplementary Figure S2B–C). Together, these analyses show that additional deletion of atypical E2Fs in *Pten*-deficient livers can partially rescue PPAR $\gamma$  signaling, as well as processes related to ribosomal function and protein synthesis.

Next, we aimed to investigate to what extent the observed gene transcription changes could be result of direct transcriptional repression or activation by atypical E2Fs. We hypothesized that the proximal promoters of the rescued genes should be enriched with E2F binding motifs compared to a randomly generated list of genes. Therefore we searched for consensus E2F-binding motifs (TTTSSCGC or highly similar) in the proximal promoters of the genes up- or down-regulated in *Pten<sup>Δ/Δ</sup>* livers and rescued by additional deletion of atypical E2Fs. We analyzed the lists of 362 rescued upwards and 276 genes rescued downwards in *78Pten<sup>Δ/Δ</sup>* livers separately. A list of 250 randomly picked genes served to detect the background level of coincidental presence of motifs, and a list of 80 well-known E2F target genes from previous RNA- and ChIP-sequencing data was used as positive control (19,29). Unexpectedly, the lists of upward or downward rescued genes did not contain more genes with at least one E2F binding motif than the randomly generated gene list (Figure 2E). Furthermore, the list of known E2F7/8 target genes contained a markedly higher percentage of E2F-motif containing genes than any of the other lists, showing that our approach is in principle feasible to pick up enrichment for E2F-binding genes (Figure 2E). Notwithstanding these findings, we observed that some genes rescued by *E2f7/8* deletion contained putative E2F binding motifs, and we asked if this limited set of genes could be primarily responsible for rescuing the PPAR $\gamma$  and steatosis phenotype in *78Pten<sup>Δ/Δ</sup>* livers. To narrow down the lists of candidate genes, we screened which of the rescued genes containing putative E2F motifs were previously shown to be bound directly by E2F7 and/or E2F8 in ChIP-sequencing experiments (19,29). In total 48 transcripts rescued by *E2f7/8* deletion were previously identified as E2F7/8 target genes with ChIP-sequencing (Supplementary Figure S3B; Supplementary Table 4). We manually curated the functions of these target genes and we noticed that expression of *Sik2* and *Irs2*, which are both involved in insulin signaling, was decreased in *Pten<sup>Δ/Δ</sup>* livers, and rescued in upward direction in *78Pten<sup>Δ/Δ</sup>* livers by RNA sequencing. We hence sought to validate these genes in larger amount of livers by quantitative PCR. Neither of these genes showed noticeable upregulation in *78Pten<sup>Δ/Δ</sup>* versus *Pten<sup>Δ/Δ</sup>* livers suggesting that *Sik2* and *Irs2* were not involved in the observed phenotypes (Supplementary Figure S3D). Finally we re-analyzed our previously published E2F7/8 ChIP-sequencing data to investigate whether the PPAR $\gamma$  target genes are bound by E2F7/8. However, proximal promoters of the PPAR $\gamma$  target gene promoters contained neither E2F7 nor E2F8 enrichment (data not shown).

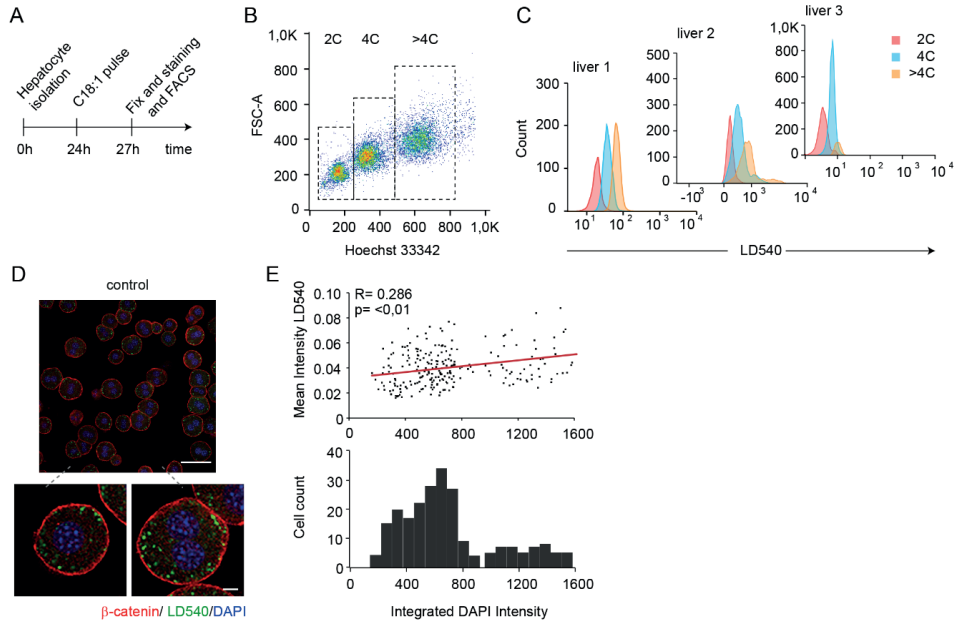
Together our transcriptomic data strongly suggest that atypical E2Fs do not alleviate steatosis in *Pten*-mutant livers via direct binding to gene promoters related to lipid metabolism. Instead, this rescue effect was most likely mediated by inhibition of polyploidization in *78Pten<sup>Δ/Δ</sup>* hepatocytes.

### **Enhanced lipid accumulation in wild-type polyploid versus diploid hepatocytes.**

Next, we explored if the polyploid state would permit a higher level of lipid accumulation also in normal hepatocytes exposed to free fatty acids. To test this, we performed single cell lipid fluorescent imaging analysis on primary hepatocytes with different ploidy status isolated from young adult wild-type mice. Subsequently we measured uptake of oleate (C18:1) oil supplements in polyploid versus diploid hepatocytes (Figure 4A). Flow cytometry analysis showed that indeed the amount of lipids, measured with the lipophilic dye LD540, increased with ploidy (Figure 4B-C). When we quantified LD540 intensity and DNA content of immunofluorescence images, we observed again a moderate positive correlation between those two parameters regardless of whether hepatocytes were mono or binucleated (Figure 4D-E and Supplementary Figure S4A-B). All together, these data indicate that the polyploid state can enhance the lipid storage capacity of hepatocytes.

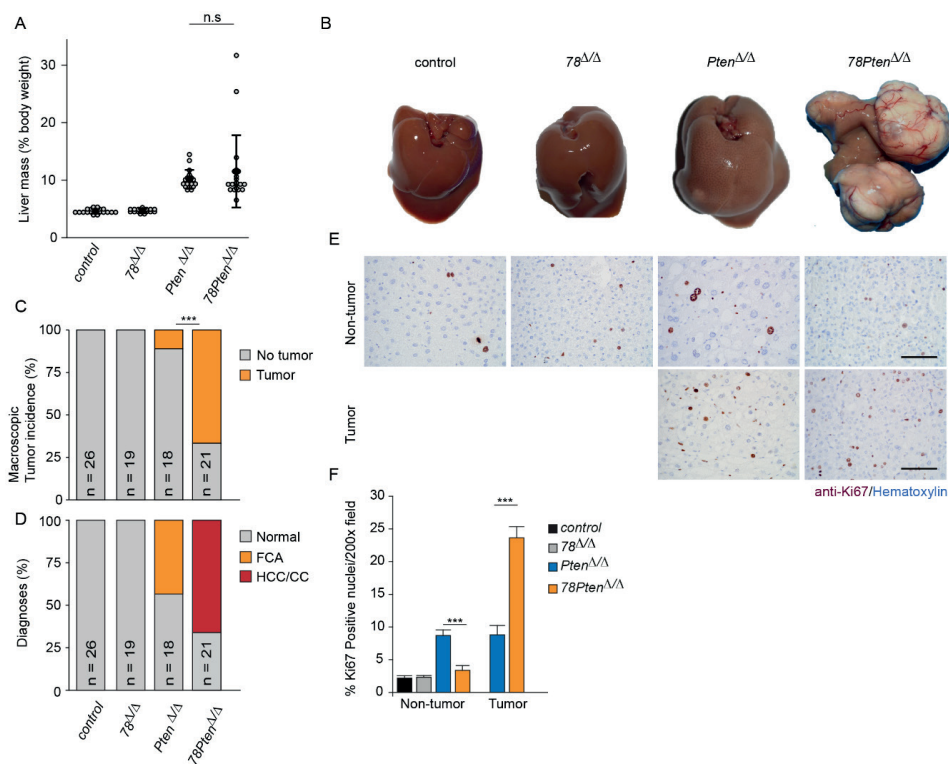
### **Blocking polyploidization accelerates liver cancer formation in *Pten*-deficient livers**

NAFLD patients are at high risk to develop liver cancer (30). Liver-specific deletion of *Pten* is an established mouse model for NAFLD that progress to liver cancer (20). To determine if inhibition of polyploidization has also impact on the progression from NAFLD towards liver cancer, we performed pathological analysis on livers from 10-months-old mice with the different genotypes. At this age, livers from *Pten<sup>Δ/Δ</sup>* mice were enlarged compared to controls (Figure 4A-B). However, we could detect only two mice with macroscopic tumor lesions. Strikingly, livers from *78Pten<sup>Δ/Δ</sup>* mice presented evident macroscopic tumor lesions, although average liver mass was comparable to *Pten<sup>Δ/Δ</sup>* liver masses (Figure 4A-C). This suggests that enhanced neoplastic growth in *78Pten<sup>Δ/Δ</sup>* liver and enhanced lipid loading in *Pten<sup>Δ/Δ</sup>* liver might compensate each other to result in similarly enlarged livers. Control and *78<sup>Δ/Δ</sup>* mice did not present any macroscopic tumors at this time point (Figure 4B-C). We next analyzed these livers histologically and confirmed that *Pten<sup>Δ/Δ</sup>* mice presented mainly premalignant lesions, characterized as focal cellular alteration (FCA; Figure 4D). Importantly, hepatocellular carcinomas (HCCs) or cholangiocarcinomas (CCs) were only found on *78Pten<sup>Δ/Δ</sup>* livers, suggesting that inhibition of polyploidization through additional deletion of *E2f7/8* markedly accelerates liver cancer formation in *Pten*-deficient livers. Consistently, *78Pten<sup>Δ/Δ</sup>* tumors showed increased proliferation, measured by Ki67-IHC staining, compared to *Pten<sup>Δ/Δ</sup>* lesions (Figure 4E-F). These results demonstrate that polyploidization is an important barrier against liver tumor progression in a mouse model for NAFLD.



**▲Figure 3: Polyploidy promotes lipid accumulation in mouse hepatocytes.** (A) Experimental set up of primary hepatocytes isolation for immunofluorescent staining and flow cytometry analysis of lipid loading. (B) Representative flow cytometry plot of hepatocytes isolated from a control mice. Hoechst 33342 and forward scatter (FSC) were used to determine level of ploidy ( $n=3$  mice). (C) LD540 fluorescence measured by FACS of 2C, 4C and >4C primary hepatocytes incubated 3hours with oleic acid from control mice ( $n=3$ mice). (D) Representative immunofluorescent staining of the lipophilic dye LD540 in primary isolated hepatocytes from control mice cultured for 3h with exogenous oleic acid (C18:1). Scale bar: 10 $\mu$ m. (E) Pearson correlation computation showing correlation between mean intensity of LD540 and integrated DAPI intensity in primary isolated hepatocytes from control mice with different ploidy incubated 3h with oleic acid.





**▲Figure 4: Blocking polyploidization enhance tumor formation in PTEN-deficient livers.** (A) Dot plot indicating liver mass/body weight percentage of 10 months old mice from the indicated genotypes (n=18-21). (B) Representative macroscopic images of 10months-old livers from the indicated genotypes. (C) Macroscopic liver tumor incidence. \*\*\* p<0,001 (Chi-square). (D) Pathology analysis of HE-stained livers. FCA= Foci of cellular alteration; HCC=hepatocellular carcinoma; CC= cholangiocarcinoma. (E) Representative immunohistochemistry pictures of Ki67-stained 10months-old liver sections from the indicated regions (tumor vs non tumor). Scale bars: 50 $\mu$ m. (F) Bar chart shows the quantification of Ki-67-positive hepatocytes in tumor and remote tissue of the indicated genotypes. Bars represent average and SEM (n=5 pictures taken with 20x objective/condition and mouse ; n=5 mice/genotype).

## DISCUSSION

The liver parenchyma displays changes in the polyploidy level of hepatocytes upon injury or stress. In particular, hepatocytes have the ability to acquire enhanced polyploid phenotype when exposed to increased lipid-related stress(5). In addition, physiological liver cell polyploidization was previously shown to function as a barrier against hepatocarcinogenesis (31,32). However, the relevance of hepatocyte polyploidization in the pathophysiology of the liver is still largely unknown. The presence of mouse models that allow the manipulation of polyploidization in the liver facilitate further investigation of this issue. On the one hand, liver-specific loss of *Pten* results in severe steatosis via activated insulin signaling and is accompanied with increased hepatocyte polyploidization (5,11). On the other hand, deletion of *E2f7/8* blocks hepatocyte polyploidization and is an established and powerful *in vivo* model to explore the relevance of polyploidy in liver diseases (10).

In this study we investigated the role of hepatocyte ploidy on lipid accumulation by comparing *controls* and *78<sup>Δ/Δ</sup>* or *Pten<sup>Δ/Δ</sup>* and *78Pten<sup>Δ/Δ</sup>* conditional knockout livers. We verified that *Pten<sup>Δ/Δ</sup>* hepatocytes showed increased hepatocyte ploidy and lipid accumulation, which is in agreement with previous findings (5,20). But surprisingly, inhibition of polyploidization via deletion of *E2f7/8* in *Pten<sup>Δ/Δ</sup>* deficient liver reduces steatosis and was accompanied with smaller lipid droplet formation. It has been shown that, polyploid hepatocytes have relatively larger cell volumes compared to diploid hepatocytes (33). Therefore, it is conceivable that the larger cell volume provides more space to increase lipid storage capacity of individual polyploid hepatocytes compared to smaller diploid hepatocytes. Indeed, comparison of murine wildtype hepatocytes of different ploidy have shown that polyploid hepatocytes are capable of accommodating more lipid droplets per cell compared to diploid hepatocytes. These findings were consistent with previous observations showing that lipid droplets in polyploid hepatocytes can grow to larger sizes than in diploid hepatocytes (5,34). Since deletion of *E2f7/8* results into formation of predominantly diploid hepatocytes, the presence of smaller lipids droplets could be related to the smaller cytoplasmic volume of these hepatocytes and consequently less lipid accumulation. In contrast, the overall number of lipid droplets per area is increased in livers with predominantly diploid cells (*78Pten<sup>Δ/Δ</sup>*) compared to livers with mostly polyploid cells (*Pten<sup>Δ/Δ</sup>*). This difference can be explained by the relative increase in cellular density in *E2f7/8* deficient liver (10). Basically, lack of large polyploid cells is compensated by increasing the number of small diploid cells per liver unit.

Previous work also showed that an increase in cell-size causes a strong increase in expression of the fatty acid transporter CD36, as well as triglyceride accumulation in liver (18). In this line, we observed that *Cd36* transcripts were upregulated in polyploid *Pten<sup>Δ/Δ</sup>* mutant livers and rescued in *78Pten<sup>Δ/Δ</sup>* livers with predominately diploid hepatocytes. Interestingly, *Cd36* is a PPAR $\gamma$  target gene, and we observed that many other PPAR $\gamma$  targets were also rescued in *78Pten<sup>Δ/Δ</sup>* livers. It is therefore conceivable that PPAR $\gamma$  signaling and CD63

expression are affected by metabolic factors differentially express in diploid versus polyploid cells. Further investigations are required to explore how polyploidization regulates PPAR signaling and CD36.

As E2F7/8 act as transcriptional repressors, we initially expected to find novel target genes involved in steatosis. Previous work suggested that genes involved in de novo fatty acid synthesis are transcriptionally controlled by E2F8 and the activating E2F family member E2F1(35,36). However, we did not observe that E2F7/8 loss caused de-repression of these lipid synthesis genes in our transcriptome analyses (data not shown). Moreover, despite in-depth gene expression analysis, we could not identify direct E2F7/8 target genes that could explain the changes in the steatosis or cancer phenotype, indicating that these phenotype changes are related to differences in the ploidy status of the livers.

Lastly, PTEN and atypical E2Fs are both known tumor suppressors in the liver, but the mechanisms of action are completely different. PTEN prevents excessive insulin signaling, fat accumulation, and polyploidization, whereas atypical E2Fs promote liver polyploidization. Physiological liver cell polyploidization was previously shown to function as a barrier against hepatocarcinogenesis (31,32). By combining genetic ablation of PTEN and atypical E2Fs, we now provide strong evidence that pathological polyploidization in NAFLD is also an important barrier against liver tumor formation. Surprisingly, this occurs independent on the degree of steatosis. This is counterintuitive, as steatosis is generally thought to drive carcinogenesis. We observed that inhibition of polyploidization reduced steatosis and PPAR $\gamma$  signaling in *Pten*-mutant livers, although tumor formation was strongly accelerated. Our data are at first sight inconsistent with a previous study showing that inactivation of PPAR $\gamma$  signaling blocks tumorigenesis in *Pten*-mutant mouse livers (27). However, the rescue was only partial, and PPAR $\gamma$  may not be the exclusive tumor-promoting pathway downstream of PI3K/AKT/PKB. For example, we observed that the tumor-suppressive Hippo signaling pathway was downregulated in *Pten*-mutant livers, and not rescued in *E2f7/8/Pten* triple mutant livers. So rather than being incompatible with this previous study, our data indicate that prevention of polyploidization overrides the potentially tumor-suppressing effect of partly reducing PPAR $\gamma$  signaling on liver tumorigenesis.

Given that NAFLD is a spectrum of chronic liver diseases that involves several metabolic dysfunctions and other factors beyond metabolism such as liver inflammation, we believe that lipid loading per se does not directly compromise the severity of the progression of the disease. Instead, massive production of proinflammatory cytokines as observed in NASH or enrichment of diploid cells via ploidy reduction may contribute to progression towards liver cancer.

## SUPPLEMENTARY MATERIAL.

**Supplementary Table 1:** PCR primers for transgene detection.

<b>Primer</b>	<b>Sequence (5'-3')</b>
Albumin-Cre_for	CCT GTT TTG CAC GTT CAC CG
Albumin-Cre_rev	ATG CTT CTG TCC GTT TGC CG
Pten_for	gAA TgC CAT TAC CTA gTA AAg CAA gg
Pten_rev floxed	ggg TTA CAC TAA CTA AAC gAg TCC
Pten_rev deleted	gAA TgA TAA Tag TAC CTA CTT CAg
E2f7_for	AGG CAG CAC ACT TGA CAC G
E2f7_rev floxed	ACT TTT GGG ACA GAG GTA GGA
E2f7_rev deleted	CCA AGA TGA AGG CCG AGA TGC TAC
E2f8_for	CTC GCA TCA TCG TCT GCT AA
E2f8_rev floxed	TAA AAA GCT TTG CGG TCG TT
E2f8_rev deleted	AAG CCA ACC TCG ATG AAT TG

4

**Supplementary Table 2:** qPCR primers.

	<b>Forward primer (5'-3')</b>	<b>Reverse primer (3'-5')</b>
Actin	<i>AGTCCTTCGTTGCCGGTCCA</i>	<i>TTTGCACATGCCGGAGCCGTTG</i>
Cidea	<i>TCCTCGGCTGTCTCAATG</i>	<i>TGGCTGCTCTTCTGTATCG</i>
Cidec	<i>ATGGACTACGCCATGAAGTCT</i>	<i>CGGTGCTAACACGACAGGG</i>
Cd36	<i>TGCACCACATATCTACCAAA</i>	<i>TTGTAACCCCACAAGAGTTC</i>
Elovl6	<i>CCGAAGATCAGCCCCAATGA</i>	<i>CGTACAGCGCAGAAAACAGG</i>
E2F7	<i>GATGCGTTTCGTGAACTCCCTG</i>	<i>AGAAACTTCTGGCACAGCAGCC</i>
E2F8	<i>GAGAAATCCCAGCCGAGTC</i>	<i>CATAAATCCGCCGACGTT</i>
Fabp4	<i>AAGGTGAAGAGCATCATAACCCT</i>	<i>TCACGCCTTTCATAACACATTCC</i>
Gapdh	<i>GAAGGTCGGTGTGAACGG</i>	<i>TGAAGGGGTCTGTTGATGG</i>
Irs2	<i>TCCAGAACGGCCTCAACTAT</i>	<i>AGTGATGGGACAGGAAGTCG</i>
Mogat1	<i>CTGGTTCTGTTTCCCGTTGT</i>	<i>TGGGTCAAGGCCATCTTAAC</i>
Pparg	<i>CTCTGGGAGATTCTCCTGTT</i>	<i>GGTGGGCCAGAATGGCATCT</i>
Pten	<i>AGACCATAACCCACCACAGC</i>	<i>TACACCAGTCCGTCCTTTC</i>
Scd-1	<i>ACCAGAGACATGGGCAAG TG</i>	<i>TGGATTGGGCTATAGGGACA</i>
Sik2	<i>ATGCACAGCCTTGGGATTGA</i>	<i>GTGCCTTGGCAACTGTTTGT</i>

**Supplementary Table 3:** KEGG and GO Molecular Process analysis.

<i>UP in Pten<sup>Δ/Δ</sup> versus control</i>			
<b>KEGG Pathway</b>	<b>Genes</b>	<b>GO Molecular Process</b>	<b>Genes</b>
PPAR signaling pathway	FABP4;GK;FABP5; PLIN4; AQP7;ACSL5; PPAR.G; PLIN2;CD36;PLTP	Triglyceride metabolic process	FABP4;GK;FABP5; GPAM; MOGAT1;CAV1; PNPLA3; APOA4;PNPLA5; LPIN3; GALK2
Amino sugar and nucleotide sugar metabolism	GALE;NAGK;FPGT; UAP1L1;PGM3;HK2;GCK	acylglycerol biosynthetic process	GK;GPAM;MOGAT1; PNPLA3;LPIN3
Lysosome	GALNS;CD63;NAPSA; PPT1;AP3S2;ARSG; AP3S1;CTSE;GUSB; LIPA;ARSB	triglyceride biosynthetic process	GK;GPAM;MOGAT1; PNPLA3;LPIN3
Pyrimidine metabolism	RRM2;UCK1;CMPK1; NUDT2;CTPS;NT5C2; DCK	neutrophil degranulation	CD63;PRCP;PLAC8;PSMB7;DP- P7;ORMDL3;MLEC;STOM;C- D36;OSTF1;GUSB;S100A11;ARS- B;GSDMD;ATP8B4;ANXA2;GCA;P- GAM1;FUCA2;CMTM6;ARPC5;PPB- P;RAP2C;GALNS;TSPAN14;VNN1;- FABP5;SLPI;PSMC2;LAMTOR1;FRK
Starch and sucrose metabolism	GYG;GBE1;TREH;HK2; GCK	neutrophil activation involved in immune response	CD63;PRCP;PLAC8;PSMB7;DP- P7;ORMDL3;MLEC;STOM;C- D36;OSTF1;GUSB;S100A11;ARS- B;GSDMD;ATP8B4;ANXA2;GCA;P- GAM1;FUCA2;CMTM6;ARPC5;PPB- P;RAP2C;GALNS;TSPAN14;VNN1;- FABP5;SLPI;PSMC2;LAMTOR1;FRK
<i>UP in Pten<sup>Δ/Δ</sup> ; rescue downwards 78Pten<sup>Δ/Δ</sup></i>			
<b>KEGG Pathway</b>	<b>Genes</b>	<b>GO Molecular Process</b>	<b>Genes</b>
Amino sugar and nucleotide sugar metabolism	GALE;FPGT;UAP1L1; PGM3;HK2	membrane raft assembly	ANXA2;S100A10
Gastric acid secretion	CHRM3;CAR2; PLCB4;CALML4;GNAI1	heart trabecula formation	FKBP1A;POLR2D
Pentose and glucuronate interconversions	KL;RPE;GUSB	positive regulation of triglyceride catabolic process	APOC2;APOA4

Fructose and mannose metabolism	PFKFB4;FPGT;HK2	lipid particle organization	HILPDA;CIDEA;CIDEC
Chemokine signaling pathway	GNGT1;SHC2;PLCB4;STAT1;PPBP;GNAI1;CCR2	positive regulation of lipoprotein lipase activity	APOC2;APOA4
<b>DOWN in <i>Pten</i><sup>Δ/Δ</sup> versus control</b>			
<b>KEGG Pathway</b>	<b>Genes</b>	<b>GO Molecular Process</b>	<b>Genes</b>
Hippo signaling pathway	TCF7L1;TGFB1;FZD5;WWC1;TCF7;FZD8;AXIN2;NKD1;PPP1CC;BMP2;CCND2;MYC;DVL3;DCHS1;FAT4;LLGL2;TEAD3	beta-catenin-TCF complex assembly	KMT2D;CREBBP;TCF7L1;TLE2;TERT;MYC;TCF7;EP300;AXIN2;MEN1
Pathways in cancer	CTBP2;PTGER1;NOTCH4;TCF7;LAMA3;PTEN;PIK3R2;IGF1R;SHH;BCL2L11;EDNRB;CCND2;TERF1;MYC;GNA12;DVL3;EP300;STAT5B;CREBBP;TCF7L1;TGFB1;FZD5;JUP;GSTO1;LAMB2;NCOA3;FZD8;AXIN2;VEGFA;BCL2;BMP2;ADCY9;RARA;CKS2;GNAS;FGFR1	regulation of transcription from RNA polymerase II promoter	FOXA1;LDB1;WWC1;PRDM2;CHD3;MED16;IRF2BPL;ELK4;SHH;EDNRB;MYC;ZMIZ2;EP300;CIC;JUNB;IER2;TEAD3;MEN1;DACT1;BRD3;KDM6B;KLF12;ZHX3;NCOA3;MKL1;TFEB;SOX12;SIRT7;HNF1A;RGMB;ETV5;NCOA2;TGFB3;HAND2;TET3;RARA;IRF5;MAML3;ZFPM1;ENH1B;HDAC4;KMT2D;NFIX;SRFBP1;CTBP2;NR1H3;TSHZ1;TSHZ2;TCF7;FOXK1;PIK3R2;CXXC5;NR2C2;SLC9A1;MXI1;PPARGC1B;BRD4;HEXIM1;IRX1;SPEN;ABCA2;STAT5B;CBX7;CREBBP;ZFHX3;TCF7L1;TGFB1;FZD5;JUP;CBX4;CBX2;SMAD9;NR2F2;SMAD6;SMARCA2;KLF2;NR2F6;HIPK2;VEGFA;BMP2;PER3;NFIB;AGO1;NFIC
Wnt signaling pathway	CREBBP;TCF7L1;CTBP2;FZD5;SERPINF1;TCF7;FZD8;AXIN2;PRICKLE1;NKD1;CCND2;ZNF3;MYC;EP300;DVL3;NOTUM;LGR5	negative regulation of transcription, DNA-templated	CDKN1C;LDB1;WWC1;IRF2BPL;ELK4;SHH;EDNRB;MYC;EP300;CIC;JUNB;MEN1;DACT1;PIAS4;TLE2;KLF12;ZHX3;SIRT7;NCOA2;THAP7;KAT6A;RARA;ZFPM1;HDAC4;NFIX;CTBP2;NR1H3;PRICKLE1;CXXC5;DEDD2;CCDC85B;MXI1;ZBTB7A;HEXIM1;IRX1;SPEN;HSPA8;CBX7;CREBBP;ZFHX3;TGFB1;ZBTB14;CBX4;CBX2;NR2F2;FOXN3;SMARCA2;KLF2;NR2F6;VEGFA;BMP2;PER3;NFIB;NFIC

Hepatocellular carcinoma	TCF7L1;TGFB1;FZD5;GSTO1;TCF7;PTEN;GAB1;FZD8;PIK3R2;AXIN2;SMARCA2;ARID1B;IGF1R;TERT;MYC;DVL3	viral process	POM121;CTBP2;RPLP1;RPS5;RPLP0;RPSA;-FURIN;VPS37B;RPL6;HIPK2;RPS26;RAB43;PTBP1;RPS18;PCBP2;RPL37A;RPL36;RPL14;PI4KA;RPS2;EIF3F;RPS21;VPS28;RPL19
Retinol metabolism	CYP2C37;CYP26A1;CYP2C68;UGT1A1;CYP2C54;CYP4A31;UGT2B38;CYP4A32;CYP1A2;CYP2C50;HSD17B6	positive regulation of transcription from RNA polymerase II promoter	FOXA1;LDB1;WWC1;PRDM2;IRF2BPL;ELK4;SHH;-MYC;ZMIZ2;EP300;JUNB;IER2;TEAD3;MEN1;KDM6B;NCOA3;MKL1;TFEB;SOX12;HNF1A;ETV5;HAND2;TET3;RARAA;IRF5;MAML3;ZFPM1;ENG;HDAC4;KMT2D;NFIIX;CTBP2;NRR113;NOTCH4;PIK3R2;NR2C2;SLC9A1;TERT;SCAP;PPARGC1B;BRD4;STAT5B;CREBBP;TGFB1;FZD5;JUP;SMAD9;SMARCA2;KLF2;HIPK2;VEGFA;BMP2;NFIB;AGO1;NFIC
<b>DOWN in <i>Pten</i><sup>Δ/Δ</sup> ; rescue upwards 78<i>Pten</i><sup>Δ/Δ</sup></b>			
Ribosome	RPS5;RPLP1;RPLP0;RPSA;MRPL14;MRPL34;RPL6;RPS26;RPS18;RPL36;RPS2;RPS21;RPL19	peptide biosynthetic process	MRPS24;RPS5;RPLP1;PABPC4;RPLP0;RPSA;FURIN;MRPL34;RPL6;RPS26;MRPL52;RPS18;RPL36;EIF4EBP2;RPS2;RPS21;RPL19
Inflammatory mediator regulation of TRP channels	CYP2C37;PPP1CC;ADCY9;CYP2C54;CYP4A31;GNAS;CYP2C50;PIK3R2;MAP2K6	translation	EEFSEC;MRPS24;RPLP1;PABPC4;RPS5;RPLP0;MRPS34;RPSA;MRPL34;RPL6;RPS26;MRPL52;TRMT112;RPS18;RPL36;EIF4EBP2;RPS2;RPS21;RPL19
Hippo signaling pathway	PPP1CC;TGFB1;WWC1;DVL3;FZD8;DCHS1;FAT4;NKD1;LLGL2;TEAD3	viral gene expression	POM121;RPS5;RPLP1;RPLP0;RPSA;-FURIN;RPL6;RPS26;RPS18;RPL36;RPS2;RPS21;RPL19
Bile secretion	ABCG8;ABCG5;ADCY9;-GNAS;KCNN2;SLC9A1	viral process	POM121;RPLP1;RPS5;RPLP0;RPSA;FURIN;RPL6;HIPK2;RPS26;RAB43;PTBP1;RPS18;PCBP2;RPL36;PI4KA;RPS2;RPS21;RPL19
Pathways in cancer	STAT5B;CREBBP;TGFB1;-JUP;PTGER1;LAMB2;NCOA3;NOTCH4;FZD8;PIK3R2;VEGFA;IGF1R;BCR;ADCY9;TERT;GNA12;CKS2;GNAS;DVL3	negative regulation of RNA metabolic process	RPS26;NCOR2;PTBP1;TGFB1;TERT;NUDT16
<b>UP in 78<i>Pten</i><sup>Δ/Δ</sup> versus control</b>			
<b>KEGG Pathway</b>	<b>Genes</b>	<b>GO Molecular Process</b>	<b>Genes</b>
PPAR signaling pathway	SCD2;PPARG;CD36;SORBS1;RXRG	response to insulin	CPEB1;TBC1D4;PPARG;SLC2A4;SORBS1;GCK

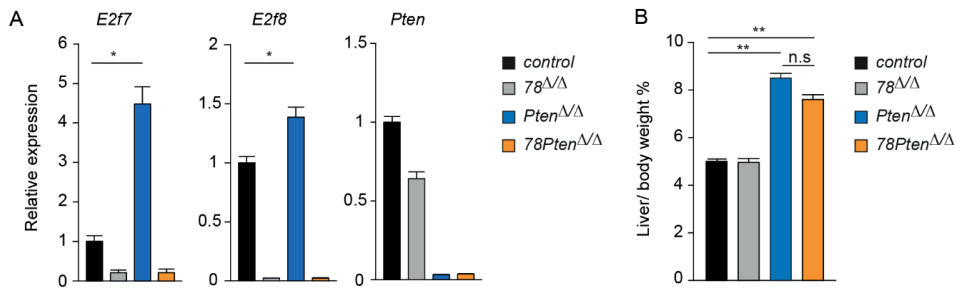


Progesterone-mediated oocyte maturation	CCNA2;MAD2L2;C-PEB1;GNAI1;MAD2L1	cellular response to peptide hormone stimulus	CPEB1;TBC1D4;PPARG;SL-C2A4;SORBS1;SLC30A10;GCK
Thyroid cancer	PAX8;PPARG;RXRG	sulfur compound catabolic process	GALNS;GPC1;OMD;CHAC1
AMPK signaling pathway	CCNA2;SCD2;PPARG;SL-C2A4;CD36	cellular response to insulin stimulus	CPEB1;TBC1D4;PPARG;SL-C2A4;SORBS1;GCK
ECM-receptor interaction	LAMB3;LAMC3;CD36;NPNT	positive regulation of protein localization to cell periphery	ARHGEF16;SORBS1;GNAI1;PLS1
<b><i>DOWN in 78Pten<sup>Δ/Δ</sup> versus control</i></b>			
<b>KEGG Pathway</b>	<b>Genes</b>	<b>GO Molecular Process</b>	<b>Genes</b>
Protein processing in endoplasmic reticulum	PDIA3;HSP90AA1;ERO1LB;HSP-90AB1;HSPA5;DERL3;EDEM2;SSR3;PDIA4;HSP90B1;DNAJC3;SEC61A1;LMAN1;DNAJB11;CANX-;STT3A;SSR1;HYOU1;CAL-R;P4HB;TXNDC5	IRE1-mediated unfolded protein response	TSPYL2;DNAJC3;SEC61A1;SER-P1;HSPA5;DNAJB11;SSR1;SRPR-B;HYOU1;PDIA5
Protein export	SEC61A1;SPCS3;HSPA5;SRPRB;SEC11A	response to endoplasmic reticulum stress	PDIA3;HSPA5;UBA5;ATP2A2;HYOU1;P4HB;PDIA5;PDIA4;HSP-90B1;TXNDC5
Steroid biosynthesis	SQLE;MSMO1;LSS;CYP51	retrograde vesicle-mediated transport, Golgi to ER	ARF4;UVRAG;TMED9;SCFD1;-SURF4;TMED3;KDELRL2;COPG1;COPZ1
Prostate cancer	HSP90AA1;HSP-90AB1;CCND1;PTEN;TGFA;HSP-90B1;FGFR1	protein N-linked glycosylation	DPAGT1;LMAN1;B3GALNT1;DERL3;OSTC;STT3A;ALG12;MAGT1
Thyroid hormone synthesis	HSPA5;CANX;LRP2;PLCB1;PDIA4;HSP90B1	Golgi vesicle transport	UVRAG;ARF4;TMED9;SURF4;USO1;TGFA;COPZ1;LMAN1;SCFD1;TMED3;KDELRL2;HYOU1;COPG1

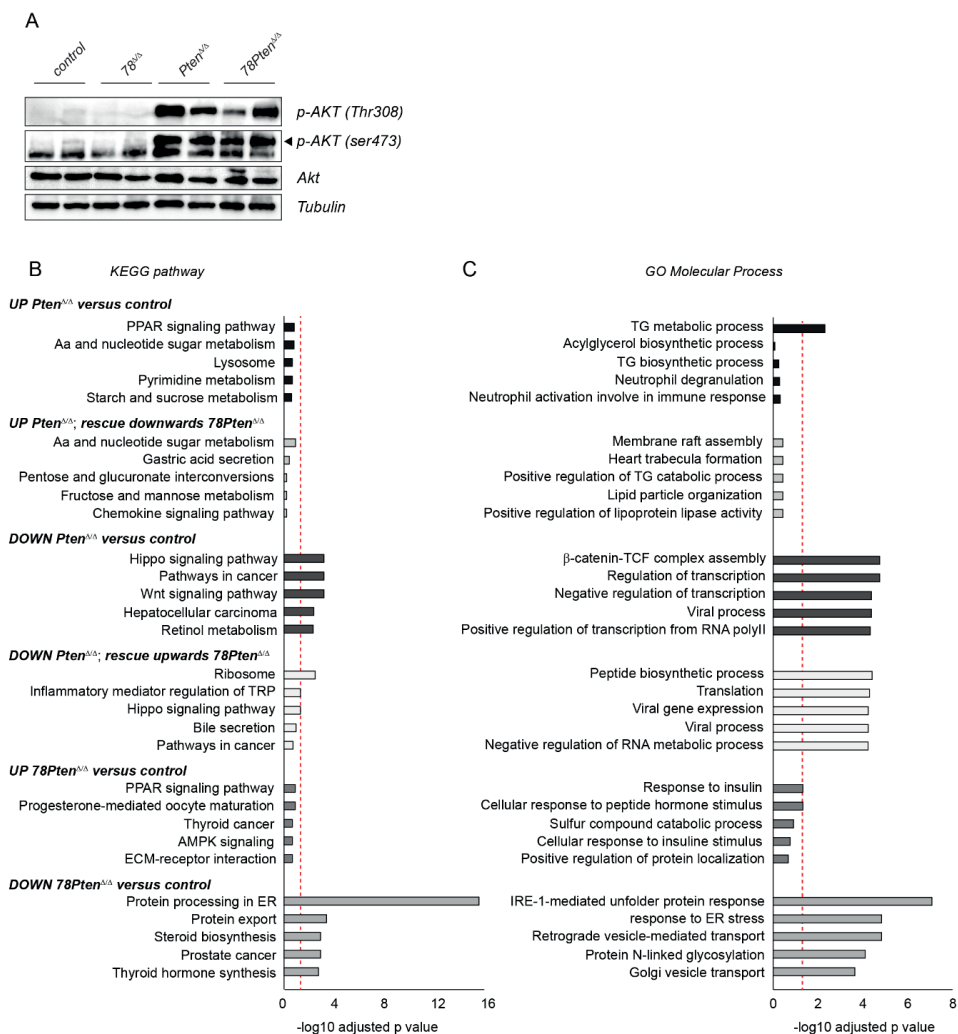
**Supplementary Table 4:** Overlapping transcripts between RNA sequencing and CHIP-sequencing data.

<i>UP in Pten<sup>Δ/Δ</sup>, rescued downwards in 78Pten<sup>Δ/Δ</sup></i>		<i>DOWN in Pten<sup>Δ/Δ</sup>, rescued upwards in 78Pten<sup>Δ/Δ</sup></i>	
<b>Gene symbol</b>	<b>Name</b>	<b>Gene symbol</b>	<b>Name</b>
E2F7	E2F transcription factor 7	PLEKHG2	Pleckstrin Homology and RhoGEF Domain Containing G2
CDC25A	Cell division Cycle 25A	ATP5G1	ATP Synthase Membrane
CDKN1A	Cyclin Dependent Kinase Inhibitor 1A	SPEN	Spn Family transcriptional repressor
RAD51AP1	RAD51 Associated Protein 1	SIK2	Salt Inducible Kinase 2
ASF1B	Anti-Silencing Function 1B Histone Chaperone	SLC25A28	Solute Carrier Family 25 Mmember 28 (encoding Mfrn2)
HAUS8	HAUS Augmin Like Complex-8	IRS2	Insulin Receptor Substrate 2
DBR1	Debranching RNA Lariats 1	ADCY9	Adenylate Cyclase 9
MTMR11	Myotubularin Related Protein 11	ZFP36L1	Zinc Finger protein Like 1
HK2	Hexokinase 2	ZFP36L2	Zinc Finger protein Like 2
RAD1	RAD1 Checkpoint DNA Exonuclease	CBX4	Chomobox 4
PTGES	Prostaglandin E Synthase	FSCN1	Fascin Actin-Bundling protein 1
CCDC51	Coiled-Coil Domain Containing 51	GAS1	Growth arrest specific 1
CHMP2B	Charged Multivesicular Body Protein 2B	GNA12	G protein subunit alpha 12
RHOA	Ras Homolog Family Member U	HIPK2	Homeodomain Interacting Protein Kinase 2
ACYP2	Acylphosphatase 2	JUNB	JunB Proto-Oncogene
TRA2A	Transformer 2 Alpha Homolog	RPL19	Ribosomal Protein L19
VOPP1	VOPP1 WW Domain Binding Protein	SLC30A3	Solute carrier family 30, member 3
		ARHGAP23	Rho GTPase Activatin Protein 23
		UBE4B	Ubiquination Factor E4B
		SF3B5	Splicing factor 3b Subunit 5
		RPS21	Ribosomal Protein S21
		RNASEH2C	Ribonuclease H2 Subunit C
		THAP7	Thap domain containing 7
		CIC	Capicua Transcriptional Repressor
		NOTUM	Notum, Palmitoleoyl-Protein Carboxylesterase
		EXOSC4	Exosome Component 4

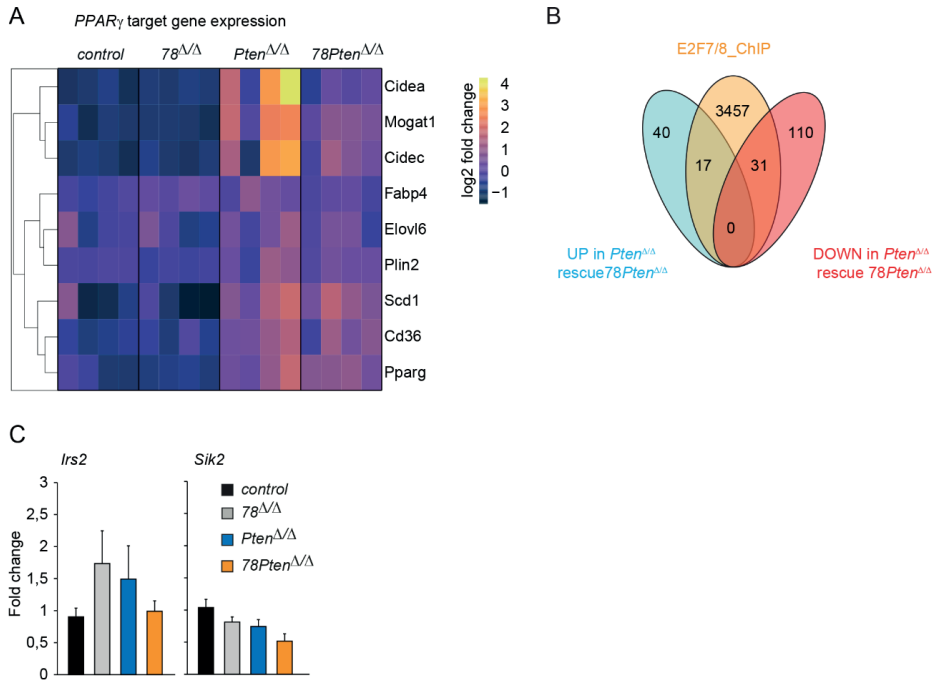
<i>UP in Pten<sup>Δ/Δ</sup>, rescued downwards in 78Pten<sup>Δ/Δ</sup></i>	<i>DOWN in Pten<sup>Δ/Δ</sup>, rescued upwards in 78Pten<sup>Δ/Δ</sup></i>
	DHTKD1 Dehydrogenase E1 and Transketolase Domain Containing 1
	KDM6B Lysine Demethylase 6B
	DUSP7 Dual Specificity phosphatase 7
	MLLT6 MLLT6, PHD Finger Containing
	ANO8 Anoctamin 8



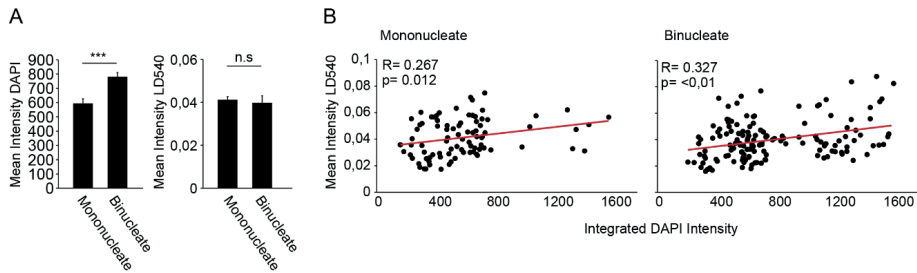
**▲Supplemental Figure 1: (A)** Transcript levels of *E2f7*, *E2f8* and *Pten* in the indicated genotypes of 16 weeks-old livers measured by quantitative PCR. Fold changes were adjusted to average of controls and GAPDH and  $\beta$ -Actin were used to normalize the expression. Bars represents average  $\pm$  SEM ( $n=5$  mice/genotype). \*  $p < 0.05$  (Mann-Whitney Rank Sum Test). **(B)** Percentage of Liver/Body weight from 16 weeks-old livers. Bar graphs represent average and SEM ( $n=8-10$  mice). \* $p < 0.05$  (Kruskal Wallis One Way Analysis of Variance on Ranks and Dunn's post-hoc correction).



**▲Supplemental Figure 2: (A)** Representative western blot showing expression levels of AKT and phosphorylated AKT (ser473 and Thr308) of 16 weeks old liver lysates of 2 mice from the indicated genotypes. (tested  $n=6$  mice/genotype). **(B)** KEGG pathway enrichment analysis showing the top 5 most strongly enriched pathways among differentially expressed genes in each of the indicated comparisons. Red dot line highlights the threshold of statistical significance (Benjamini-Hochberg corrected  $p < 0.05$ ). **(C)** Gene ontology (GO) analysis showing the top 5 most strongly enriched pathways among differentially expressed genes in each of the indicated comparisons. Red dot line highlights the threshold of statistical significance (Benjamini-Hochberg corrected  $p < 0.05$ ).



**▲Supplemental Figure 3: (A)** Heatmap showing 2log-fold change in expression relative to the mean expression of control livers of *Pparg* and a panel of its target genes in RNA-sequencing data from 16 weeks old livers. **(B)** Venn diagram showing overlapping genes with at least 1 E2F motif identified in our RNA sequencing and available ChIP-seq data collected from HeLa. **(C)** Transcript expression of *Irs2* and *Sik2* in 16weeks-old livers from the indicated genotypes. Fold changes were adjusted to average of controls and GAPDH and  $\beta$ Actin were used to normalize the expression. Data represent average  $\pm$  SEM ( $n=6$  controls;  $n=4$  78 $\Delta/\Delta$ ,  $n=9$  *Pten* $\Delta/\Delta$ ,  $n=8$  78*Pten* $\Delta/\Delta$ ).



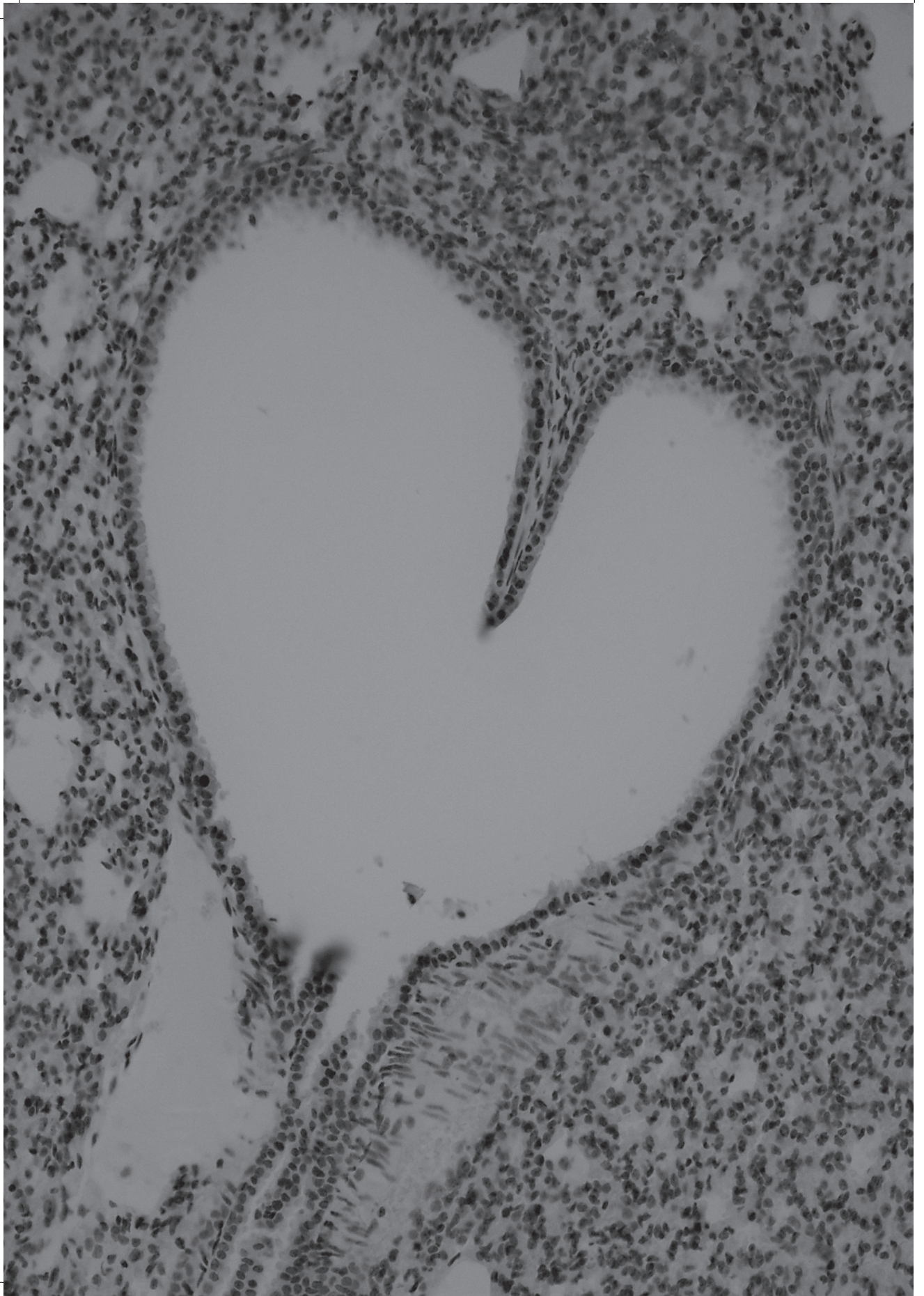
**▲Supplemental Figure 4: (A)** Mean intensity of DAPI and LD540 signal of immunofluorescent images of mononucleate and binucleate hepatocytes. ( $n=87$  mononucleate;  $n=146$  bi-nucleate). \*\*\* $p<0.001$  (Mann-Whitney Rank Sum Test). **(B)** Pearson correlation computation showing correlation between mean intensity of LD540 and integrated DAPI intensity in primary isolated mononucleated and binucleated hepatocytes from control mice with different ploidy incubated 3h with oleic acid.

## REFERENCES

- (1) Mitra S, De A, Chowdhury A. Epidemiology of non-alcoholic and alcoholic fatty liver diseases. *Transl Gastroenterol Hepatol* 2020 -4-05;5.
- (2) Fabbrini E, Sullivan S, Klein S. Obesity and nonalcoholic fatty liver disease: biochemical, metabolic, and clinical implications. *Hepatology* 2010 Feb;51(2):679-689.
- (3) Cusi K. Role of insulin resistance and lipotoxicity in non-alcoholic steatohepatitis. *Clin Liver Dis* 2009 Nov;13(4):545-563.
- (4) Michelotti GA, Machado MV, Diehl AM. NAFLD, NASH and liver cancer. *Nat Rev Gastroenterol Hepatol* 2013 Nov;10(11):656-665.
- (5) Gentric G, Maillet V, Paradis V, Couton D, L'Hermitte A, Panasyuk G, et al. Oxidative stress promotes pathologic polyploidization in nonalcoholic fatty liver disease. *The Journal of clinical investigation* 2015;125(3):981-992.
- (6) Fox DT, Duronio RJ. Endoreplication and polyploidy: insights into development and disease. *Development* 2013 -01-01;140(1):3-12.
- (7) Edgar BA, Zielke N, Gutierrez C. Endocycles: a recurrent evolutionary innovation for post-mitotic cell growth. *Nature Reviews Molecular Cell Biology* 2014 -03;15(3):197-210.
- (8) Celton-Morizur S, Desdouets C. Polyploidization of liver cells. *Polyploidization and Cancer* 2010:123-135.
- (9) Duncan AW, Taylor MH, Hickey RD, Hanlon Newell AE, Lenzi ML, Olson SB, et al. The ploidy conveyor of mature hepatocytes as a source of genetic variation. *Nature* 2010;467(7316):707-710.
- (10) Pandit S, Westendorp B, Nantasanti S, van Liere E, Tooten PCJ, Cornelissen PWA, et al. E2F8 is essential for polyploidization in mammalian cells. *Nat Cell Biol* 2012;14(11):1181-1191.
- (11) Celton-Morizur S, Merlen G, Couton D, Margall-Ducos G, Desdouets C. The insulin/Akt pathway controls a specific cell division program that leads to generation of binucleated tetraploid liver cells in rodents. *J Clin Invest* 2009 -7-1;119(7):1880-1887.
- (12) Chen H, Ouseph MM, Li J, Pécot T, Chokshi V, Kent L, et al. Canonical and atypical E2Fs regulate the mammalian endocycle. *Nat Cell Biol* 2012 Nov;14(11):1192-1202.
- (13) Sladky VC, Knapp K, Soratroi C, Heppke J, Eichen F, Rocamora-Reverte L, et al. E2F-Family Members Engage the PIDDosome to Limit Hepatocyte Ploidy in Liver Development and Regeneration. *Dev Cell* 2020 Feb 10;52(3):335-349.e7.
- (14) Muramatsu Y, Yamada T, Moralejo DH, Mochizuki H, Sogawa K, Matsumoto K. Increased polyploid incidence is associated with abnormal copper accumulation in the liver of LEC mutant rat. *Res Commun Mol Pathol Pharmacol* 2000;107(1-2):129-136.
- (15) Lazzarini Denchi E, Celli G, de Lange T. Hepatocytes with extensive telomere deprotection and fusion remain viable and regenerate liver mass through endoreduplication. *Genes Dev* 2006 -10-01;20(19):2648-2653.
- (16) Toyoda H, Bregerie O, Vallet A, Nalpas B, Pivert G, Brechot C, et al. Changes to hepatocyte ploidy and binuclearity profiles during human chronic viral hepatitis. *Gut* 2005 Feb;54(2):297-302.
- (17) Duncan AW, Hanlon Newell AE, Bi W, Finegold MJ, Olson SB, Beaudet AL, et al. Aneuploidy as a mechanism for stress-induced liver adaptation. *J Clin Invest* 2012 Sep;122(9):3307-3315.
- (18) Miettinen TP, Pessa HKJ, Caldez MJ, Fuhrer T, Diril MK, Sauer U, et al. Identification of transcriptional and metabolic programs related to mammalian cell size. *Curr Biol* 2014 -03-17;24(6):598-608.
- (19) Kent L, Rakijas J, Pandit S, Westendorp B, Chen H, Huntington J, et al. E2f8 mediates tumor suppression in postnatal liver development. *J Clin Invest* 2016;126(8):2955-2969.

- (20) Horie Y, Suzuki A, Kataoka E, Sasaki T, Hamada K, Sasaki J, et al. Hepatocyte-specific Pten deficiency results in steatohepatitis and hepatocellular carcinomas. *J Clin Invest* 2004 /06/15;113(12):1774-1783.
- (21) Stiles B, Wang Y, Stahl A, Bassilian S, Lee WP, Kim Y, et al. Liver-specific deletion of negative regulator Pten results in fatty liver and insulin hypersensitivity. *PNAS* 2004 -02-17 00:00:00;101(7):2082-2087.
- (22) Soriano P. Generalized lacZ expression with the ROSA26 Cre reporter strain. *Nat Genet* 1999 -01;21(1):70-71.
- (23) Robinson MD, McCarthy DJ, Smyth GK. edgeR: a Bioconductor package for differential expression analysis of digital gene expression data. *Bioinformatics* 2010 -01-01;26(1):139-140.
- (24) Love MI, Huber W, Anders S. Moderated estimation of fold change and dispersion for RNA-seq data with DESeq2. *Genome Biol* 2014;15(12):550.
- (25) Xie Z, Bailey A, Kuleshov MV, Clarke DJB, Evangelista JE, Jenkins SL, et al. Gene Set Knowledge Discovery with Enrichr. *Curr Protoc* 2021 -03;1(3):e90.
- (26) Thoolen B, Maronpot R, Harada T, Nyska A, Rousseaux C, Nolte T, et al. Proliferative and nonproliferative lesions of the rat and mouse hepatobiliary system. *Toxicol Pathol* 2010;38(7 Suppl):5S-81S.
- (27) Patitucci C, Couchy G, Bagattin A, Cañeque T, de Reyniès A, Scoazec J, et al. Hepatocyte nuclear factor 1 $\alpha$  suppresses steatosis-associated liver cancer by inhibiting PPAR $\gamma$  transcription. *J Clin Invest* 2017 -05-01;127(5):1873-1888.
- (28) Pan D. The hippo signaling pathway in development and cancer. *Dev Cell* 2010 -10-19;19(4):491-505.
- (29) Westendorp B, Mokry M, Groot Koerkamp, Marian J A, Holstege FCP, Cuppen E, de Bruin A. E2F7 represses a network of oscillating cell cycle genes to control S-phase progression. *Nucleic Acids Res* 2012;40(8):3511-3523.
- (30) Nagaya T, Tanaka N, Komatsu M, Ichijo T, Sano K, Horiuchi A, et al. Development from simple steatosis to liver cirrhosis and hepatocellular carcinoma: a 27-year follow-up case. *Clin J Gastroenterol* 2008 -10;1(3):116-121.
- (31) Zhang S, Zhou K, Luo X, Li L, Tu H, Sehgal A, et al. The polyploid state plays a tumor suppressive role in the liver. *Dev Cell* 2018 -2-26;44(4):447-459.e5.
- (32) Lin Y, Zhang S, Zhu M, Lu T, Chen K, Wen Z, et al. Mice With Increased Numbers of Polyploid Hepatocytes Maintain Regenerative Capacity But Develop Fewer Hepatocellular Carcinomas Following Chronic Liver Injury. *Gastroenterology* 2020 -05;158(6):1698-1712.e14.
- (33) Watanabe T, Tanaka Y. Age-related alterations in the size of human hepatocytes. A study of mononuclear and binucleate cells. *Virchows Arch B Cell Pathol Incl Mol Pathol* 1982;39(1):9-20.
- (34) Xu W, Wu L, Yu M, Chen F, Arshad M, Xia X, et al. Differential Roles of Cell Death-inducing DNA Fragmentation Factor- $\alpha$ -like Effector (CIDE) Proteins in Promoting Lipid Droplet Fusion and Growth in Subpopulations of Hepatocytes. *J Biol Chem* 2016 -02-26;291(9):4282-4293.
- (35) Denechaud P, Lopez-Mejia IC, Giral A, Lai Q, Blanchet E, Delacuisine B, et al. E2F1 mediates sustained lipogenesis and contributes to hepatic steatosis. *J Clin Invest* ;126(1):137-150.
- (36) Shimada Y, Kuninaga S, Ariyoshi M, Zhang B, Shiina Y, Takahashi Y, et al. E2F8 promotes hepatic steatosis through FABP3 expression in diet-induced obesity in zebrafish. *Nutr Metab* 2015 -5-20;12.





# Chapter 5

---

## General Discussion

In this thesis, we aimed to explore the consequences of manipulating E2F-dependent transcription in tumor formation and progression employing transgenic mouse models. We showed that activity of atypical E2Fs, E2F7 and E2F8, is critical to suppress liver tumor progression (Chapter 2 & 3). Interestingly, they can also promote tumorigenesis in lungs and pituitary glands (Chapter 3). These contradicting results might be related to tissue cell-type specific functions of atypical E2Fs in regulating transcriptional events during the cell cycle. Furthermore, atypical E2Fs possesses functions that reach beyond normal cell cycle control, because they are also key regulators of abortive cell cycles required for liver cell polyploidization and thereby altering for instance lipid accumulation in the liver (chapter 4). In this chapter, we would like first to discuss the opposing roles of atypical E2Fs in either inhibiting or promoting tumorigenesis. In the second part, I will outline potential translating strategies to target the tumor promoting E2F activity in cancer patients.

## **ATYPICAL E2Fs: TUMOR SUPPRESSORS OR ONCOGENES?**

Atypical E2Fs regulate many genes whose expression is essential for proper progression through the cell cycle. Nevertheless, their role in cancer development is still under debate. To date, some studies have shown that atypical E2Fs act as tumor suppressors but other studies claimed that they function also as oncogenes (1-5). In this thesis we employed knock-out models of atypical E2Fs and we developed a new transgenic mouse model with whole-body inducible E2F7 and -8 overexpression. This offered the unique possibility to compare and study the consequences of manipulating E2F-dependent transcription, via atypical E2Fs, during spontaneous and chemical-induced tumorigenesis in a variety of tissues. We learned that atypical E2F display abilities to suppress and promote tumorigenicity. To better understand the opposing roles of atypical E2Fs in tumorigenesis, we discuss below the possible mechanisms of action of atypical E2Fs in regulating transcription, polyploidization and angiogenesis.

### **Transcription**

It is firmly established that atypical E2Fs act as repressors of a large network of genes essential for DNA replication, DNA repair and DNA metabolism. In fact, atypical E2Fs inhibit proliferation of cancer cells *in vitro* (6-10). Moreover, studies with conditional deletion of *E2f7* and *E2f8* in mouse livers and skin resulted in enhanced cancer development, supporting a tumor suppressive function(1,2). In line with this observation, results presented in chapter 2 demonstrated that ectopic expression of atypical E2Fs can inhibit liver cancer growth, whereas overexpression of an atypical DNA binding-mutant E2F without transcriptional activity cannot block liver tumor growth. These *in vivo* findings clearly support a model where atypical E2Fs function as tumor suppressor via transcriptional repression of E2F target genes in the liver.

However, there are *in vitro* studies using human lung and liver cancer cell lines claiming that E2F8 can promote tumor growth (3,4). More specifically, these last studies proposed that ectopic expression of E2F8 can act as transcriptional activator of cyclin D1 (*CCND1*) and UHRF1 in hepatocellular carcinoma cells. This discrepancy might be explained by the fact that E2F7/8 can function as activators in a tissue or context-dependent way. Other E2Fs exhibit dual roles switching from activators to repressors depending on the context (11). However, the results presented in chapter 2 demonstrated that proliferation of cancer cells was mainly carried out by cells whose ectopic expression of atypical E2Fs was low or null. Ectopic E2F7/8 invokes a strong negative selection pressure which lead to an increased risk for tumor recurrence in the long run. These results suggest that mild repression of E2F targets is not sufficient to inhibit cancer cell proliferation and thus the oncogene effect of atypical E2Fs might be determined by their expression levels and the capacity to repress E2F targets in specific cells. Therefore, it is conceivable that the studies presented above by *Deng and Park* were performed with hepatoma cell line clones with modest E2F8 activity, which would result in minimal repression of E2F targets and therefore increased tumorigenic capacity. We also showed that life-long overexpression of E2F7/8 promoted tumorigenesis in the lungs (Chapter 3). The tumor promoting mechanism is currently unknown, but might be also dependent on its transcriptional activity, because a transcriptionally inactive mutant form of atypical E2F does not promote lung tumorigenesis.

Owing to the large number (>100) of E2F-regulated genes, it is difficult to dissect which specific target genes are critical for cancer cell cycle progression. We explored some of them, for example DNA replication and DNA repair factors, and we demonstrated for the first time that boosted expression of atypical E2Fs induced replication stress (RS) via repression of the aforementioned factors. Given that E2F7/8 represses E2F targets during late S and G2, these findings suggest that repression of E2F-dependent transcription during these period alters the replication capacity of cells and precludes cell cycle progression. Of note, mild repression of E2F-transcription also induces, to a lesser extent, replication stress, although the outcome in terms of cell cycle fate decision-making differs. Cells experiencing RS became vulnerable to accumulation of DNA damage during S phase. Thus, cells must decide either to repair the damage and continue cycling, or arrest and exit the cell cycle or go into programmed cell death (apoptosis) due to replication catastrophe (12). This decision is to a large extent controlled by E2F transcription(13,14). Cells can tolerate low levels of atypical E2Fs, albeit at the expense of DNA damage and perhaps even genomic instability. But high levels trigger stalling of the replication machinery and replication catastrophe leading to cell death. Several studies have demonstrated that reduced expression of DNA repair genes, such as BRCA deficiency, contributed to genomic instability and caused a variety of cancers (15). Therefore, chronic repression of E2F targets (including *BRCA1* and *BRCA2*) might eventually be detrimental for cells and results in cellular transformation. Together, to assess the anti-tumor or pro-tumor activity of E2F7/8, it is critical to investigate their protein expression

levels. Given that their expression levels may differ between individual cells, analysis of single cells may help to understand the heterogeneous response. Moreover, it would be interesting to see whether sustained boosted expression of atypical E2Fs in the liver would permanent arrest liver tumor cells and therefore block tumor growth.

Another point for discussion is whether the timing of manipulating E2F-dependent transcription matters to prevent tumorigenesis. Regulation of E2F-target genes is precisely coordinated through the cell cycle (6,16,17). In particular, RB ensures proper G1-S transition by repressing E2F-dependent transcription while atypical E2Fs repress the same targets during late S and G2. Given that RB and atypical E2Fs cooperate in several processes such as cellular senescence (18), we hypothesized that their cooperation might also be important to prevent tumorigenesis. In chapter 3 we found evidence that atypical E2Fs and RB prevented or promoted tumorigenesis in a context and tissue-specific manner. In the liver, we hypothesized that deletion of RB and atypical E2Fs would lead to further deregulation of E2F targets, thus explaining the increased proliferation observed in liver tumor tissue. However, our experimental evidence is insufficient to formally exclude differences in expression of E2F targets, because we looked at expression in bulk cell lysates. This analysis does not account for variability between the cell cycle fates and thus expression of E2F targets. This same analysis performed on sorted single cells labelled with the FUCCI (Fluorescent Ubiquitination Cell cycle Indicator) system could expedite further investigation of this issue in the future. Instead, we found that additional deletion of atypical E2Fs on RB-mutant tumors altered cell cycle profile marked by an increase of 4C cell populations. Previous studies have shown that deletion of RB in livers can cause activation of the DNA damage checkpoint (19). In addition, E2F7/8 loss can cause defects in the DNA damage checkpoint (20). Therefore, their combined action could be essential to maintain genomic integrity. Our results suggest that atypical E2Fs might function as a backup mechanism for tumors that loss or mutate RB by acting in a different and later checkpoint, although we observed opposing results in pituitary glands with RB heterozygous background. Thus, this checkpoint-based evidence might be specific for certain tissues.

Conceptually, the findings from this thesis indicate that expression levels of atypical E2Fs as well as the timing of their activation play a critical role on their biological functions. Acute or severe overexpression of E2F7/8 resulted in inhibition of cancer cell proliferation. Whereas chronic or modest expression contributed to cancer. This phenotype is shared by many chemotherapeutic drugs (21). Thus, the findings from this thesis provide a rationale to interfere with the regulation of E2F7/8 as a therapeutic approach to block the proliferation of cancer cells. Moreover, boosted expression of atypical E2Fs may induce sensitivity to chemotherapeutics that also cause replication stress. Nevertheless, this regulation must be tightly controlled in a precise and timely manner.



## Polypliodization

Polypliodization, the addition of one or multiple complete sets of chromosomes, can occur in some cells as a normal developmental process, whereas in others it occurs as a result of stress (22,23). In the liver, for example, physiological polypliodization is associated with the development and differentiation of hepatocytes during postnatal growth (24,25), whereas pathological polypliodization arises upon oxidative stress or chronic viral infection as a putative protective mechanism(26,27). These findings suggest that polypliod hepatocytes might account for specific functions. Accordingly, tetraploidy prevents formation of hepatocellular carcinoma, presumably because polypliod cells may possess extra copies of tumor suppressor genes and buffer the effect of gene-inactivating mutations due to DNA damaging agents (28). Moreover, early tumor lesions in human liver cancer patients are characterized by the expansion of diploid hepatocytes as well as in carcinogen-induced rodent models (29). These findings challenge the old dogma which claimed that polypliod cells foster aneuploidy and consequently are more prone to develop cancer (30).

We previously showed that E2F7/8 deficient livers are composed predominantly of diploid hepatocytes (31). Interestingly, these livers developed spontaneous liver cancer (2), suggesting that E2F7/8 -dependent polypliodization might have a tumor suppressive function in the liver. This is consistent with data shown in chapter 3 and 4 of this thesis. In support of this hypothesis, we recently demonstrated that E2F7 and -8 transcriptionally repressed the PIDDosome, an important multiprotein complex that limits polypliodization in the liver. Deletion of PIDDosome components in conditional knockout mice caused a marked increase in hepatocyte ploidy (32). Of note, hyper-polypliodization caused by PIDDosome deficiency protected livers from HCC (33). Altogether, these studies suggest that E2F7 and -8 are key components of the molecular pathway that facilitates physiological hepatocyte polypliodization and, consequently inhibit liver tumorigenesis. These findings are a clear demonstration of the importance of tissue context on the effects of atypical E2Fs on tumorigenesis.

## Tumor angiogenesis

E2F7/8 appear to repress tumor angiogenesis (formation of blood vessels derived from pre-existing vessels). Loss of atypical E2Fs during tumor formation promoted vessel branching in subcutaneous engrafted tumors from transformed mouse embryonic fibroblasts (34). However, this neo-vascularization did not result in enhanced tumor growth. Considering these results, it seems unlikely that atypical E2Fs plays a tumor suppressive role in the liver via repressing angiogenesis. Nevertheless, we cannot exclude that this effect is again tissue-specific, as atypical E2Fs can also form a transcriptional complex with the hypoxia inducible factor 1 (HIF-1) to stimulate the vascular growth factor A (VEGF-A) promoter activity (35). We did not evaluate this role extensively in this thesis, but we examined in chapter 2 whether tumor vascularization differed between control and tumors overexpressing E2F7 or -8 by analyzing the amount of

blood vessels in each condition (immunohistochemistry analysis of Isolectin B4). The data revealed no differences in the apparent vascularization of the tumors in the different condition. Further research is needed to understand whether these effects are dependent on tumor type or tissue-specific and whether they interfere with tumorigenesis.

Taken together, atypical E2Fs are involved in many cell type specific processes such as transcription, polyploidization and angiogenesis that are known to impact tumorigenesis. Further mechanistic studies including single cell studies are required to better understand the action of atypical E2Fs in cancer. Endogenous levels of atypical E2Fs exhibit significant variability on their effect on cell fate decisions. Our results support a model in which low levels of atypical E2Fs permit proliferation whereas intermediate expression levels stall the cell cycle and very high levels drive apoptosis through replication catastrophe in cancer cells. Therefore, depending on the average levels of atypical E2Fs and the extent of cell-cell variability, opposing effects can be observed in experiments performed on the same system. This model is further supported by the fact that other E2F members, namely E2F1, also dictate their downstream phenotypes based on their expression levels (36). These results illustrated the complexity of understanding the activity of atypical E2Fs. Moreover, the analysis of bulk population of cells might oversimplify the interpretation of the results. Individual cycling cancer cells display substantial heterogeneity in E2F target deregulation (20). Thus, analysis of single cells would be a more powerful tool to further understand their heterogeneous regulation and, most likely, allow us to make more clear conclusions about their relevance in tumorigenesis.

## **FROM THE BENCH TO THE CLINICS: MANIPULATION OF E2F ACTIVITY TO INHIBIT CANCER PROGRESSION.**

### **Importance of targeting E2F-dependent transcription during tumorigenesis.**

Upregulation of E2F-dependent transcription is frequently observed in a variety of cancer types and proposed to drive uncontrolled proliferation of cancer cells and is correlated with a poor prognosis for the patients. Moreover, increased E2F-dependent transcription activity was recently proposed to mediate oncogene-induced replication stress (37). Therefore, targeting E2F activity has been recognized as an important and selective antitumor strategy.

### **Attempts to manipulate E2F activity in patients.**

During the past couple of decades, extensive efforts on developing strategies to target E2Fs in the clinics have been made. Owing to the difficulties of targeting transcription factors, the only drugs that received the approval from FDA (US Food and Drug Administration) and affect E2F activity are those targeting CDK4 and CDK6 (referred as CKD4/6 inhibitors). Inhibition of



CDK4/6 results in RB hypo-phosphorylation, inactivation of E2F activity and blocks G1/S transition (38). Therefore, their mechanism of action of CDK4/6 inhibitors seems to heavily relies on the control of E2F transcription during S phase. Their efficacy to inhibit tumor growth has been widely demonstrated although drug resistance is a frequently occurring problem (39). There is solid evidence that some of the resistance mechanisms involve persistent E2F target gene expression (40). It is therefore conceivable that resistance to CDK4/6 inhibitors involves E2F-controlling mechanisms and therefore, specific targeting of E2F activity might help to override tumor relapses. Recently, it has been suggested that long-lasting effects upon drug (CDK4/6i) washout were accompanied by accumulation of replication stress (41). In clinical practice, the CDK4/6i palbociclib is typically given in cycles which include a drug-holiday week (42). Therefore, one could envision a possibility of combining CDK4/6 inhibitors with other genotoxic drugs to exacerbate the anti-proliferative effect and overcome tumor resistance. We propose that modulation of E2F activity is a possible alternative to deal with CDK4/6i resistance. To date several approaches have been described, including peptides that interfere with the binding of E2F activators to its consensus DNA sequence or small molecules that inhibit E2F activity (43–45). Despite the potent inhibitory effect on the proliferation capacity of the tested cells, it also often triggered cellular toxicity. This harmful effect on cancer cells would, however, be very detrimental for normal cells, which also rely on this program to control the cell cycle. Therefore, attempting to modulate E2F-dependent transcription in cancer patients must be carefully evaluated beforehand to minimize side effects. A summary of already tested strategies and the reasons that might explain why they are still in pre-clinical stages are discussed below.

### **Inhibitors of E2F activity with small molecules**

Initial studies showed that a small molecule, a pan-E2F-inhibitor (HLN006474), downregulated E2F-dependent transcription and decreased cell proliferation and induced apoptosis in melanoma and lung cancer cells (45,46). This molecule binds to E2Fs via hydrogen bonds and inhibited the DNA-binding activity of E2F (45). Initial characterization revealed a high efficiency in blocking cell proliferation. However, this was only observed when maintained for long exposure. Short time exposures lead to deregulation of E2F targets which, – although unlikely–, could lead to an increase in cell growth and adaptation of cells to elevated E2F-dependent transcription. Moreover, inhibition of E2F might lead to repression of pro-apoptotic proteins and increased genomic instability. Therefore, although the authors of these studies demonstrated that inhibition of E2F activity may have therapeutic potential in certain cell cultures, they raised concerns related to unwanted consequences of pan-E2F inhibitors that need to be further investigated. One additional concern that arises from these studies is the methodology. Taken into account that all the experiments were performed in two-dimensional culture, it is well possible that experiments using *in vivo* models will present more variation

or different outcome due to, in part, the high redundancy between E2F family members and their complex regulation (47). Therefore, follow-up investigations with this drug are necessary to determine the impact of inhibiting E2F activity in cancer patients.

A second compound which was described to interfere with E2F activity by the authors is ly101-4B, a nucleoside analogue. This compound could efficiently suppress cell viability of pancreatic ductal adenocarcinoma (PDAC)-derived cells and seemed to have higher affinity for cells with elevated levels of E2F activity (48). However, the authors only focused on the efficacy of this compound but its mechanism of action was not determined. It is conceivable that ly101-4B do not directly inhibit E2F activity. Instead, it inhibits DNA replication and therefore it correlates with reduced E2F activity. Thus, additional experiments need to be performed to address how the mechanism of action of this compound in better detail.

In summary, although the strategy to target E2F activity with pan-inhibitors seemed to work in 2D models, their efficacy needs to be tested in preclinical mouse models. Moreover, the complex transcriptional and post-translational regulation of E2F members should be considered for the optimal efficacy.

### **Inhibition of E2F activity with peptides and truncated E2F proteins**

Another strategy that has been explored is to inhibit E2F activity by designing peptides that interfere with the DNA binding activity or its association with DPs. Introduction of these peptides into cancer cells led to apoptosis, which correlated with a decrease in E2F activity (49-51). Most of these peptides were designed specifically to target E2F1, under the rationale that E2F1 is high in several human cancers and correlates with poor prognosis (43,44,52,53). For instance, some of these peptides bound tightly to an immobilized consensus in E2F1 promoter sequence and, when couple to penetratin (PEP), were cytotoxic to many malignant cells (43,44). Others prevented the dimerization between E2F1 and its DP partners, which consequently inhibited E2F1 transcription (54). Therefore the concern mentioned before in regard to the redundancy between E2F family member and their possible compensation still remains. Accordingly, regrowth of tumors occurred when the treatment with E2F1 penetrating-peptide was stopped in xenograft models (44). Moreover, these studies indicated that blocking the DNA binding activity of E2F in cancer cells efficiently impaired proliferation without major systemic toxicity. Nevertheless, blocking E2F DNA-binding activity might, in theory, interfere with the function of RB protein, which binds to DNA via E2F. Therefore, ideally, this therapies should be applied locally in RB-deficient tumors.

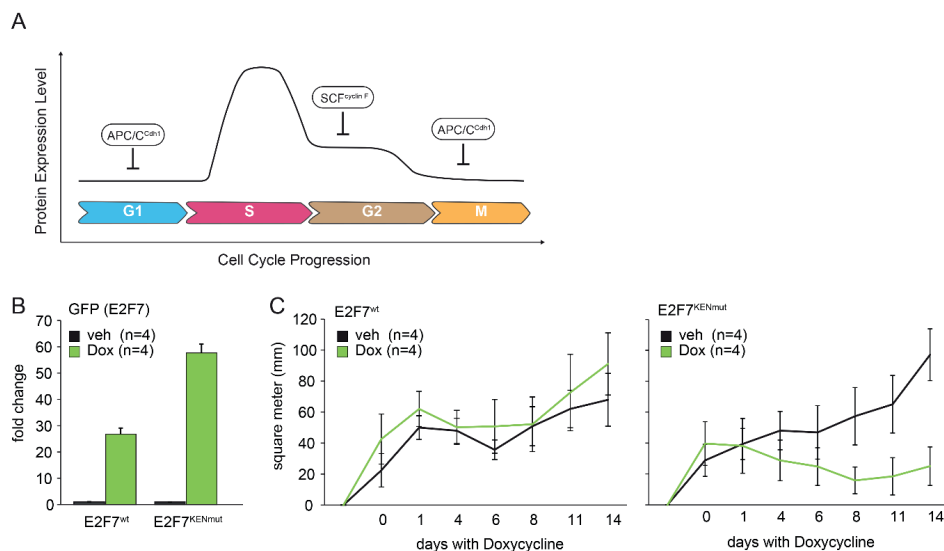
In addition to the peptides, truncated E2F1 proteins had also the ability to induce apoptosis and impaired tumor growth (55,56). These studies delivered a truncated form of E2F1 which lacks the transactivation domain and cell cycle-promoting effects via adenoviral therapy. Tumors treated with Ad-mediated E2F1 mut exhibited extensive apoptosis and reduced size. Nevertheless, once more the mechanism of action is not well studied and the delivery of these truncated proteins might be challenging due to possible immune reaction when applied systemically.

### **E2F-responsive oncolytic virus**

The use of virus as oncolytic agents for tumor therapy has been widely tested in a number of cancers (review(57)). Given that cancer cells are more actively transcribing E2F-responsive genes than normal cells (58), employing viral vectors that incorporate E2F-responsive promoters was a tempting idea. Briefly, oncolytic therapies control expression of viral early gene(s) required for replication with tumor-selective promoter(s). In this case, oncolytic adenoviral vectors use the tumor selective E2F1 promoter to limit expression of the viral E1A transcription unit, essential for replication and thus viral life cycle, in tumor cells. Using this technology, researchers were able to efficiently place E2F-responsive promoters into the genome of oncolytic adenoviruses and deliver these viruses into tumor cells and xenograft mouse models, and demonstrated a significant therapeutic advantage(59). This strategy resulted in increased production of several E2F-responsive viral genes, increased viral replication and cell lysis specifically of tumor cells with high E2F activity(59,60). Moreover, the usage of this strategy has demonstrated low toxicity in mice and veterinary patients and showed promising results in clinical trials (61-63). However, tumor growth inhibition was maintained over a prolonged time period but not totally eradicated. This could indicate low viral penetration into solid tumors. It is therefore critical to determine which factor(s) compromised the efficacy of this approach to pursue its application in the routine clinical use. A way of improving viral penetration is, for instance, the co-administration of hyaluronidase, enzyme that helps to degrade the extracellular matrix, and showed to improve the spreading of oncolytic viruses within tumors (64).

### **Therapeutic targeting of atypical E2Fs.**

Previous studies demonstrated that atypical E2Fs are potent tumor suppressors in liver and skin (1,2). This tumor suppression function is mainly mediated by the transcriptional repression of E2F target genes, which are involved in cell cycle progression, DNA damage response and apoptosis. In chapter 2 of this thesis, we demonstrated that boosting atypical E2F repressor activity can efficiently block deregulated E2F-dependent transcription, leading to reduced proliferation and impaired liver tumor growth without major effect on overall health status (65). Conceptually, these results indicate that manipulation of atypical E2Fs might be an efficient strategy to suppress tumor cell proliferation. However, we also observed some cells which managed to re-enter S-phase with mild replication stress and DNA damage despite overexpression of E2F7 leading to tumor relapse. Given that E2F7 levels peak during in S/G2 phase, these “escapees” might have been able to keep cycling because E2F7 is degraded during G1 (10). Previous data from our lab showed that mutant cell lines which failed to degrade E2F7/8 during G1, had very high levels of E2F7/8, halted cell cycle progression and underwent cell death (10). These data indicated that in order to achieve a strong inhibitory effect on the proliferation of tumor cells, atypical E2Fs need to be highly and continuously



**▲Figure 1: Regulation of atypical E2Fs activity to ensure proper cell cycle progression. (A)** Post-translational mechanisms regulating protein expression of atypical E2Fs during the cell cycle: APC/C<sup>dh1</sup> degrades atypical E2Fs in G1 phase to trigger E2F target gene expression for G1-S transition. Atypical E2Fs levels peak at early S phase and are later -G2- partially degraded by SCF<sup>Cyclin F</sup>. In order to allow mitotic progression, atypical E2Fs are fully eliminated by again APC/C<sup>dh1</sup>. **(B)** Quantitative PCR of E2F7-GFP transcript in HeLa cells with doxycycline-induced E2F7<sup>wt</sup> and E2F7<sup>KENmut</sup> after 24h of doxycycline treatment. **(C)** Xenograft growth curves. HeLa cells from B were injected into the flanks of nude mice and then we waited until palpable tumors appeared (day 0). Doxycycline was administrated *ad libitum* in pellets for 14 days. Tumors were monitored every 2-3 days.

expressed during the entire cell cycle. But, how to achieve that? For long time, transcription factors were considered as “undruggable” targets. Currently, there are several ways to target them, including modulation of their expression or degradation, preventing DNA binding or by blocking protein/protein interactions (66). In our lab, we unraveled three different post-translational mechanisms that control the oscillatory expression of atypical E2Fs during the cell cycle, in particular APC/C and SCF complexes, which target them for proteasomal degradation (10,14,67) (Figure 1A).

Importantly, these studies identified the domains in E2F7 and -8 where these potent degradation systems target atypical E2Fs to modulate their expression. APC/C<sup>dh1</sup> targets the KEN domain during G1 (10), checkpoint kinase 1 (Chk1) phosphorylates E2F7 and -8 together with 14-3-3 proteins via an RxxS Chk1-substrate motif in response to DNA damage (14), and cyclin F binds to both E2F7 and -8 via a canonical CY motif during G2 (67). Manipulation of these binding sites *in vitro* demonstrated that protein oscillation of atypical E2Fs is important for orderly cell cycle progression. Preliminary *in vivo* data in our lab

showed that stable KEN-mutant version of E2F7 blocked tumor growth in xenografts more efficiently than wild-type E2F7 induction (Figure 1B-C). Conceptually, these findings indicate that interfering the degradation of E2F7 would boost its repressive function throughout the entire cell cycle. So far, stabilization of E2F7 during G1, via mutation in KEN motif, seems to be sufficient to strongly inhibit tumor cell proliferation. This approach could be applied to patients via, for instance, delivery of chemically stabilized E2F7 KEN-mutant mRNA in lipid nanoparticles.

Cancer cells heavily rely on DNA repair mechanisms to deal with DNA damage. A clear example of this is the use of PARP inhibitors for the treatment of BRCA mutated tumors (68). This strategy is also known as synthetic lethality and it occurs when the perturbation of two genes simultaneously results in the loss of viability, while the loss of either gene alone is viable. Since atypical E2Fs also function as transcriptional repressor of DNA repair genes, including BRCA1/2 and Rad51, a possible targeting strategy would be to trigger “hyperactive” atypical E2Fs, for example via blocking their proteasomal pathways (cdh1, cyclin F), and combine it with PARP inhibitors. In support to this hypothesis, two studies indicated that loss of E2F7 conferred resistance to DNA damaging drugs by elevating expression of DNA repair genes (69,70). Another option would be to hyper-activate atypical E2Fs in combination with CDK4/6 inhibitors to overcome the loss of sensitivity observed with current treatment using CDK4/6 inhibitors (such as palbociclib). A study demonstrated that breast cancer patients resistant to palbociclib treatment exhibit persistent E2F target gene expression, indicating that resistance might involve E2F-dependent transcription mechanisms(40). Lastly, Chk1 inhibitors have been predicted to activate E2F7/8 under replication stress conditions (14). Presumably, this would imply that Chk1 inhibitors represent another attractive alternative to boost atypical E2Fs. Perhaps the combination with peptides blocking the binding of proteasomal regulators (Cdh1/cyclin F) to atypical E2Fs with Chk1 inhibitors would potentially lead to super-activation of atypical E2Fs and efficient down regulation of E2F dependent transcription. Moreover, it may help to overcome the tumor resistance mechanisms frequently encountered by Chk1 inhibitors which imply upregulation of E2F targets (71). Therefore, inhibition of E2F targets alone or in combination with current cancer therapies is a possibility that should be further explored and considered to complement current treatment strategies.

Nevertheless, stabilization of E2F7/8 as a potential cancer treatment is likely to trigger also some undesirable side effects. Despite targeting tumor cells, normal cells with rapid turnover, such intestinal cells, could also be affected and potentially eradicated. This could lead to abnormal absorption of nutrients and worsen the status of the patient. In the next section of this discussion we examine the advantages of avoiding systemic “hyperactivation” of atypical E2Fs by targeting specific tissues, such as the liver, where hepatocytes rarely proliferate under normal conditions and therefore side effects would be less likely.

**Liver cancer is an attractive candidate for E2F7/8 stabilizing therapy.**

Our findings and other studies indicate that the liver is particularly sensitive to increased E2F transcriptional input (2,72). For instance, increased copy numbers of E2F activators -1 and -3b in the whole body led to increased incidence of HCC in mice without affecting the rest of the tissues (72). The reason behind this observation is a matter of speculation, but it might have to do with exposure of hepatocytes to persistent DNA-damaging insults, resulting from the detoxification function of the liver. This stimulates re-entry of hepatocytes into the cell cycle to regenerate damaged areas in the liver, a process highly dependent on E2F signaling (13,14). Thus, the liver might be more sensitive than other organs to increased E2F transcription.

Another reason is the fact that E2F-dependent transcription is confined mainly to cycling cells. In the liver, most cells are normally quiescent, thus only rapidly proliferating cells may be affected by therapies which manipulate E2F activity. Accordingly, in chapter 2 of this thesis, we demonstrated that ubiquitous induction of atypical E2Fs inhibited liver tumor growth without a major impact on the healthy surrounding cells (65). Therefore, targeting E2F activity in organs with low basal proliferation rates, such as the liver, could open a novel therapeutic avenue for cancer patients whose tumors have higher proliferative rate than the surrounding tissue.

Lastly, E2F inhibition in HCC is attractive, because it is relatively easy to target drugs to the liver. To date, few nanocarrier technologies such as peptides and lipid nanoparticles have been investigated for liver-specific applications (73). Lipid nanoparticles have been increasingly recognized as vehicles for systemic delivery of gene therapies, such as siRNA or mRNA, to the liver and HCC (74,75), and have been utilized in clinical trials (76-78). Peptides or oncolytic viruses are also technologies applied for liver specific treatment, as mentioned above in the discussion. Based on these approaches and the knowledge we generated with mutant versions of E2F7/8, it would be interesting to prove whether it is possible to boost atypical E2F expression in cycling hepatocytes via delivery of mRNA in one of these carriers. Nevertheless, these techniques must be further optimized in order to fulfill specific needs such as increased cellular targeting and protection from degradation.

**CONCLUSION**

In this thesis we focused on further understanding the consequences of manipulating E2F-dependent transcription, via atypical E2Fs, in the context of cancer development and progression as well as in fatty liver disease. We, together with others, demonstrated that the E2Fs are a complex family of transcriptional regulators whose coordinated expression and activity are essential to ensure proper cell cycle progression and maintenance of genomic stability. It is clear that E2F-dependent transcription is highly heterogeneous between different types of cycling cells, in particular, is elevated in cancer cells. Therefore, E2F-controlling mechanisms might efficiently allow to block cancer cell proliferation. Finally, there is accumulating evidence

that cancer cells rely on excessive E2F activity to develop resistance to chemotherapy like, for instance, in the case of PARP inhibitors or CDK4/6 inhibitors. Therefore, targeted repression of E2F-dependent transcription might be an excellent strategy to complement current therapies. In this thesis, we present data demonstrating that it might be possible in the future to apply our proposed strategy, consisting on “hyperactivating” atypical E2Fs, in the clinic although still further research is necessary.



## REFERENCES

- (1) Thurlings I, Martínez López LM, Westendorp B, Zijp M, Kuiper R, Tooten P, et al. Synergistic functions of E2F7 and E2F8 are critical to suppress stress-induced skin cancer. *Oncogene* 2017;36(6):829-839.
- (2) Kent L, Rakijas J, Pandit S, Westendorp B, Chen H, Huntington J, et al. E2f8 mediates tumor suppression in postnatal liver development. *J Clin Invest* 2016;126(8):2955-2969.
- (3) Park S, Platt J, Lee J, López Giráldez F, Herbst R, Koo J. E2F8 as a Novel Therapeutic Target for Lung Cancer. *J Natl Cancer Inst* 2015;107(9).
- (4) Deng Q, Wang Q, Zong W, Zheng D, Wen Y, Wang K, et al. E2F8 contributes to human hepatocellular carcinoma via regulating cell proliferation. *Cancer Res* 2010;70(2):782-791.
- (5) Ye L, Guo L, He Z, Wang X, Lin C, Zhang X, et al. Upregulation of E2F8 promotes cell proliferation and tumorigenicity in breast cancer by modulating G1/S phase transition. *Oncotarget* 2016;7(17):23757-23771.
- (6) Westendorp B, Mokry M, Groot Koerkamp, Marian J A, Holstege FCP, Cuppen E, de Bruin A. E2F7 represses a network of oscillating cell cycle genes to control S-phase progression. *Nucleic Acids Res* 2012;40(8):3511-3523.
- (7) Di Stefano L, Jensen M, Helin K. E2F7, a novel E2F featuring DP-independent repression of a subset of E2F-regulated genes. *EMBO J* 2003;22(23):6289-6298.
- (8) Maiti B, Li J, de Bruin A, Gordon F, Timmers C, Opavsky R, et al. Cloning and characterization of mouse E2F8, a novel mammalian E2F family member capable of blocking cellular proliferation. *J Biol Chem* 2005;280(18):18211-18220.
- (9) Logan N, Delavaine L, Graham A, Reilly C, Wilson J, Brummelkamp T, et al. E2F-7: a distinctive E2F family member with an unusual organization of DNA-binding domains. *Oncogene* 2004;23(30):5138-5150.
- (10) Boekhout M, Yuan R, Wondergem A, Segeren H, van Liere E, Awol N, et al. Feedback regulation between atypical E2Fs and APC/CCdh1 coordinates cell cycle progression. *EMBO Rep* 2016;17(3):414-427.
- (11) Chong J, Wenzel P, Sáenz Robles MT, Nair V, Ferrey A, Hagan J, et al. E2f1-3 switch from activators in progenitor cells to repressors in differentiating cells. *Nature* 2009;462(7275):930-934.
- (12) Ciccio A, Elledge SJ. The DNA Damage Response: Making it safe to play with knives. *Mol Cell* 2010 -10-22;40(2):179-204.
- (13) Bertoli C, Herlihy A, Pennycook B, Kriston Vizi J, de Bruin, Robertus A M. Sustained E2F-Dependent Transcription Is a Key Mechanism to Prevent Replication-Stress-Induced DNA Damage. *Cell Rep* 2016;15(7):1412-1422.
- (14) Yuan R, Vos HR, van Es RM, Chen J, Burgering BM, Westendorp B, et al. Chk1 and 14-3-3 proteins inhibit atypical E2Fs to prevent a permanent cell cycle arrest. *EMBO J* 2018 03 01;37(5).
- (15) Moynahan ME, Jasin M. Mitotic homologous recombination maintains genomic stability and suppresses tumorigenesis. *Nat Rev Mol Cell Biol* 2010 Mar;11(3):196-207.
- (16) Bertoli C, Skotheim JM, de Bruin, Robertus A. M. Control of cell cycle transcription during G1 and S phases. *Nat Rev Mol Cell Biol* 2013 -8;14(8):518-528.
- (17) Cuitiño MC, Pécot T, Sun D, Kladney R, Okano-Uchida T, Shinde N, et al. Two Distinct E2F Transcriptional Modules Drive Cell Cycles and Differentiation. *Cell Rep* 2019 -06-18;27(12):3547-3560.e5.

- (18) Aksoy O, Chicas A, Zeng T, Zhao Z, McCurrach M, Wang X, et al. The atypical E2F family member E2F7 couples the p53 and RB pathways during cellular senescence. *Genes Dev* 2012;26(14):1546-1557.
- (19) Bourgo RJ, Ehmer U, Sage J, Knudsen ES. RB deletion disrupts coordination between DNA replication licensing and mitotic entry in vivo. *Molecular biology of the cell* 2011 Apr;22(7):931-939.
- (20) Segeren HA, van Rijnberk LM, Moreno E, Riemers FM, van Liere EA, Yuan R, et al. Excessive E2F Transcription in Single Cancer Cells Precludes Transient Cell-Cycle Exit after DNA Damage. *Cell Rep* 2020 Dec 01;33(9):108449.
- (21) Ask A, Persson L, Rehnholm A, Frostesjö L, Holm I, Heby O. Development of resistance to hydroxyurea during treatment of human myelogenous leukemia K562 cells with alpha-difluoromethylornithine as a result of coamplification of genes for ornithine decarboxylase and ribonucleotide reductase R2 subunit. *Cancer Res* 1993 -11-01;53(21):5262-5268.
- (22) Davoli T, de Lange T. The causes and consequences of polyploidy in normal development and cancer. *Annu Rev Cell Dev Biol* 2011;27:585-610.
- (23) Physiological significance of polyploidization in mammalian cells. *Trends in Cell Biology* 2013 /11/01;23(11):556-566.
- (24) Duncan AW. Aneuploidy, polyploidy and ploidy reversal in the liver. *Semin Cell Dev Biol* 2013 -04;24(4):347-356.
- (25) Gentric G, Desdouets C. Polyploidization in liver tissue. *Am J Pathol* 2014 -02;184(2):322-331.
- (26) Gentric G, Maillat V, Paradis V, Couton D, L'Hermitte A, Panasyuk G, et al. Oxidative stress promotes pathologic polyploidization in nonalcoholic fatty liver disease. *The Journal of clinical investigation* 2015;125(3):981-992.
- (27) Toyoda H, Bregerie O, Vallet A, Nalpas B, Pivert G, Brechot C, et al. Changes to hepatocyte ploidy and binuclearity profiles during human chronic viral hepatitis. *Gut* 2005 Feb;54(2):297-302.
- (28) Zhang S, Zhou K, Luo X, Li L, Tu H, Sehgal A, et al. The polyploid state plays a tumor suppressive role in the liver. *Dev Cell* 2018 -2-26;44(4):447-459.e5.
- (29) Celton-Morizur S, Desdouets C. Polyploidization of liver cells. *Polyploidization and Cancer* 2010:123-135.
- (30) Storchova Z, Pellman D. From polyploidy to aneuploidy, genome instability and cancer. *Nat Rev Mol Cell Biol* 2004 /01;5(1):45-54.
- (31) Pandit S, Westendorp B, Nantasanti S, van Liere E, Tooten PCJ, Cornelissen PWA, et al. E2F8 is essential for polyploidization in mammalian cells. *Nat Cell Biol* 2012;14(11):1181-1191.
- (32) Sladky VC, Knapp K, Soratroi C, Heppke J, Eichen F, Rocamora-Reverte L, et al. E2F-Family Members Engage the PIDDosome to Limit Hepatocyte Ploidy in Liver Development and Regeneration. *Dev Cell* 2020 Feb 10;52(3):335-349.e7.
- (33) Sladky VC, Knapp K, Szabo TG, Braun VZ, Bongiovanni L, van den Bos H, et al. PIDDosome-induced p53-dependent ploidy restriction facilitates hepatocarcinogenesis. *EMBO reports* 2020 November 23;n/a(n/a):e50893.
- (34) Weijts, B G M W, Westendorp B, Hien BT, Martínez López LM, Zijp M, Thurlings I, et al. Atypical E2Fs inhibit tumor angiogenesis. *Oncogene* 2018;37(2):271-276.
- (35) Weijts, Bart G. M. W., Bakker WJ, Cornelissen PWA, Liang K, Schaftenaar FH, Westendorp B, et al. E2F7 and E2F8 promote angiogenesis through transcriptional activation of VEGFA in cooperation with HIF1. *EMBO J* 2012 Oct 03;31(19):3871-3884.

- (36) Shats I, Deng M, Davidovich A, Zhang C, Kwon JS, Manandhar D, et al. Expression level is a key determinant of E2F1-mediated cell fate. *Cell Death Differ* 2017 /04;24(4):626-637.
- (37) Kotsantis P, Silva LM, Irmischer S, Jones RM, Folkes L, Gromak N, et al. Increased global transcription activity as a mechanism of replication stress in cancer. *Nat Commun* 2016 -10-11;7(1):1-13.
- (38) Rivadeneira DB, Mayhew CN, Thangavel C, Sotillo E, Reed CA, Graña X, et al. Proliferative suppression by CDK4/6 inhibition: complex function of the retinoblastoma pathway in liver tissue and hepatoma cells. *Gastroenterology* 2010 May;138(5):1920-1930.
- (39) O'Leary B, Finn RS, Turner NC. Treating cancer with selective CDK4/6 inhibitors. *Nat Rev Clin Oncol* 2016 /07;13(7):417-430.
- (40) Ma CX, Gao F, Luo J, Northfelt DW, Goetz M, Forero A, et al. NeoPalAna: Neoadjuvant Palbociclib, a Cyclin-Dependent Kinase 4/6 Inhibitor, and Anastrozole for Clinical Stage 2 or 3 Estrogen Receptor-Positive Breast Cancer. *Clin Cancer Res* 2017 Aug 01;23(15):4055-4065.
- (41) Crozier L, Foy R, Mouery BL, Whitaker RH, Corno A, Spanos C, et al. CDK4/6 inhibitors induce replication stress to cause long-term cell cycle withdrawal. *bioRxiv* 2021 -02-04:2021.02.03.428245.
- (42) Pernas S, Tolaney SM, Winer EP, Goel S. CDK4/6 inhibition in breast cancer: current practice and future directions. *Ther Adv Med Oncol* 2018;10:1758835918786451.
- (43) Xie X, Bansal N, Shaik T, Kerrigan J, Minko T, Garbuzenko O, et al. A novel peptide that inhibits E2F transcription and regresses prostate tumor xenografts. *Oncotarget* 2014;5(4):901-907.
- (44) Xie X, Kerrigan J, Minko T, Garbuzenko O, Lee K, Scarborough A, et al. Antitumor and modeling studies of a penetratin-peptide that targets E2F-1 in small cell lung cancer. *Cancer Biol Ther* 2013;14(8):742-751.
- (45) Ma Y, Kurtyka C, Boyapalle S, Sung S, Lawrence H, Guida W, et al. A small-molecule E2F inhibitor blocks growth in a melanoma culture model. *Cancer Res* 2008;68(15):6292-6299.
- (46) Kurtyka CA, Chen L, Cress WD. E2F inhibition synergizes with paclitaxel in lung cancer cell lines. *PLoS One* 2014;9(5):e96357.
- (47) Chen H, Tsai S, Leone G. Emerging roles of E2Fs in cancer: an exit from cell cycle control. *Nat Rev Cancer* 2009;9(11):785-797.
- (48) Lan W, Bian B, Xia Y, Dou S, Gayet O, Bigonnet M, et al. E2F signature is predictive for the pancreatic adenocarcinoma clinical outcome and sensitivity to E2F inhibitors, but not for the response to cytotoxic-based treatments. *Sci Rep* 2018 -05-29;8(1):1-12.
- (49) Bandara LR, Girling R, Thangue NBL. Apoptosis induced in mammalian cells by small peptides that functionally antagonize the Rb-regulated E2F transcription factor. *Nat Biotechnol* 1997 /09;15(9):896-901.
- (50) Montigiani S, Müller R, Kontermann RE. Inhibition of cell proliferation and induction of apoptosis by novel tetravalent peptides inhibiting DNA binding of E2F. *Oncogene* 2003 /08;22(32):4943-4952.
- (51) Fabbriozzi E, Le Cam L, Polanowska J, Kaczorek M, Lamb N, Brent R, et al. Inhibition of mammalian cell proliferation by genetically selected peptide aptamers that functionally antagonize E2F activity. *Oncogene* 1999 Jul 29;18(30):4357-4363.
- (52) Nelson MA, Reynolds SH, Rao UNM, Goulet A, Feng Y, Beas A, et al. Increased gene copy number of the transcription factor E2F1 in malignant melanoma. *Cancer Biol Ther* 2006 Apr;5(4):407-412.
- (53) Iwamoto M, Banerjee D, Menon LG, Jurkiewicz A, Rao PH, Kemeny NE, et al. Overexpression of E2F-1 in lung and liver metastases of human colon cancer is associated with gene amplification. *Cancer Biol Ther* 2004 Apr;3(4):395-399.

- (54) Kaelin WG. E2F1 as a target: promoter-driven suicide and small molecule modulators. *Cancer Biol Ther* 2003 Jul-Aug;2(4 Suppl 1):48.
- (55) Gomez-Gutierrez JG, Garcia-Garcia A, Hao H, Rao X, de Oca-Luna RM, Zhou HS, et al. Adenovirus-Mediated Expression of Truncated E2F-1 Suppresses Tumor Growth In Vitro and In Vivo. *Cancer* 2010 -9-15;116(18):4420-4432.
- (56) Bell LA, O'prey J, Ryan KM. DNA-binding independent cell death from a minimal proapoptotic region of E2F-1. *Oncogene* 2006 /09;25(41):5656-5663.
- (57) Mullen JT, Tanabe KK. Viral oncolysis. *Oncologist* 2002;7(2):106-119.
- (58) Parr MJ, Manome Y, Tanaka T, Wen P, Kufe DW, Kaelin WG, et al. Tumor-selective transgene expression in vivo mediated by an E2F-responsive adenoviral vector. *Nat Med* 1997 /10;3(10):1145-1149.
- (59) Jakubczak JL, Ryan P, Gorziglia M, Clarke L, Hawkins LK, Hay C, et al. An oncolytic adenovirus selective for retinoblastoma tumor suppressor protein pathway-defective tumors: dependence on E1A, the E2F-1 promoter, and viral replication for selectivity and efficacy. *Cancer Res* 2003 Apr 01;63(7):1490-1499.
- (60) Dubensky TW. (Re-)Engineering tumor cell-selective replicating adenoviruses: a step in the right direction toward systemic therapy for metastatic disease. *Cancer Cell* 2002 May;1(4):307-309.
- (61) Nokisalmi P, Pesonen S, Escutenaire S, Särkioja M, Raki M, Cerullo V, et al. Oncolytic Adenovirus ICOVIR-7 in Patients with Advanced and Refractory Solid Tumors. *Clin Cancer Res* 2010 -06-01 00:00:00;16(11):3035-3043.
- (62) Rojas JJ, Cascallo M, Guedan S, Gros A, Martinez-Quintanilla J, Hemminki A, et al. A modified E2F-1 promoter improves the efficacy to toxicity ratio of oncolytic adenoviruses. *Gene Ther* 2009 /12;16(12):1441-1451.
- (63) Laborda E, Puig-Saus C, Rodriguez-García A, Moreno R, Cascalló M, Pastor J, et al. A pRb-responsive, RGD-modified, and hyaluronidase-armed canine oncolytic adenovirus for application in veterinary oncology. *Mol Ther* 2014 May;22(5):986-998.
- (64) Guedan S, Rojas JJ, Gros A, Mercade E, Cascallo M, Alemany R. Hyaluronidase Expression by an Oncolytic Adenovirus Enhances Its Intratumoral Spread and Suppresses Tumor Growth. *Mol Ther* 2010 -07;18(7):1275-1283.
- (65) Moreno E, Toussaint MJM, van Essen S, Bongiovanni L, van Liere E, Koster M, et al. E2F7 is a potent inhibitor of liver tumor growth in adult mice. *Hepatology* 2020.
- (66) Lambert M, Jambon S, Depauw S, David-Cordonnier M. Targeting Transcription Factors for Cancer Treatment. *Molecules* 2018 -6-19;23(6).
- (67) Yuan R, Liu Q, Segeren H, Yuniati L, Guardavaccaro D, Lebbink R, et al. Cyclin F-dependent degradation of E2F7 is critical for DNA repair and G2-phase progression. *EMBO J* 2019;38(20):e101430.
- (68) Fong PC, Boss DS, Yap TA, Tutt A, Wu P, Mergui-Roelvink M, et al. Inhibition of poly(ADP-ribose) polymerase in tumors from BRCA mutation carriers. *N Engl J Med* 2009 Jul 09;361(2):123-134.
- (69) Clements KE, Thakar T, Nicolae CM, Liang X, Wang H, Moldovan G. Loss of E2F7 confers resistance to poly-ADP-ribose polymerase (PARP) inhibitors in BRCA2-deficient cells. *Nucleic Acids Res* 2018 /09/28;46(17):8898-8907.
- (70) Mitxelena J, Apraiz A, Vallejo Rodríguez J, García Santisteban I, Fullaondo A, Alvarez Fernández M, et al. An E2F7-dependent transcriptional program modulates DNA damage repair and genomic stability. *Nucleic Acids Res* 2018;46(9):4546-4559.

- (71) Blosser WD, Dempsey JA, McNulty AM, Rao X, Ebert PJ, Lowery CD, et al. A pan-cancer transcriptome analysis identifies replication fork and innate immunity genes as modifiers of response to the CHK1 inhibitor prexasertib. *Oncotarget* 2020 -01-21;11(3):216-236.
- (72) Kent L, Bae S, Tsai S, Tang X, Srivastava A, Koivisto C, et al. Dosage-dependent copy number gains in E2f1 and E2f3 drive hepatocellular carcinoma. *J Clin Invest* 2017;127(3):830-842.
- (73) Polymer- and lipid-based nanoparticle therapeutics for the treatment of liver diseases. *Nano Today* 2010 /08/01;5(4):296-312.
- (74) Witzigmann D, Kulkarni JA, Leung J, Chen S, Cullis PR, van der Meel R. Lipid nanoparticle technology for therapeutic gene regulation in the liver. *Adv Drug Deliv Rev* 2020 Jul 02,.
- (75) Lipid nanoparticles for hepatic delivery of small interfering RNA. *Biomaterials* 2012 /09/01;33(25):5924-5934.
- (76) Akinc A, Zumbuehl A, Goldberg M, Leshchiner ES, Busini V, Hossain N, et al. A combinatorial library of lipid-like materials for delivery of RNAi therapeutics. *Nat Biotechnol* 2008 May;26(5):561-569.
- (77) Judge AD, Robbins M, Tavakoli I, Levi J, Hu L, Fronda A, et al. Confirming the RNAi-mediated mechanism of action of siRNA-based cancer therapeutics in mice. *J Clin Invest* 2009 Mar;119(3):661-673.
- (78) Pecot CV, Calin GA, Coleman RL, Lopez-Berestein G, Sood AK. RNA interference in the clinic: challenges and future directions. *Nat Rev Cancer* 2011 -1;11(1):59-67.









# Chapter 6

---

## Addendum

Nederlandse samenvatting

Academic summary

Resumen

Acknowledgements

Curriculum Vitae

List of publications

## NEDERLANDSE SAMENVATTING

Ons lichaam bestaat uit triljoenen cellen die samen onze organen en weefsels vormen. Alle cellen slaan informatie op, maar kunnen deze ook lezen en gebruiken. Informatie is opgeslagen in DNA in zones die genen worden genoemd. Genen coderen voor eiwitten, die op hun beurt een breed scala aan functies uitvoeren. Eén van die functies is celdeling. De productie van een eiwit vereist een tussenstap die gen transcriptie wordt genoemd. Tijdens gen transcriptie wordt de nucleotidevolgorde van een gen gekopieerd naar een RNA-molecuul. RNA wordt vervolgens vertaald in eiwitten. Als cellen delen worden alle genen doorgegeven aan twee dochter cellen. Hiervoor moet het genetisch materiaal eerst verdubbelen. Om te zorgen dat dit zonder fouten gebeurt, beschikt de cel over een controle systeem dat controleert of alle genen op tijd en zonder fouten worden gekopieerd. Fouten in het verdubbelen van DNA kunnen catastrofale gevolgen hebben. Als genen per ongeluk dubbel worden gekopieerd, verdwijnen of kleine veranderingen ondergaan kan dat leiden tot kanker. Veel genen die het verdubbelen van DNA in goede banen leiden worden aangestuurd door een bepaalde groep eiwitten: de familie van E2F transcriptiefactoren. Mensen hebben verschillende E2Fs. E2Fs 1-3 bijvoorbeeld activeren de genen die DNA kopiëren, terwijl E2Fs 4-8 ze juist remmen. E2Fs worden op hun beurt gereguleerd door RB. RB remt celdeling en kan dus ook kanker tegengaan. Het gen dat codeert voor RB is vaak beschadigd in kankercellen waardoor E2F hyperactief wordt. Een verkeerd functionerend RB is geassocieerd met het ontstaan van tumoren en verdere ontwikkeling daarvan. Als bij kanker RB beschadigd is, betekent dat vaak een slechte prognose voor de patiënt. Opvallend genoeg zijn E2F7 en E2F8, die net als RB ook celdeling tegengaan, bijna nooit beschadigd in kanker. Dit bracht ons tot de hypothese dat het kunstmatig activeren van E2F7 en E2F8 in kankercellen, celdeling zou kunnen remmen.

In dit proefschrift onderzoeken we de gevolgen van het manipuleren van E2F7 en E2F8 gen-activiteit. We bekijken het effect op tumorformatie en -groei, en onthullen het moleculaire mechanisme dat daaraan ten grondslag ligt. Om dit te doen hebben we genetisch gemodificeerde muismodellen ontwikkeld. We hebben atypische E2F's (E2F7 en E2F8) specifiek in bepaalde weefsels verwijderd dan wel geactiveerd. Dit hebben we ook gedaan in combinatie met het uitschakelen van andere belangrijke tumor remmers als RB en *phosphatase and tensin homolog* PTEN.

Ten eerste hebben we gevonden dat sterk activeren van E2F7 en E2F8 ertoe leidt dat kankercellen niet kunnen delen. We zagen dat het de cellen niet meer lukte DNA te verdubbelen. Dat zorgt ervoor dat DNA schade accumuleert en lever tumoren niet meer groeien. Dit duidt op een tumor remmende rol voor atypische E2F's in de lever (**Hoofdstuk 2**). Aan de andere kant zagen we dat het chronisch remmen van genen die door E2F's worden gereguleerd, tumoren ontstonden in longweefsel. Mogelijk komt dat door toegenomen instabiliteit van het DNA in die cellen. Vaak ging dit gepaard met DNA schade (**Hoofdstuk 3**). Deze bevindingen suggereren dat de *in vivo* functies van door E2F's gereguleerde genen verder strekken dan het remmen van celdeling alleen.

Ten tweede leidde het activeren van E2F tot tumoren in de lever, maar remde het juist tumoren in de hypofyse in muismodellen waarin RB deels is uitgeschakeld. Deze resultaten bevestigen dat atypische E2Fs en RB weefsel-specifiek het ontstaan van tumoren reguleren (**Hoofdstuk 3**).

Ten derde hebben we het effect onderzocht van polyploidisatie —het door een cel verkrijgen van meer dan twee sets genetisch materiaal— op het ontwikkelen van *non-alcoholic fatty liver disease* (NAFLD) en het ontwikkelen van lever kanker. We hebben een muis met een lever-specifieke deletie van atypische E2F's gekruist met een muis waarin PTEN was geïnactiveerd. PTEN deletie zorgt voor hepatomegalie, steatose —vet-ophoping— en leverkanker in combinatie met meer polyploidisatie. Bij het vergelijken van levers van muizen zonder Pten (polyploïde levers) met muizen zonder atypische E2F's en Pten (diploïde levers), ontdekten we dat de opslagcapaciteit van lipiden en dus de ernst van steatose hoger is in polyploïde levers in vergelijking met levers die voornamelijk diploïde hepatocyten bevatten. Belangrijk is dat polyploidisatie nog steeds een belangrijke barrière was tegen het ontstaan van levertumoren (**Hoofdstuk 4**). In het laatste hoofdstuk bespraken we de algemene resultaten van de onderzoeken die in dit proefschrift worden gepresenteerd (**Hoofdstuk 5**). We concentreerden ons op de tegengestelde rollen van atypische E2F's bij het onderdrukken of bevorderen van tumorigeniciteit. We bespraken deze bevindingen in de context van hun rol in de regulatie van transcriptie, polyploidisatie en angiogenese — nieuwe bloedvatvorming—. Ten slotte stellen we ook toekomstige strategieën voor om E2F-activiteit als potentiële antikankerbehandelingen te richten, aangezien E2F-afhankelijke transcriptie vaak wordt opgereguleerd in een verscheidenheid aan kankertypes en correleert met een slechte prognose bij patiënten.

Tezamen hebben de experimenten in dit proefschrift bijgedragen aan het vergroten van ons begrip van de rol van atypische E2F's en RB bij kanker en leveren ze wetenschappelijk bewijs om nieuwe therapeutische toepassingen voor oncologie te ontwikkelen.

## ACADEMIC SUMMARY

Our bodies contain trillions of strictly organized cells which form our tissues and organs. All these cells have the common ability to store, retrieve and translate information. These instructions are encoded by close to 30,000 genes written in the DNA, which encode proteins that carry out a huge number of different functions in the cell, including cell division itself. The production of a protein requires an intermediate step called gene transcription. During gene transcription, the nucleotide order of a gene is copied to an RNA molecule. RNA is then translated into proteins. When a cell divides, all genes are passed on to its daughter cells, which requires accurate DNA duplication. Cells possess a cell cycle control system that ensures that the genome is properly duplicated in a timely and coordinated manner and, importantly, checked for potential errors. If errors occur during DNA replication, it could result in detrimental consequences for the next generation of cells, such as gene amplifications, gene deletions, or gene mutations. All these gene alterations can trigger diseases such as cancer. A large number of genes involved in proper DNA replication are regulated by the family of E2F transcription factors. Human cells have multiple E2Fs, which can either activate (E2F1-3) or inhibit (E2F4-8) the expression of those target genes. The retinoblastoma (Rb) protein is another important regulator of DNA replication, as it can inhibit the activator E2Fs. Rb is a key inhibitor of the cell cycle and thus important to prevent tumor formation. The gene encoding Rb (RB gene) is often lost or mutated in cancer, resulting in hyperactivated E2F transcription. These alterations are frequently associated with tumor initiation, progression and poor prognosis. Importantly, E2F7 and -8 are also inhibitors of the cell cycle and prevent tumorigenesis; however, in contrast to RB, they are rarely mutated in cancer. These observations led us to hypothesize that artificial activation of the mechanism that inhibits E2F-dependent genes, such as induction of E2F7 and E2F8, might efficiently block cancer cell proliferation.

In this dissertation, we aim to explore the consequences of manipulating E2F-dependent transcription in tumor formation and progression and elucidated the molecular mechanisms involved. To this end, we created unique genetically-modified mouse models in which we altered E2F-dependent transcription in specific tissues, via deletion or overactivation of atypical E2F repressors (E2F7 and E2F8), either alone or in combination with deletion of other important tumor suppressors, such as RB and PTEN.

First, we found that acute downregulation of E2F transcription by boosting expression of E2F7 and E2F8 impaired the ability of cancer cells to progress through the cell cycle. Specifically, DNA replication was impaired, leading to severe accumulation of DNA damage and blockage of liver tumor growth, supporting a tumor suppressive role of atypical E2Fs in liver tissue (**Chapter 2**). However, we also demonstrated that chronically repressing E2F-target gene expression resulted in spontaneous tumorigenesis in lung tissue potentially due to high genomic instability. This condition results frequently in the accumulation of mutations within the genome (**Chapter 3**). Thus, these results suggest that *in vivo* functions of atypical E2Fs

repressors extend beyond the control of cell proliferation. Second, hyperactivated E2F-dependent transcription led to spontaneous liver tumorigenesis but prevented formation of pituitary tumors in specific mouse models lacking RB. These findings allowed us to confirm that atypical E2Fs and RB control tumorigenesis in a tissue cell-type specific manner (**Chapter 3**).

Third, we investigated the impact of polyploidization —when a cell contains more than two paired sets of chromosomes— on the development of non-alcoholic fatty liver disease (NAFLD) and its progression towards liver cancer. We bred mice harboring a conditional deletion of atypical E2Fs in the liver, to block hepatocyte polyploidization, with phosphatase and tensin homolog (Pten) deleted mice. *Pten* deletion causes hepatomegaly, steatosis —lipid accumulation— and liver cancer at a later stage accompanied by enhanced polyploidization. When comparing livers from mice lacking *Pten* (polyploid livers) with mice lacking *atypical E2Fs* and *Pten* (diploid livers), we found that the lipid storage capacity and thus severity of steatosis is higher in polyploid livers compared to livers containing mainly diploid hepatocytes. Importantly, polyploidization was still an important barrier against liver tumorigenesis (**Chapter 4**). In the last chapter we discussed the overall results of the studies presented in this thesis (**Chapter 5**). We focused on the opposing roles of atypical E2Fs in either suppressing or promoting tumorigenicity. We discussed these findings in the context of their roles in the regulation of transcription, polyploidization and angiogenesis —new blood vessel formation—. Lastly, we also propose future strategies to target E2F activity as potential anti-cancer treatments as E2F-dependent transcription is frequently upregulated in a variety of cancer types and correlates with poor prognosis in patients.

Overall, the studies described in this thesis have contributed to furthering our understanding of the role of atypical E2Fs and RB in cancer and are providing scientific evidence to develop novel therapeutic options in oncology.

## RESUMEN

Nuestro cuerpo contiene más de 30 billones de células que están estrictamente organizadas en distintos tipos y constituyen los diferentes tejidos y órganos. Todas estas células tienen la capacidad común de almacenar, recuperar y traducir información. Las instrucciones para emplear estas capacidades están codificadas por cerca de 30.000 genes, los cuales se encuentran en el ácido desoxirribonucleico (ADN). Estos genes codifican proteínas encargadas de llevar a cabo una gran cantidad de diferentes funciones celulares, incluyendo la propia división celular. La producción de una proteína requiere un paso intermedio llamado *transcripción*. Durante la transcripción, los nucleótidos que comprenden un gen se copian para formar una molécula de ARN. Finalmente, el ARN se traduce mediante la *traducción* en proteínas. Cuando una célula se divide, todos los genes deben traspasarse a sus células hijas, lo que requiere una *duplicación* precisa del ADN. Las células poseen un sistema de control del ciclo celular que garantiza que el genoma se duplique correctamente de una manera oportuna, coordinada y, lo que es más importante, verifique que no se produzcan errores. Si durante el proceso de la duplicación del ADN se produjeran errores, la siguiente generación celular podría adquirir graves consecuencias, como por ejemplo amplificación de genes, supresión de material genético o mutaciones genéticas. Todas estas modificaciones genéticas pueden desencadenar enfermedades como el cáncer. Una gran cantidad de genes codificadores de proteínas involucrados en la regulación de la replicación del ADN están a su vez regulados por la familia de factores de transcripción E2F que, como su nombre indica, son parte de las herramientas centrales de la transcripción en las células. Las células humanas tienen múltiples E2F que pueden activar (E2F1-3) o reprimir (E2F4-8) la expresión de genes específicos y, por tanto, la transcripción. La proteína del retinoblastoma (Rb) es una proteína también encargada de la regulación de la replicación del ADN, ya que puede inhibir la función de los E2F activadores. De modo que Rb es una importante inhibidora del ciclo celular y por lo tanto supresora de tumores. El gen que codifica esta proteína (gen RB) sufre a menudo mutaciones o se pierde en células cancerígenas, que como consecuencia poseen una hiperactivación de la transcripción regulada por E2Fs. Esta característica está asociada frecuentemente con el inicio, la progresión y el pronóstico reservado de los tumores. Es importante destacar que E2F-7 y -8 son también inhibidores del ciclo celular y previenen la formación de tumores. Pero, a diferencia de RB, es muy poco frecuente encontrarlos alterados en la enfermedad del cáncer. Teniendo en cuenta estas observaciones, mis compañeros y yo planteamos una hipótesis de trabajo basada en la activación artificial de mecanismos que puedan inhibir la transcripción de genes regulados por E2Fs. Por ejemplo, inducir E2F-7 y E2F-8 en las células cancerígenas para bloquear la proliferación de estas células, lo que conllevaría a una posible reducción de la masa tumoral.

Durante mi tesis doctoral nuestro objetivo era explorar las consecuencias de manipular la expresión de los genes regulados por E2Fs en la formación y progresión de tumores, y entender los mecanismos moleculares involucrados en dicha manipulación. Para ello hemos

creado modelos únicos de ratones manipulados genéticamente en los que podemos regular la expresión de los genes regulados por E2Fs a través de la supresión o hiperactivación de los represores E2F-7 y E2F-8 (o también llamados E2F atípicos), ya sean solos o en combinación con la supresión de otros genes supresores tumorales importantes como son RB o PTEN.

Primero, descubrimos que la regulación negativa y aguda de la transcripción de los E2F a través de la hiperactivación de E2F7 y E2F8 resultó en la discapacidad de las células cancerígenas para progresar a través del ciclo celular. En concreto la replicación del ADN resultó afectada, lo que provocó una acumulación de daño en el ADN y un bloqueo del crecimiento del tumor hepático. Estos efectos respaldan el papel que desempeñan los E2F atípicos como tumores supresores en el tejido hepático (**Capítulo 2**). Sin embargo también demostramos que la represión crónica o durante un largo plazo de los genes regulados por E2Fs resultó en la aparición espontánea de tumores en el tejido pulmonar. Creemos que se debe a la acumulación de inestabilidad genómica. Esta condición resulta con frecuencia en la acumulación de mutaciones en el genoma (**Capítulo 3**). Por lo tanto las funciones *in vivo* de los E2F atípicos se extienden más allá del control de la proliferación celular. Demostramos en segundo lugar que la hiperactivación de los genes regulados por E2Fs, mediante el uso de modelos de ratones específicos que contienen el gen RB suprimido, resultó en la aparición de tumores hepáticos pero impidió la formación de tumores en la glándula pituitaria. Gracias a estos hallazgos pudimos confirmar que los E2F atípicos y RB controlan la formación de tumores de una manera específica dependiendo del tipo celular y del tejido (**Capítulo 3**).

En tercer lugar investigamos el impacto de la poliploidización —cuando una célula contiene más de dos pares de cromosomas— en el desarrollo de la enfermedad del hígado graso o esteatosis hepática debido a causas no alcohólicas (EHGNA), y su progresión hacia el cáncer de hígado. Para ello criamos ratones que contienen suprimidos los E2F atípicos en el hígado, lo cual resulta en el bloqueo de la poliploidización en los hepatocitos, en combinación con ratones a los cuales se les elimina la fosfatasa y un homólogo de la tensina en el cromosoma 10 (PTEN). Los ratones sin PTEN desarrollan hepatomegalia, esteatosis —acumulación anormal de grasa— y posteriormente cáncer de hígado, todo ello acompañado de un aumento de la poliploidización. Al comparar hígados de ratones que carecen PTEN (hígados poliploides) con ratones que carecen de E2F atípicos y PTEN (hígados diploides), demostramos que la capacidad para almacenar grasas, y por lo tanto la gravedad de la esteatosis, es mayor en hígados poliploides en comparación con hígados que contienen principalmente hepatocitos diploides. Además es importante destacar que la poliploidización desempeña un papel importante contra la progresión del cáncer hepático (**Capítulo 4**). En el último capítulo discutimos en general los resultados de los estudios presentados en esta tesis (**Capítulo 5**). Nos centramos principalmente en discutir la doble función de los E2F atípicos en el control de la formación tumoral. Y discutimos estos resultados en el contexto del papel que estos desempeñan en la regulación de la transcripción, poliploidización y la angiogénesis —formación de nuevos vasos sanguíneos—.



Por último, proponemos también posibles estrategias futuras basadas en la manipulación de la actividad de los E2F en el tratamiento contra el cáncer. Estas estrategias tienen como fundamento el hecho de que en una gran variedad de tipos de cáncer, la expresión de los genes regulados por E2F se observa frecuentemente incrementada y se relaciona con un pronóstico desfavorable para los pacientes.

Se puede concluir que los estudios descritos en esta tesis han contribuido a la mejora en el entendimiento de las funciones los E2F atípicos y RB en la enfermedad del cáncer y proporcionan evidencia científica para desarrollar nuevas opciones terapéuticas en el ámbito de la oncología.

## ACKNOWLEDGEMENTS

My mind brings me to June 2014 when, just after my graduation, I found out I would start my research experience abroad in the department of Pathobiology in Utrecht. It was meant to be a 9 month internship, just 9 months of getting experience in a laboratory to hopefully then start a PhD. And it became true. I started my PhD on March 2016 in the same group and department. Lucky me, I was going to spend the next years surrounded by the best colleagues ever, and have one of the best times of my life. Accomplishing a PhD is not an easy journey but I now finally finished “The book”! A book which would not have been possible to write without the support and help of numerous people. I would like to take this opportunity to personally thank some people that have been there for me and supported me throughout this entire period.

First and foremost, I would like to thank **Alain**. Thank you very much for giving me the opportunity to join your lab and involving me in this project. You have been kind, supportive, and an excellent mentor. I learnt a lot from your broad knowledge, your critical thinking and your favorite “brain-storm sessions”. I must admit that in some of those brain-storm sessions you managed to burn some of my neurons, but luckily you also stimulated some others. Thanks for your helpful input. Also, you were very patient with my fast way of talking and I will always try to remember to breathe between my sentences. You were always available for any questions or issues, even during your busiest moments. I admire your capacity to combine your busy agenda with your family, the lab, and your multiple responsibilities at the university. Once again, thank you Alain for all your dedication, trust, and mentorship. I will keep all the good memories your lab has provided me forever. By the way, I hope it is time to light the fire of the BBQ you promised me when I would finish my thesis.

**Bart**, my daily captain. Thank you very much for your tireless, constant, useful, and kind supervision. Besides it “being your job”, you have provided me constant motivation and support throughout my PhD. I admire your approach to do science (focused and smart), your critical insights and how you always shared your thoughts and comments in a calm way to support all of us. I will really miss the spot-on 5 minutes (which easily turned to be 1 hour) discussions in the corridor, coffee machine or in Teams. I must say that your challenging questions, your capacity of see both sides of a story and your patience has helped me a lot to growth as a researcher. We even did a trip together, all the way to Mount Snow in Vermont. One of the best experiences during my PhD and so much fun. It was very cool to drive in those mountains with you, eating massive burgers with 1 L of cola on the side and do sightseeing in Boston. Thank you Bart for all your great input, your trust, your daily support and all those fun moments inside and outside the lab.

**Hilda**. Thank you very much for your help, your patient and permanent support inside and outside the lab. From the first moment I stepped foot in the lab you were the one who helped me with the thousands of PCRs, handling the mice, and anything else I would ask you

to help me with. Those long days in the GDL allowed me to get closer to you and I will always be grateful for how you have treated me all these years. Thank you also very much for your delicious framboise ham, I loved the morning toasties with it. I hope you keep enjoying the retirement, sitting in the garden and taking care of all your plants.

Thanks to my PhD committee, **Saskia van Mil** and **Geert Kops**. Your support and advice in the yearly meetings were of great help. Also, together with the rest of the reading committee, **Celia Berkers**, **Bart van der Sluis**, and **Andreas Villunger**, thank you for taking the time to assess this doctoral dissertation.

“The Doctors to Be”, or should I say “De Bruin talents”? :p. I was very lucky to be surrounded by such good and motivational people. I am the first in line to defend but I cannot wait to attend all of your defenses in the near future, almost doctors. **Jet**, my partner in crime. There is little I can write that I have not already told you. Since the moment I stepped into this lab you demonstrated to me how good a person you are. I am so happy I met you. Thank you for explaining to me molecular stuff, your advice, your help, and your unconditional support. I will forever admire your perseverance, your incredible strength, your wisdom, and your zumba skills(:p). Fun in the lab but so much fun also outside. Smaragdplein, Jan van Foreeststraat, King’s night and day, Spain, Athens, Macumba, ... so many good memories, and more to come for sure. It is an honor to have you as my paranimf and best friend! Almost there with your PhD, keep going! **Qingwu**, the next warrior in line. The most friendly and hard-working person in the lab. You have the ability to always help people with a smile, especially with your favorite technique, Liu Blotting. Keep going, I believe you will end up with a very nice thesis very soon. And also, if you keep playing tennis as often as you do, not even Roger Federer will be able to beat you :p. **Thomas**, our most international PhD. Your fun Italian character together with your hands-on attitude and creativity helps to do good science and keep the positive environment in the lab. Good luck tackling the complexity of senescent cells and tumor microenvironment and of course, finishing your PhD. **Anneloes**, bonita, EV expert. Who would ever guess that I managed to convince my little princess to dance in a latin party? Haha. It clearly shows how adventurous you are. But also, such a hard-worker, responsible, and super motivated. I am really impressed by how you combined your veterinary studies with a demanding research internship in our lab. I hope your dedication and motivation will be recognized with a nice PhD position. And of course, we will keep having a lot of fun outside the lab, probably in a coming soon Macumba party :p. To all the students, with special reference to **Anne**, **Jan** and **Morgan**, who passed through the lab these years and contributed to keep the good vibes and hard-working environment. And of course to **Vivian**, thanks for your great job in the newly established DNA repair team :p. I am sure you will find a nice PhD position after this, good luck!!

**Elsbeth**, thanks for helping out with experiments and all the management support we get from you in the lab. **Saskia**, bedankt voor het altijd klaar staan met je geweldige expertise in het

omgaan met muizendingen. Het was erg leuk om tijd met je te delen in de GDL en je geweldige hulp bij het processing, embedding, staining en organiseren. Ik zal onze zangdagen, bijpassende schokdagen echt missen. **Bram**, good luck with the postdoc and I hope you get the grant you recently applied. **Tara**, thanks for arranging all the meetings and always being so kind.

I would also like to thank to the best pathologists of the group, **Laura** and **Rachel**. Girls, thank you very much for your support, your wise advice, and your analysis in my studies. You were always available when I had any questions or needed experienced eyes to look at the slides. Rachel, thank you also for the British touch to some of my work. It was a real pleasure to work closely with both of you, and I learnt a lot from your experience. Rachel, I will see you very soon, it is very nice that you are coming back to the group.

I want to thank all former and present colleagues in the Pathobiology Department of the Veterinary Faculty; **Kim, Nica, Bernardo, Nermin, Javier, Mark, Eric, Heni, and Tim**. The Christmas dinners and the gatherings were fun. I wish you all the best in your futures. Also **Martijn, Martin, Bernd**, and **Chris**, from the department of Biochemistry. I really enjoyed our collaboration trying to isolate hepatocytes and gaining an insight into the world of lipidomics. **Ger**, thanks for all the sorting support and doing FACS during the period we were still sitting in the Androclus building.

**Pieter**, thanks for all the support I received from you during the first year. You were the first person to teach me some Dutch words, although not always the nicest ones (i.e. “Rot op”). It was nice to do PCRs with you and see how almost every mouse started shaking when they saw you coming (joking of course). **Yuan**, the EMBO guy, thanks for the great times in the lab. Luckily, all those million western blots gave you such good publications and a great thesis. You have set the bar very high. **Matondo**, it was very nice to meet you in the lab and I am glad I had the opportunity to be involved in your PTEN story. Thanks for your patience and your help in the lab. I am looking forward to going to Tanzania again.

The **RMCU** and **Hubrecht community**, thanks for the warm welcome in this cool (and cold) building. The move of our lab to the Hubrecht building was with no doubt one of the best decisions taken. A building full of hard-working and smart people interacting day-to-day with a common purpose, perform high quality research. The Hubrecht borrels, thanks to whomever came up with organizing these events every Friday, what a fantastic idea! Thanks to everyone with whom I had the opportunity to have a beer with :p. **Enric**, muchas gracias por tu apoyo, tu motivación, tus constantes ideas y las risas que me has hecho pasar desde que te conozco. No sé si aquí o en Valencia pero espero no quedarme sin probar tu famosa paella. **Sonia**, guapa, madrileña tenías que ser :p. Gracias también por tu apoyo y tu motivación. La verdad que quejarse con alguien que a la vez te sube el ánimo es mucho más fácil. Venga, mucho ánimo que ya te queda menos para terminar a ti también y vas a tener una tesis magnífica. **Guy**, the only one that dared to share room in “our section”. Thanks for the fun and help. **Ed**, western blot buddy, I believe you can manage to complete your thesis, cheer up!

**Joaquín**, que no me entere yo que alguien te quita tu sitio en la esquina eh?:-p. Es un placer haberte conocido y te deseo mucha suerte con tu proyecto. **Alexandro, Suzy, Magdalena, Cornelike, Cindy, Manon, Monique, Loes, Saskia**, thanks for contributing to such a nice work environment on the 5<sup>th</sup> floor. **Gautam**, or Gautman, as I called you for almost a year, thanks for your help introducing us to prime editing, and all your funny stories and beers in the borrels. Good luck finishing up your PhD. **Jamie**, the king of “blond princesses”! Thanks for your British input and your -funny- abusing jokes :p. **Stefan, Renier**, thanks for your patient and your support during sorting.

The animal care takers from the GDL, with a special mention to **Wout** and **Anja**, thanks for all your support and taking such good care of our mice.

Lastly, I would like to thank the other half, my life outside the lab. To begin with, “**Utrecht bonitas**”. You girls were definitely a key cornerstone during my PhD. Thanks for all your support and fun times. **Vic**, que te voy a decir que no te haya dicho ya. Que no sé qué hubiera hecho sin ti este periodo. Gracias por tu incondicional apoyo, tu cariño y tus consejos. Desde que te has ido a Valencia, Utrecht no es igual sin ti. Te echo de menos. Menos mal que ya tienes cortinas en la habitación de invitados porque me da que la voy a utilizar frecuentemente. Ah, y que me hace tanta ilusión ser tu paraninf en tu defensa, es todo un honor. **Jet**, I already thank you above but again, you know how much you mean for me inside and outside the lab, thanks. **Amalia**, thanks for all the listening, support and nice gin & tonics on Fridays. Too bad that corona arrived and we had to stop our visits to Stand & Co, I hope we can pick up that routine again :p. We also passed through a few tough moments during the PhD together. I am very glad you were always there for anything I needed and to cheer me up no matter what. Now, last effort to finish the PhD, Χαμογελάστε ! **Helena**, mi catalana favorita :p. Admiro tu creatividad, tus consejos y tu don en la cocina. Gracias por todos los cafés y galletitas a escondidas en la office. Ir de compras, quejarnos de los estudiantes y los proyectos, gossipear y morir haciendo intensity. Me alegro mucho de que nuestros caminos se hayan cruzado en el Hubrecht. Ahora, un último empujón para terminar la tesis y poder irte a construir tu casita que llevas diseñando todo este tiempo :p. **Arwa**, habibi, your sweetness and strength are really admirable. Thanks for all the fun in our shopping sessions, your wise advice and for painting my nails so professionally :p. Love you habibi. **Tal**, esa energía para tirar hacia delante y tu fuerza me han demostrado en poco tiempo que eres una crack. Muchas gracias por acogerme en tu casa durante un mes, la verdad que ya solo por escuchar las historias de Edo hizo que mereciera mucho la pena. Ánimo con el PhD, esa lucha contra las garrapatas la tienes casi ganada. **Martita**, la más marchosa. Tienes unas vibes geniales y con tu positividad y tu energía me has motivado un montón de veces. Ah bueno y gracias por ser mi celestina en el Hubrecht, jijiji. **Janine**, the best photographer of the group. Thanks for the cool video of Florence, your spontaneous photos and for your down-to-earth and motivational spirit. I wish you all the best back home and we must organize a trip to visit you very soon. **Maya**, guapa, vecina. Gracias

por esas cervecitas al sol en Jan van Foreeststraat, tu actitud tan positiva y tu motivación. Dentro de nada estamos las 2 peleando por los mismo puestos de trabajo ya verás jajaja. Ánimo en los últimos meses del PhD, ya casi casi lo tienes. **Sanna**, thanks for your kindness and calmness. I like a lot your nice figures with worms, I am sure they will all end up in nice publications for your thesis. And very brief last sentence for all of you. Let's all repeat a "Florence-like" trip very soon! Maybe to Valencia to visit Vic, or to Portugal to visit Janine, but let's do it!!

Thanks to my Greek/ Italian/ Dutch community, **Elenaki, Annaki, Thijs** and **Alberto**. Thank you guys for being close to me these years. For your support, your care, and your sweetness. **Elenaki**, my sweet friend, thanks for all the times we motivated each other, we enjoyed the sun on your terrace, your encouragement, and your honesty. I really appreciate spending time with you. **Alberto**, master of delicious lasagna and pizzas and bread. Thanks for your calm attitude and your funny jokes, making it a pleasure to hang out with you guys. And I am really looking to your wedding, I hope we can have a well-deserved party! **Annaki**, can I adopt your kids? What a lovely family you guys formed over these years and I am so happy I have seen it all from the beginning. Thanks for being there all this time. **Thijs**, I hope I can keep -almost- winning you in "The Trains" and having nice gin & tonics together. Let's keep the fun going!

**Annelot, Shyro**. You two are the perfect example of unwavering strength and planning/organizing skills. Thank you guys for your inspiring attitude, your support and your love all these years. I learnt a lot from you two. Especially in relation to building a house; sanding, making holes and screwing :p. I hope we can keep enjoying nice dinners in your fantastic garden, make a nice trip to Denia, and taking care of your beautiful daughter. **Anne**. The most energetic and motivational person in the whole of Utrecht. Thanks for all the fun and support. I really enjoyed the time we spent together the first year and all your jokes and stories. Hope we can finally meet again in your new house :-). **Ruby**, it was really nice to share that first year together with you in the lab. Your ambition, your wise ideas, and your calmness were really something to look up to!

To all the "**Parnassos people**". **Begoña, Camila, Alan, Paula, Arturo, Isa, Jordi, Javi, Alexander, Rosalia**. You guys gave me life during the first year in Utrecht. I will always remember all those fun evenings in the corridor of Parnassos, the long nights in Chupitos and the energy I got from all of you, thank you!

**Lucía**, todos estos años separadas pero a la vez sintiéndote siempre tan cerca. Gracias por todo tu apoyo. Y a sabes lo mucho que significas para mí y todo lo que siempre me has ayudado, gracias. **Cris, Loro**. Cual es nuestro siguiente destino? :). Gracias chicas por siempre haber estado ahí durante estos años, vuestro apoyo en momentos difíciles, nuestras escapadas y nuestras videollamadas de 2 horas. Os quiero. **Cris**, estoy segura que tu motivación y tremenda responsabilidad y el hacer bien las cosas te va a convertir en al mejor jefa de "Figuroa e hijos" :p. No puedo esperar a que te den tu nueva casa y poder estrenar la habitación de invitados (o debería llamarla "de Eva y Loro":p). **Loro**, no hay persona con más perseverancia, ambición

y tan trabajadora como tú. Te has embarcado en una experiencia muy similar a la mía y estas viendo que no siempre es fácil, pero quien lo sigue lo consigue. Ánimo que estoy segura que tu tan ansiada residencia va a llegar muy pronto y vas a seguir demostrando lo que vales. Y a mucha otra gente y amigos, entre ellos, **Marga, Lola, Puro, Borja, Oyola** (quien nos iba a decir que íbamos a acabar siendo “ciudadanos del mundo” :p), **Cabárcenos y Cabarcenitos, José y Miguel** (mis cataneros favoritos), **Isabel, Nacho, Cruz, Goyo**, que de alguna manera u otra habéis estado ahí para apoyarme y compartir buenos momentos juntos durante estos años. **Jacinto, Pedro, Toñi**, que ilusión me hace poder compartir el momento de mi defensa con vosotros. Vuestra motivación por la profesión veterinaria es digna de admiración y sin vuestro apoyo no hubiera vivido algunas de las experiencias que me facilitasteis durante mi carrera, gracias.

**Niels**, guapuchino, thanks for your support and your care during the last phase of my PhD. Your fantastic cooking skills (lekker rendam), the beer-pong competitions, the long Netflix sessions, our paseitos and in summary, your company, made the awkward pandemic times passed rather smoothly next to you. I look forward to explore and to enjoy more of this world together. Maybe we should take **Benjamin** along to be our *chofer, dj* and beer provider :p.

A mi **familia**. Gracias por vuestro apoyo y vuestro cariño. Me da mucha pena haberme perdido tantos eventos familiares durante estos años pero he agradecido enormemente vuestras visitas en pelotón (hasta 5 personas en 25 metros cuadrados :p) o vuestras videollamadas. **Tia Rosa** que ilusión me hace que vengas a la defensa de la tesis, me aseguraré que tengas una silla con buenas vistas :p. **Yayita**, te quiero mucho mucho. Sabes que esta tesis os la dedico también tanto a ti como al abuelo, que en paz descanse. “*A usted nuncale nuncale, pues puequele puequele*”. Sin vuestro cariño y vuestra motivación para siempre esforzarme al máximo nunca hubiera llegado hasta aquí. Gracias por tu apoyo yaya, y por siempre tener aceitunas en tu despensa a la espera de mi visita :p. **Abuela Isabel**, te quiero.

**Alvarito**, te quiero mucho. Tengo poco que decirte porque al igual que papá y mamá has estado estos años ahí para apoyarme y motivarme a terminar, gracias. A ver si os venís prontito Ana y tu a visitarme, os cedo mi casa :p.

Y por último **mamá, papá**, esta tesis os la dedico a vosotros por vuestro amor incondicional, vuestro apoyo y el haber estado siempre ahí. Lo he conseguido! En la universidad de Utrecht, papá (madre mía la de veces que oírte hablar de esta universidad antes de venir). Se que han sido años difíciles con la distancia, la pandemia, ... pero he de agradeceros la oportunidad y el sacrificio de todos estos años para hacer que mi experiencia en Holanda haya sido posible. Os quiero!

This was it!

I have spoken.



## CURRICULUM VITAE



Eva Moreno was born on September 16<sup>th</sup> 1991 in Madrid, Spain. She attended and graduated from the Montserrat high school of Madrid before enrolling at Alfonso X University, Madrid, at the faculty of Veterinary Medicine in 2009. During her 5-year studies she worked as Veterinary Intern at Indra-Vetersalud Companion Animal Clinic. She obtained her Master degree in Veterinary Science Medicine in 2014. Having developed great interest in understanding more in depth the mechanisms driving the pathologies she observed during her masters, mainly cancer, she applied for a research internship at the Pathobiology Department of the Veterinary Faculty at Utrecht University, in the lab of Professor

Alain de Bruin. For over a year, she performed experiments and learned several molecular techniques that allowed her to obtain a PhD position in the same lab in March 2016 under the supervision of Prof. Dr. A. de Bruin (Promotor) and Dr. B. Westendorp (Co-promotor). During this period she joined several general and specialized courses related to cancer biology offered by the PhD program “Cancer, Stem Cells & Developmental biology” at Utrecht University, as well as presented her work in some national and international conferences. The results obtained during her time as a PhD student are presented in this thesis.

## LIST OF PUBLICATIONS

**Moreno E**, Pandit SK, Toussaint MJM, Bongiovanni L, Harkema L, van Essen SC, van Liere EA, Westendorp B, de Bruin A. “Atypical E2Fs either counteract or cooperate with RB during tumorigenesis depending on tissue context”.

*Cancers*. 2021 Apr; 13(9): 2033

**Moreno E**, Toussaint MJM, van Essen SC, Bongiovanni L, van Liere EA, Koster MH, Yuan R, van Deursen JM, Westendorp B, de Bruin A. “E2F7 Is a Potent Inhibitor of Liver Tumor Growth in Adult Mice”.

*Hepatology*. 2021 Jan;73(1):303-317.

Segeren HA, van Rijnberk LM, **Moreno E**, Riemers FM, van Liere EA, Yuan R, Wubbolts R, de Bruin A, Westendorp B. “Excessive E2F Transcription in Single Cancer Cells Precludes Transient Cell-Cycle Exit after DNA Damage”.

*Cell Rep*. 2020 Dec 1;33(9):108449

Bongiovanni L, Brachelente C, **Moreno E**, Welle MM. Canine Epithelial Skin Tumours: Expression of the Stem Cell Markers Lgr5, Lgr6 and Sox9 in Light of New Cancer Stem Cell Theories.

*Vet Sci*. 2020 May 8;7(2):62.

Sladky VC, Knapp K, Soratroi C, Heppke J, Eichin F, Rocamora-Reverte L, Szabo TG, Bongiovanni L, Westendorp B, **Moreno E**, van Liere EA, Bakker B, Spierings DCJ, Wardenaar R, Pereyra D, Starlinger P, Schultze S, Trauner M, Stojakovic T, Scharnagl H, Fava LL, Fojjer F, de Bruin A, Villunger A. “E2F-Family Members Engage the PIDDosome to Limit Hepatocyte Ploidy in Liver Development and Regeneration”.

*Dev Cell*. 2020 Feb 10;52(3):335-349.e7.

Matondo RB, **Moreno E**, Toussaint MJM, Tooten PCJ, van Essen SC, van Liere EA, Youssef SA, Bongiovanni L, de Bruin A. “Atypical E2f functions are critical for pancreas polyploidization”.

*PLoS One*. 2018 Jan 12;13(1):e0190899

